PB83-250191

Fates and Biological Effects of Polycyclic Aromatic Hydrocarbons in Aquatic Systems

Savannah River Ecology Lab., Aiken, SC

Prepared for

Environmental Research Lab., Athens, GA

Jul 83

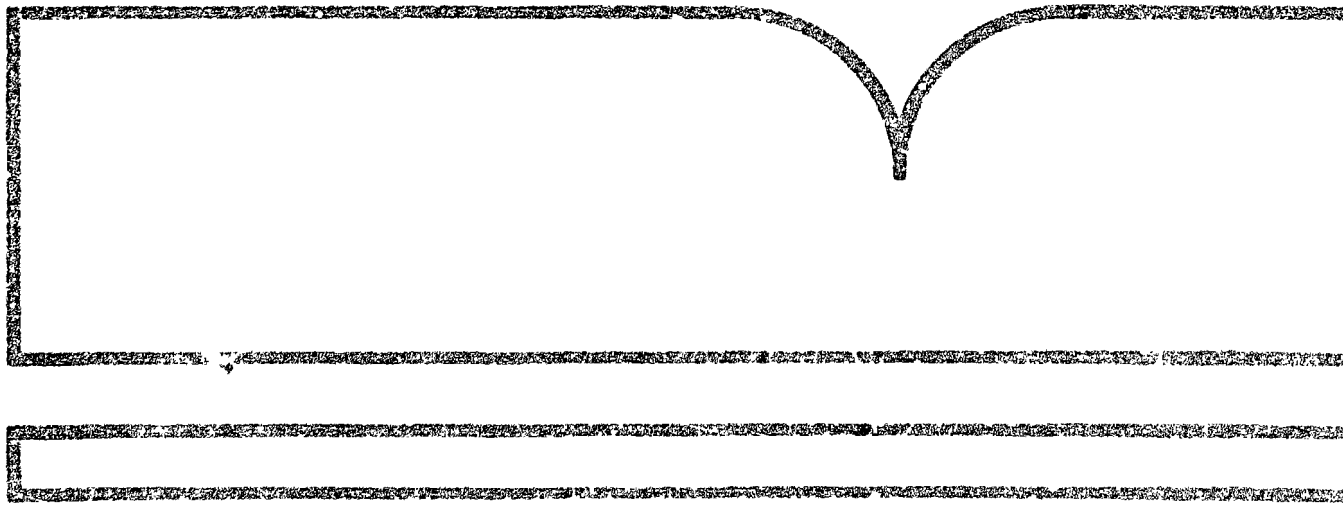

TECHNICAL REPORT DATA
(Please read Instructions on the reverse before completing)

1. REPORT NO.	2.	3. RECIPIENT'S ACCESSION NO.
EPA-600/3-83-053		PB83 250191

4. TITLE AND SUBTITLE	5. REPORT DATE
Fates and Biological Effects of Polycyclic Aromatic Hydrocarbons in Aquatic Systems	July 1983
	6. PERFORMING ORGANIZATION CODE
7. AUTHOR(S)	8. PERFORMING ORGANIZATION REPORT NO.
John P. Giesy, Steven M. Bartell, Peter F. Landrum, Gordon J. Leversee, and John W. Bowling	
9. PERFORMING ORGANIZATION NAME AND ADDRESS	10. PROGRAM ELEMENT NO.
Savannah River Ecology Laboratory U.S. Department of Energy P.O. Drawer E Aiken SC 29801	CCULIA
	11. CONTRACT/GRANT NO.
	78-D-X0290
12. SPONSORING AGENCY NAME AND ADDRESS	13. TYPE OF REPORT AND PERIOD COVERED
Environmental Research Laboratory--Athens GA Office of Research and Development U.S. Environmental Protection Agency Athens GA 30613	Final, 6/78-5/81
	14. SPONSORING AGENCY CODE
	EPA/600/01

15. SUPPLEMENTARY NOTES

16. ABSTRACT

This research project was conducted to test the hypothesis that fates of polycyclic aromatic hydrocarbons (PAH) in ecosystems can be predicted by mechanistic simulation models based on easily measured properties of the compounds in this homologous series. To accomplish this goal our research efforts were in four major areas: (1) development of a mechanistic, predictive simulation model based on kinetic rather than thermodynamic considerations; (2) development of analytical and quality assurance protocols forthe extraction and quantification of PAH associated with biological and geological matrices; (3) laboratory studies to determine the vectors of and rate constants for uptake, depuration and biotransformation of PAH by aquatic organisms and sediments; (These studies also examined the effect of PAH concentration, temperature and other exogenous factors on rate constants and determined whether rate constants were first order.) and (4) a microcosm study to compare the results of simulation and laboratory scale studies to a larger scale ecosystem study.

17. KEY WORDS AND DOCUMENT ANALYSIS

a. DESCRIPTORS	b. IDENTIFIERS/OPEN ENDED TERMS	c. COSATI Field/Group

18. DISTRIBUTION STATEMENT	19. SECURITY CLASS (This Report)	21. NO. OF PAGES
RELEASE TO PUBLIC	UNCLASSIFIED	245
	20. SECURITY CLASS (This page)	22. PRICE
	UNCLASSIFIED	

EPA Form 2220-1 (9-73)

PB83-250191

EPA-600/3-83-053
July 1983

FATES AND BIOLOGICAL EFFECTS OF POLYCYCLIC AROMATIC HYDROCARBONS IN AQUATIC SYSTEMS

by

John P. Giesy, Steven M. Bartell, Peter P. Landrum, Gordon J. Leversee, John W. Bowling

Savannah River Ecology Laboratory
University of Georgia
P.O. Drawer E
Aiken, South Carolina 29801

Interagency Agreement
78-D-X0290

between

U.S. Department of Energy
and
U.S. Environmental Protection Agency

Project Officer
Harvey W. Holm
Environmental Systems Branch
Environmental Research Laboratory
Athens, Georgia 30613

ENVIRONMENTAL RESEARCH LABORATORY
OFFICE OF RESEARCH AND DEVELOPMENT
U.S. ENVIRONMENTAL PROTECTION AGENCY
ATHENS, GEORGIA 30613

DISCLAIMER

This report has been reviewed by the Savannah River Ecology Laboratory, U.S. Environmental Protection Agency, and approved for publication. Approval does not signify that the contents necessarily reflect the views and policies of the U. S. Environmental Protection Agency, nor does mention of trade names or commercial products constitute endorsement or recommendation for use.

FOREWORD

Environmental protection efforts are increasingly directed towards preventing adverse health and ecological effects associated with specific compounds of natural or human origin. As part of this Laboratory's research on the occurrence, movement, transformation, impact, and control of environmental contaminants, the Environmental Systems Branch studies complexes of environmental processes that control the transport, transformation, degradation, and impact of pollutants or other materials in soil and water and assesses environmental factors that affect water quality.

Polycyclic aromatic hydrocarbons (PAH) from natural and man-made sources are widely distributed in the environment and pose potential health problems to aquatic animals and humans. An important phase in addressing these problems is developing an understanding of the cycling and fate of these compounds. This report presents the development and evaluation of a theoretical, predictive model of the fate of PAH based on easily measured characteristics of the compounds and the environments to which they may be released.

William T. Donaldson
Deputy Director
Environmental Research Laboratory
Athens, Georgia

ABSTRACT

This research project was conducted to test the hypothesis that fates of polycyclic aromatic hydrocarbons (PAH) in ecosystems can be predicted by mechanistic simulation models based on easily measured properties of the compounds in this homologous series. To accomplish this goal our research efforts were in four major areas. 1) Development of a mechanistic, predictive simulation model based on kinetic rather than thermodynamic considerations; 2) Development of analytical and quality assurance protocols for the extraction and quantification of PAH associated with biological and geological matrices; 3) Laboratory studies to determine the vectors of and rate constants for uptake, depuration and biotransformation of PAH by aquatic organisms and sediments. These studies also examined the effect of PAH concentration, temperature and other exogenous factors on rate constants and determined if rate constants were first order; and 4) A microcosm study to compare the results of simulation and laboratory scale studies to a larger scale ecosystem study.

Laboratory studies indicated that anthracene and benzo (a) pyrene are rapidly biotransformed by fish and dipteran larvae but not by periphyton communities. Biotransformation had a significant effect on the steady state concentrations of parent compound and biotransformation products. These results demonstrated that predictions of steady state concentrations based on ^{14}C-labeled parent compound and the octanol-water partitioning coefficient of the parent compound would be in error. Thus, the octanol-water partitioning coefficient would not be a good predictor of the behavior of PAH in aquatic organisms. Uptake and depuration rate constants were first order for fish but not dipteran larvae. Induction of biotransformation and changes of this rate over time means that results from short-term pharmacokinetic studies, using radio-labeled compounds, will be misleading for compounds which are biotransformed.

Anthracene (approximately 12 $\mu g \cdot \ell^{-1}$) was acutely toxic to bluegill sunfish dosed in outdoor channels microcosms. This mortality was not observed in laboratory studies and was shown to be a photo-toxic mechanism. Therefore, laboratory studies must be conducted under the same lighting conditions if the results of these studies are to be realistic representations of field conditions.

The modeled processes that influenced PAH transport included losses to volatilization, photolytic degradation, sorption to suspended particulate matter and sediments and net uptake by biota. The biota in the model included phytoplankton, periphyton, rooted macrophytes, bacteria, zooplankton, two functionally defined benthic invertebrate components and two functionally defined categories of fish. Model simulations were compared to results of experiments conducted in artificial streams. A 0.6 μmolar

solution of anthracene in ethanol was continuously added into the headwaters for 15 days followed by termination of anthracene input. The model accurately predicted the dissolved anthracene concentration through time and space. Uptake by periphyton was overestimated by the model; however, the rate of depuration of anthracene by periphyton was reasonably simulated. Photolytic degradation appeared to be the most important pathway of flux within the channels, both experimentally and in the simulations.

This report was submitted in fulfillment of Interagency Agreement No. EPA-78-D-X0290 by the Savannah River Ecology Laboratory with the U.S. Environmental Protection Agency. This report covers the period June 1, 1978 to May 31, 1981, and work was completed as of May 31, 1981.

CONTENTS

FIGURES

TABLES

ACKNOWLEDGEMENTS

The cooperation and support of the staff of the University of Georgia's Savannah River Ecology Laboratory (SREL) is much appreciated. The research and report preparation were supported, in part, by interagency agreement No. DE-AC09-76SR00819 between the United States Department of Energy and SREL. We wish to acknowledge the technical support of James Cheatham and Susan Giddings. We wish to thank Ms. Jean Coleman, Tonya Willingham and Debbie Perks for their help in preparing this report. Karen Brown assisted with sampling and statistical analyses of experiments on sediment studies.

SECTION 1

INTRODUCTION

Polycylic (polynuclear) aromatic hydrocarbons (PAH or PNA) are a homologous series of compounds composed of 2 or more condensed benzene rings with occasional incorporations of cyclopentene rings, such as in the fluorenes or "hetero-octanes" (N, O or S). PAH derived from natural (Andelman and Snodgrass, 1974) and man-made sources are widely distributed in the environment. PAH occur as natural products in plants and microbes and natural pyrolytic processes, such as forest fires and volcanic activity, and human activities such as manufacturing and fossil fuel conversion (Braunstein et al., 1977; Harrison et al., 1975; and Suess, 1976). Inputs to aquatic systems are due to human activities, as found in east coast near-shore marine sediments (Hites, et al., 1977) or of natural origin in sediments of pristine lakes (Brown and Starnes, 1978) and marine sediments (LaFlamme and Hites, 1979). LaFlamme and Hites (1978) reviewed the sources of PAH in the environment and concluded that while some of the PAH could be from natural sources, most of the PAH were from pyrolytic processes due to human activities. PAH released to the environment by human activities are due to oil spills and fossil fuel conversion (Neff, 1979). Over 230,000 metric tons of PAH enter the oceans and surface waters of the world each year (Neff, 1979). The American Petroleum Institute (1978) has compiled a lengthy review of the sources and environmental concentrations of PAH in the environment. Inputs of PAH into aquatic systems are expected to increase with the commencement of the synthetic fuels program and emphasis on coal combustion as a primary energy source (Gehrs et al., 1976). After reviewing the available literature on projected effluent concentrations, solubility, degradation waste treatment efficiency and acute and chronic effects of coal conversion effluents, Herbes et al. (1976) concluded that higher molecular weight polycyclic and heteroaromatic compounds possess the greatest potential for bioaccumulation, carcinogenic and mutagenic effects in aquatic animals and man, and acute toxicity to aquatic organisms. Thus, the importance of developing predictive models of PAH fate in aquatic systems must be emphasized (Baughman and Lassiter, 1978). For this reason we undertook two lines of research: 1) to develop an understanding of the cycling and fate of these compounds including bioaccumulation, sorption, degradation and transformation in a quasi-natural environment and 2) to determine effects of PAH compounds on aquatic ecosystems.

Toxic, mutagenic, and carcinogenic properties of PAH have been much studied (LaVoie et al., 1979; Norden, et al., 1979). Many PAH are carcinogenic or have carcinogenic biotransformation products (Christensen et al., 1975; Neff, 1978) and may be hazardous to man through biomagnification or be directly mutagenic to aquatic organisms (Neff, 1979).

Mechanisms of PAH biotransformation, mode of action, and analyses in biological and geological matrices have been much studied and this literature has been reviewed (Braunstein et al., 1977; Jones and Leber, 1979; Neff, 1979; Bjorseth and Dennis, 1980). However, few studies have attempted to integrate laboratory, field and simulation studies.

Assessment of health risks, associated with introduction of PAH into the environment, depends in part upon quantification of environmental transport and subsequent dose concentrations experienced by inhabitants (Crawford and Leggett, 1980). Estimates of transport and dose are independent of the specific nature of the threat to human health, either directly through contamination of potable water, for example, or indirectly through damage to ecological life support systems.

We have the recent experiences, for example, of worldwide distribution of DDT and PCB in aquatic life of many rivers and bays, mercury and cadmium poisonings of the populations in certain industrial areas, and vinyl chloride exposure of industrial workers. These experiences arose from accidental release, uncontrolled industrial releases, and unsafe overuse. In order to avoid these types of experiences in future years with the thousands of new chemicals being released to the environment, a toxic effects testing strategy is needed which will "flag" potential problem contaminants prior to their widespread dispersal. This testing strategy should cover both plant and animal species and be concerned with acute and chronic exposures. Because of restrictions on time, resources and human cognitive capacity, a number of techniques have been established to assess probable effects of trace contaminants. These techniques include toxicity tests on individual or standard organisms, individual bioaccumulation tests, measurement of physical properties of the chemical, environmental monitoring, studies in simple systems and investigation of transport and degradation.

To depend only on retrospective environmental studies to elucidate the knowledge required to avoid adverse effects is to court disaster. Rather, what is urgently required is a systematic program of investigation the scale of which time and resources permit expeditious acquisition of the essential data and understanding. While the tests listed above provide useful information, they do not consider complex interactions between biotic and abiotic components of the environment and do not allow for evaluation of complex biological interactions. Over time, very subtle effects may have serious impacts on populations or communities as they modify complex interdependencies.

The so-called "benchmark" techniques have been developed on the assumption that the chemical and physical characteristics of a trace contaminant will determine its effects on the biocenose and how it fluxes and cycles through the environment and that the fate of a compound can be predicted by simple first or second principles. While this assumption has not been tested and may, in fact, be untestable, correlative studies indicate that the assumption is somewhat valid. However, low predictability and high variability indicate that the correct parameters are not being measured for each compound or that the interactions between the compounds of interest with biotic and abiotic components are non-additive. That is,

there are significant interaction terms which can not be evaluated by simple tests or knowledge of the first principles of trace contaminants.

Because of the vast difference between simple laboratory tests and complex field situations, scientists have formed conceptual and operational bridges between the two systems. These include models of theoretical conceptualization of how complex systems operate. Computer science has provided the bookkeeping capacity to describe these systems with complex linear and non-linear functions. The science of modeling and environmental predictability suffers from a lack of steady state conditions, rate constants and an understanding of the most important parameters for increasing the power of predictability. If the correct physical and chemical parameters of both an organic compound of interest and the environment to which it is being released are known, a model could be constructed to predict the gross movement of the compound of interest within that environment. This model could also include degradation and transformation due to hydrolysis, photolysis and by biota. Another useful type of model of ecosystems are the simplified subsets of ecosystems called microcosms (Metcalf et al., 1971; Lee and Takahashi, 1977; Lu et al., 1977; Giesy, 1980). We feel that a microcosm approach (artificial streams) allowed us to evaluate a predictive model under more natural, complex conditions with control of inputs and replication of the experimental conditions.

For example, most information on plutonium indicated that it was not ecologically hazardous since it was not readily taken up by plant roots or assimilated through the intestinal wall of animals. Hence, its presence in the environment was more a problem of physical transport in air and soils, and its biological significance, with regard to effects, was limited to inhalation or movement into wounds. Later, field data showed quantities of plutonium in trophic levels and tissues where it was not expected. Studies were conducted which showed that in the environment plutonium can be organically complexed by microorganisms in the soil, and that it was then much more available for transfer through food chains all the way up to vertebrate consumers of the vegetation. Effects within the system could then be predicted based on new modes of entry within the intact system, and a change in rate constants for transfers between components within the system.

Thousands of different PAH compounds are chemically possible. Therefore, application of elaborate screening protocols (Duthie, 1977) to individual PAH in order to estimate major processes of transport, accumulation, and degradation is impractical for purposes of risk analysis. However, it is important to answer questions about these compounds such as: Can human exposure be limited by more rigorous drinking water treatment aimed at removing organics? Do the various compounds become concentrated in and magnified by trophic levels culminating in human exposure? Is concentration in various trophic components proportional to time and concentration of exposure? What are the rates of accumulation and elimination from various components? What are the rates of uptake and elimination relative to immobilization rates by sorption processes and photo- and microbial

degradation rates. Because of the large number of compounds and environments to be evaluated a certain level of predictability must be achieved.

This study tested the hypothesis that a theoretical predictive model of the fate of PAH compounds or classes of compounds in a given environment, or class of environments, can be constructed based on characteristics of the compound of interest and the environment to which it is released. This report describes a test of the hypothesis that the transport of three PAH, anthracene, naphthalene, and benzo(a)pyrene, in lotic systems (streams, rivers, reservoirs) could be predicted from the fundamental chemistry of individual PAH which embodies sufficient information for prediction. While we do not feel that a simple characteristic, such as molecular weight is necessarily the best parameter, from which to predict environmental fates, we feel that the law of parsimony dictated that we try a simple parameter, such as molecular weight, to try to make predictions from and determine where this simplification fails to predict accurately. Many modeling efforts rely on measured properties, such as octanol-water partitioning coefficients, which are a function of first principles of a compound. These measured parameters often integrate several properties of compounds, which is an advantage because more information can be included in a single empirically measured value. However, these coefficients must be measured, which is time-consuming and they may be less accurate than molecular weight measurements.

We feel that a coordinated synthesis of information on ecosystem structure and function is required to assess environmental impacts of any technology which must ultimately be interfaced with the environment. While this research was on PAH compounds (anthracene and benzo(a)pyrene specifically) it tested the hypotheses that valid generalizations about the behavior of general classes of organic compounds in complex environments can be made from knowledge about the compounds obtained in relatively simple laboratory studies and the environments to which these compounds are released. Knowledge of this type can be transferred to other organic compounds and has broad applicability.

Anthracene was chosen as a model PAH for laboratory, field and simulation studies because it is a commercially important PAH which is produced in large quantities and used extensively as a reagent in organic synthesis (Archer et al., 1979). Anthracene has also been used frequently as a model PAH for studies of environmental fate and transport in aquatic systems (Ausmus et al., 1980) or physiological disposition in aquatic biota (Roubal et al., 1977). Anthracene is non-carcinogenic (NAS, 1972) and relatively non-toxic (NAS, 1972; Deickman and Gerarde, 1969).

SECTION 2

CONCLUSIONS

The results of the laboratory studies demonstrated that PAH are rapidly biotransformed by bluegill sunfish and chironomid larvae but not unionid clams or periphyton assemblages. Biotransformation rates were affected by temperature and time of exposure. The rates of biotransformation also affected the bioconcentration factors predicted from short-term pharmacokinetic studies. Temperature and food ration also affected rates of uptake and depuration. Uptake and depuration were first-order with respect to forcing function concentrations. Depuration was generally multiphasic with some of the biotransformation products bound to tissues, such that they were very slowly depurated.

Recovery of PAH from geological materials such as sediments, was inversely proportional to time of exposure. Internal standards added at the time of extraction did not allow accurate determination of extraction efficiencies. Drying of sediments resulted in reduced recovery of anthracene from sediment. Capillary gas-liquid chromatography coupled to mass spectrometry (GC/MS) showed that anthracene could be extracted from sediments and separated from interfering peaks but anthraquinone (a transformation product of anthracene) could not.

Dissolved, naturally occurring organic acids (humic acids) reduced the availability of anthracene, benzo(a)pyrene and dimethylbenzanthracene to D. magna but increased the availability of 3-methylcholanthracene and dibenzanthracene. The presence of particulates also reduced the availability of PAH to D. magna.

The simulation model, Fate of Aromatics Model (FOAM), was developed to predict the fates of PAH from molecular weight of the PAH of interest and parameters of the ecosystem to which it is to be released. FOAM accurately simulated and predicted the flux along physical-chemical pathways. However, the model was less accurate in predicting the accumulation and biotransformation of PAH by aquatic biota. Future versions of predictive simulation models should be kinetically based, as FOAM is, if accurate information on cycling is to be predicted. However, this type of model requires a great amount of information. Because of the scale of the input parameters, models such as FOAM will be useful in describing overall processes and fluxes along different pathways but will not be very useful in simulating the concentrations of PAH and PAH transformation products in individual biotic components. Also, some of the physical processes, which are important in determining the fates of PAH in natural systems, are discontinuous functions or catastrophic events, such as storms, which do not lend themselves to mathematical simulations. Therefore, models of the

type developed here will always be limited to relatively gross predictions. Accurate predictions of concentrations in individual types of organisms may not be attainable.

The channels microcosms were useful for testing the reliability of FOAM to simulate the behavior of PAH in a complex ecosystem. However, the greatest utility of the channels microcosm was in allowing studies to be conducted under more natural conditions than allowed by laboratory systems. From these studies we learned that exposure to sunlight during exposure to anthracene was acutely toxic. Thus, laboratory studies do not accurately predict toxicity observed under more natural conditions. While microcosms may not be used as a central monitoring tool, they are useful in studies of classes of compounds and to verify laboratory and simulation conclusions. Because of their scale, however, microcosms will never be useful in validation of long-term or global simulation models. The test of the benchmark hypotheses was only partly supported by our studies. Future simulations will need to consider more complex measures of chemical behavior. The proposed use of octanol/ water partitioning coefficients shows promise for predicting uptake by organisms but not biotransformation. Thus, the benchmark approach will probably not give adequate predictions of the dynamics of organic compounds in complex environments.

SECTION 3

RECOMMENDATIONS

Future studies of the fates and effects of trace contaminants should be conducted in laboratory, field and simulation modes concurrently. All three modes of investigation added to the overall understanding of the dynamics of PAH in aquatic ecosystems.

Simulation models should be developed to predict general behavior of PAH in aquatic systems. That is, to determine when the greatest mass of PAH accumulates and where the most sensitive ecosystem components are. Where physical and chemical processes dominate, simulation models will be able to accurately predict the overall dynamics of PAH, but rare events of large magnitude will reduce the accuracy of predictions on a short-term basis. Optimization of time step duration relative to system level variability needs to be further investigated to increase the accuracy of predictive models.

The current state of predictive simulation models will not allow the accurate prediction of concentrations of single PAH in individual species but can be useful in simulating overall processes in a gross manner. Future simulations should be kinetic in nature but the relationships used to predict rate constants need to be based on structure-activity relationships.

The channels microcosms used in this study were sufficient to test some simulation processes and we recommend the use of this type of a system in future studies. However, microcosms of this magnitude will not be useful as screening tools. The utility of the realism of such systems was demonstrated by the photo-toxic effect observed in the microcosm, which was not observed under laboratory conditions. We suggest this type of system needs to be used to validate processes which are indicated by laboratory and/or simulations because they allow testing in a more complex and more natural system than that of the laboratory, while not releasing trace contaminants to the biosphere.

SECTION 4.0

LABORATORY STUDIES

SECTION 4.1

INTRODUCTION

A series of laboratory studies was conducted to determine rate constants for uptake, depuration and biotransformation of PAH in several isolated components of aquatic systems. The components studied were water, sand, organic sediments, periphyton, daphnia, chironomids, fish and clams. Beside determining rate constants for uptake, depuration and biotransformation, these studies investigated the effects of factors such as temperature, presence or absence of substrate, and concentration of PAH on rate constants. The goal of these studies was to supply independent estimates of rate constants and to determine the precision with which these rate constants could be measured in the laboratory. The rate constants could be used to parameterize the simulation model as well as to develop statistical relationships between rate constants and first principles of the compounds of interest.

Subsequent comparison of rate constants and state variables measured under controlled laboratory conditions could be compared to those observed in microcosm studies and those predicted from simulation models. Such comparisons can provide estimates of relative variability as well as relative importance of pathways and interactions to be used in formulating and modifying the predictive simulation model.

SECTION 4.2

ANTHRACENE SORPTION AND DESORPTION BY ORGANIC SEDIMENTS

INTRODUCTION

When PAH are added to aquatic systems they rapidly become associated with suspended and bottom sediments (Dunn, 1976; Lee and Takahashi, 1977; Muller and Böhnke, 1977; Lee et al., 1978; Giddings et al., 1978; Herbes and Schwall, 1978; Teal et al., 1978; Prahl and Carpenter, 1979; Gearing et al., 1980; Hinga et al., 1980). A number of techniques for extracting organic compounds from solid matrices are available and different extraction efficiencies have been reported for each (Kooke et al., 1981). Therefore laboratory studies were designed to determine the best extraction conditions and quantification techniques. Rate constants for sorption of anthracene by organic sediments were also determined.

MATERIALS AND METHODS

Extraction Procedures

The first set of experiments was conducted to determine the best extraction protocol (Figure 4.2.1). The methods which were common to these two experiments are given first, with the methods which were specific to each experiment afterward.

Two different sediments were used in these studies. Upper Three Runs Creek (UTRC) sediment is a fine, silty sediment high in organic matter (~ 20% by weight). Steel Creek sediment is a coarse, sand-clay mixture with little organic matter. Sediment from the two streams was collected with a glass beaker and sieved through 5 mm opening stainless steel screen into a stainless steel bucket. ^{14}C-anthracene used to spike the sediments had a specific activity of 3.3 mCi·mmol^{-1}. All soxhlet extractions were done for 18 h. Liquid scintillation counting was done using 12 mls of Research Products International 3a70b counting cocktail. Counting time was 10 minutes per sample with a Beckman Model LS 8100 liquid scintillation counter.

High pressure liquid chromatography analyses were done on a Varian Model 5000 LC, which was equipped with a Varian 30 cm MCH-10 reverse phase column operated at 30°C, and a flow rate of 1 ml·min^{-1}. Solvents were 35% acetonitrile in water initially, programmed to 100% acetonitrile in 40 minutes, held at 100% for 10 minutes, with a return to initial conditions for 5 minutes before the next injection. Injections were done automatic-

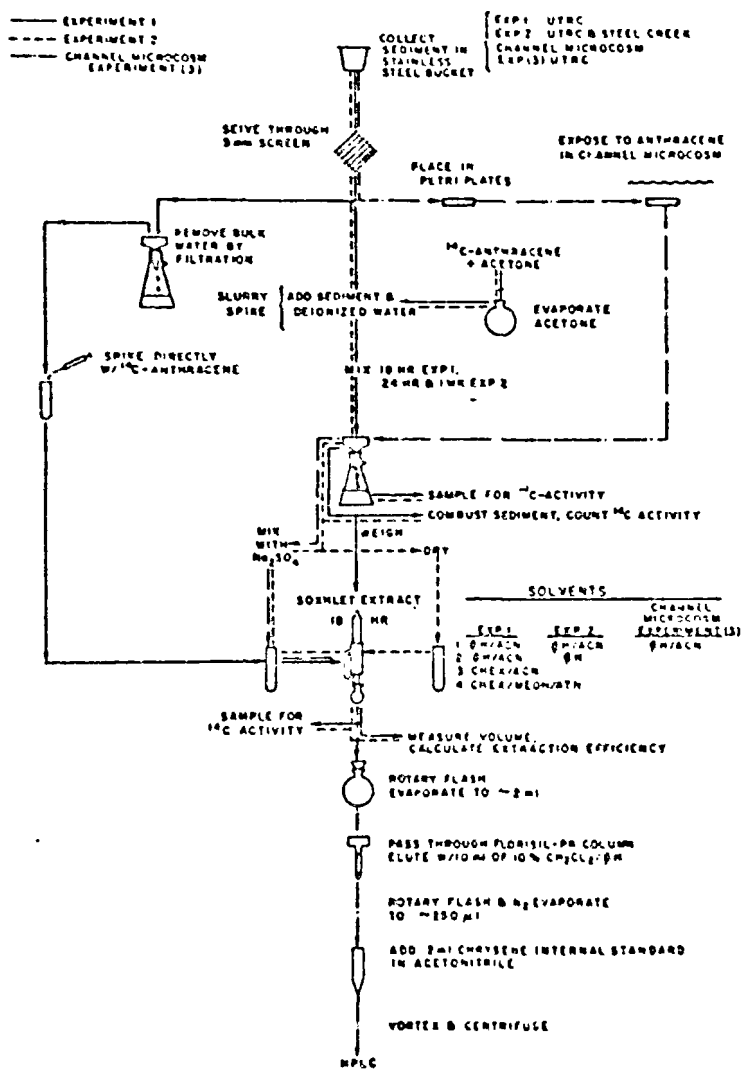

Figure 4.2.1. Flow diagram of procedures used to spike, extract and analyze anthracene in stream sediment.

ally by a 25 µl sample loop. The detector was a 254 nm fixed-wavelength uv detector, connected to a Varian CDS 111-L integrator, and a strip chart recorder. A fluorescence detector with 360 nm excitation and > 460 nm emission wavelength filters, connected to a second strip chart recorder was operated downstream from the UV detector. Quantitation was by the internal standards method with chrysene as the internal standard.

Combustion of sediment for unextracted ^{14}C was done on a Packard Tricarb sample oxidizer. ^{14}C-CO_2 was trapped in 7 ml of a CO_2 trapping agent and added to 12-15 ml of counting cocktail. Prior to combustion, sediment samples, ~ 250 mg each, were mixed with cellulose powder and Combustaid® to improve combustion efficiency.

The first experiment was conducted to determine the solvent system which allowed the greatest recovery of anthracene from sediment, while minimizing the extraction of interfering compounds. In addition, we wanted to determine if direct spiking and more natural incorporetion gave similar estimates of extraction efficiency. The flow diagram for this experiment is given by the solid line in Figure 4.2.1 Three solvents were used to extract UTRC sediment, which had been slurry spiked. Three aliquants of 10g, wet filtered weight were soxhlet extracted with each of three solvent systems (Table 4.2.1).

The second experiment was conducted to compare variation in extraction efficiency due to sediment type, time of equilibration between sediment and anthracene, the effect of sediment moisture on the extraction of anthracene from wet or dry sediment, and solvent type (polarity). The flow diagram for this experiment is given by the dashed line in Figure 4.2.1. The experimental design was a completely randomized 2^4 factorial with 3 replications per treatment combination (Table 4.2.2). Spiked sediment slurries were mixed for 24 h or 1 wk before extraction. Wet sediment samples were soxhlet extracted immediately after filtration. Dry sediment was air-dried in a hood for 24 h. Extraction time was 18 h with either 100 ml of benzene or 35 ml of acetonitrile + 65 ml of benzene. Crude extracts were sampled for quantification of ^{14}C activity.

Anthracene and anthraquinone peaks were separated on an OV101 capillary column and mass spectra recorded to determine if the compounds which were being spearated and identified were anthracene and anthraquinone. The relative ion intensities of the peaks which we had identified as anthracene and anthraquinone are given in Figures 4.2.2 and 4.2.3 respectively. The retention indexes (RI) were calculated with equation 4.2.1. The HPLC protocol separated anthracene, anthraquinone and chrysene well (Fig. 4.2.4). However, sediment extracts often contained a compound which eluted very near anthraquinone (Fig. 4.2.4). This peak was almost always present but often obscured the anthraquinone in spiked samples. The retention indices of the anthracene standard and an anthracene sample extracted from sediment were 1717 and 1712 respectively. The retention indices of anthraquinone standard and sample were 1807 and 1789 respectively. The retention indices indicated that the peaks we had chosen as anthracene and anthraquinone in our chromatograms of sediment extracts were accurate. However, to

TABLE 4.2.1. EXTRACTION OF ^{14}C-ANTHRACENE FROM DIRECT AND SLURRY SPIKED UTRC SEDIMENT

Treatment	N	Solvent System[a]	Fraction Recovered		
			$\bar{x}$	SD	CV
1 Direct Spike	3	35 ml ACN + 65 ml ϕH	.976	.020	2.05
2 Slurry Spike	3	35 ml ACN + 65 ml ϕH	.808	.030	0.37
3 Slurry Spike	3	35 ml ACN + 65 ml Chex	.771	.015	1.95
4 Slurry Spike	3	16 ml MEOH + 42 ml ATN + ml CHEX	.898	.027	3.01

[a]ACN = Acetonitrile

ϕH = Benzene

ATN = Acetone

CHEX = Cyclohexane

MEOH = Methanol

TABLE 4.2.2 EXPERIMENTAL DESIGN TO DETERMINE EFFECTS OF SEDIMENT TYPE, EQUILIBRATION TIME, MOISTURE CONTENT AND POLARITY OF SOLVENT ON EXTRACTION EFFICIENCY OF ANTHRACENE FROM SEDIMENT

	Main Effects		
Sediment Type	Spike Time	Moisture	Solvent[a] System
Steel Creek	24 hr	Wet	ϕH ϕH/ACN
		Dry	ϕH ϕH/ACN
	1 wk	Wet	ϕH ϕH/ACN
		Dry	ϕH ϕH/ACN
UTRC	24 hr	Wet	ϕH ϕH/ACN
		Dry	ϕH ϕH/ACN
	1 wk	Wet	ϕH ϕH/ACN
		Dry	ϕH ϕH/ACN

[a] ϕH = Benzene, ACN = Acetonitrile.

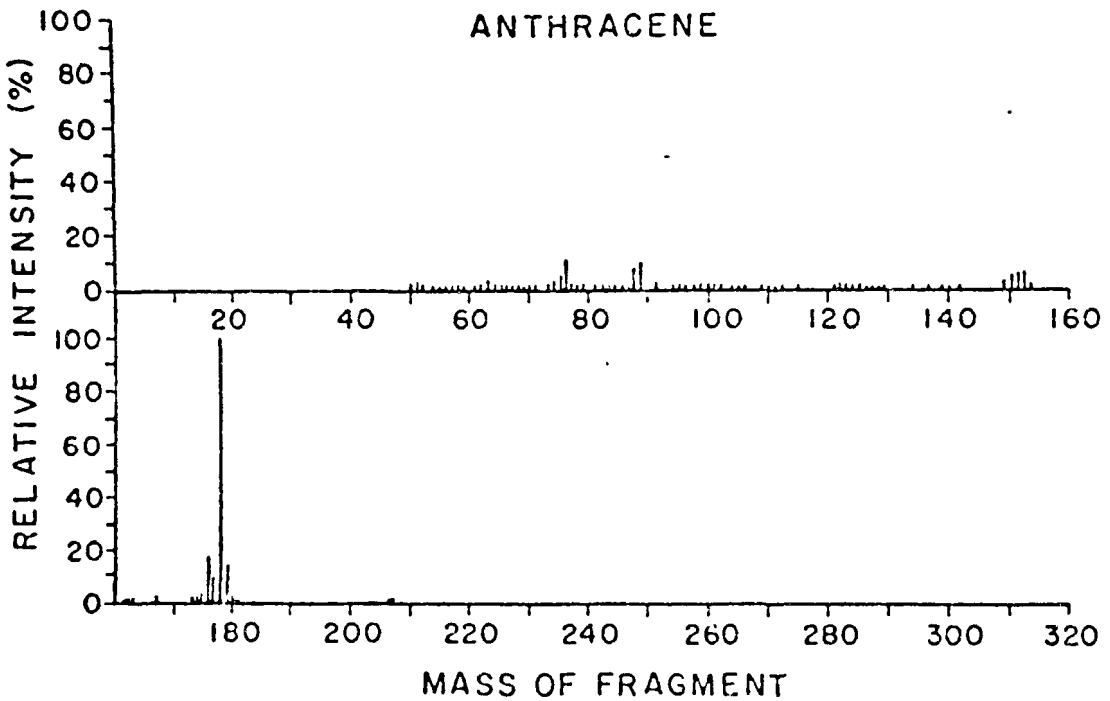

Figure 4.2.2. Relative ion intensities of anthracene. OV101 capillary column, 2°C min. increase in temperature.

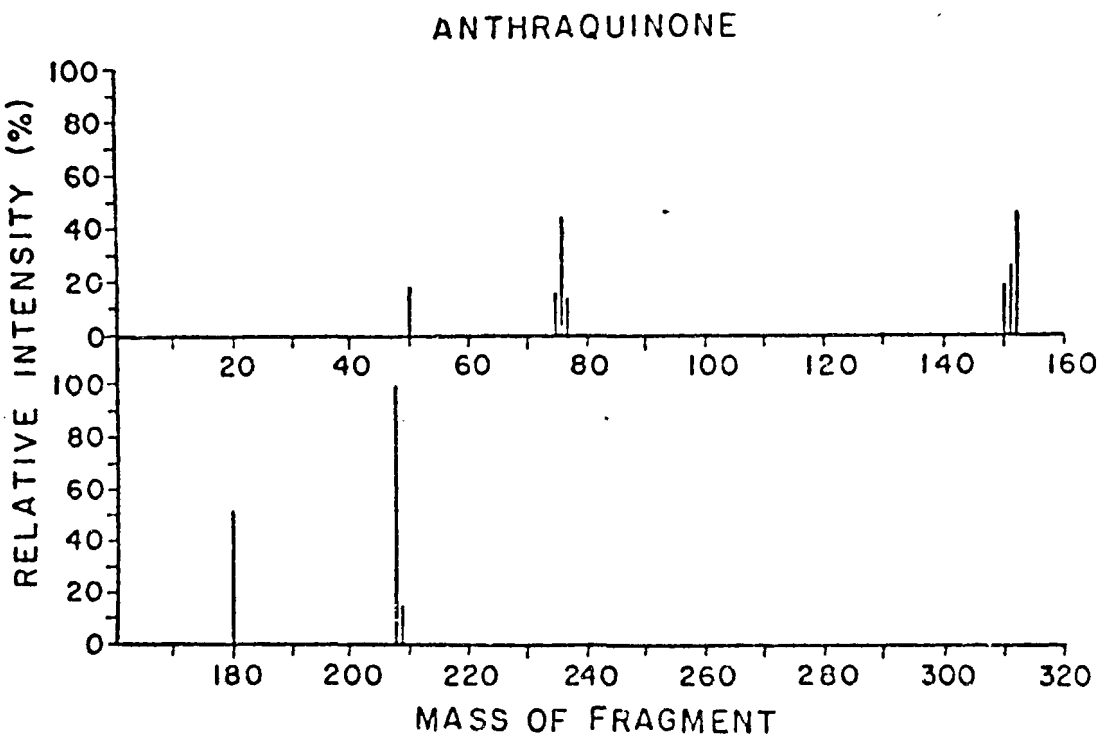

Figure 4.2.3. Relative ion intensities of anthraquinone. OV101 capillary column 2°C min. increase in temperature.

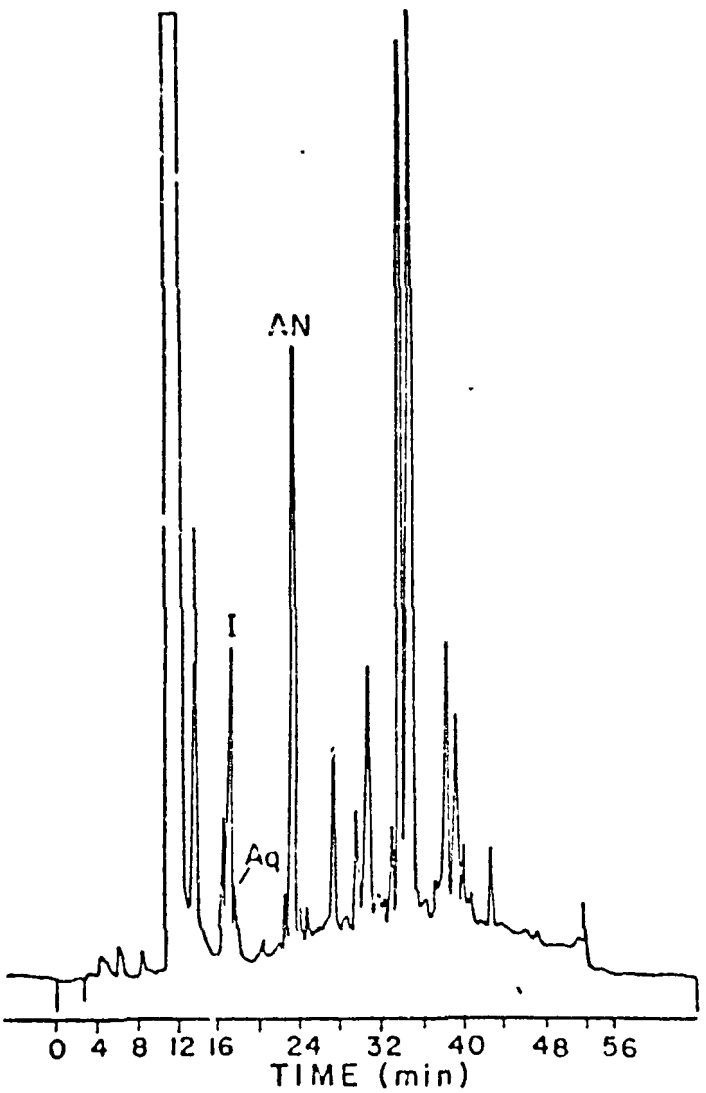

Figure 4.2.4. High pressure liquid chromatograms of anthracene and anthraquinone extracted from sediment with 35/65 ml acetonitrile/benzene. 254 nm UV detection. I = interferring peak, AN = anthracene, Aq = anthraquinone.

check the accuracy of our determinations further we examined the mass spectra of these peaks.

The retention indices and matching coefficients were calculated using equations 4.2.1 and 4.2.2.

$$RI = \frac{SU - SR1}{SR2 - SR1} \times 200 \qquad 4.2.1$$

where: RI = Retention Index

SU = Scan Number of unknown peak
SR1 = Scan Number of first hydrocarbon standard peak (C_{16})
SR2 = Scan Number of second hydrocarbon standard peak (C_{17})

The matching coefficient of our sample peaks and standard peaks were calculated from the mass spectra of anthracene and anthraquinone (Figs. 4.2.5 - 4.2.9) and equation 4.2.2. The matching coefficients for anthracene and anthraquinone were 81.4 and 99.9% respectively.

$$MC = \left[1 - \frac{/\sum_{i=1}^{n}(RIST - RISA)/}{\sum_{i=1}^{n}(RIST + RISA)} \right] \times 100\% \qquad 4.2.2$$

where: MC = Matching Coefficient
$RIST_i$ = Relative intensity of each mass fragment in the standard peak
$RISA_i$ = Relative intensity of each mass fragment in the sample peak
i = ith ion fragment
n = Number of confirming ions

A laboratory study was performed to determine the rate constants for uptake and depuration from a quiescent sediment. Upper Three Runs Creek sediments were placed in crucibles with a volume of 4.8 ml and top surface area of 4.2 cm^2. Crucibles were placed in a flow through exposure system and exposed to 35 $\mu g \cdot \ell^{-1}$ of ^{14}C-anthracene. The flow rate through the system was adjusted so that the concentration of anthracene in the water was not significantly depleted due to uptake by the sediment. The uptake rate constant was calculated by assuming first order kinetics and initial rates conditions.

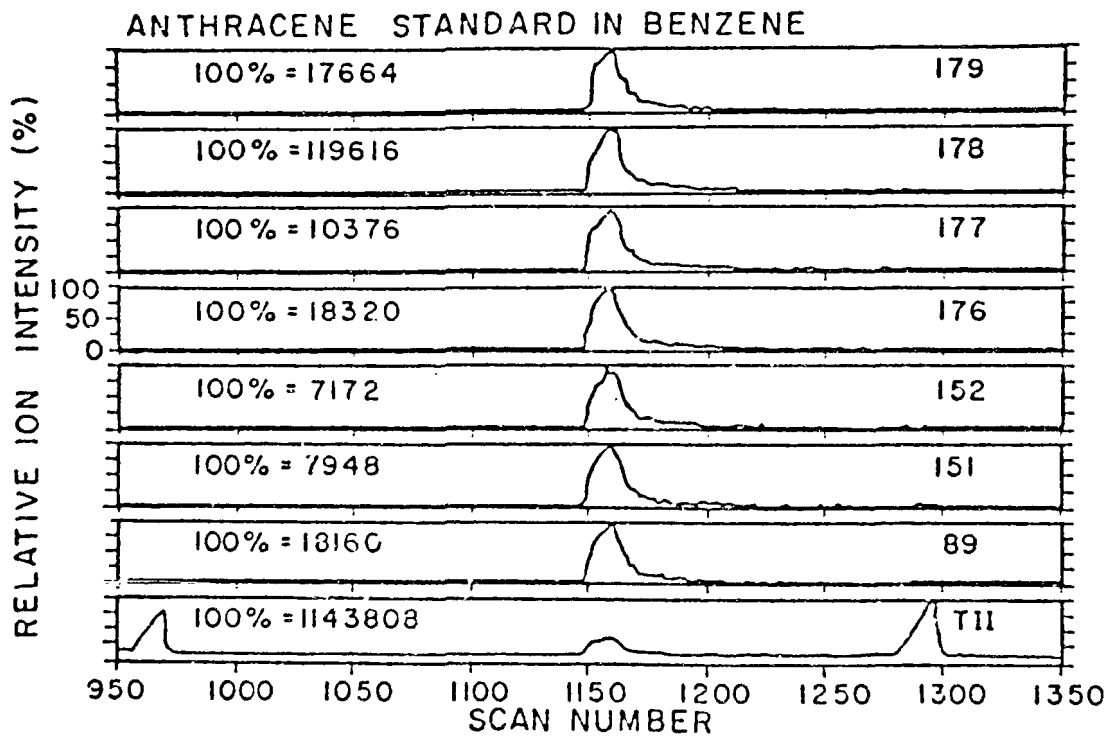

Figure 4.2.5. Relative ion intensities of 7 mass fragments of anthracene in benzene.

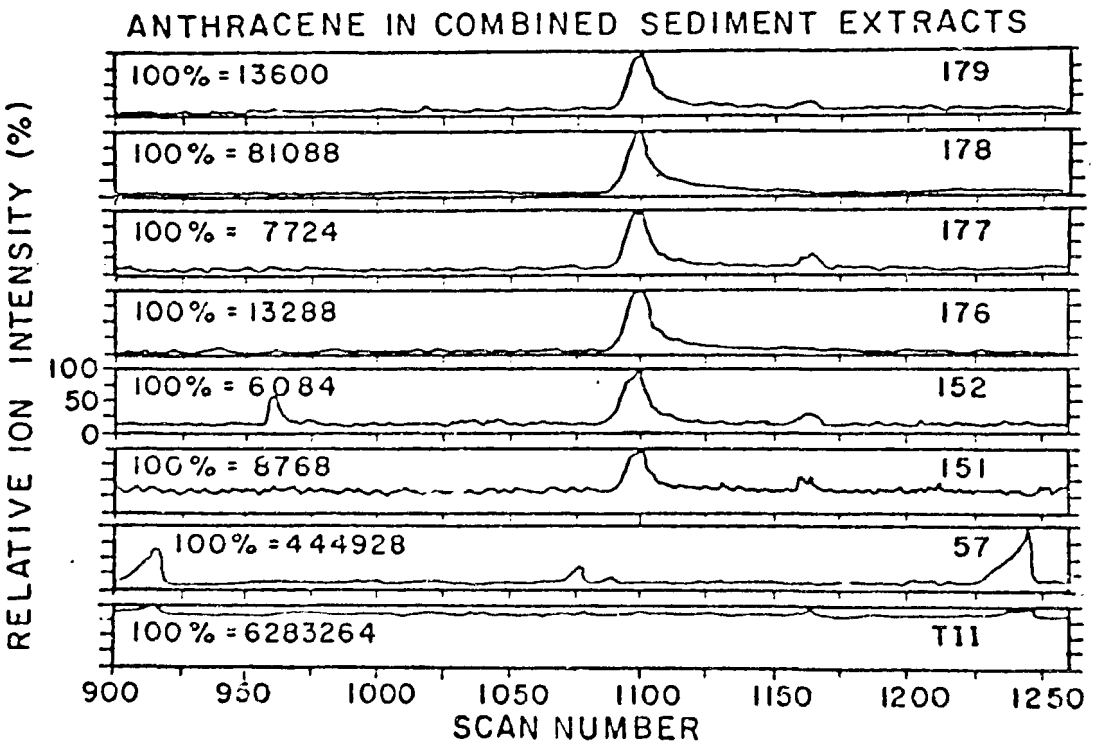

Figure 4.2.6. Relation ion intensity of anthracene in sediment extracts.

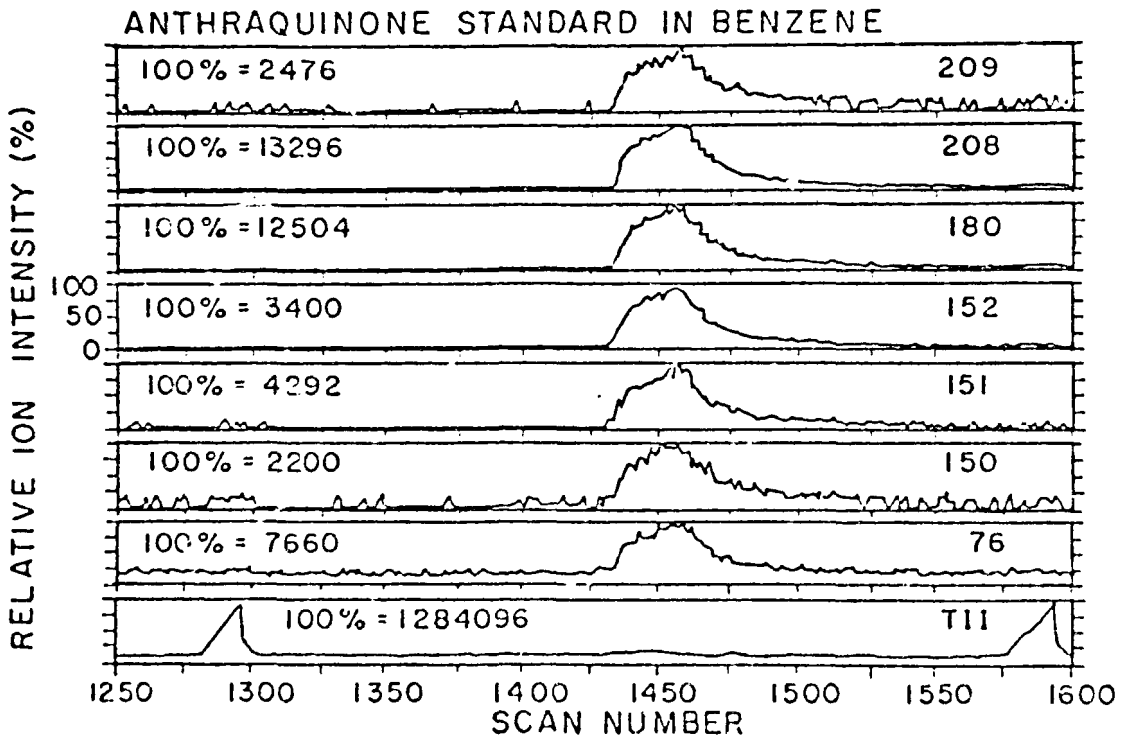

Figure 4.2.7. Relative ion intensities of mass fragments of anthraquinone standard in benzene.

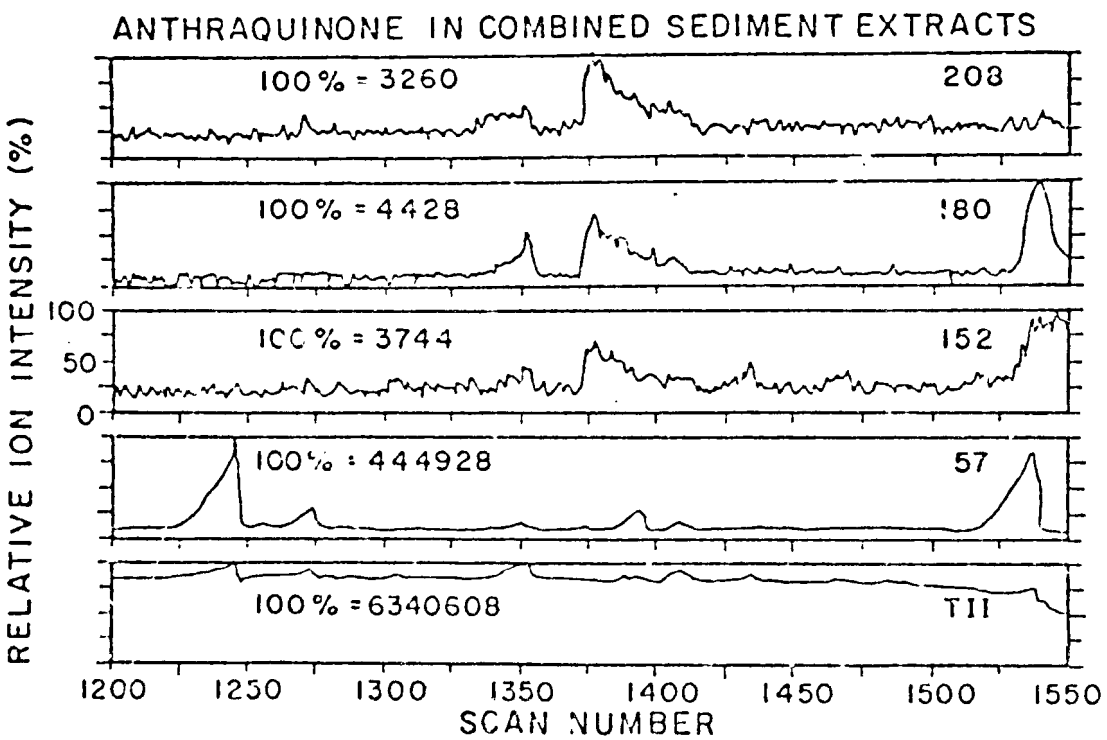

Figure 4.2.8 Relative ion intensities of mass fragments from anthraquinone in sediment extracts.

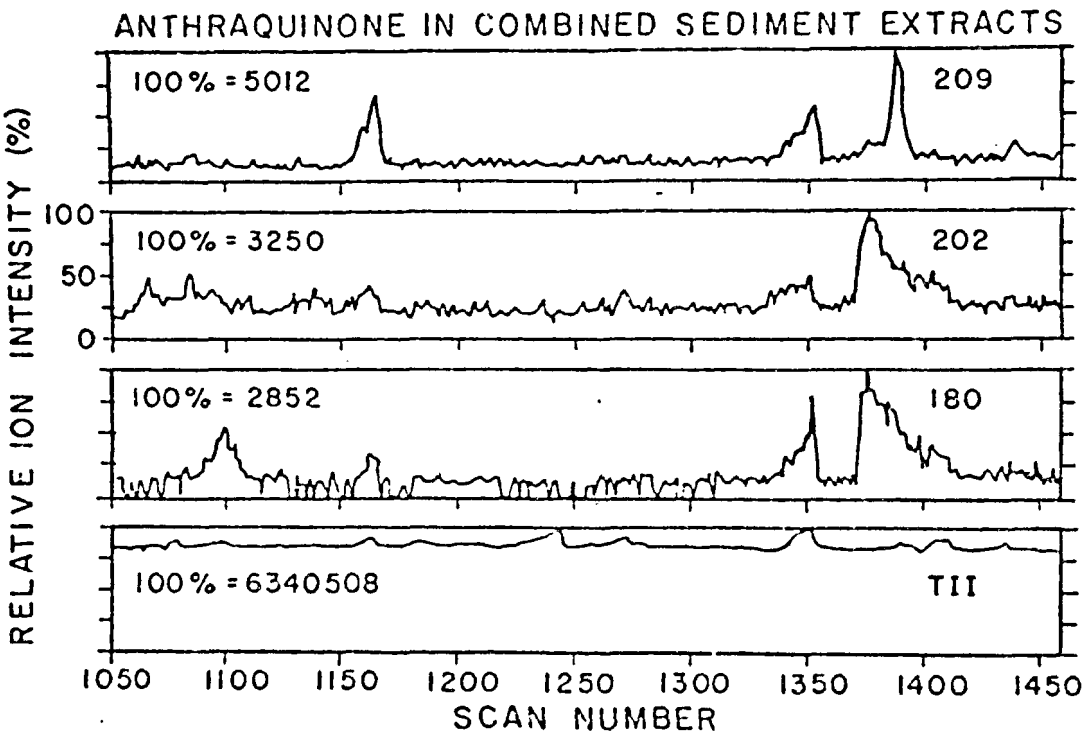

Figure 4.2.9. Relative ion intensities of mass fragments from anthraquinone in sediment extracts.

RESULTS AND DISCUSSION

Solvent Systems

The recovery of ^{14}C-anthracene added to the samples immediately before extraction did not give the same extraction efficiency from samples, which had been spiked as a slurry (Table 4.2.1). Thus, spikes added just prior to sediment extraction are not useful in determining the efficiency of an extraction procedure for extracting anthracene from a particular sediment.

The greatest extraction efficiency of "naturally incorporated" anthracene was by the most polar solvent system, which was methanol, acetone and cyclohexane (Table 4.2.1). However, this solvent mixture extracted much of the polyphenolic humic substances from the sediment which could not be easily separated from anthracene before analysis. The mixture of acetonitrile and cyclohexane yielded anthracene in two solvent phases and was not practical when all of the relative merits of the solvent systems were considered. We adjudged the acetontrile-benzene solvent mixture to be the most practical extraction system. The recovery of anthracene, using the acetonitrile-benzene mixture was only slightly less than that with the more polar mixture but the selectivity for anthracene was greater.

The results of the factorially designed experiment are presented as mean recovery and standard deviations of the factorial main effects (Table 4.2.3) and analysis of variance (Table 4.2.4). All of the main effects were statistically significant. This indicates that all of the factors examined significantly affect the efficiency of extraction of anthracene from sediment. The two-way interaction terms between equilibration time and moisture content and equilibration time and solvent polarity were also significant so that the exact magnitude of the main effects of these treatments can not be interpreted directly. The three-way interaction term was also statistically significant. Thus, any discussion of the two-way interactions must be guarded. The two-way interaction between moisture content and solvent polarity was highly significant for Steel Creek sediment but not statistically significant for the more organic sediment from UTRC (Table 4.2.4).

Similar generalizations could be made for both the sediment types studied. The longer anthracene is equilibrated with sediments, in an aqueous slurry, the lower the recovery (Table 4.2.3). This is probably due to partitioning into clay lattice spaces and sediment organic matter.

Incomplete extraction of PAH from sediments has been a continuing problem and has affected the qualitative as well as quantitative analytical results (Gearing et al., 1978). Lake et al. (1980) reported that because of varying extraction efficiencies close agreement among results from different laboratories should not be expected.

When equilibrated for 24h, recovery was greater from wet-extracted sediment than dry-extracted Steel Creek sediment. The opposite trend was observed for UTRC. After one week of equilibration this effect was not observed.

TABLE 4.2.3. EFFECT OF TIME OF EQUILIBRATION, MOISTURE CONTENT, SEDIMENT TYPE AND SOLVENT POLARITY ON EXTRACTION OF ^{14}C-ANTHRACENE FROM STEEL CREEK AND UTRC SEDIMENT

Treatment[b,c]	Steel Creek $\bar{x}$[a]	Steel Creek SD	Steel Creek CV	UTRC $\bar{x}$[a]	UTRC SD	UTRC CV
24hr, Wet, ϕH	.971	.037	3.83	.796	.040	4.97
24hr, Wet, ϕH/ACN	.879	.024	2.72	.783	.061	7.81
24hr, Dry, ϕH	.454	.047	10.4	.819	.026	3.12
24hr, Dry, ϕH/ACN	.707	.026	3.73	.860	.012	1.34
1wk, Wet, ϕH	.315	.017	5.23	.253	.130	51.5
1wk, Wet, ϕH/ACN	.547	.032	5.77	.470	.035	7.49
1wk, Dry, ϕH	.455	.003	0.58	.719	.038	5.31
1wk, Dry, ϕH/ACN	.533	.010	1.82	.741	.004	0.59
Main Effects						
Spike time-24hr	.75	.21	28.0	.81	.05	6.2
1wk	.45	.10	22.2	.55	.22	40.0
Moisture- Wet	.68	.27	39.7	.58	.25	43.1
Dry	.54	.11	20.4	.78	.06	7.7
Solvent- ϕH	.55	.26	47.3	.65	.25	38.5
System ϕH/ACN	.67	.15	22.4	.71	.16	22.5

[a] Average fraction recovered of initial sediment ^{14}C activity

[b] Refer to Table 4.2.2 for explanation of treatments

[c] ϕH = Benzene, ACN = Acetonitrile

TABLE 4.2.4. ANOVA OF EXPERIMENTAL RESULTS GIVEN IN TABLE 4.2.1

		Steel Creek			UTRC		
Source	DF	SS	MS	F	SS	MS	F
A(Spike Time)	1	.5049	.5049	695.45[a]	.4334	.4334	133.75[a]
B(Moisture)	1	.1192	.1192	164.19[a]	.2623	.2623	81.00[a]
C(Solvent System)	1	.0832	.0832	114.60[a]	.0269	.0269	8.30[a]
A x B	1	.2452	.2452	337.74[a]	.1525	.1525	47.07[a]
A x C	1	.0075	.0075	10.33[a]	.0166	.0166	5.12[b]
B x C	1	.0138	.0138	19.01[a]	.0074	.0074	2.29 NS
AxBxC	1	.0980	.0980	134.99[a]	.0235	.0235	7.25[b]
Error	16	.0110	.0007		.0520	.0032	
Total	23	1.0830			.9746		

[a]Significant at $P \leq 0.01$

[b]Significant at $P \leq 0.05$

NS = Not significant at $P \leq .05$

PAH are generally extracted from wet sediments (Windsor and Hites, 1979) because it has been observed that drying sediments reduces the recovery. This effect may be due to volitalization or to other physical processes which cause the PAH to bind more tightly to sediments upon drying. In this study we observed greater extraction efficiencies from wet Steel Creek sediments and dry UTRC sediments. This may be due, in part, to the different organic contents of the two sediment types. This accounts for the equilibration time-moisture interaction term. After being equilibrated for a longer period of time the extraction efficiency was no longer affected by sediment moisture because of migration of anthracene into organic and donon spaces. The benzene-acetonitrile solvent system was significantly better at recovering anthracene from both sediment types.

From the mass fragment spectrum for anthracene (Fig. 4.2.3) we selected masses 179, 178, 177, 176, 152, 151 and 89 and monitored the relative ion intensity of a standard in benzene (Fig. 4.2.5) and determined that our standard was pure. We then monitored the relative ion intensities of masses 179, 178, 177, 176, 152, 151 and 57 in a sediment extract. The fact that the onset of all of these peaks was in the same scan number indicates that all of the material which eluted in this peak was anthracene. An analysis of our anthraquinone standard in benzene was done for mass fragments 209, 208, 188, 152, 151, 150 and 76 (Fig. 4.2.7). This analysis showed that our anthraquinone standard was also pure. A similar analysis of mass fragments 209, 180, 152 and 57 (Fig. 4.2.8) and mass fragments 209, 208 and 160 (Fig. 4.2.9) in sediment extracts in benzene demonstrated an impurity in the peak in our samples which we had tentatively identified as anthraquinone. The 209 mass fragment peak in scan 1390 is not in the same scan as the 208 and 160 mass fragments, which have peaks in scan 1375 (Fig. 4.2.9). This information indicates that there is a unknown compound which also has 208 and 160 mass fragments, as does anthraquinone, which elutes slightly sooner than those from anthraquinone. This compound does not seem to have a very intense 209 mass fragment. Therefore, we did not report anthraquinone recoveries from our sediment. Maher et al. (1978) also found colored organics were extracted from sediments which interfered with subsequent quantification of PAH compounds. In a study of extracts from marine sediments, Overton et al. (1977) found that capillary column chromatography was able to distinguish between indigenous hydrocarbons of contemporary origin and those known to be associated with fossil hydrocarbon pollution of marine sediments.

First-Order Rate Constants

The first order rate constant for sorption was reported on both a mass and area of sediment basis. Based on mass of sediment the rate constant for uptake was 0.04 min^{-1}, assuming a density of approximately 1 for the silty sediment used in this study. While the sediment density is slightly greater than 1, this will not significantly affect the rate constant. The first order rate constant for sorption, based on surface area of sediment was found to be 0.009 $ml \cdot cm^{-2} \cdot min^{-1}$. These values relate to the rate

of sorption as well as diffusion into the quiescent sediment and are not the rate constants which would be derived for sorption in completely mixed systems.

SECTION 4.3

EFFECT OF HUMIC ACIDS ON BIOAVAILABILITY AND TRANSPORT OF PAH

INTRODUCTION

Evidence suggests that the most important pathway of bioaccumulation of PAH is direct uptake from water by simple partitioning into lipids (Neeley, et al., 1974). It has been demonstrated that humics in freshwater systems may form stable complexes affecting the transport of trace organic compounds including pesticides (Wershaw, et al., 1969) and cholesterol (Hassett and Anderson, 1979). In marine systems, dissolved organic matter (DOM) reportedly increased the solubility of n-alkanes (Boehm and Quinn, 1974) and decreased the uptake of aromatic and other petroleum hydrocarbons by the vivalve Mercenaria mercenaria (Boehm and Quinn, 1976). It is generally believed that DOM in rivers is precipitated on exposure to seawater and deposited in estuarine and nearshore marine sediments (Gardner and Menzel, 1974; Hedges and Parker, 1976). The potential for deposition of trace contaminants in estuarine sediments is largely unknown.

The effects of humics on direct uptake of PAH by Daphnia magna and the potential for salting-out or co-precipitation of PAH-humics at estuarine salinities were determined in laboratory studies. Studies on humics as they affect PAH accumulation in D. magna were conducted to determine 1) if a "standard" humic acid (Aldrich®) at one concentration (2 $mg \cdot \ell^{-1}$ DOC) affected the bioaccumulation of several PAH, 2) if observed effects in some PAH varied predictably with humic concentration, 3) if observed effects changed over a range of PAH concentrations, some of which exceeded limits of water solubility, and 4) if humics in natural waters behaved similarly. In addition, the potential for salting-out of PAH-humics was determined for six PAH at one concentration of Aldrich® humics in 20°/oo artificial seawater.

METHODS AND MATERIALS

Benzo(a) pyrene, napthalene, anthracene, 1, 2, 5, 6 - dibenz anthracene, dimethyl benz(a)anthracene and 3-methylcholanthrene (Table 4.3.1) were studied. Stocks of PAH were diluted in solvents as shipped and added to water in volumes of 1-30 $\mu l \cdot \ell^{-1}$. The ^{3}H - dibenzanthracene specific activity was adjusted to 1027 $mCi \cdot mmol^{-1}$ by addition of unlabeled dibenzanthracene (Aldrich, 97% pure) to water at the time of labeling. Water was labeled in bulk (1-2 ℓ) and thoroughly shaken for one to two min.

Table 4.3.1. Radio-labeled PAH used in bioavailability studies.

Compound	Label	Specific Activity	Solvent	Radiopurity	Source
benzo(a)pyrene	7,10-^{14}C	21.7	toluene	$\geq$ 96	Amersham Batch 29
napthalene	1-^{14}C	8.8	ether	$\geq$ 98	California bionuclear lot 2545
anthracene	9-^{14}C	3.3	acetone	$\geq$ 98	California bionuclear lot 770824
1,2,5,6-dibenzanthracene	^{3}H(G)	30.3x10^{3}	benzene	$\geq$ 97	New England Nuclear lot 1253-021
7,12-dimethyl benzo(a)anthracene	dimethyl ^{14}C	97.4	benzene	$\geq$ 98	New England Nuclear lot 1267-176
3-methylcholanthrene	6-^{14}C	57.0	benzene ethanol 9:1	$\geq$ 98	New England Nuclear lot 1231-171

Test water was prepared by adding inorganic salts to deionized water (Milli-Q®) (Table 4.3.2).

Table 4.3.2. Inorganic salts added to test water and resulting water quality parameters.

Added Salt	$mg \cdot \ell^{-1}$
$NAHCO_3$	48
$CaSO_4 \cdot 2H_2O$	30
$MgSO_4$	30
KCl	2.0

Water Quality Parameters	
pH	7
hardness	20 $mg \cdot \ell^{-1}$ as $CaCO_3$
Alkalinity	120 $mg \cdot \ell^{-1}$ as $CaCO_3$
Conductivity	130 $\mu mhos \cdot cm^{-2}$

A humic stock solution was prepared from Aldrich humic acid (H-1675-2, Lot #082091) as follows: 1) humics dissolved in 0.1 N NaOH; 2) centrifuged at 13,000 x g for 30 min; 3) pH adjusted to 2 with 6.0 N HCl and allowed to stand for 18 h; 4) humic acid precipitate was collected by centrifugation (4000 x g for 20 min). The above steps were repeated three times, the final humic solution adjusted to pH 7, and dialyzed repeatedly against deionized water until conductivity was < 10 µmho. Stock humics were added to labeled test water to a final, nominal concentration of 2.0 $mg \cdot \ell^{-1}$ DOC. Total carbon and inorganic carbon were determined by a Beckman Model 915B Carbon Analyzer and DOC was calculated by differences.

Daphnia magna from laboratory cultures (Athens Environmental Research Laboratory, U.S. EPA, Athens, GA.) were exposed to PAH in paired one liter beakers with and without humics (60-70 Daphnia ℓ^{-1}), for six h. Five samples of ten animals were removed by pipet from each test water, collected on nylon netting, rinsed quickly in 50 ml deionized water, and poured through a Millipore filter apparatus. Animals were collected on tared 25 mm Type HA cellulose acetate filters, dried over desiccant for 24-48 h and sample dry weights determined on a Cahn Model 4700 Electrobalance. Animals

and filters were combusted in a Packard Model 306 sample oxidizer, $^{14}CO_2$ and $^{3}H_2O$ collected in suitable trapping agents, and counted by liquid scintillation counting.

To evaluate the importance of natural particulates and DOC on B(a)P bioavailability, similar experiments were conducted using water from Upper Three Runs Creek (UTRC) and Skinface Pond on the Department of Energy's Savannah River Plant, near Aiken, SC. B(a)P uptake was determined in water directly from the creek, in water filtered through Whatman GFC precombusted (550° C, 8 h) glass fiber filters (0.45 μm) to remove particulates, and in filtered water UV photo-oxidized (LaJolla Scientific Co.) to remove DOC.

Salting-out of PAH - Humic Complexes:

Each of the six PAH was dissolved in 0.5 L of water in paired beakers containing Milli-Q water with humics (8.5 mg·ℓ$^{-1}$ DOC) and without humics (0.2 mg · ℓ$^{-1}$ DOC). Initial PAH concentrations were determined from triplicate assays of activity in 1 ml water samples. A nominal salinity of 20 o/oo was obtained by adding sea salts (Instant Ocean, Aquarium Systems, East Lake, OH.) to each beaker and PAH in solution after 24 h was determined as above.

RESULTS AND DISCUSSION

Bioconcentration in Daphnia magna

Concentrations of five PAH were determined in Daphnia magna after 6 h exposures in water with Aldrich® humics (DOC = 2.0 mg·ℓ$^{-1}$) and in water without humics (DOC ≤ 0.2 mg·ℓ$^{-1}$). Daphnia in humic waters had significantly lower concentrations of benzo(a)pyrene (BaP) (-24.5%) than comparable animals in non-humic waters (Table 4.3.3). On the other hand, humics increased daphnia concentrations of methylcholanthrene (MC) (+210%). Humics had little effect on dimethylbenzanthracene (-13.1%) or dibenzanthracene (+19.1%), and while the effect on anthracene (-46.7%) appeared large, it was not significant due to large sample variance. Results reported assume that all radioactivity was parent compound. These results are significant for two reasons: 1) they demonstrate that humics at low concentrations affect bioaccumulation of some PAH; 2) they demonstrate that humics may either increase or decrease bioaccumulation.

Evidence from this and other studies suggest that results reported for the 6h uptake tests were not transient differences but were representative of steady state differences for all PAH tested. In preliminary 24 h uptake studies, steady state radioactivity in D. magna was reached within 6 h for naphthalene, anthracene and BaP. Approximately 60-80% of steady state was reached after 6 h with DMBA, DBA and MC. In no case did the relative difference between daphnia PAH in humic and non-humic waters change after 6 h. In Daphnia pulex, Southworth, et al., (1978) reported that 6-h exposures produced steady state concentrations of naphthalene and anthracene, while up to 24 h were required for benzanthracene, results consistent with

Table 4.3.3. Effect of Aldrich® humic acids on PAH accumulation by D. magna.

PAH	PAH Concentration ($\mu g \cdot \ell^{-1}$)	Humic Concentration (DOC in $mg \cdot \ell^{-1}$)	Bioaccumulation[a] (6 h)	Bioconcentration[b] Factor
Anthracene	1.96	0.2	82.3 (19.7)	607
mw 178.2		2.0	43.9 (4.0)	319
Benzo(a)pyrene	1.15	0.2	131.6 (7.3)	2745
mw 252.3		2.0	99.4 (7.7)	2158
Dimethylbenz-anthracene	0.33	0.2	64.2 (23.2)	968
mw 256.3		2.0	55.8 (30.0)	666
Methyl cholanthrene	1.29	0.2	34.0 (7.4)	667
mw 268.3		2.0	105.5 (10.8)	2064
Dibenzanthracene	0.73	0.2	20.3 (0.8)	652
mw 278.4		2.0	24.2 (2.4)	773

[a]Bioaccumulation: (nmoles PAH $\cdot g^{-1}$ dry wt. D. magna; Dry wt/Wet wt Ratio = 0.06)

[b]Bioconcentration factor: $\frac{\text{ng PAH} \cdot g^{-1} \text{ wet wt D. magna}}{\text{ng PAH} \cdot ml^{-1}}$

[c] $\bar{X}$ (SE) n = 5.

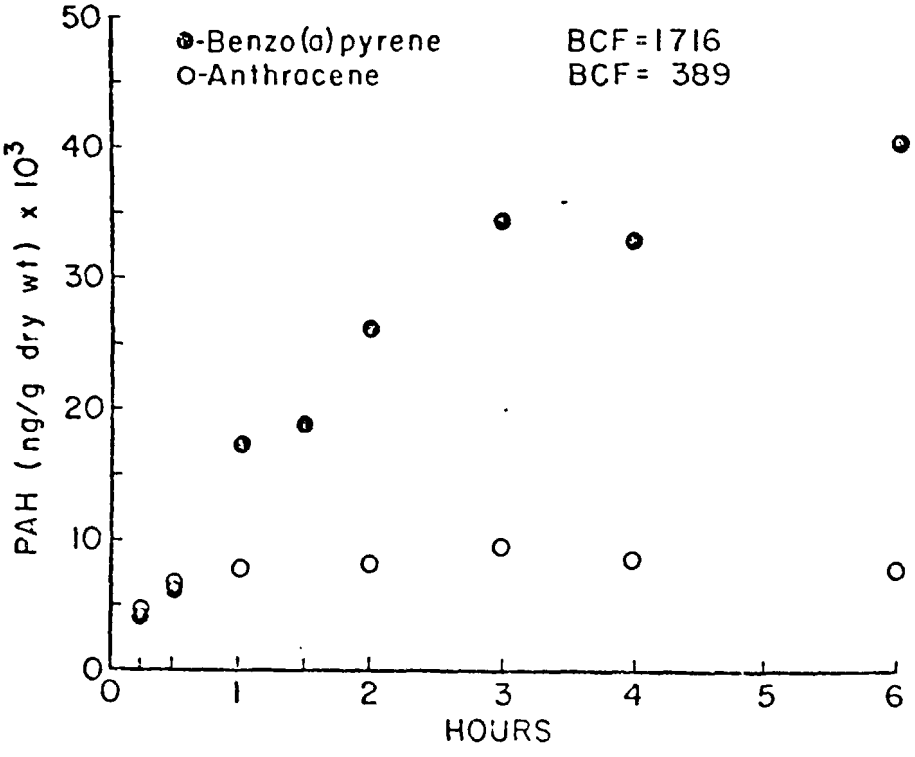

Figure 4.3.1. Accumulation of B(a)P and anthracene by D. magna as a function of time.

our observations. Previous studies have shown that daphnia have relatively slow PAH biotransformation rates relative to accumulation rates (Herbes and Risi, 1978; Leversee, et al., 1981). In this study with ^{14}C-BaP, after 6 h, parent compound represented 91.3 ± 2.1% of test water activity and 92.8 ± 0.8% of D. magna activity respectively. Active biotransformation and excretion of PAH reported for some invertebrates and fish are probably not important factors in D. magna PAH accumulation.

The effect of varying Aldrich® humic acid concentrations (0.3-5.7 mg·ℓ$^{-1}$ DOC) on daphnia accumulation of BaP, anthracene, and naphthalene was determined. Humics significantly reduced the accumulation of BaP and anthracene, but did not affect naphthalene (Table 4.3.4). In this simple unsubstituted PAH series, the effect of humics was greatest for BaP > anthracene > naphthalene, which is consistent with the order of reported octanol-water partition coefficients. This suggests that hydrophobic PAH may be partitioned competitively between daphnia lipids and humics. Although the effect of humics on BaP and anthracene was greatest at highest humic concentrations, there was not a simple linear relation between humic concentration and daphnia PAH concentration. The greatest effect was found between no humic (0.2 mg·ℓ$^{-1}$ DOC) and 1-2 mg·ℓ$^{-1}$ DOC. Additional data at several concentrations of PAH and humics will be necessary before dismissing the possibility that predictive sorption isotherms can be developed for PAH like BaP and anthracene, but these data suggest that such a possibility is unlikely.

Table 4.3.4. Effect of Aldrich® humic acids on PAH accumulation by D. magna.

PAH	Humic Concentration (DOC in mg·ℓ$^{-1}$)	Bioaccumulation (6h)	Bioconcentration[b] Factor
Benzo(a)pyrene[c] mw 252	0.3	139.2 (14.2)	1716
	1.5	90.9 (7.6)	979
	5.7	72.6 (5.7)	838
		$F_{2,12}$=12.19 (P<.005)	
Anthracene mw 178	0.3	37.2 (2.0)	389
	1.5	34.9 (2.0)	362
	5.7	31.0 (1.1)	340
		$F_{2,12}$=3.16 (P<0.1)	
Naphthalene mw 128	0.3	1.7 (0.2)	61
	1.5	1.6 (0.2)	74
	5.7	1.8 (0.1)	57
		$F_{2,6}$=0.95 (NS)	

[a]Bioaccumulation: n moles PAH·g^{-1} dry wt D. magna. $\bar{X}$ (SE), n=5. Naphthalene n=3.

[b]Bioconcentration Factor: $\frac{\text{ng PAH·g}^{-1}\text{ wet wt D. magna}}{\text{ng PAH·ml}^{-1}\text{ water}}$

[c]Initial B(a)P water concentration was 1.5 μg·ℓ$^{-1}$ (6.0 mM); Anthracene was 7.2 mM; Naphthalene was 6.6 mM.

Salting - out

An initial study was conducted with BaP to determine the range of salinities producing a salting-out effect and the time to steady state water concentrations. Initial concentration of Aldrich® humic acid was 8-10 mg·ℓ$^{-1}$ DOC in all studies. At 17-25°/oo salinity, 70% of BaP was lost from the water column after 24 h (Fig. 4.3.2). Below 5°/oo, no salting out was apparent. In beakers where significant salting out occurred, a fine organic floc was evident on bottom and sides of the beaker. PAH mass balance was greater than 95% in all cases, indicating that unaccountable losses were minimal.

Co-precipitation of all six PAH studied was determined at 20°/oo salinity after 24 h. In the presence of humic acids, PAH concentrations at 24 h were reduced significantly (5-79%) below initial values for all PAH

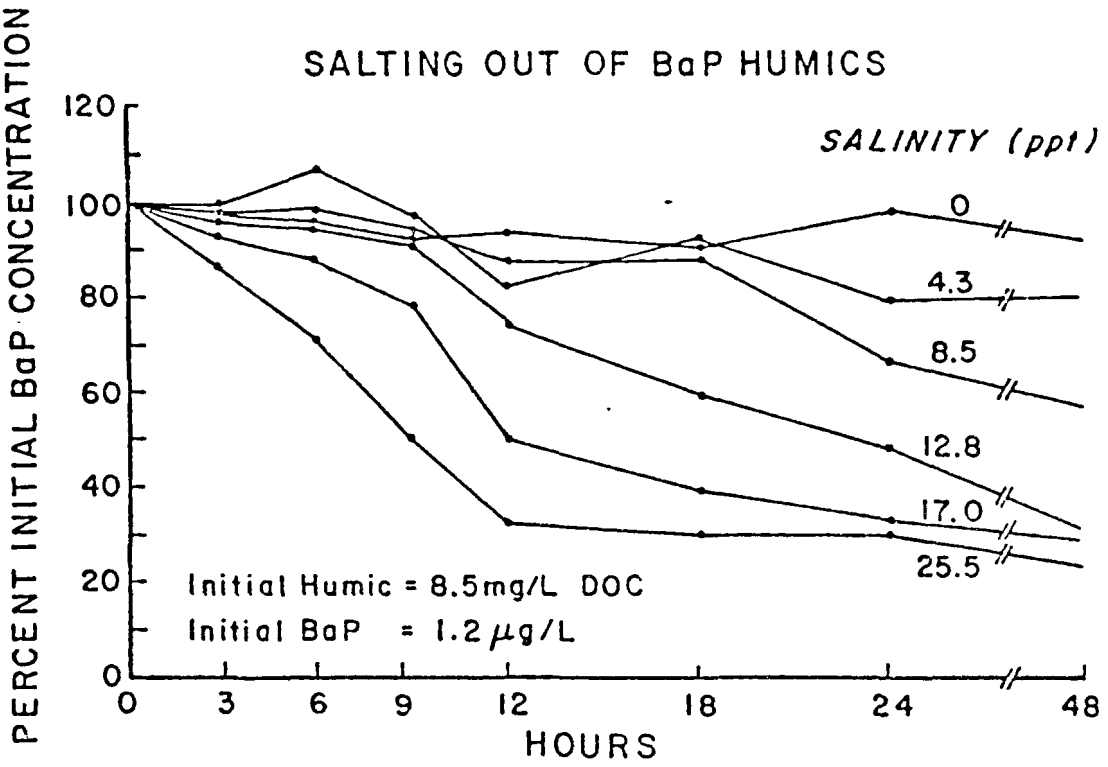

Figure 4.3.2. Salting-out of BaP at six salinities in the presence of Aldrich humics.

(Table 4.3.6). In water without humics, salting out was found only for MC (-12.5%) and DBA (-15.2%). Mass balances were all in excess of 93%, and no losses were observed from control beakers (PAH in Milli-Q® water). DOC at 24 h was not determined.

Table 4.3.5. Effect of Skinface Pond and Upper Three Runs Creek organics and particulates on B(a)P accumulation by Daphnia magna.

Water Source and Treatment	Organic Carbon ($mg \cdot \ell^{-1}$)	Bioaccumulation[a] (6 hour)	Bioconcentration[b] Factor
Upper Three Runs Creek			
Untreated	10.0	227.4 (12.0)[c]	2571
Filtered (0.45μm)	5.5	304.4 (7.1)	3581
Filtered-oxidized	0.2	367.2 (13.9)	4656
Skinface Pond			
Untreated	12.2	70.4 (2.6)[d]	903
Filtered (0.45μm)	--	156.2 (5.6)	2312
Filtered-oxidized	0.2	206.7 (13.1)	3292

[a] Mean (SE), n=5. Values = nmole $\cdot g^{-1}$ dry weight

[b] $\frac{mg\ BaP \cdot g^{-1}\ wet\ weight\ Daphnia}{ng\ BaP \cdot ml^{-1}\ water}$

[c] ANOVA: $F_{2,12} = 37.87$ $p < .001$.

[d] ANOVA: $F_{2,12} = 67.84$ $p < .001$.

Table 4.3.6. Salting - out of PAH in water with and without humics[a].

PAH	Time (H)	PAH ($\mu g \cdot \ell^{-1}$) Without Humics[b]	PAH ($\mu g \cdot \ell^{-1}$) With Humics[c]
Naphthalene	T = 0	2.10 (0.02)[d]	2.21 (0.07)
mw 128.2	T = 24	2.13 (0.16)	1.56 (0.04)
Anthracene	T = 0	2.81 (0.01)	2.81 (0.10)
mw 178.2	T = 24	2.90 (0.05)	2.55 (0.04)
Benzo(a)pyrene	T = 0	1.21 (0.04)	1.26 (0.01)
mw 252.3	T = 24	1.18 (0.05)	0.39 (0.03)
Dimethylbenzanthracene	T = 0	0.91 (0.01)	0.78 (0.05)
mw 256.3	T = 24	0.96 (0.03)	0.39 (0.01)
Methylcholanthrene	T = 0	1.04 (0.04)	1.02 (0.04)
mw 268.3	T = 24	0.91 (0.10)	0.25 (0.00)
Dibenzanthracene	T = 0	0.72 (0.01)	0.72 (0.02)
mw 278.4	T = 24	0.61 (0.01)	0.15 (0.00)

[a]Salinity in all cases 20o/oo, Instant Ocean Salts.

[b]Water without humics: Dissolved Organic Carbon = 0.2 $mg \cdot \ell^{-1}$ at T = 0.

[c]Water with Aldrich® humic acids: DOC = 10.0 $mg \cdot \ell^{-1}$ at T = 0.

[d]All values = $\bar{X}$ (SE), N = 3.

While the importance of PAH sorption to suspended mineral and organic particulates has been recognized (Karickhoff, et al., 1979), the role of dissolved organic matter has received little attention. Hassett and Anderson (1979) reported that DOM in river water reduced the efficiency for solvent extraction of cholesterol. Boehm and Quinn (1976) found that dissolved organic matter (DOM) in sea water increased the solubility of n-alkanes and isoprenoid hydrocarbons, but had no effect on the solubility of the PAH phenanthrene and anthracene. Landrum and Giesy (1981) reported that sorption of B(a)P to XAD-4 resins is reduced by the presence of humics.

The importance of humics on the environmental fate of hydrophobic PAH like B(a)P is clear from this study. Our results show that B(a)P bioaccumulation is significantly reduced by humic concentrations of 2.0 $mg \cdot \ell^{-1}$ DOC. Downstream transport of hydrophobic PAH may be increased by humics

depending on particulate load, character of humics, and partitioning among these compartments. Precipitation of humic PAH complexes by increasing salinity, as reported here for B(a)P, may represent a significant pathway for accumulation of PAH in estuarine sediments. Thus, this work demonstrates that fresh water humics may significantly affect results of studies on PAH bioavailability and environmental transport.

SECTION 4.4

UPTAKE, DEPURATION AND BIOTRANSFORMATION KINETICS OF BENZO(A)PYRENE AND ANTHRACENE BY PERIPHYTON COMMUNITIES

INTRODUCTION

Algae are the foundation of most aquatic food webs, thus, changes in the size, structure or metabolic activity of the algal community may have important effects on the structure and function of the entire aquatic community. While many stream systems are not autotrophic, the periphyton community may be important to critical species or at critical periods during the growing season. Also, the periphyton community can be an important accumulator of organic compounds. Thus, periphyton communities may be an important component of simulation models by removing organics from solution, biotransforming trace organics or acting, directly or indirectly, as a source of these compounds to foraging insects and other components of the food web, directly or indirectly.

The effects of hydrocarbons on algae have been investigated (Soto et al., 1975; Schindler et al., 1975; Soto et al., 1979a and 1979b; and Giddings, 1979) but few studies have been made of the uptake, depuration and biotransformation, which are needed for dynamic simulation models (Payer and Soeder, 1975; Walsh et al., 1977).

Evidence suggests that the most important pathway of bioaccumulation by periphyton is direct uptake from water by simple partitioning of B(a)P into lipids (Neeley, et al., 1974). Elimination from biota includes partitioning of parent compound into clean water and active biotransformation and excretion of metabolites (Neff, 1979). Reported biotransformation potential is great in midge larvae (Leversee, et al., 1981a) and fish (Lee, et al., 1972b; Bend et al., 1979), and is minor in Daphnia (Southworth, et al., 1978). The potential for food chain bioaccumulation is still not resolved. It has been shown that there is significant accumulation of naphthalene by Chlamydomonas angulosa with no apparent biotransformation (Soto, et al., 1975). In marine microcosms, Lee, et al. (1978) reported accumulation, and no apparent biotransformation, of B(a)P and other PAH by phytoplankton. Accumulation of B(a)P from algal food by hardshell clam larvae is reported to equal that of direct uptake from water (Dobroski and Epifanio, 1980). In freshwater lotic systems, periphyton represents an important primary producer for food chains and may serve as the functional organic substrate for PAH accumulation.

A series of studies was conducted, under laboratory conditions, to determine the rates of uptake, depuration and biotransformation of the PAH compounds, benzo(a)pyrene and anthracene by periphyton communities on glass slides. These studies were designed to provide information not only on rate constants and biotransformation but also on community seasonal differences, as well as length of colonization time.

MATERIALS AND METHODS

Periphyton Communities

Natural periphyton communities were collected from two streams on the U. S. Department of Energy's Savannah River Plant near Aiken, South Carolina. Upper Three Runs Creek (UTRC) is a deep, fast-flowing, blackwater stream in which diatoms comprised approximately 90% of the winter periphyton community. Eunotia incisa and Eunotia sudetica were the dominant forms. The water quality of UTRC is given in Giesy and Briese, 1978. Castor Creek, by comparison, is a shallow, partially beaverdam-impounded system in which the periphyton community was more diverse. Species of filamentous and non-filamentous desmids from the genera (Hyalotheca, Desmidium, Spondylosium, Netrium, Euastrum and Pleurotaenium) accounted for approximately 50% of the Castor Creek attached flora. Various diatom species, particularly Anomoeoneis serians var. Apiculata and Frustulia rhomboides, were representative of the remainder of the community.

Exposure

Naturally colonized glass microscope slides (7.62 x 2.54 cm) in plexiglass slide holders were harvested after 3 or 5 weeks colonization from UTRC and after 3 or 6 weeks colonization from Castor Creek, beginning in January of 1980. These slides, with their attached communities, were exposed to 7,10 ^{14}C-Benzo(a)pyrene (B(a)P) (Amersham-Searle, specific activity 21.7 mCi·mmol^{-1}) in a laboratory flow-through system. The anthracene used in these studies was 9, ^{14}C labelled (Cal. Biochem., specific activity 3.3 mCi·mmol^{-1}, Lot #770824). Millipore filtered (0.45 µm) stream water was labelled in bulk with ^{14}C-BaP approximately one hour before exposure was begun. Labelled water was gravity fed from a 40ℓ glass head tank, via stainless steel tubing and micrometer valves, to each of six 250 ml glass staining dishes. Flow rates averaged 100 ml·h^{-1} and were sufficient to maintain a constant B(a)P water concentration of 1.0 µg·ℓ$^{-1}$. They did not simulate stream flow conditions. Six slides, supported in stainless steel wire mesh baskets, were placed in each staining dish. Experiments were performed under gold fluorescent light ($\lambda \geq 500$ nm) to minimize photolysis of B(a)P anthracene. Uptake, biotransformation and autoradiographic studies were conducted simultaneously.

Uptake and Depuration Rate Constants

Slides used in the determination of uptake rates were removed from the flow-through system after 0.25, 1, 2, 4, 8 and 24 h of exposure. One slide from each of three reservoirs was harvested at each of the six sampling times. After removal from the dosing system, each slide was allowed to air dry and the periphyton were then scraped into a tared paper thimble. Samples were dried in a dessicator for 24 h and weighed on a Mettler Model HL52 Balance. They were then combusted in a Packard Model 306 sample oxidizer and $^{14}CO_2$ collected in a scintillation cocktail consisting of 15 ml of Permafluor® and 5 ml of Carbosorb®. ^{14}C activity was subsequently measured in a Beckman Model LS-8100 liquid scintillation counter with quench correction using the sample channels ratio method.

Uptake data were fit to linear least squares regressions on a concentration (ng PAH$\cdot g^{-1}$ dry weight) and a slide surface area (ng PAH$\cdot cm^{-2}$) basis. Data were analyzed using Procedure GLM, Statistical Analysis System (Barr, et al., 1979). First order uptake rate constants were calculated from the flux of the initial uptake rate and depuration rate constants from the slope of the log-linearized depuration regression.

Autoradiography

Dipping emulsion autoradiographic techniques were used to visualize sites of ^{14}C-B(a)P accumulation. Two slides were removed at each sampling time, dipped in 2% Lugol's solution for ca. 30 seconds and then allowed to air dry overnight. Standard autoradiographic techniques using Kodak NTB-2 dipping emulsion were used in processing the samples (Gude, 1968). Slides were stored in light-tight boxes for 5 days, then developed and mounted in Permount. Resultant autoradiographs were examined and photographed on a Zeiss Model IM-35 inverted microscope.

Biotransformation

The biotransformation potential of periphyton communities was determined by analyzing periphyton for ^{14}C as B(a)P and B(a)P-transformation products (non-B(a)P ^{14}C). Periphyton were assayed by a combination of solvent extraction, thin layer chromatography (TLC) and liquid scintillation counting (LSC). More specific methods are given in section 4.3. In order to demonstrate that any observed breakdown of B(a)P was the result of some living cellular process and not of phenomena such as photooxidation, a "dead cell control" was used in the study of biotransformation. Two slides each of living and dead periphyton (fixed for 0.5 h in 4% Lugol's solution and rinsed prior to exposure) were sampled after 0.25, 4 and 24 h exposure. Living periphyton were immediately placed in Lugol's solution (4%) to insure cessation of any ongoing biotransformation of B(a)P. Since subsequent measurements of ^{14}C activity of this Lugol's solution revealed ^{14}C concentrations at or below background, it was felt that no appreciable loss of activity occurred during this step. Following overnight storage (-20°C), periphyton were scraped from slides and sample wet weights were

measured. Samples were stored in glass scintillation vials at -20°C under benzene: ethyl acetate (1:1, V/V). Samples were warmed to room temperature and extracted by grinding in a Ten Broeck glass homogenizer with benzene: ethyl-acetate (1:1, V/V). Homogenates were centrifuged at 1000 rpm for 0.5 h and (IEC model HN-S centrifuge) supernatant volumes adjusted to 10 ml. ^{14}C activity in pellets was determined as a measure of bound compound.

For TLC analysis, the supernatant was sampled (0.5 ml) to determine activity, and the volume was reduced to 100 µl by N_2 evaporation. It was then co-chromatographed with B(a)P standards on Merck Silicanized Silica Gel 60 channel plates. Plates were developed in 9:1 hexane:benzene and visualized using ultraviolet light. Each sample channel was divided into a B(a)P section (the standard B(a)P spot ± 1 cm), R_f > B(a)P (less polar) and R_f < B(a)P (more polar). Each section was scraped from the plate and transferred to a scintillation vial with cocktail (Research Products International 3a70B®) for ^{14}C activity measurement.

In addition to determining levels of these compounds in periphyton, the breakdown of B(a)P dissolved in experimental water was monitored as well. Water samples (3 x 100 ml) were collected at time "0" and subsequently at 0.25, 4 and 24 h and frozen (-20°C). Samples were thawed, acidified to pH 4, and extracted sequentially with benzene (3 x 50 ml) and ethyl acetate (3 x 50 ml). Extracts were combined, dried over anhydrous Na_2SO_4, reduced in volume and run on TLC plates as described above.

RESULTS

Periphyton Communities

The Castor Creek and UTRC periphyton communities differed markedly in both species composition and amount of biomass accumulation after 3 or 6 wk colonization of glass slides. Approximately 50% (relative abundance) of the Castor Creek attached flora consisted of desmids, including such ornate species as Desmidium coarctatum (6%), Hyalotheca sp. (14.5%), Spondylosium pulchrum (16%) and Euastrum pinnatum (4%). Diatoms, particularly Anomoeoneis serians var. apiculata (32%) and Frustulia rhomboides (12%), represented the remainder of the community. Mucilaginous secretions are common in members of the Desmidiaceae, and extensive sheaths surrounded D. coarctatum and S. pulchrum. In comparison, the diator-dominated UTRC community, consisted primarily of Eunotia incisa (40%) and Eunotia sudetica (21%). This diatom community appeared to provide less in the way of both adsorptive surface area and mucilage secretion. Periphyton biomass on Castor Creek slides was greater than UTRC after both 3 wk ($\bar{X}$ = 2.99 vs. 1.72 mg dry weight/slide) and 6 wk of colonization ($\bar{X}$ = 6.88 vs. 5.36 mg dry weight/slide).

Uptake

B(a)P was rapidly accumulated from water by both UTRC and Castor Creek periphyton communities. Uptake of ^{14}C-B(a)P was linear during the first 24 h of accumulation when expressed as a function of concentration (r^2 = .59-.93) and slide surface area (r^2 = .85-.93) (Fig. 4.4.1). Biphasic uptake, consisting of a rapid surface sorption followed by slower accumulation during the first 24 h was suggested by the positive y-intercepts in all cases (Fig. 4.4.1). Approximately 37% of the total B(a)P present in the UTRC samples after 4 h was accumulated within the first 15 minutes of exposure. For Castor Creek periphyton, this value was 26%. The uptake rates determined on a surface area basis from regression plots differed significantly between the two streams after similar colonization periods ($P < .01$), and between colonization periods within streams ($P < .01$). Uptake rates, on a concentration basis, were more variable than those normalized to surface area so significant effects were more difficult to demonstrate. Accumulation by periphyton which had been colonizing for 6 wk in Castor Creek was significantly greater ($P < 0.01$) than by that which had only been colonized for 3 wk. The slides which were colonized in UTRC had the lowest biomass and were the only ones which approached steady state concentrations of B(a)P (Fig. 4.4.1). The comparatively low regression r^2 (0.59) of accumulation of B(a)P by the UTRC periphyton after 3 wk of colonization suggests a departure from linearity. A semi-log plot of the same data only slightly improved the fit (r^2 = 0.66) (Fig. 4.4.1C).

The uptake flux can be determined as the initial slope of the linear regressions. The first-order rate constants can then be calculated with equation 4.4.1.

$$J_i = C_w \cdot K_u \qquad (4.4.1)$$

where

J_i = initial uptake flux
C_w = water concentration
K_u = uptake rate constant

Autoradiography

Autoradiographs suggest surface sorption and sheath complexation as the principal mechanisms of B(a)P accumulation by algae of both communities. Although it is not possible to differentiate conclusively between intra vs. extracellular accumulation without the use of ultra-thin sectioning techniques (R. Knoechel, pers. comm.), label did appear to consistently accumulate on cell surfaces. There is virtually no label associated with the shrunken protoplast of Netrium digitus (Fig. 4.4.2). The extensive mucilaginous sheaths surrounding Desmidium coarctatum and Spondylosium pulchrum readily complexed B(a)P (Fig. 4.4.2). Dense labelling of the diatom Neidium viridis var. amphigomphus was unique (Fig. 4.4.2). Unlabelled controls did not show concentrations of silver grains within or around algae, although a background level was apparent.

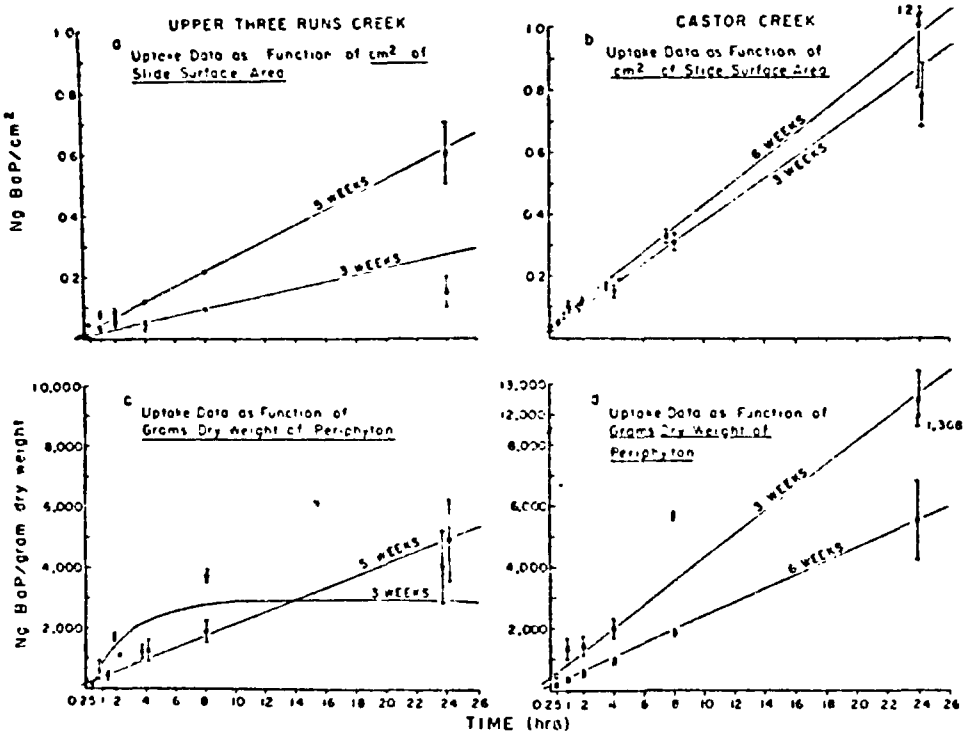

Figure 4.4.1. Accumulation of ^{14}C B(a)P by periphyton communities from UTRC and Castor Creek which had been colonized for 3 or 5 wk. Accumulation is normalized to a surface area (a and b) and dry weight basis (c and d). Each point represents the mean of 3 replications with confidence interval = $\pm$ SD.

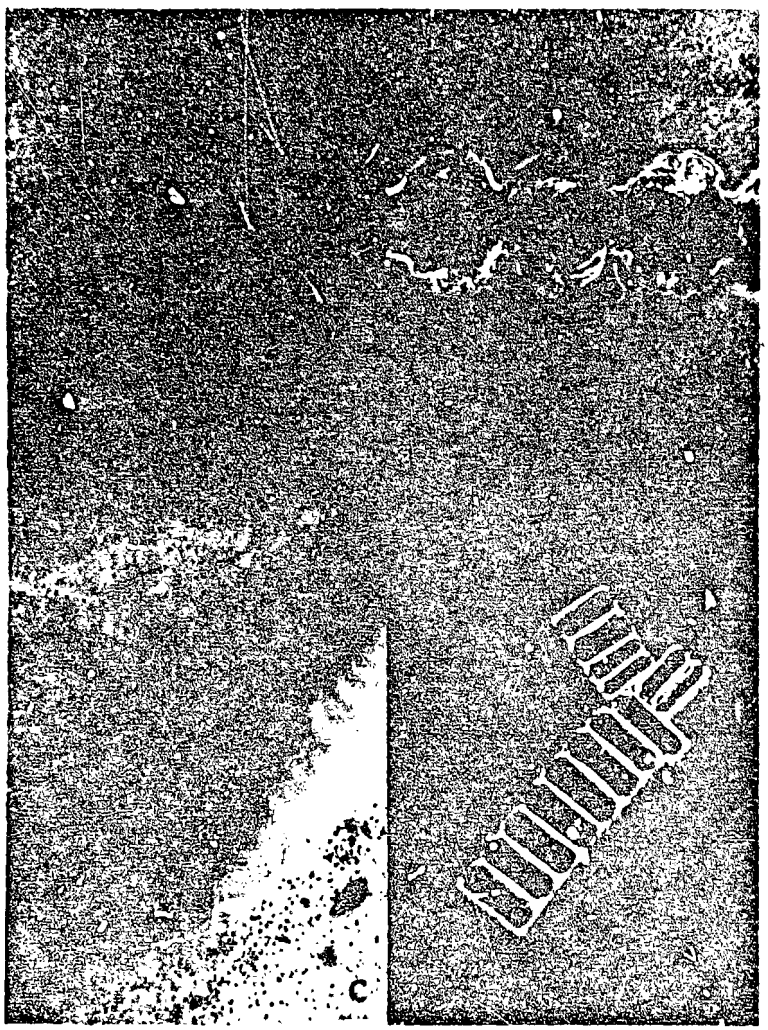

Figure 4.4.2. Autoradiographs illustrating the deposition of ^{14}C B(a)P in A) Desmidium coarctatum, B) Spondylosium pulchrum, C) Netrium digitus, D) Neidium iridis, and E) Eunotia sp. All autoradiographs are 500X magnification.

Biotransformation

Neither UTRC nor Castor Creek periphyton communities exhibited significant biotransformation of ^{14}C-B(a)P within 24 h. In both living periphyton and dead cell controls, approximately 85-90% of total ^{14}C after 24 h was B(a)P (Figs. 4.4.3 and 4.4.4). Histograms representing the percent of ^{14}C activity as B(a)P and B(a)P-transformation products at 0.25, 4, and 24 h exposures reveal no substantial differences between living and dead periphyton communities for either stream or either colonization period (Fig. 4.4.5). Significant apparent transformation of ^{14}C-B(a)P occurred over 24 h in flasks containing experimental water only. Approximately 90% of total ^{14}C was B(a)P after 0.25 h, while only 62% remained as B(a)P after 24 h. In previous studies with fish, exposure water analyzed the same day without freezing never contained more than 12% B(a)P transformation products after 24 h.

Anthracene

A set of studies was conducted to determine the uptake and depuration rate constants for anthracene in periphyton communities colonized in UTRC. The accumulation of anthracene during 24 h was linear, except for an initial rapid accumulation (Fig. 4.4.6). This initially very rapid uptake results in a positive y-intercept for linear regressions. The uptake flux was estimated as the slope of the overall linear regression. The first-order uptake rate constant was 0.04h^{-1}.

After 24 h exposure to anthracene, plates and the associated periphyton were transferred to clean water and desorption followed (Fig. 4.4.7). Desorption was rapid. The rate constant for depuration was 0.17h^{-1} which means that the half time for elimination was 4 h. However, there was a residual of approximately 4 ng anthracene·cm^{-2} which was not eliminated after 30 h of depuration.

DISCUSSION

Results of our study suggest that community species composition can significantly affect uptake rates of PAH by periphyton. This conclusion is consistent with our observations that 1) Castor Creek periphyton had significantly greater B(a)P uptake rates, 2) Castor Creek periphyton, dominated by structurally ornate desmids with extensive gelatinous sheaths, differed markedly from the diatom-dominated UTRC community, and 3) autoradiographs demonstrated the relative importance of B(a)P sorption to cell surfaces, especially to sheath material. The larger biomass on Castor Creek slides did not appear to cause the greater uptake rates observed, since results expressed on an area basis were not significantly different between periphyton from the two streams.

Our results suggest that uptake rates vary as a function of colonization period, or community biomass. One would expect an increase in biomass to yield a concomitant increase in the concentration of PAH per

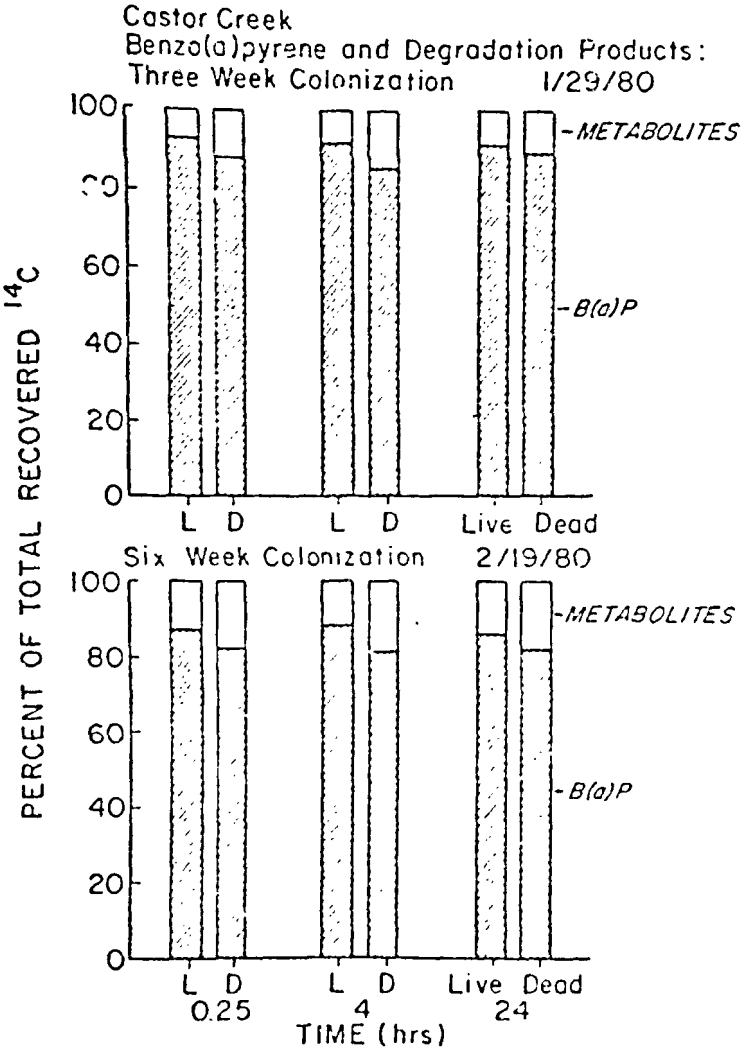

Figure 4.4.3. Percent of recovered ^{14}C as B(a)P, shaded, and non-B(a)P, unshaded, extracted from Castor Creek periphyton. The upper figure represents periphyton from a three week colonization, while the lower figure represents periphyton from a six week colonization period. Samples of both live and dead periphyton were taken after 0.25, 4 and 24 h.

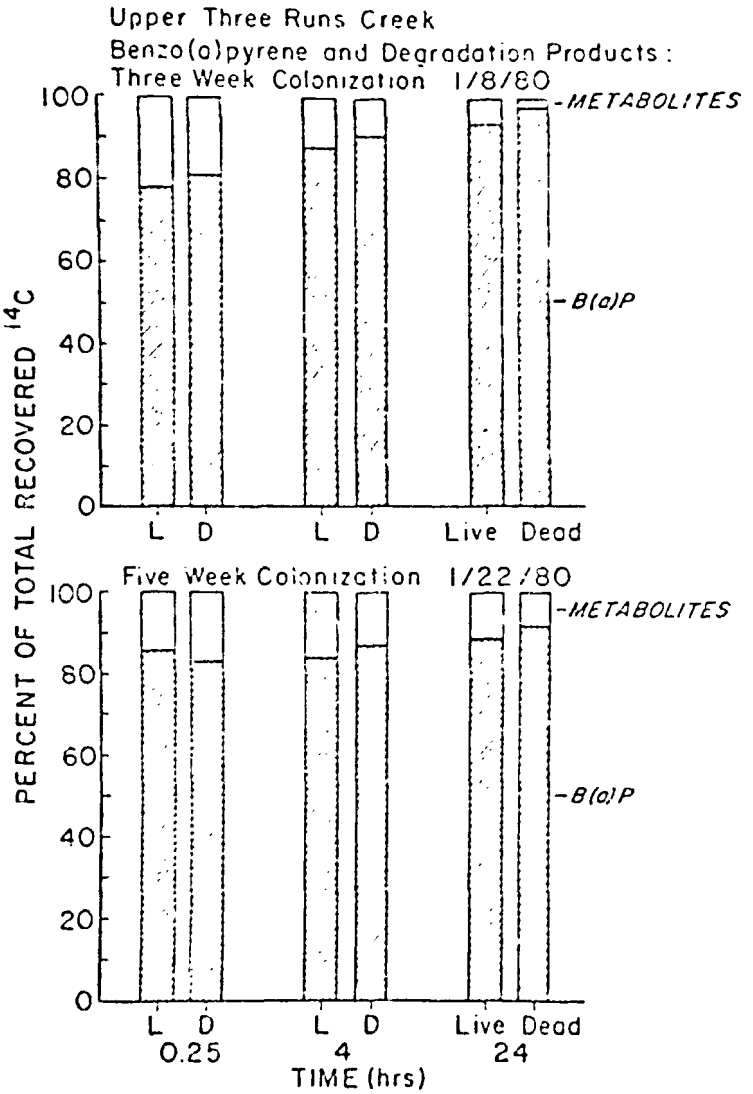

Figure 4.4.4. Percent of recovered ^{14}C as B(a)P, shaded, and non-B(a)P, unshaded, extracted from Upper Three Runs periphyton. The upper figure represents periphyton from a three week colonization while the lower figure represents five weeks of colonization. Samples of both live and dead periphyton were taken after 0.25, 4 and 24 h.

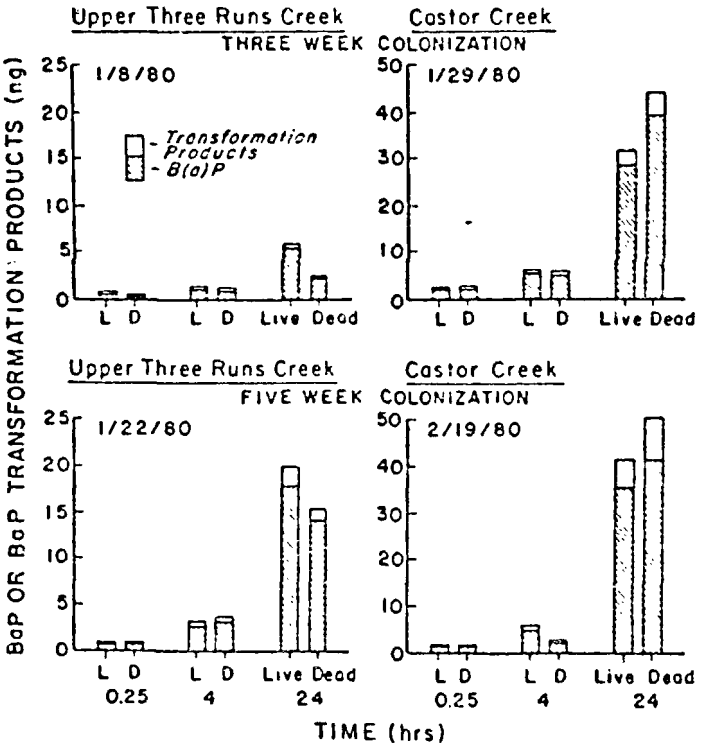

Figure 4.4.5. Histograms of quantities of B(a)P shaded, and non-B(a)P, unshaded, ^{14}C in Upper Three Runs and Castor Creek periphyton. Samples of live and dead periphyton were taken after 0.25, 4 and 24 h.

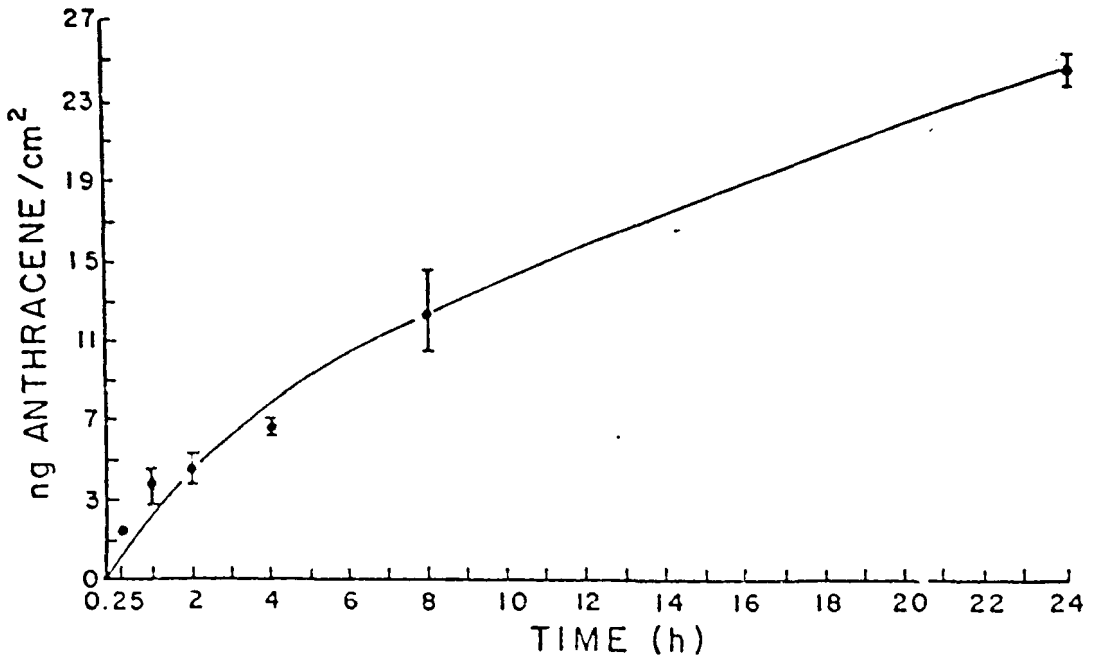

Figure 4.4.6. Accumulation of ^{14}C-anthracene by periphyton which colonized glass slides in UTRC. Mean biomass/slide = 0.4 mg, dry weight·cm^{-2}. Anthracene concentration in water = 22 µg·ℓ$^{-1}$. Concentrations are normalized to an area basis but can be converted to a biomass basis with the conversion factor given. Each point represents the mean of 3 slides. Confidence intervals are ± SD.

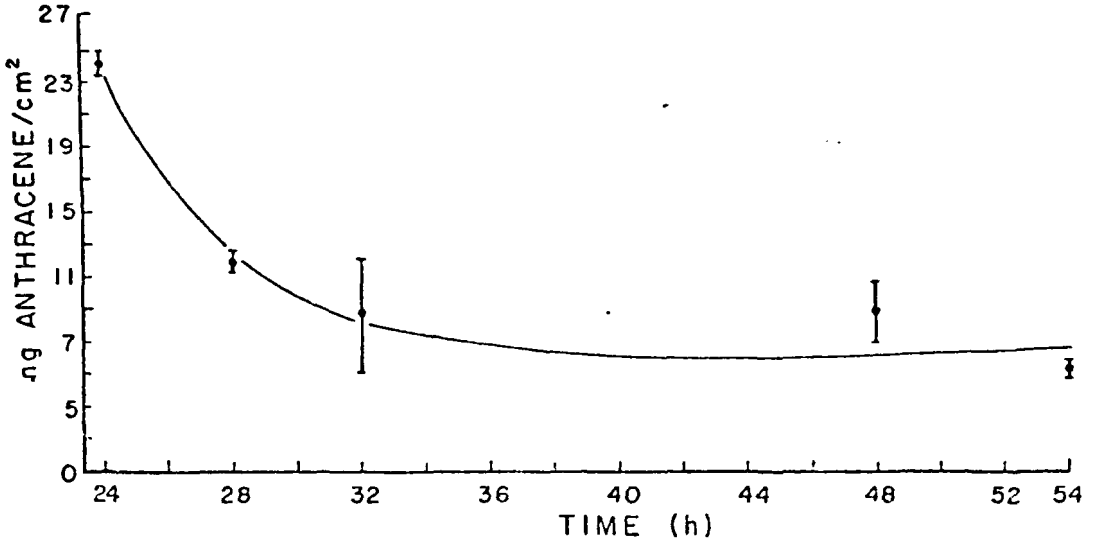

Figure 4.4.7. Desorption of ^{14}C-anthracene from UTRC periphyton which had been exposed to ^{14}C-anthracene for 24 h. Each point represents the mean of three slides. Confidence intervals are ± SD. Mean periphyton biomass = .4 mg, dry weight·cm^{-2}.

unit substrate surface area as more of a given substrate is covered by periphyton growth. The maximal effect of biomass on uptake rate should be realized when the entire substrate becomes covered by a layer of periphyton growth. As the community becomes more layered with time, only the uppermost strata should actually be exposed to levels of PAH within a 24 hour period. Any further increase in biomass should not increase uptake rate, but rather, should increase the length of time necessary for a particular community to achieve steady state, and the absolute capacity of that community for accumulation of compound. Thus, uptake rates, on a concentration basis, would be expected to decrease after a critical minimum thickness, or mass, of periphyton has been reached. Our data show slower uptake rates, on a concentration basis, after longer colonization times. Similar results have been reported for the accumulation of selected radionuclides (Co^{60}, Zn^{65}, Ru^{106}, Cs^{137}) by periphyton (Neal et al., 1967). Uptake was linear over a certain range of biomass, but as mass increased, accumulation was not proportional. Uptake rates are best expressed on a surface area rather than a concentration basis.

The statistically significant differences in B(a)P uptake rates between UTRC and Castor Creek periphyton must be interpreted cautiously since no steady state equilibrium was achieved. The steady state bioconcentration factor (BCF) can be estimated from the ratio of uptake rate coefficient (K_u) to depuration rate coefficient (K_d). Preliminary depuration results (for Castor Creek) were too variable to accurately estimate K_d; however, the relatively slow B(a)P depuration observed (only a 25% reduction in ^{14}C activity after 24 h) indicates that B(a)P will not be quickly released from periphyton once complexed. The range of expected values for K_u, K_d, and BCF for periphyton from other streams, such as northern hardwaters, would be of interest.

The achievement of steady state is most probably linked to the rate at which the compound can diffuse through the multi-layered periphyton community. The plateau observed in the low biomass UTRC three week old community suggests an approach to saturation of this thin periphyton layer. In contrast, the 5 week old UTRC community, and both the 3 and 6 week old Castor Creek communities, are still in a linear phase of uptake after 24 h. These findings are in agreement with those reported for Zn^{65} adsorption by periphyton communities where accumulation was largely a surface phenomenon and ultimate biomass saturation was diffusion-dependent (Rose and Cushing, 1970). Complete saturation of periphyton will be a function of community thickness and exposure time. Exposure times of several weeks may be required to achieve steady state for various PAH in mature periphyton communities.

Biotransformation has been suggested as a significant degradative pathway for PAH in aquatic environments. Pseudomonad bacteria in culture have been found to transform B(a)P and fluoranthene (Barnsley, 1975), as well as anthracene (Evans et al., 1965). Bacteria in petroleum-contaminated stream sediments have been found to transform ^{14}C-labelled naphthalene, anthracene, B(a)P and dibenzanthracene to $^{14}CO_2$, polar transformation products and bound material (Herbes and Schwall, 1978; Herbes et al., 1977). In general, both freshwater (Soto et al., 1975) and marine phyto-

plankton (Lee et al., 1977) have not demonstrated an ability to biotransform PAH, but do accumulate considerable amounts. Our data indicate that the periphyton communities examined did not actively biotransform B(a)P in 24-h exposures. The non-B(a)P ^{14}C material present in periphyton (as much as 20% of total ^{14}C) was attributed to non-specific B(a)P breakdown or binding since no difference between living periphyton and that fixed in Lugol's solution was observed. No separate measure of viability or enzyme activity in fixed controls was made, but apparent active biotransformation of methyl parathion by sediment bacteria autoclaved up to 20 minutes has been observed (David Lewis, pers. comm.). The experiments reported here were conducted under low intensity gold fluorescent light ($\lambda \geq 500$ nm) to reduce photolysis of B(a)P. The importance of photosynthetically coupled B(a)P uptake and transformation in natural exposures remains to be determined.

The deposition of B(a)P in heterotrophically dominated communities may differ from the trend reported above. Biotransformation of B(a)P may be significant in environments such as densely canopied stream areas where P/R ratios are reduced. McIntire (1975) observed the tendency for periphyton developing on rocks in a stream to exhibit characteristic layering with time. He noted an outer, photosynthetically active, layer and in time the development of a heterotrophic layer between this outer layer and the substratum surface. Thus, the biotransformation capabilities of a given community may not be uniform throughout. The concentration of B(a)P transformation products may vary along a vertical transect down through the community. The growth of Chlorella vulgaris #29, a heterotrophic variety, has reportedly been stimulated by exposure to crude oil (Graham and Hutchinson, 1975). Chronic low level exposure to PAH, such as B(a)P, may work to restructure the periphyton community and favor heterotrophic growth.

Where periphyton cover a significant area of stream bottom, this community may equal or exceed the importance of organic sediments in determining the fate of B(a)P and other PAH. The observed property of composition-dependent rates of uptake for periphyton communities may serve to significantly alter the responses of distinct lotic systems to B(a)P perturbations. Rates of accumulation and capacity for accumulation to B(a)P input will vary between streams supporting divergent periphyton flora and within the same stream as seasonal changes in periphyton composition occur. On a smaller scale, variations in response to B(a)P input between reaches of a particular stream, e.g. pool vs. riffle area or canopied vs. open area, will occur due to associated variation in algal species composition. The phenomenon of patchiness in the microdistribution of algal species has been frequently reported (Bruno and Lowe, 1980; Douglas, 1957; Duthie, 1965). This property of periphyton distribution ensures that local variations in B(a)P concentrations will occur.

Periphyton may represent a significant pathway for food chain bioaccumulation. While direct uptake from water is usually considered the most important pathway, trophic transfer of B(a)P from the diatom Thalassiosira pseudonana to larvae of the marine hard clam Mercenaria mercenaria was reportedly equal to that of direct uptake from water (Dobroski and Epi-

fanio, 1980). Grazing benthic invertebrates may accumulate B(a)P in a similar manner.

When uptake and depuration rate constants, which were derived in these laboratory studies, were used in the simulation model, the predicted concentrations of anthracene in periphyton were very similar to those observed in periphyton in the channels microcosm (see section 5.4).

In summary, periphyton represent a significant and previously unexamined sink for B(a)P in stream systems. Clearly, additional work is needed to confirm the observed low biotransformation rates, as well as to determine the physical or physiological basis of community differences in B(a)P uptake rates.

SECTION 4.5

UPTAKE DEPURATION AND BIOTRANSFORMATION OF BENZO(a)PYRENE BY THE MIDGE, CHIRONOMUS RIPARIUS

INTRODUCTION

Larval midges (Chironomidae) are abundant benthic organisms which burrow in sediments and have been shown to accumulate trace contaminants (Kawatski and Bittner, 1975; Derr and Zabik 1972). Chironomids are a major food source for larger macroinvertebrates and smaller fish, and link both aquatic and terrestrial food chains through emergent adults.

This study of B(a)P kinetics in chironomids was conducted to 1) construct descriptive models of B(a)P uptake and elimination kinetics, 2) compare uptake and elimination coefficients determined using one and two compartment models, 3) determine the ability of chironomids to metabolize B(a)P and the effect of biotransformation on bioconcentration factor, 4) determine the contribution of exoskeleton to total bioaccumulation and 5) determine the effect of bottom substrate on depuration rate.

MATERIALS AND METHODS

Uptake and Depuration

Chironomus riparius larvae were collected from a sewage outfall on Badfish Creek near Madison, Wisconsin, and reared in the laboratory at the Savannah River Ecology Laboratory for several generations. Cultures were maintained in gallon glass jars that contained well aerated substrate of previously washed and fermented ground paper towels. Approximately one gram of a mixture of dog biscuits, TetraMin® flake fish food shrimp pellets, and Cerophyll® (powdered nettle leaves) was added to the jars every three days during the three week larval stage. After two days as pupae, adults emerged, mated and oviposited in the jars. Fourth instar larvae had a mean dry weight of 0.39 mg (SD = 0.2, n = 50) and a dry to wet weight ratio of 0.095.

Benzo(a)pyrene (7,10-^{14}C) was used as purchased from Amersham/Searle in two lots, CFA472 Batch 26 (specific activity 60.7 mCi·mmol^{-1}) and Batch 29 (specific activity 21.7 mCi·mmol^{-1}). The specific activities were confirmed with a Varian Model 5000 high pressure liquid chromatography system. Radiochemical purity determined by thin layer chromatography was greater than 99%. All preparative, analytical, and experimental procedures were

performed under gold fluoreascent light ($\lambda \geq 500$ nm) to minimize photodegradation of B(a)P.

Well water (pH 7.1) was aerated and centrifuged to remove particulates (> 0.15 μ). Water was labeled in bulk (7-10 ℓ) and dispensed into replicate test chambers after a 1 to 2 h equilibration. Actual water concentrations were determined from calculations based on dpm·ml^{-1} and known B(a)P specific activity. Concentrations ranged between 0.6 - 1.5 μg B(a)P·ℓ$^{-1}$.

Uptake experiments (in triplicate) were performed in 1) 0.35 ℓ staining dishes which contained 0.2 ℓ of water and 20 chironomids; 2) 6.0 ℓ aquaria which contained 1-2 ℓ of water and 100 - 200 chironomids. Samples of 10 chironomids were taken after 0.25, 0.5, 1.0, 1.5, 2, 4, and 8 h. Each staining dish provided a single sample of 10 chironomids for total ^{14}C and 10 for analysis of biotransformation products. The biomass to volume ratios ranged from 0.020 - 0.039 mg dry wt·ml^{-1} water. The range of biomass to volume ratios in both uptake and depuration experiments was due to differences in water volume. The chironomid larvae were approximately the same size in all experiments.

Depuration experiments were performed by transferring 100-200 chironomids, labeled for eight hours, into 6 ℓ glass aquaria, which contained 1 to 2 ℓ of clean water. Ten chironomids as well as one ml of water were taken from the aquaria after 0.5, 1.0, 1.4, 2.0, 4, 8, 15, 24 and 48 h. Mass to volume ratios ranged from 0.035-0.070 mg dry wt·ml^{-1} water. Addition of paper towel with associated microflora provided a food source, to avoid starvation effects, and a substrate allowing normal behavioral patterns. Substrate was not used in uptake experiments, because sorption and microbial biotransformation would have confounded exposure calculations.

Samples of 10 chironomids were combusted in a Packard Model 306 sample oxidizer and collected in a scintillation cocktail consisting of 17 ml Permafluor® and 5 ml Carbosorb®. Internal and external standards indicated a $^{14}CO_2$ recovery greater than 99% and no carry-over. Water and solvent samples were placed directly into a premixed commercial cocktail (Research Products International 3a70B®). All sample activities were measured with a Beckman Model LS8100 liquid scintillation counter and corrected for quench using internal and external standards and the sample channels ratio method.

Biotransformation

Both animals and water were analyzed for ^{14}C- B(a)P and transformation products. Chironomids were assayed by a combination of solvent extraction, thin layer chromatography (TLC), and liquid scintillation counting (LSC). Thirty chironomids (10 from each replicate) were homogenized in a Ten Broeck tissue homogenizer with five drops of concentrated HCl. The acid homogenate was extracted sequentially by homogenizing with benzene (5 ml nanograde), diethylether (2 x 10 ml, anhydrous), and ethylacetate (5 ml nanograde). The organic solvents were combined, a 2 x 0.5 ml aliquot counted, and the remaining volume determined. The samples were dried with anhydrous sodium sulfate and the volume reduced to approximately 100 μl by

rotary flash evaporation and evaporation under a nitrogen stream. The samples were brought to 500 µl with diethylether and activity determined on a 25 µl aliquot. Recovery of ^{14}C-B(a)P from spiked chironomids was 92.3 ± 3%.

Samples were spotted onto thin layer plates and chromatographed in pentane:diethylether (9:1, V/V) in an unsaturated system. Developed plates were divided into five sections corresponding to B(a)P, hydroxylated metabolites, the origin, and two others. The sections were scraped from the plate and ^{14}C activity measured. Chironomid extracts were also analyzed by high pressure liquid chromatography (see below). All samples were kept frozen (-20°C) prior to analysis.

Water from an eight hour uptake experiment was analyzed for metabolites by 2-dimensional TLC. The pH was adjusted to 4.0 with glacial acetic acid and water was passed through 100 ml of wet XAD-4 resin precleaned by the method of Garnas (1975). No breakthrough of radioactivity was detected by counting aliquots of water which passed through the resin column. The resin column was eluted sequentially with 250 ml each of diethylether and acetone. The solvents were combined and ^{14}C activity of one ml subsamples determined. Solvents were dried by the addition of 50 ml petroleum ether followed by passage over anhydrous sodium sulfate. Volume was reduced as previously described and metabolites were isolated by 2-dimensional TLC with pentane:ether (9:1, V/V) and toluene:methylene chloride:methanol (25:10:1, V/V/V) (Pitts et al., 1978). The spots were identified with UV light and quantified by LSC. Standards of B(a)P metabolites for TLC co-chromatography were obtained from the National Cancer Institute's Standard Chemical Reference Repository.

Water was also analyzed for B(a)P by high pressure liquid chromatography (HPLC). After chironomids were removed, 200 ml water samples were taken from uptake aquaria and uptake controls (no chironomids) and extracted with hexane (3 x 50 ml). The three hexane extracts from each water sample were combined and dried with anhydrous sodium sulfate. Extract volumes were reduced to < 0.25 ml as previously described, diluted to 0.5 ml with methanol and analyzed by a Varian Model 5000 HPLC system with a 254 nm fixed wavelength detector. Recovery of ^{14}C - B(a)P from spiked water was 77.6 ± 6%. Separations were made with a Micro-Pak MCH-10 reverse-phase column (35 cm long) equipped with a Whatman guard column of Co·Pel C_{18} ODS on 35 µm particles using gradient programmed elution conditions at 28°C (Johnson et al., 1977). The gradient was from 75% acetonitrile:25% water to 90% acetonitrile. Acetonitrile (90%) was pumped through the column for five min before recreating the initial conditions.

Chironomid extracts were analyzed by HPLC with a Varian Fluorichrome detector with 7-54 and 7-60 excitation filters (bandpass 250-390 nm, peak 360 nm) and 4-76 and 3-72 emission filters (bandpass 430-650 nm, peak 525 nm). Gradient elution was from 30% acetonitrile to 90% acetonitrile in water at 2%·min^{-1}.

Data Analysis

Distribution of B(a)P and metabolites in a static uptake test is represented schematically in Figure 4.5.1. The data supported the assumptions of 1) constant water B(a)P concentration, 2) low water metabolite concentration ($K_{dm} \simeq 0$). Under these conditions, bioconcentration of total ^{14}C was described by equation 4.5.1.

$$\frac{d\,C_a}{dt} = K_u \cdot C_w - (K_d + K_{dm}) \cdot C_a \qquad (4.5.1)$$

where

C_a = ^{14}C concentration in animal ($ng \cdot g^{-1}$, wet wt)

C_w = ^{14}C concentration in water ($ng \cdot ml^{-1}$)

K_u = B(a)P uptake rate constant (h^{-1})

K_d = B(a)P depuration rate constant (h^{-1})

K_{dm} = Metabolite depuration rate constant (h^{-1})

Low metabolite concentration in water and high metabolite concentration in chironomids suggested that $K_{dm} << K_u$, and a single overall depuration rate constant designated K_d was assumed. Equation 4.5.2 is the integral form of equation 4.5.1 using these assumptions.

$$C_a = (K_u/K_d) \cdot C_w \cdot (1 - e^{-(K_d \cdot t)}) \qquad (4.5.2)$$

This is the familiar first order equilibrium model, and at steady state, the bioconcentration factor (BCF) can be calculated as shown in equation 4.5.3.

$$C_a/C_w = K_u/K_d = BCF \qquad (4.5.3)$$

A simple two compartment model (equation 4.5.4) which did not assume constant water concentration but does assume constant mass within the system was also used to estimate K_u and K_d (Giesy et al., 1980).

$$Q_a = [(K_u \cdot Q_{total}) / (K_u/K_d)]\ (1-e^{-(K_u + K_d)t}) \qquad (4.5.4)$$

where

Q_a = mass of ^{14}C in animals

Q_{total} = total mass of ^{14}C in experimental system

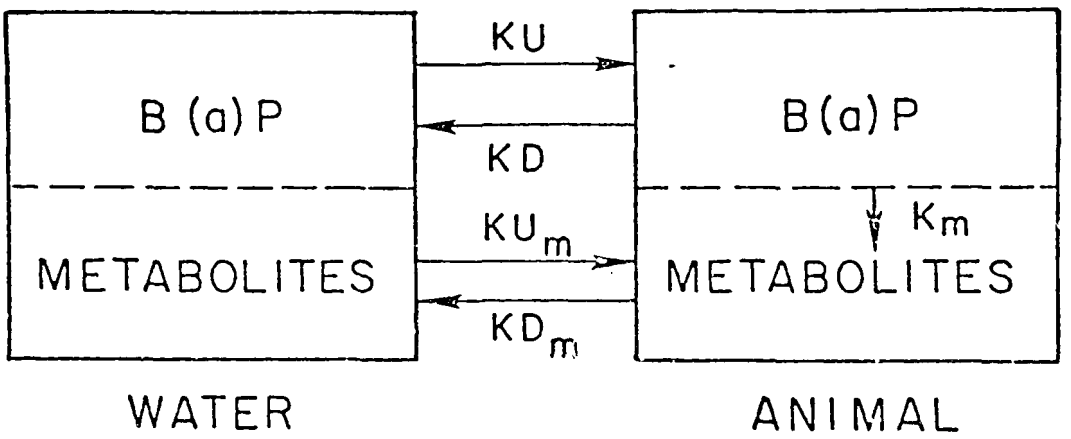

Figure 4.5.1. Distribution of B(a)P and metabolites in static uptake test.

Large concentrations of metabolites in chironomids indicated a large biotransformation rate. There were insufficient data to merit independent estimates of K_{um} using a model analagous to equation 4.5.1 for chironomid metabolite accumulation. The importance of biotransformation was shown instead by comparing calculated BCF (K_u/K_d) with steady state total ^{14}C and B(a)P. Loss of ^{14}C in depuration experiments was biphasic. Rate coefficients were estimated from semi-log plots by linear least-square fits.

Rate constants, steady state concentrations and asymptotic 95% confidence limits were estimated by the Marquardt iterative least squares procedure (Procedure NLIN, Statistical Analysis System, Barr et al., 1979).

RESULTS AND DISCUSSION

Data from triplicate uptake experiments were fit to one compartment and two compartment models (Table 4.5.1). Kinetics of ^{14}C accumulation were accurately described by the one compartment model. Bioaccumulation was rapid and steady state activity was approached after eight hours.

The uptake rate constant (K_u) for the one compartment model was 214 ± 20 h^{-1} when calculated from water and animal concentrations. A one compartment model is only appropriate if water concentration is constant. When calculated from activity measurements, water concentration was 1.38 ± 0.32 ng · ml^{-1} (X± SE, n = 3) initially and did not decrease significantly during the course of the experiment (1.11 ± 0.25 ng·ml^{-1} after 8 h). Analysis by TLC and HPLC indicated no measurable amounts of non-B(a)P materials in the control water (no chironomids) or after two hours in water containing chironomids. After eight hours, water containing chironomids had 86% of ^{14}C as B(a)P and 14% as unidentified metabolites. It was concluded that water activity through eight hours was an acceptable measure of B(a)P concentration.

If water concentration changes significantly, and observed losses are into the animals, a two compartment model is required. Two compartment models have a major advantage in not requiring a constant source term; however, a knowledge of total mass is required. They can be used in experimental systems where mass additions can be controlled but may be of limited use in natural systems with unknown mass additions.

The depuration rate constant (K_d = 0.22 ± 0.04 h^{-1}) was estimated using the one-compartment model from data collected during the exposure phase. The time required for loss of 50% of ^{14}C was between 3-4 h. The two compartment model estimate of the same constant (K_d = 0.15 ± 0.001 h^{-1}) was in good agreement.

Depuration rate constants were also estimated by placing exposed animals in clean water (Figure 4.5.2). A semi-log plot of depuration shows a slope change between four and five hours, which suggests biphasic depuration. Animals in chambers containing substrate depurated about 60% of initial activity within 4 h. The initial depuration rate constant (K_d = 0.22 h^{-1}) agrees well with the overall depuration rate constant calculated

Table 4.5.1. Bioaccumulation parameter estimates for total ^{14}C in Chironomus riparius using one and two - compartment models.

Model and Assumptions	Parameter Estimates		Depuration Half-life (hr)
One Compartment $C_a = (K_u/K_d) \cdot C_w \cdot (1-e^{-(K_d \cdot t)})$ Assumes Constant Infusion B(a)P Concentration Units - ($ng \cdot g^{-1}$ wet weight in animal; $ng \cdot ml^{-1}$ in water)[a]	K_u 214 ± 20	K_d 0.22 ± 0.04	3.1
Two Compartment $Q_a=[(K_u \cdot Q_{total})/(K_u+K_d)](1-e^{-(K_u+K_d)t})$ Assumes constant B(a)P Mass Balance within experimental system	K_u 0.039 ± 0.003[b]	K_d 0.15 ± 0.001	4.8

[a] Assumes density of water is 1 $g \cdot ml^{-1}$

[b] In concentration units 0.039 ± 0.003 h^{-1} = 190 ± 15 h^{-1}, which compares favorably with one compartment model.

All parameter estimates = Mean ± SE, for pooled data from triplicate experiments.

K_u = Uptake rate constant (h^{-1}); K_d = Depuration rate constant (h^{-1}); Q_a = Mass ^{14}C as B(a)P (ng) in experimental system; t = hr.

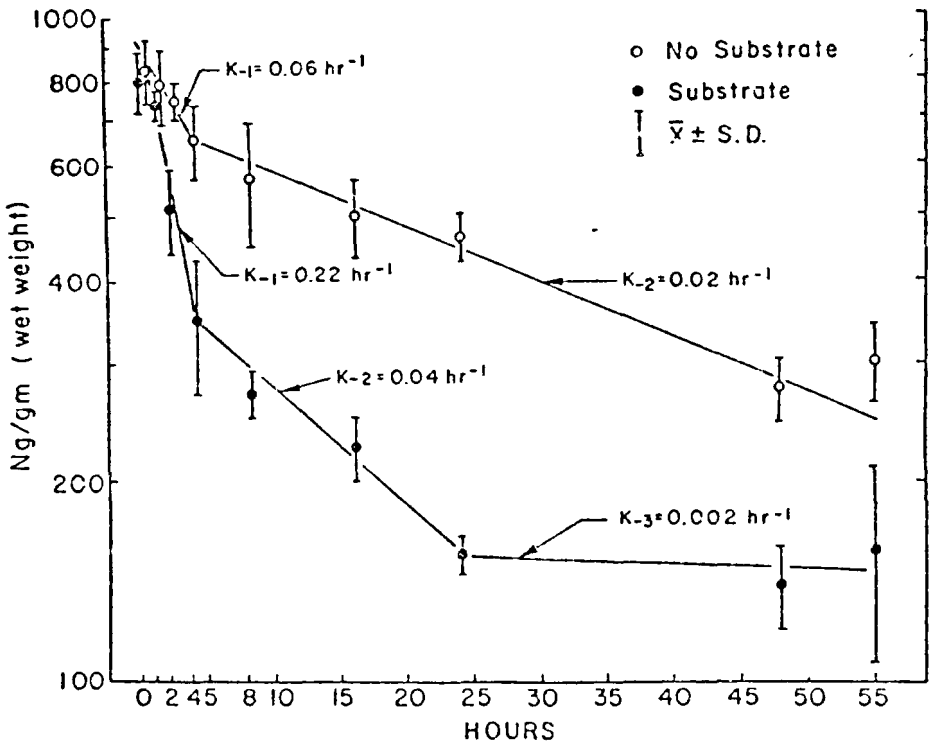

Figure 4.5.2. Depuration of ^{14}C by C. riparius with and without substrate. Concentration is expressed as ng ^{14}C B(a)P · g^{-1} (wet weight) chironomid, assuming all ^{14}C is B(a)P. Each point is the mean of 3 determinations ± SD.

from the accumulation data. The initial depuration includes a component due to K_d from 4-24 h. This component was comparatively small (K_d = 0.04 h^{-1}) and accounted for 22% of initial activity released. Between 24-55 h, 19% of the maximum ^{14}C concentration attained remained as bound B(a)P and metabolites. Animals exposed to clean water in the absence of substrate also exhibited biphasic depuration but the rates were consistently slower. Approximately 23% of the initial activity was rapidly released. The slower depuration was not complete when the experiment was terminated after 55 h. As noted, the initial depuration rate constant was similar to the overall depuration constant derived from a monophasic model and that for B(a)P the monophasic model was adequate to summarize the data. This initial rate constant gives the best overall estimate of net flux of B(a)P and metabolites from chironomids for ecological fate studies.

The mechanism by which substrate increased depuration in chironomids is unknown but may involve increased biotransformation of B(a)P related to gut processes, an active role by bacterial food, behavioral changes by chironomids on the paper towel substrate, or increased gut contents into which the ^{14}C labeled compounds can partition. Simple clearance of gut contents was probably not important in observed initial depuration since animals were starved for eight hr prior to exposure and for eight hr during exposure. More rapid depuration by feeding animals may be due to partitioning of B(a)P from the animal into uncontaminated food. Synthesis and excretion of the peritrophic membrane has been shown to facilitate excretion of DDT by mosquito larvae (Abedi and Brown, 1961) and may be important. Alternatively, Herbes and Risi (1978) reported that feeding decreased the rate of depuration of anthracene from Daphnia pulex. Only 10% of activity in chironomids was associated with exoskeleton (Figure 4.5.3). Therefore, surface losses were probably not important in the initial depuration rates we observed. Exoskeleton may influence initial uptake rates in chironomids since nearly 50% of activity after 0.5 h was in the exoskeleton.

BIOTRANSFORMATION

Information on biotransformation is important in hazard assessment because some metabolites of B(a)P are mutagenic and carcinogenic (Lehr et al. 1978). The biotransformation of B(a)P by C. riparius was rapid. After 1 h 43 ± 2% ($\bar{X}$ ± SE) of chironomid ^{14}C activity existed as non-B(a)P metabolites, as determined by TLC, and after 8 h 72 ± 2% was non-B(a)P (Table 4.5.2 and Figure 4.5.4). The large percentage of metabolites was not due to B(a)P oxidation on TLC plates as evidenced by a 92.3 ± 3% recovery of ^{14}C - B(a)P from spiked chironomid controls. Biotransformation of organic compounds is common and has been reported for chironomids (Kawatski and Bittner 1975, Estenik and Collins 1979). The rate of biotransformation, calculated from metabolite activity and known B(a)P specific activity, was 3.2 ± 0.5 nmol · g dry weight^{-1} · h^{-1} (Table 4.5.2). This rate compares favorably, with that for conversion of aldrin to dieldrin (1.44 nmol · g^{-1} · h^{-1}) reported by Estenik and Collins (1979). The large biotransformation rate at 0.5 h is likely due to sampling time errors, as suggested by the

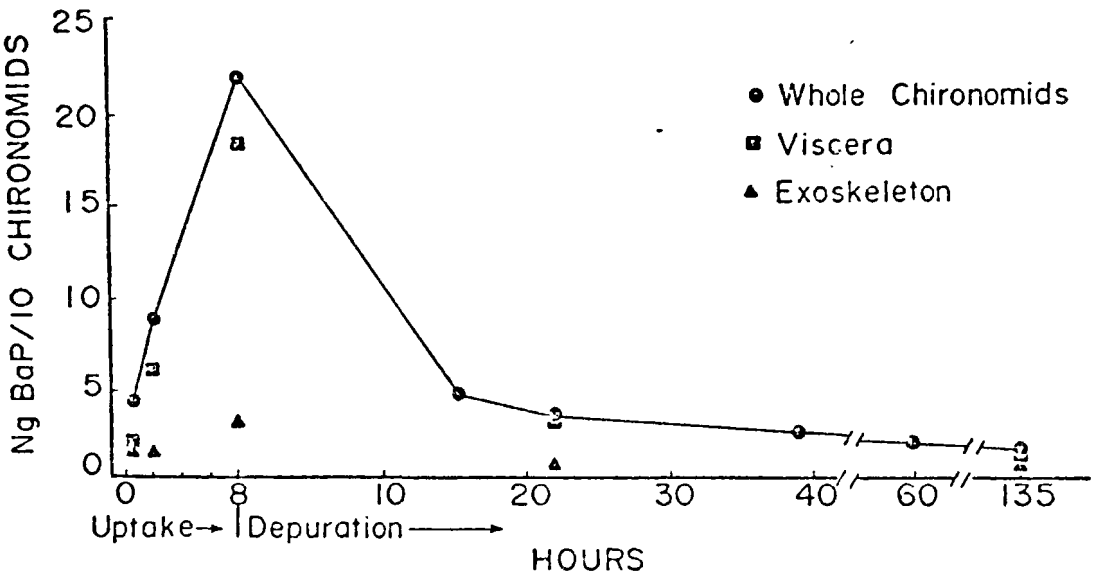

Figure 4.5.3. Uptake and loss of ^{14}C in whole C. riparius, exoskeleton and viscera. Each point represents the mean of 3 determinations ± SD.

Table 4.5.2. biotransformation of ^{14}C - B(a)P by Chironomus riparius.

HOURS	% RECOVERY[a]	^{14}C - B(a)P ($ng \cdot g^{-1}$) TLC	HPLC	% METABOLITES[b]	BIOTRANSFORMATION RATE ($nmol \cdot g^{-1} \cdot h^{-1}$) TLC	HPLC
0.5	142 ± 33 [c]	767 ± 137	N.D.	57 ± 9	7.4 ± 3.0	N.D.
1.0	103 ± 23	1166 ± 199	N.D.	43 ± 2	3.6 ± 0.7	N.D.
2.0	97 ± 13	1349 ± 217	2180 ± 286	57 ± 2	3.6 ± 0.9	1.9 ± 0.7
4.0	80 ± 4	1935 ± 115	2372 ± 115	60 ± 2	2.7 ± 0.3	2.2 ± 0.3
8.0	77 ± 6	2085 ± 291	2760 ± 286	72 ± 2	2.7 ± 0.6	2.4 ± 0.9

[a] DPM of sample extracted/DPM of sample combusted.

[b] $\frac{\text{DPM Total - DPM B(a)P}}{\text{DPM Total}} \times 100.$

[c] Mean ± SE, n = 3.

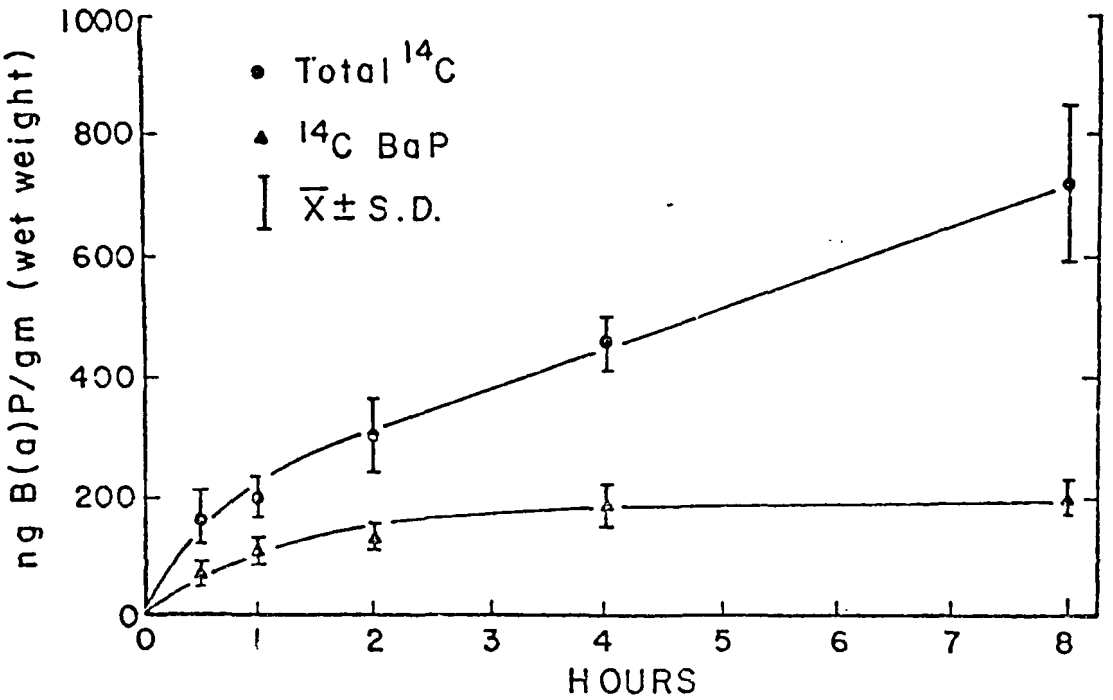

Figure 4.5.4. Accumulation of ^{14}C B(a)P (Δ) as determined by TLC, and B(a)P plus metabolites (o) expressed as ng B(a)P · g^{-1} (wet weight) chironomid. Each point represents the mean of 3 determinations ± SD.

large standard error. While the data are not sufficient for careful statistical analysis, it was concluded that there was no apparent change in biotransformation rate with time.

The rapid biotransformation observed will cause the bioconcentration factor (BCF) reported in terms of parent compound to be very low. Indeed, Lu et al. (1977) reported a BCF of "0" for B(a)P in fish due to complete biotransformation. The high uptake rate constant and BCF reported here in terms of ^{14}C suggest very large accumulation of B(a)P metabolites, some of which may be carcinogenic. Accumulation of metabolities may be the most important aspect of environmental risk assessment for certain PAH. For this reason we have reported both an apparent BCF (total ^{14}C) and a true BCF (parent compound only). The major metabolites depurated into water during the uptake phase were polar compounds. Using co-chromatography of authentic standards, the major metabolite was determined to be 3-hydroxy-B(a)P and represented 4.4% of water activity after 8 hr. This compound has also been reported as the major metabolite in mammals (Nebert and Gelboin 1968). The 3-hydroxy B(a)P was fluorescent blue on the original TLC plate, but became a fluorescent red air oxidation product on co-chromatography plates.

Small amounts of three other metabolites were detected. These had relative abundances of I) 0.35, II) 0.06 and III) 0.015 compared to 3-hydroxy B(a)P. Metabolite I had an Rf value corresponding to 7-hydroxy-B(a)P in the original 2-dimensional TLC plate, but apparently degraded and did not move from the origin after transfer and co-chromatography with standard. Metabolites II and III were tentatively identified as the 9,10- and 7,8-dihydrodiols of B(a)P respectively. In general, the metabolites were quite labile and degraded relatively rapidly, even in the dark at -20°C under organic solvent. Some of the polar compounds observed may have resulted from degradation during storage of both water and chironomid extracts. Rapid analysis after sampling is recommended.

It was assumed that all ^{14}C was B(a)P and an apparent BCF (ng B(a)P $\cdot$ g^{-1} wet weight/ng B(a)P $\cdot$ ml^{-1}) of 650 was calculated from chironomid steady state activity at eight h. An estimate of 970 was obtained using the ratio K_u/K_d. The presence of substantial quantities of non-B(a)P materials in chironomids (Figure 4.5.4, Table 4.5.2) indicated that biotransformation was significant, and the actual BCF was about 200. B(a)P was at apparent steady state after 4 - 8 h (Figure 4.5.4). Lu et al. (1977) reported a similarily low BCF of 107-149 for B(a)P in mosquito larvae, with only 46% of the activity present as parent compound. Southworth et al. (1978) predicted a BCF of 13,000 for B(a)P in D. magna calculated from the octanol-water partition coefficient, but assumed no biotransformation. The difference in BCF between Daphnia and both chironomids and mosquito larvae was probably related to active biotransformation and excretion processes in the latter.

These studies demonstrate that donor controlled linear compartment models may be used to predict steady state bioaccumulation of B(a)P and metabolites (total ^{14}C) in Chironomus riparius. However, the BCF for parent compound is reduced by a factor of three relative to that of ^{14}C by

active biotransformation of B(a)P in this species. The frequently used correlations between octanol-water partition coefficient and bioaccumulation may not be adequate for predictions of B(a)P fate in many species.

SECTION 4.6

EFFECTS OF TEMPERATURE AND ANTHRACENE CONCENTRATION ON UPTAKE, DEPURATION AND BIOTRANSFORMATION OF ANTHRACENE BY *CHIRONOMUS RIPARIUS*

INTRODUCTION

Midges, important inhabitants of a variety of aquatic habitats (Oliver, 1971), often represent the largest number of tax and individuals in benthic communities (Jonasson, 1978). *Chironomus riparius* is often abundant (10^4 individuals·m^{-2}) in polluted streams (Gower and Buckland, 1978). *C. riparius* is able to metabolize aldrin (Escenik and Collins, 1979) and the PAH benzo(a)pyrene (Leversee *et al.*, 1981a). Thus, midges living in periphyton and sediment may be important in the biotransformation of PAH and other lipophilic compounds which concentrate in those substrates. Midges may also be an important vector of mobilization of PAH from sediments to high trophic levels. Emergence of winged adults from environments polluted with PAH may increase the export from aquatic to terrestrial environments.

Anthracene was chosen for study as a representative of the homologous series of PAH because of its relatively low volatility (Southworth, 1979), intermediate water solubility (Leo, 1975), and presence in contaminated aquatic systems (Sheldon and Hites, 1978).

Regulatory agencies are faced with predicting the fates of large numbers of compounds. Mathematical simulation models may be useful for this purpose. However, few rate constants for uptake, depuration or biotransformation are available for use in mechanistic, predictive, simulation models. Also, the effect of external forcing functions on conditional rate constants is unknown. If conditional rate constants for uptake, depuration and biotransformation are not independent of the forcing function, a statistical relationship may be needed for prediction of these constants.

Two important forcing functions that affect the dynamics of compounds within aquatic systems and organisms are temperature and concentration of chemical. One aspect of our study was to determine the relationship between PAH concentration and the uptake and depuration rate constants and bioconcentration factor (BCF) in midge larvae. The relationship between concentration of PAH in water and in aquatic animals has been studied in *Daphnia* (Southworth *et al.*, 1978) and *Callinectes sapidus* (Lee *et al.*, 1976).

A second aspect of this study was to determine the effects of temperature on uptake, depuration, biotransformation, and BCF. Other authors have observed a negative correlation between temperature and uptake or retention of trace organic compounds in coho salmon, copepods (Collier et al., 1978) and clams (Fucik and Neff, 1977; Harris et al., 1977). However, Fossato and Canzonier (1976) reported that BCF was not a direct function of temperature in mussels. Also, a temperature optimum has been found for the mixed function oxidase system which is responsible for the biotransformation of anthracene and other xenobiotics in aquatic organisms (Lee et al., 1979; Estenik and Collins, 1979).

MATERIALS AND METHODS

Midges

Chironomus riparius larvae were collected from a sewage outfall on Badfish Creek near Madison, Wisconsin. Cultures were maintained using a method similar to that described by Leversee et al. (1981a) at the Savannah River Ecology Laboratory for over 20 generations at 25°C. Animals used for experiments at different temperatures were acclimated for 2 to 3 days prior to exposure to anthracene. Overall mean weight of 5 dry midges was 3.0 ± 0.1 mg (x ± 95% CI, n = 334) and ranged from 2.2 ± 0.2 mg (n=30) to 3.9 ± 0.2 (n=30). The mean wet to dry weight ratio was 8:1.

Water and Anthracene

Well water (pH 7.1) was aerated for several days and filtered through 0.45 µm Milipore® filters to remove particulates. Anthracene ($3.3 mCi \cdot nmol^{-1}$, 9-^{14}C) was obtained from California Bionuclear Corp. (Lot #770824) and used without further purification. Radiochemical purity was determined by thin layer chromatography to be greater than 98%. All preparative analytical and experimental procedures were performed under gold fluorescent light ($\lambda \geq 500nm$) to minimize phototransformation of anthracene.

Dosing and Sampling

Accumulation flux and uptake and depuration rate constants were measured at four concentrations (1.7, 8.7, 22.3 and 30.5 $\mu g \cdot \ell^{-1}$) at 25°C, and three temperatures (16, 25, and 30°C) at 22 $\mu g \cdot \ell^{-1}$. Uptake experiments were conducted in flow-through systems with a flushing rate of 1-2 volumes per hour to maintain a constant anthracene concentration and minimize the accumulation of both ^{14}C labeled biotransformation products and metabolites. Anthracene concentrations were monitored throughout the study. Three or four replicate samples of 5 midges were taken after approximately 0.5, 1, 2, 4, 8, 12, 20, and 30 h (Figure 4.6.1). While sampling intervals varied slightly among experiments, actual length of exposure was used for computations. For depuration of anthracene and biotransformation products, midges exposed to anthracene for 9 h were transferred to uncontaminated

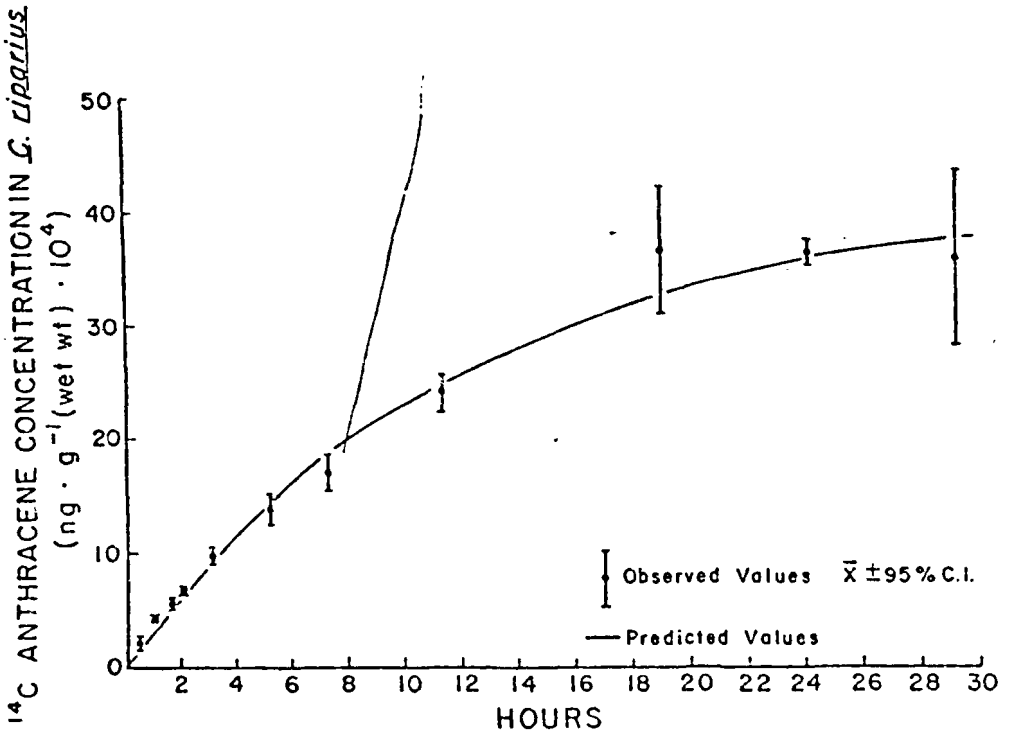

Figure 4.6.1. Accumulation of ^{14}C anthracene by C. riparius at 25°C and 22 $\mu g \cdot \ell^{-1}$. Each point represents the mean ± 2 SE of 3 replicates. The line represents the least squares fit of equation 2.

aerated water containing paper towel substrate. Three replicate samples of 5 midges and a sample of water taken after 1, 2, 4, 8, 16, 24, and 30 h. Water was changed if activity was twice background.

Biotransformation rates of anthracene were measured at three temperatures (16, 25, and 30°C) at 22 $\mu g \cdot \ell^{-1}$. Four replicate samples of 30 midges were taken after 0.5, 1, 2, and 4 h. At 30°C, samples were also taken after 9 and 18 h.

Extraction and Analysis

Water samples were placed directly into the counting cocktail (3a70B®, Research Products International) for ^{14}C activity determination. Midges were dessicated overnight at room temperature in glass dessication chambers and weighed on a model 4700 Cahn Electrobalance. Total ^{14}C in midges was collected in a 4 ml Carbosorb® and 15 ml RPI 3a70B® scintillation cocktail by combustion by a model 306 Packard sample oxidizer. Internal and external standards indicated ^{14}C recovery greater than 99% and no carryover of ^{14}C.

Biotransformation products of anthracene were measured in undessicated midges which had been blotted dry. Samples were stored in a solution of ethylacetate:acetone (4:1, V/V) at -40°C until they were extracted. Samples were homogenized in a Ten Broeck homogenizer and extracted twice with 5 ml of ethylacetate:acetone (4:1, V/V) and once with 5 ml of cyclohexane. The extracts were combined and filtered through Whatman #40 paper. The extract was evaporated to 0.5 ml under a stream of nitrogen. Activity was determined from a 50-µl aliquant. The filter paper was burned, counted, and reported as unextractable metabolite. Mean (± 95% CI) recovery of spiked samples was 88 ± 11% (n=5).

Aliquants of 200 ul were spotted and chromatographed on precoated silica gel thin layer chromatography plates (E. Merck) in hexane:benzene (9:1, V/V) and pentane:ether (9:1, V/V). Developed plates were sectioned into 4 to 5 parts corresponding to the origin, anthracene, and 2 and 3 other spots visualized by UV light. Spots were scraped into RPI 3a70B for ^{14}C activity determination. The origin, non-anthracene spots and filter paper are reported as total metabolite (see Figure 4.6.6). Biotransformation rates were determined by dividing total metabolite by duration of exposure (see Figure 4.6.5).

^{14}C activity of all samples was determined using a Beckman model 8100 liquid scintillation counter. The samples were corrected for background, quench and counting efficiency. The quench and counting efficiency were corrected using a quench curve and the samples channels ratio method. Counting efficiency for water and combusted insects were 85% and 87% respectively.

Data Analysis

Rate constants, BCF and asymptotic 95% confidence limits were estimated by Marquardt iterative least squares proceedures (proceedure NLIN, Statistical Analysis System, Barr et al., 1979), with a one compartment donor dependent model (equations 4.6.1 and 4.6.2) (Giesy et al., 1980; Hamelink 1977).

$$\frac{dC_a}{dt} = (K_u \cdot C_w) - (K_d \cdot C_a) \qquad (4.6.1)$$

where:

C_a = concentration of ^{14}C in midge (anthracene equivalents)

C_w = concentration of ^{14}C in water (anthracene equivalents)

K_u = uptake rate constant

K_d = depuration rate constant

t = exposure time (h).

Since CW was constant and assuming 1 ml water = 1 g, the integrated analytical solution of equation 4.6.1 is given by equation 4.6.2.

$$C_a = \frac{K_u}{K_d} C_w (1-e^{-(K_d \cdot t)}) \qquad (4.6.2)$$

At steady rate state the BCF can be related to the rate constants for uptake and depuration by equation 4.6.3.

$$\frac{C_a}{C_w} = \frac{K_u}{K_d} = BCF \qquad (4.6.3)$$

Since K_u and K_d were estimated simultaneously by numerical methods, they were highly correlated. Bias introduced into one estimate by violating assumptions can affect the other. Therefore, we estimated K_u and K_d by several other techniques which made different assumptions.

Independent estimates of K_u were also calculated from slopes of tangents to the uptake curve at 1 h. This initial rates technique assumes a first order relationship with respect to CW and no initial depuration (K_u = slope / C_w). The overall depuration rate constant (K_d) was also estimated from data collected during the clearance period, when midges were not exposed to anthracene. The overall depuration rate constant was estimated from the slope of the first log-linear component of the depuration curve. The component K_{ds}, contributing to the overall K_d were estimated concurrently by equation 4.6.4.

$$C_{at} = \sum_{i=1}^{n} C_{ai} \cdot e^{-(K_{di} \cdot t)} \qquad (4.6.4)$$

where:

C_{at} = concentration in midge at time t

t = time from cessation of exposure

C_{ai} = initial concentration in i^{th} component

i = individual depuration component

K_{di} = depuration rate constant for i^{th} component

n = number of independent depuration components

RESULTS AND DISCUSSION

Uptake

Uptake of ^{14}C-anthracene was rapid and approached steady state in 25 to 45 h (Figure 4.6.1). The uptake rate constant for ^{14}C increased by a factor of approximately 3 over the concentration range 1.7 to 30.5 $\mu g \cdot \ell^{-1}$ (Figure 4.6.2). Few studies have computed rate constants for the accumulation of PAH by aquatic invertebrates. However, Herbes and Risi (1978) report a first-order uptake rate constant of 1.01 h^{-1} for anthracene accumulation by Daphnia pulex.

As exposure time increased, K_u based on ^{14}C generally decreased (Table 4.6.1). Since K_u and K_d were estimated simultaneously from ^{14}C data, they may be biased by accumulation of biotransformation products. This will be discussed more fully in the sections on depuration and biotransformation.

The decrease of K_u may also be due to a decline in swimming and activity. The speed of the normal swimming motion of midges decreased as duration of exposure increased. Midges in uncontaminated water also showed the same activity patterns. Slower swimming activity could be expected to increase the boundary layer of less concentrated anthracene and thus reduce exposure concentration. Respiration and metabolic rates, as manifested in swimming rates (Walshe, 1949) could also influence uptake rate. K_u values measured at 25° and 30°C were not significantly different, but were higher than that determined at 16° (Table 4.6.1).

Depuration

Depuration rate constants were greater at higher anthracene concentrations (Table 4.6.1). As exposure time increased, a larger fraction of the ^{14}C was in the bound than extractable pools. Therefore, K_d decreased with

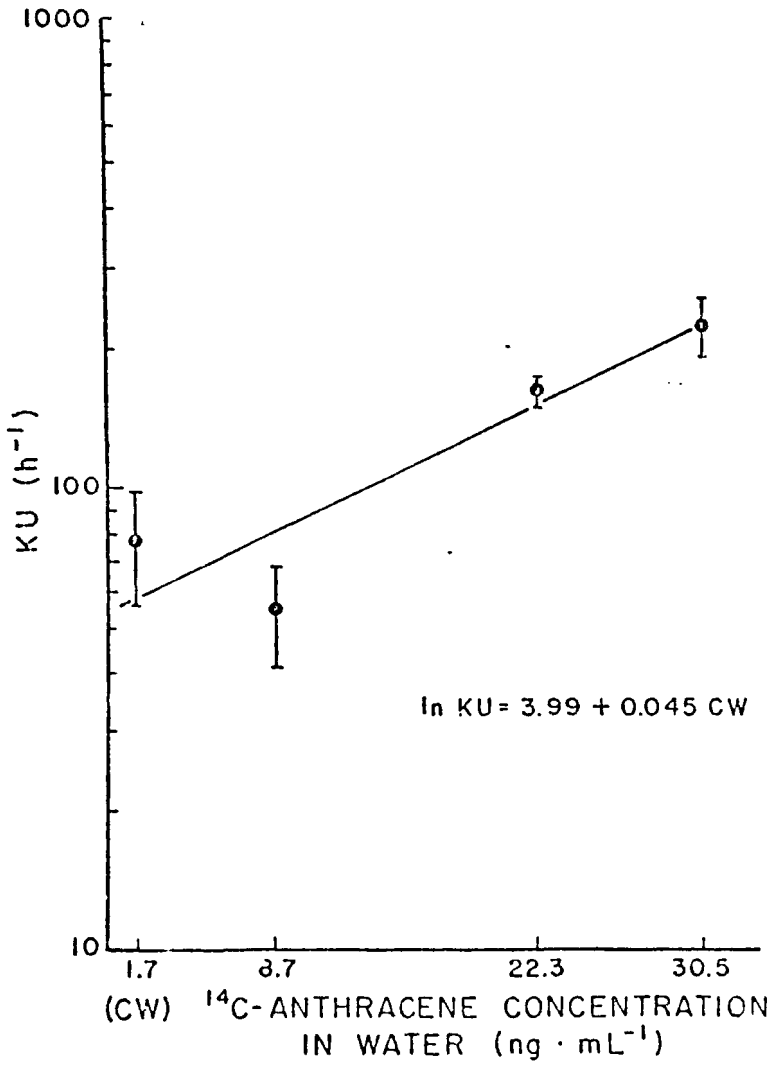

Figure 4.6.2. Log K_u for C. riparius at 4 different concentrations of anthracene in water. Estimate ± asymptotic 95% CI.

Table 4.6.1. Uptake (K_u) and depuration (K_d) rate constants in C. riparius at four concentrations and three temperatures (estimate ± 95% CI).

Concentration $\mu g \cdot \ell^{-1}$	Temperature (°C)	K_u (h^{-1})			K_d (h^{-1})			
		1h[ab]	10h[c]	30h[c]	10h[c]	30h[c]	3h[d]	30h[e]
1.7	25	82	77±21	68±13	0.070±0.073	0.035±0.019	0.077±0.023	0.311±0.224
8.7	25	79	54±13	74±10		0.041±0.014	0.215±0.078	0.236±0.098
22.3	25	193	161±12	155±16	0.107±0.021	0.085±0.014	0.158±0.176	0.247±0.101
30.5	25	265	222±32	143±20	0.276±0.070	0.078±0.017	0.093±0.014	0.177±0.120
22.2	16	128	116±10	102±11	0.091±0.023	0.053±0.011	0.144±0.027	0.250±0.457
22.3	25	193	161±12	155±16	0.107±0.021	0.085±0.014	0.158±0.018	0.247±0.102
22.7	30	153	152±14	152±16	0.089±0.026	0.089±0.015	0.260±0.139	0.363±0.231

a. Duration of test. All values estimated from concentration of ^{14}C-anthracene in midges ($ng \cdot g^{-1}$ wet weight).
b. Estimated from tangent to slope at 1 h.
c. Estimated from ^{14}C-anthracene uptake experiments using donor dependent model (equations 4.6.1 and 4.6.2).
d. Measured as slope during initial 3 h depuration in uncontaminated water and paper towel substrate after 9 h exposure.
e. First component of overall depuration rate constant calculated with equation 4.

time, since a smaller proportion of the ^{14}C material was available for depuration. Polar biotransformation products have been shown to be eliminated more slowly by many aquatic animals (Landrum and Crosby, 1981a and 1981b).

Depuration rate constant was not affected by temperature (Table 4.6.1). Because most metabolic functions are temperature dependent over the normal temperature range encountered by animals one would expect that both biotransformation and active elimination would be affected by temperature. The fact that we see no effect of temperature on the depuration rate constant, based on ^{14}C activity, is probably due to a complex interaction of temperature effects on metabolism, excretion and anthracene biotransformation.

When midges, which had accumulated anthracene, were placed in water with paper towel substrate, no effects of temperature or concentration on K_d were observed. K_d values, calculated from the donor dependent model (Equation 4.6.2), were generally lower in the absence of paper towel substrate than when paper towel substrate was present (Table 4.6.1). Leversee et al. (1981) observed greater rates of depuration of benzo(a)pyrene, (B(a)P), from C. riparius in the presence of paper towel than in the absence of paper towel.

We observed biphasic depuration of ^{14}C-anthracene (Figure 4.6.3). The two phases may represent depuration of anthracene from two storage compartments, or depuration of anthracene and its biotransformation products which are more polar. Herbes and Risi (1978) observed a multiphasic depuration of anthracene from Daphnia pulex. Resolution of these questions would be difficult in the midge and our studies were not designed to resolve them.

However, we did resolve the overall depuration rate constant into several component parts. In each case where we determined the overall and more rapid depuration rate constants the overall rate constant estimate was slower than the estimate of the rapid phase (Table 4.6.1). This indicates that our estimate of the overall K_d is intermediate between the more rapid and slower rates. The overall depuration rate constant, as estimated by equations 1 and 2 should be a weighted average of the multiple rate constants (equation 4.6.5).

$$K_{do} = \frac{\sum_{1}^{i} C_i \cdot K_i}{\sum_{1}^{i} C_i} \qquad (4.6.5)$$

where:

K_{do} = overall depuration rate constant

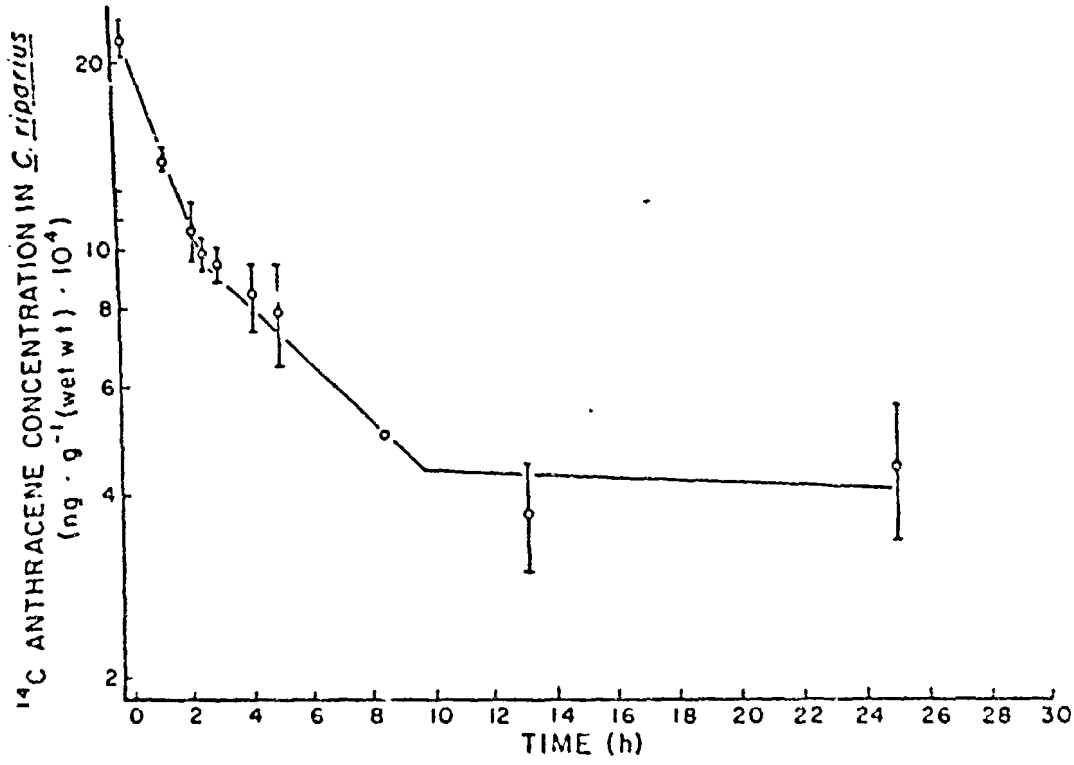

Figure 4.6.3. Depuration of ^{14}C anthracene by C. riparius in uncontaminated water and paper towel substrate at 30°C. $\bar{X} \pm 2$ Se, n = 3.

C_i = initial concentration of i^{th} component

K_i = i^{th} depuration rate constant

For predicting body burdens in populations we feel that this level of resolution is not necessary and advocate use of the overall depuration rate constant. If one needs to resolve depuration rate constants, we suggest that estimates be made by fitting the data, using equation 4.6.4, by interative least squares techniques rather than the "back stripping" technique of Wagner (1975). It can be seen that unless the sample size is large, the confidence intervals for the estimates are very large (Table 4.6.1).

After two depuration phases had been identified, a residual of approximately 20% of the initial ^{14}C still remained bound in the animal at 30°C (Figure 4.6.3). This residual was depurated very slowly or not at all. The slope of the log-transformed ^{14}C concentration as a function of time was not significantly different from zero.

Biotransformation

The biotransformation rate was maximum at 25°C (Figures 4.6.4 and 4.6.5). Because the biotransformation rate was high, percent anthracene was minimum at 25°C. The mass of anthracene in the midges, however, was maximum at 30°C because accumulation of ^{14}C was as high, but biotransformation was lower at 30° than at 25°C.

The temperature effect indicates that the enzymes responsible for the biotransformation are responding optimally at 25°C. Estenik and Collins (1979) found *in vitro* aldrin expoxidation activity in *C. riparius* by mixed function oxidase was greatest at 30°C. Thus, the decline in biotransformation from 25° to 30°C was probably due to a decline in the overall physiological state of the midges and not due to enzyme efficiency. Additional evidence for reduced physiological fitness at 30°C was seen in culture growth. Cultures of midges maintained at 30°C did not remain viable, whereas those at 25°C propagated successfully.

At 16°C, the overall biotransformation rate was slower than at higher temperatures (Figure 4.6.6). Additionally, the proportion of biotransformation anthracene that was unextractable was smaller at 16°C. This suggests that biotransformation involves several processes which respond differently to temperature. Likewise, Varanasi *et al.* (1981) found that the relative concentrations of different naphthalene biotransformation products in starry flounder also changed with temperature.

The biotransformation rate decreased during the first 4 h (Figure 4.6.5). This may have been due to a decline in respiration, as discussed earlier, or to a build-up of biotransformation products and end product inhibition. Leversee *et al.* (1981a) found a similar decrease in biotransformation rate in midges exposed to B(a)P. However, at 30°C biotransformation rate tended to increase after 4 h (Figure 4.6.5).

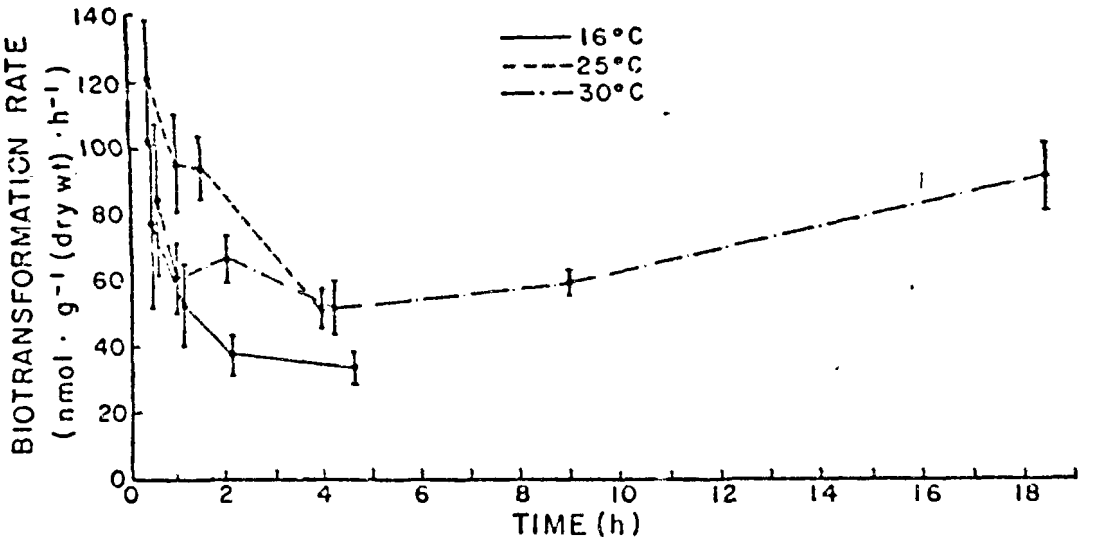

Figure 4.6.4. Biotransformation rate after 1 h exposure as a function of temperature. $\bar{X} \pm 2$ SE, n = 4.

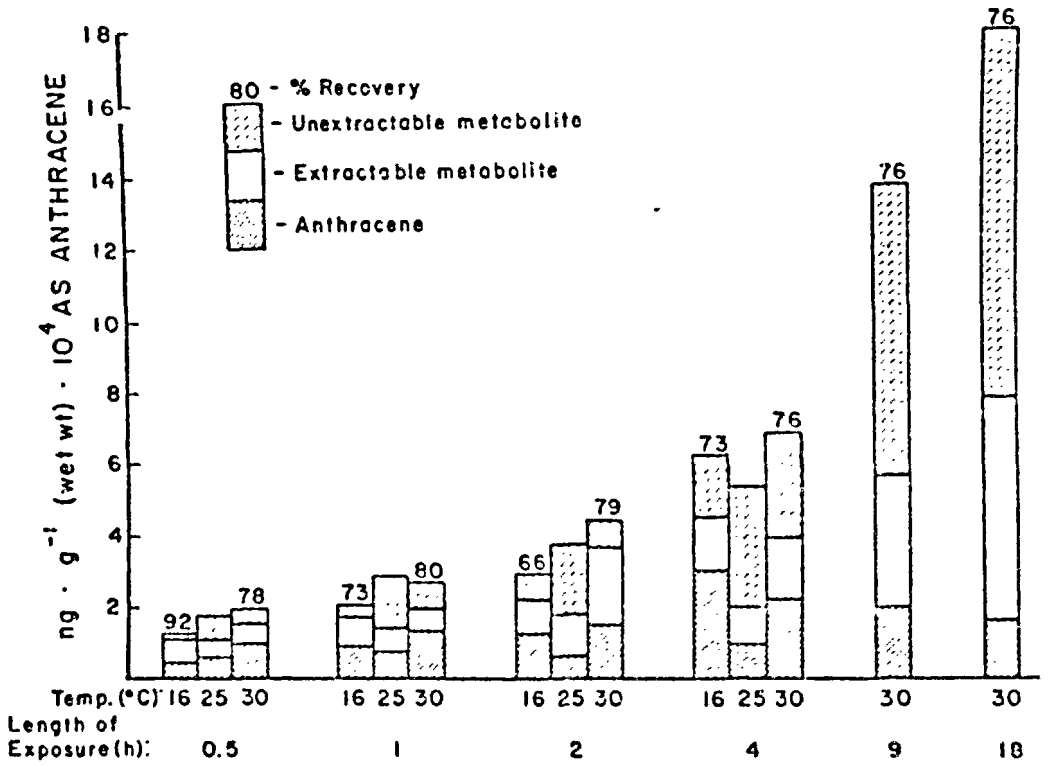

Figure 4.6.5. Biotransformation rate as a function of time of exposure and temperature. $\bar{X} \pm 2$ SE, n = 4.

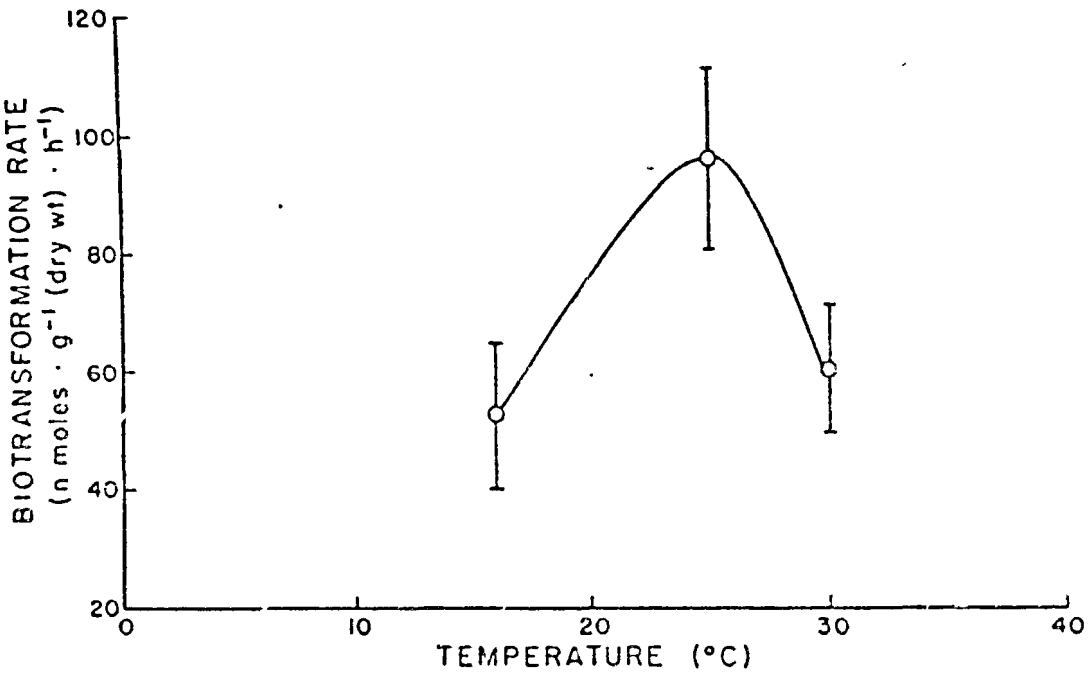

Figure 4.6.6. Biotransformation of ^{14}C anthracene at 16, 25 and 30°C. $\bar{X}$ $\pm$ 2 SE, n = 4.

At 30°C, the percent of ^{14}C that was anthracene decreased with length of exposure from 48% at 0.5 h to 9% at 18 h (Figure 4.6.6). The trend was less pronounced at the other temperatures. Between 4 and 18 h, anthracene concentration decreased by 2/3 while the ^{14}C activity rose by a factor of 2.7. However, at all temperatures percent unextractable ^{14}C increased with time.

Bioconcentration Factor

Bioconcentration factor (BCF), calculated using $K_u \cdot K_d^{-1}$ based on ^{14}C, was not affected by temperature or concentration in the water (Table 4.6.2). Other studies with aquatic organisms, Canton et al. (1978), Blanchard et al.

Table 4.6.2. Bioconcentration factors (BCF) for ^{14}C-anthracene in the midge C. riparius. BCF for total ^{14}C was calculated from $K_u \cdot K_d^{-1}$ after 10 and 30 h of uptake. BCF for anthracene was calculated from concentrations of anthracene at 4 hr. $\bar{x}$ ± 95% CI.

Concentration ($ng \cdot ml^{-1}$)	Temp (°C)	BIOCONCENTRATION FACTORS		
		14C		Anthracene
		10 h	30 h	4 h
1.7	25	915±532	1964±722	
8.7	25		1817±388	
22.3	25	1503±206	1820±136	
30.5	25	804±104	1843±180	
22.2	10	1277±245	1915±228	132±39
22.3	25	1503±206	1820±136	47±15
22.7	30	1697±384	1702±119	95±5

(1977) and Wilkes and Weiss (1971) have likewise shown that BCF was constant at different concentrations. Similarly, bioaccumulation was found to be unaffected by temperature in Mytilus edulis (Fossato and Canzonier, 1976). Bioconcentration factor predicted from the 30 h data set was usually higher than BCF from the 10 h data. The difference is probably due to accumulation of non-anthracene ^{14}C. The BCF calculated for anthracene in biotransformation studies was more than an order of magnitude lower than ^{14}C-BCF, due to rapid biotransformation of anthracene. Steady state had not been reached by 4 h so a true BCF can not be calculated. Interesting-

ly, at 30°C, the concentration factor at 18 h was 68 ± 17, which is 2/3 of the concentration factor at 4 h. Concentration factor was lowest at 25°C and reflected the biotransformation rate.

BCF was more strongly affected by differences in biotransformation rate due to temperature than by differences in uptake rate due to temperature. For example, BCF was highest at 16°C because biotransformation was lowest, even though uptake rate and concentration were also lowest at 16°C. Consequently, caution must be exercised in comparing BCF for metabolically transformable compounds. As we found with anthracene in chironomids, ^{14}C-BCF leads to overestimation of bioconcentration potential.

Benzo(a)pyrene and Anthracene

Since octanol:water partitioning coefficient has been positively correlated with BCF (Neely et al., 1974), benzo(a)pyrene (BaP) would be expected to have a larger BCF than anthracene. The ^{14}C-BCF of anthracene (915 at 1.7 ng·ml^{-1}) was similar to BCF for B(a)P in C. riparius (970 at 1.0 ng·ml^{-1}) (Leversee et al., 1981a). Though both K_u and K_d were slower for anthracene, the ^{14}C-BCF values were similar for anthracene and B(a)P because their relative proportions remained constant. The 4 h accumulation factor based on parent compound was approximately 4 times greater for B(a)P (200) than for anthracene (47), as might be expected from the octonol:water partitioning coefficient predictions. Bioaccumulation was calculated using parent compound at 4 h, since steady state was not easily recognizable. The difference between BCF based on ^{14}C and BCF based on parent compound for anthracene compared respectively to those for B(a)P indicates a slower elimination of anthracene biotransformation product. Relative rates of biotransformation on a molar basis were similar for B(a)P (2.7 nmol·g^{-1}·h^{-1} at 4 nmol·ℓ$^{-1}$) and anthracene (51 nmol·g^{-1}·h^{-1} at 125 nmol·ℓ$^{-1}$) considering the difference in concentration.

CONCLUSIONS

1. Accumulation of ^{14}C-anthracene is described by the model $\frac{dC_a}{dt} = (K_u \cdot C_w) - (K_d \cdot C_a)$ (Equation 4.6.1).

2. Uptake rate constants are temperature and concentration dependent.

3. Bioconcentration factor based on ^{14}C is not affected by concentration or temperature.

4. Bioconcentration factor based on anthracene is minimum at 25°C and is inversely proportional to rate of biotransformation.

SECTION 4.7

UPTAKE, DEPURATION AND BIOTRANSFORMATION OF ANTHRACENE BY THE CLAM, ANODONTA IMBECILLIS

INTRODUCTION

Uptake and release of polycyclic aromatic hydrocarbons (PAH) and other petroleum hydrocarbon compounds by marine bivalve molluscs have been the focus of much research in recent years. Being sessile filter feeders, clams are readily exposed to pollutants (Nunes and Benville, 1979), and it has been suggested that these organisms could be used as worldwide monitors of hydrocarbon pollution (Stegeman and Teal, 1973; Goldberg, 1975; Fossato and Canzonier, 1975; Dunn and Stitch, 1975; DeSalvo et al., 1975; Bravo et al., 1978). The general conclusions of past studies of hydrocarbon interactions with clams have been that 1) uptake is rapid (Nunes and Benville, 1979), but can be highly variable (Jackim and Wilson, 1977), 2) depuration consists of several release compartments (i.e. fast and slow) (Dunn and Stitch, 1976) and depuration half-life is directly dependent on the length of exposure to a pollutant (Boehm and Quinn, 1977; Jackim and Wilson, 1977), and 3) biotransformation of hydrocarbons by molluscs is minimal or nonexistent (Carlson, 1971; Lee et al., 1972; Dunn and Stitch, 1976; Nunes and Benville, 1979). This lack of biotransformation is probably due to the fact that molluscs are deficient in mixed function oxidase enzymes (Neff et al., 1976; Bend et al., 1977; Moore, 1979). Molluscs have also been found to selectively concentrate PAH compounds relative to other hydrocarbons (Lake and Kershmer, 1977).

PAH studies concerning freshwater invertebrates have centered on Daphnia sp. (Herbes and Risi, 1978; Southworth et al., 1978) and chironomids, which have been shown to have a high biotransformation potential (this report). The primary objective of this study was to determine fluxes and rate constants for uptake, depuration and biotransformation of anthracene by the freshwater clam Anodonta imbecillis. The symmetry of the anthracene molecule lowers the number of possible metabolites compared to other PAH compounds, such as benzo(a)pyrene, making the assessment of biotransformation readily feasible. An ideal freshwater monitor organism the paper-shell clam, A. imbecillis, is a common member of the benthic community of lakes and large rivers of North America, Europe, and Asia (Pennak, 1953).

MATERIALS AND METHODS

Anodonta imbecillis were collected August 4, 1980 by SCUBA from PAR pond (on the Savannah River Plant, Aiken, S.C.) at depths from 1.5 to 3.0 meters. Clams were returned to the lab and held for 2 days in a tank containing aerated, PAR pond water at 25°C. Twenty-four hours before the experiment was initiated, eight clams of similar size ($\bar{X}$ valve length = 7.07 ±.315 cm) were cleaned externally, and placed in individual aquaria containing filtered (0.45 µm), aerated, PAR pond water to allow for gut clearance. The clams were blotted and weighed before transfer to experimental chambers. Mean tissue weight was 17.41 ±.82 gm, wet weight.

14-C anthracene was added in bulk to > 0.45 um filtered PAR pond water allowed to equilibrate for 2 hours, and then 1.1 ℓ was added to each of the 5.0-ℓ (covered) glass experimental aquaria. To allow for adsorption to the walls, the aquaria were left for an additional hour. The final equilibrated concentration of 14-C anthracene was 31 $ug \cdot \ell^{-1}$ (0.68 $uCi \cdot \ell^{-1}$). Experiments were conducted at 25 ± 1°C.

Water samples were taken after 0.0, 0.5, 1.0, 3.0, 5.0, 13.0, and 24.0 h and the anthracene concentrations were determined by liquid scintillation counting (LSC). One ml of water was added to 12 ml of a premixed counting cocktail (Research Products International 3a70B®). All activity measurements were made by a Beckman Model LS8100 liquid scintillation counter, and were corrected for quenching using internal and external standards and sample channels ratio. All procedures involving anthracene were performed under gold flourescent light ($\lambda \geq 500$ nm) to minimize photodegradation.

After 24 h of exposure to anthracene, three of the remaining six clams (2 died during the experiment and were not used in the analysis) were removed and frozen for extraction and analysis. The other three clams were placed in aquaria containing 2.0 ℓ of uncontaminated filtered PAR pond water for depuration studies. Before transfer to freezer bags or depuration chambers the clams were dipped in clean pond water and allowed to drain to remove 14-C activity from loosely bound water on the surface of the shells. Water samples were taken after 0.0, 0.5, 1.0, 1.5, 3.0, 5.0, 12.0, and 24.0 h, and water activity was measured by LSC to determine the rate of depuration from the clams.

For tissue analysis, individual clams were homogenized in a Ten Broeck tissue homogenizer. Emptied shells were blotted and wet weight determined. 14-C combustion analysis was used to determine the final total anthracene tissue concentration. Tissue extracts were analyzed by thin-layer chromatography (TLC) and HPLC to determine concentrations of possible biotransformation products of anthracene. Clam homogenate (0.25 ml) was combusted in a Packard Model 306 sample oxidizer® for 1 min., and was collected in scintillation vials with 5 ml Carbosorb® and 13 ml Permaflour®. Previous experiments showed, by use of internal and external standards, that recovery of $14\text{-}CO_2$ was 90% but possible contamination of the oxidizer lowered the percent recovery to 81% during this experiment. Oxidized samples accounted for 95 ± 27% of the 14-C anthracene in tissues as was predicted from water data and the mass balance assumption. Extractions for TLC, and

extraction and analysis procedures for HPLC are given in Section 4.6. TLC separations were made on silica gel plates, one set with hexane-benzene (9:1, V/V) and another set with pentane-ether (9:1, V/V) as solvents. The position of anthracene was determined by comparison to standards parallel to the samples. Recovery by this technique was 70.7% ± 3.5 (95% C.I.) for anthracene and 79.3% ± 2.9 for anthraquinone, a possible biotransformation product of anthracene. After visualization with UV light, areas 1 cm above and below the 14-C anthracene and metabolite spots were scraped from the plates and placed in LSC vials containing counting cocktail for subsequent analysis.

Since changes in water anthracene concentration were used to measure uptake and depuration by A. imbecillis, it was necessary to determine the contribution of the shells alone. Weighted and sealed shells were used in an uptake and depuration experiment which duplicated that with live clams. Surface area was determined for the shells in all experiments. Uptake and depuration data obtained from living clams were corrected for calculated contribution from shells.

A Marquardt iterative least squares method was used to estimate first order rate constants and asymptotic 95% confidence limits (PROC NLIN, Statistical Analysis System, Barr et al., 1979). Because the dosing system used in these studies was closed, a two compartment model was used to estimate the first order rate constants for uptake and depuration (Equations 4.7.1-4.7.4).

$$\frac{dQ_a}{dt} = K_{uqw} - K_{dqa} \qquad (4.7.1)$$

$$AO = Q_w + Q_a \qquad (4.7.2)$$

assuming equation 4.7.2 is true and integrating gives:

$$QA = \frac{K_u \cdot AO}{(K_u + K_d)} 1 - e^{-(K_u + K_d) \cdot t} \qquad (4.7.3)$$

and

$$Q_w = \frac{-K_u \cdot AO + AO(1 + K_u \cdot e^{-(K_u + K_d) \cdot t})}{(K_u + K_d)} \qquad (4.7.4)$$

where:

Q_a = mass of anthracene in clam of time t

Q_w = mass of anthracene in water at time t_o

K_u = first order uptake rate constant

K_d = first order depuration rate constant

AO = total mass of anthracene in system

t = time

t_o = time zero

RESULTS AND DISCUSSION

Shells

A two compartment model (Equation 4.7.4) was used to estimate K_u and K_d for shells. K_u and K_d were 0.092 h^{-1} and 0.362 h^{-1} respectively during the first 5.0 h of the experiment. Only data from the first 5.0 h of uptake by shells were used because of loss of anthracene from the water (> 20% after 5.0 h). Loss was primarily attributed to adsorption of compound to dust particles which accumulated on the surface of the water during the sample period. After 24 h of depuration, steady state was reached, and only 12% of 14-C anthracene had been released by the shells (Figure 4.7.1). This type of almost irreversible adsorption raises doubt about the use of a two compartment model to predict the uptake of this compound by the shells, or at least in this case, the use of the term 'depuration rate constant'. Instead of a depuration rate constant, K_d most likely represents a substrate saturation rate constant.

After 24 h exposure to 31 µg anthracene·ℓ^{-1}, clams had accumulated 0.71 ± 0.098 µg anthracene/g wet weight ($\bar{X}$ ± SD) of soft tissue (Figure 4.7.2). The predicted steady state concentration (CSS) of 0.75 had been reached by this time. The first order rate constants for uptake and depuration are given in Table 4.7.1. Uptake appeared to be biphasic for this experiment (Figure 4.7.2). However, due to the absence of data points between 13 and 24 h, where the phase shift is suggested to occur, short term multicompartmentalization for uptake in these clams is merely speculative. The literature on compartment theory is incomplete for short term uptake circumstances since no previous experiment has exhaustive'y studied the first 24 h of exposure of clams to organic compounds. The overall uptake rate constant was estimated as a single value. The two component nature of the uptake may have been due to saturation of a pool such as the extrapallial fluid, followed by partitioning into the soft tissue of the clam. In order to estimate overall rate constants for the 24 h uptake period, the 13 h data was omitted for use in the two compartment model since in this experiment multiphasic uptake was assumed to be additive. The model used here assumed that all of the anthracene accumulated by the clams was from exposure to anthracene dissolved in the water. This assumption is supported by the work of Dobrenki and Epifanio (1980) which showed that the hard clam (Mercinaria mercinaria) accumulated more B(a)P directly from water than from B(a)P-containing food.

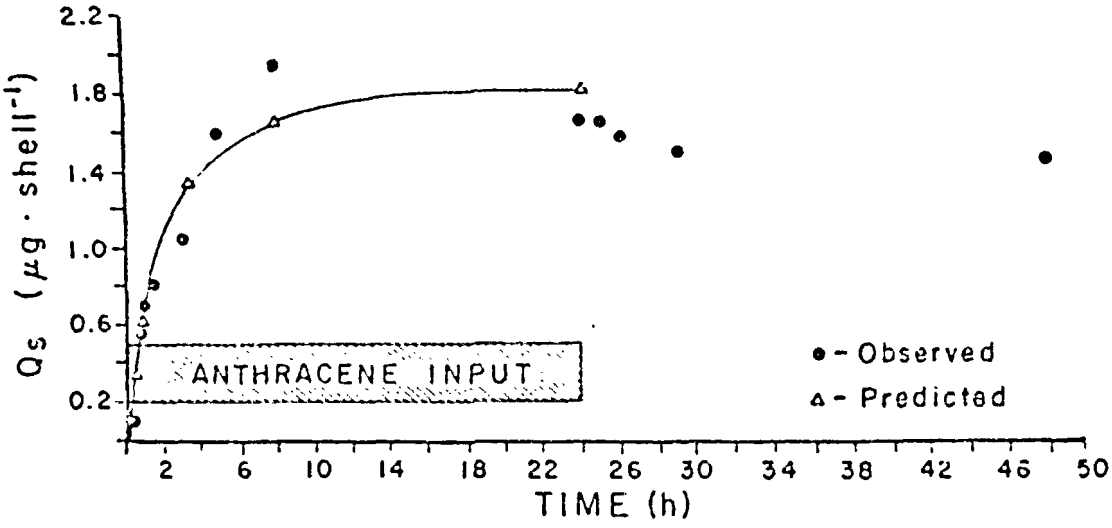

Figure 4.7.1. Accumulation of anthracene by A. imbecillis shell as a function of time. The fitted line is based on the first 5 h of uptake only because of loss of anthracene from the water, which did not go to the clams. This results in a decrease in the amount of anthracene associated with the shells (points after 24 h).

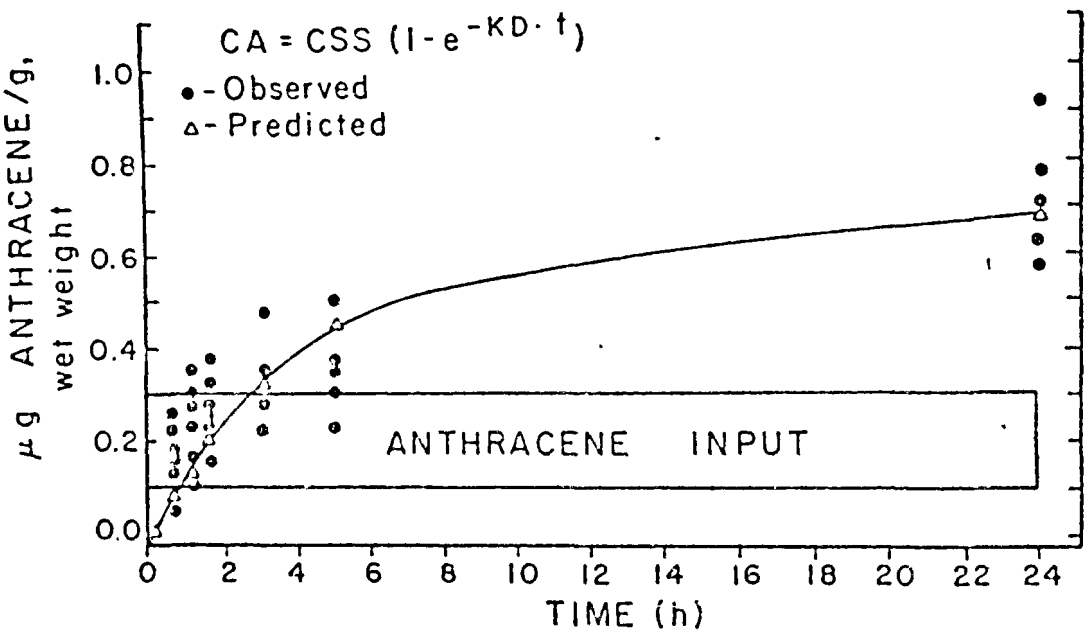

Figure 4.7.2. Accumulation of anthracene by soft tissues of A. imbecillis as a function of time.

Table 4.7.1. First order rate constants for uptake and depuration of anthracene by A. imbecillis from 31 µg anthracene. Estimated by Marquardt iterative least squares procedure.

	Estimate	Asymptotic SE	F and P of F
SHELLS			
K_u[1]	0.092	0.015	$F_{2,26} = 184$ P<0.0001
K_d[2]	0.362	0.126	
SOFT TISSUE			
K_u[1]	0.0052	0.0006	$F_{2,40} = 215$ P<0.0001
K_d[2]	0.216	0.033	
K_d[3]	0.200	0.079	$F_{2,24} = 57$ P<0.001

[1]Overall uptake rate constant with units $\ell \cdot (h \cdot g)^{-1}$, wet weight

[2]Overall depuration rate constant estimated during uptake phase, with units h^{-1}.

[3]Single component depuration rate constant estimated during depuration phase, with units h^{-1}.

Depuration studies showed that compound release is biphasic during a 24 h period with a shift in the depuration rate occurring between 1.5 and 3.0 h after removal from exposure to 14-C anthracene. A multiphasic depuration model (Equation 4.7.4) gave estimates of 0.118 h^{-1} for K_d^1 (0 - 1.5 hrs) and 0.011 h^{-1} for K_d^2 (3.0 - 24.0 hrs) (Fig 4.7.3). The depuration rate constant estimate (K_d) from the two compartment model was similar to the overall depuration rate constant K_d^1 estimated from the two component depuration model. The dispersion in the data was such that we also used a single component depuration model to estimate K_d phase (Table 4.7.1). The overall depuration rate constant was similar to that estimated from data collected during the anthracene exposure. However, it can be seen that

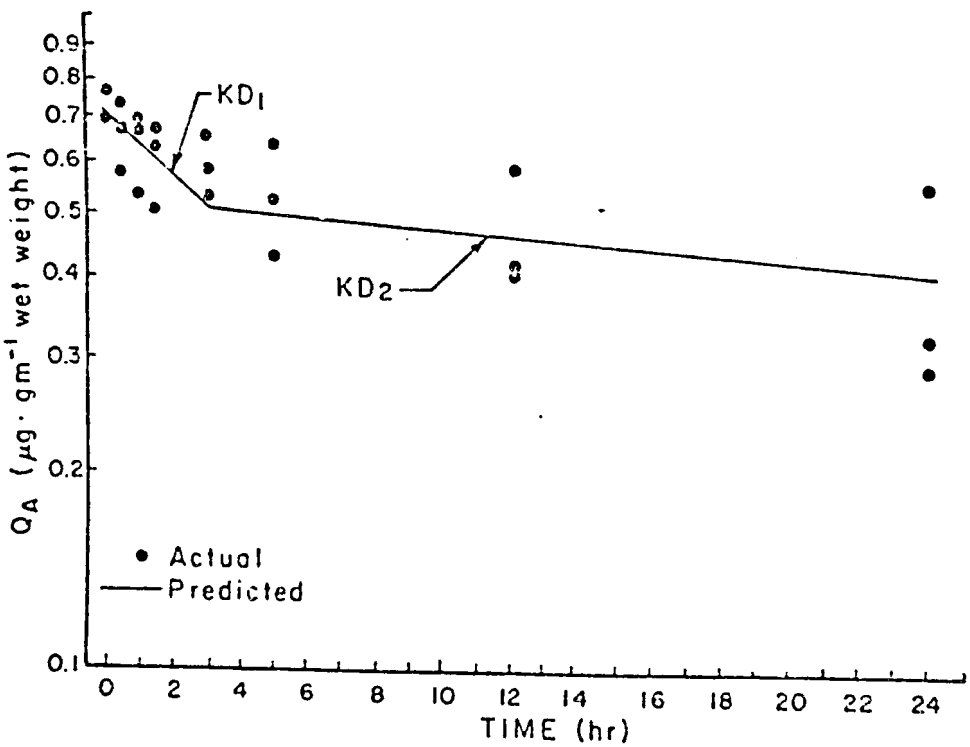

Figure 4.7.3. Depuration of anthracene from the clam A. imbecillis. The data have been fit to a two component depuration model (Equation 4 7.8).

this rate constant is too great and that there is a slow loss of anthracene which is not accounted for by this model. Therefore the best estimate of the overall depuration rate constant is $0.118 h^{-1}$. However, even this constant alone would predict the loss of anthracene from the clams to be more rapid than it really is.

The rates of depuration of PAH from molluscs has been shown to be non-selective, and slower than from fish or shrimp (Neff et al., 1976). Several investigators have suggested multiphasic depuration of toxins by aquatic organisms (Dunn and Stitch 1976, Herbes and Rishi 1978, Nunes and Benville 1979, Boehm and Quinn 1977, Blumer et al., 1970, Stegemen and Teal 1977, Fossato and Canzonier 1976) but again none of these studies dealt with short term components as in this study. The depuration half-life of 14-C anthracene in A. imbecillis had not been reached by the end of the sample period and, assuming the occurrence of no more phase shifts, the estimated half-life is approximately two days. Multiphasic depuration and depuration times which are long relative to the length of the uptake period are consistent with findings in the literature.

In a study with Anodonta cataractae, McLeese et al. (1979) found $K_u = 0.125\ h^{-1}$ and $K_d = 0.015\ h^{-1}$ for the uptake and depuration of an organophosphate pesticide. While the depuration rate constant is similar to the K_d obtained in this experiment, the uptake rate constant in the McLeese paper is much larger. A lowering of K_u could possibly be due to the absence of food in this experiment. It can be argued that a clam which is actively feeding will accumulate more toxic burden, due to digestion and assimilation of food material laden with the toxic substance, than a clam which is siphoning for respiration only. This feeding effect is unknown and deserves further study. The different natures of the chemicals used by McLeese et al. (1979) and this study may also affect K_u. The predicted concentration from 336 h exposure to 31 μg anthracene$\cdot \ell^{-1}$, which was the average concentration to which clams were exposed in the channels microcosms, from uptake and depuration rate constants reported here for laboratory studies is 1.2 μg anthracene$\cdot g^{-1}$, dry weight of soft tissue. This value is more than an order of magnitude less than the 16.7 μg anthracene$\cdot g^{-1}$, dry weight, actually observed in clams collected from the channels microcosms after 336 h exposure. The reasons for this difference could be many. Foremost, is that the laboratory studies were conducted for short periods of time and may underestimate the actual rate of accumulation. We observed clams in the laboratory to remain closed much of the time. Because the laboratory studies were done for short periods of time the clams may not have been able to acclimate rapidly enough to give rate constants representative of those observed in the field. We conclude that laboratory determined rate constants may not adequately describe the actual kinetics of accumulation of PAH compounds in natural environments.

Biotransformation

After 24 h of exposure, little of the ^{14}C-anthracene had been biotransformed. Only 0.9 ± 0.6% of the ^{14}C had been biotransformed after 24 h

of uptake. After a subsequent 24 h depuration period only 1 ± 0.8% of the ^{14}C remaining in the soft tissues was biotransformed.

These findings are similar to those of Dunn and Stitch's (1976) suggestion that bivalve molluscs do not possess the capability to metabolize petroleum hydrocarbons, and that indeed "the organism's only defense against toxins is slow depuration" (Nunes and Benville 1979; Carlson 1972). Stegeman and Teal (1973) also found depuration from clams to be slow, and accumulation to be dependent on lipid content. Lake and Kerchner (1977) reported that depuration of PHA from molluscs was non-selective.

It was observed during the uptake portion of this study that the clams were sporadically closing, and were remaining closed for periods up to 0.5 h. During depuration, the clams did not exhibit this behavior and were rarely observed to be closed throughout the sample period. It appears that A. imbecillis are sensitive to either the 14-C anthracene or the acetone which was used as a solvent for the anthracene. In either case, the ability of these clams to detect small amounts of foreign substance (30 $\mu g \cdot \ell^{-1}$ 14-C anthracene and 15 $\mu l \cdot \ell^{-1}$ acetone) is worth noting.

CONCLUSIONS

Sealed and weighted shells of Anodonta imbecillis adsorb 14-C anthracene in what can be termed an irreversible fashion. Non-feeding clams take up significant amounts of 14-C anthracene in 24 h, and this uptake may be biphasic, although further study is needed to validate compartmentalization of uptake. A low uptake rate constant, compared to that from an experiment with Anodonta cataractae, may be due in part to the absence of food in this study. The first order rate constants determined from short-term, simple laboratory accumulation studies, result in an overestimation of the concentrations attained by A. imbecillis when compared to clams in the channels microcosms. This may be due to many factors, such as current, filtering time, temperature, suspended particulates or other factors. The important fact is that the laboratory derived rate constants are poor predictors of field observations (see Section 6.5).

SECTION 4.8

UPTAKE, DEPURATION, AND BIOTRANSFORMATION OF ANTHRACENE AND BENZO(A)PYRENE IN BLUEGILL SUNFISH

Direct uptake from water to fish has been shown for several PAH including naphthalene, alkylated naphthalenes, anthracene, and benzo(a)pyrene (Lee et al., 1972a; Anderson et al., 1974; Neff et al., 1976; Roubal et al., 1978; Melancon and Lech, 1978). PAH can undergo biotransformation to more polar compounds in vitro (Pedersen and Hersberger, 1974; Bend et al., 1979; Ahokas et al., 1979) and in vivo (Lee et al., 1972; Roubal et al., 1977; Lu et al., 1977; Lu et al., 1978; Statham et al., 1978; Melancon and Lech, 1979). Because some members of the PAH group are procarcinogens, there is a concern for the presence of PAH residues and biotransformation products in edible fish.

Bioconcentration factors, ratio of compound concentrations in fish to their concentrations in water at steady state, have been successfully predicted from correlations with the octanol-water partition coefficient (Neely et al., 1974; Veith et al., 1979 a and b). The partition coefficients of the larger PAH suggest that they should bioconcentrate to a high degree. However, chemicals that are readily biotransformed may not behave according to predictions based on the parent compound. Southworth et al. (1980) observed smaller bioconcentration factors than expected for azaarenes because of their rapid biotransformation in minnows. Competing rates of biotransformation and exchange at the gill are probably important in determining the overall bioconcentration of PAH, as well.

The present study was designed to measure rates of uptake, biotransformation, and elimination of ^{14}C-labeled anthracene and benzo(a)pyrene in bluegill sunfish (Lepomis macrochirus) during and following short-term exposures in water. Distribution of ^{14}C activity in fish tissues was also determined. The observed rate constants and calculated bioconcentration factors were compared to estimates based on partition coefficients.

METHODS

Juvenile bluegills (100 - 600 mg) were obtained from the Millen National Fish Hatchery, Millen, Georgia. They were maintained at 20-22°C in filtered, recirculating test water for at least two weeks prior to testing. No significant mortalities occurred during transport or acclimation. No signs of stress were observed during any of the testing. Water for acclimation and testing was taken from Upper Three Runs Creek, a blackwater

stream within the U. S. Department of Energy's Savannah River Plant near Aiken, South Carolina. Because of its extremely low mineral content (60 umhos·cm^{-1}), the water was amended with salts to produce a standard soft test water. Water quality characteristics were: pH 7.4-7.6, hardness 43 mg·ℓ$^{-1}$ as $CaCO_3$, alkalinity 30 mg·ℓ$^{-1}$ as $CaCO_3$, and conductivity 140 umhos·cm^{-1}. Well water, used for several uptake experiments, had similar quality but lacked the colored organic material found in the blackwater stream water and was amended to give the same hardness characteristics as the amended stream water. Humic acids (Aldrich Chemical Co., molecular wt. > 300,000; 3.6 g dry wt·ml^{-1}) were added to well water at a concentration of 1 mg·ℓ$^{-1}$ for certain uptake experiments.

Uptake, depuration, and biotransformation were studied with 9-^{14}C anthracene (California Bionuclear Corp., specific activity of 3.3 mCi·mmol^{-1}) and 7-10-^{14}C benzo(a)pyrene (Amersham-Searle, specific activity of 21.7 mCi·mmol^{-1}). The radiopurity of the compounds was determined by two-dimensional, thin layer chromatography (TLC). The purities of anthracene and benzo(a)pyrene were 97.4 ± 2.6 and 96%, respectively.

Uptake Phase

Exposures were performed at 23-24.5°C in covered 5-l all-glass aquaria. All test water was aerated, passed through a Sorvall SS-1 continuous-flow centrifuge to remove particulates, and spiked directly with ^{14}C anthracene or B(a)P. After mixing, the test water was distributed to the aquaria. Fish were sorted by size and introduced to the tanks at rates of 100-500 mg fish·ℓ$^{-1}$. No aeration or feeding was provided during testing. At appropriate time intervals, fish were netted, blotted dry, wrapped in aluminum foil, and frozen at -20°C.

Depuration Phase

Fish used for depuration tests were transferred to clean flowing water after 4 h exposure. The fish were held in 5-l all-glass flow-through chambers with uncontaminated, unfiltered test water at a flow rate of 1 - 1.3 ℓ·h^{-1}. Hydrocarbons eliminated by the fish were trapped on a 75 ml Amberlite® XAD-4 resin column (Rohm and Haas) placed downstream, as described by Crosby et al. (1979). No significant radioactivity was detected in the column eluent during any depuration experiment. The resin was eluted with diethyl ether, acetone, and methanol according to the method of Garnas (1975). Trapping efficiency of anthracene was 97 ± 3% and elution efficiency was 89 ± 10%.

Analysis

Fish to be analyzed were weighed before and after being freeze-dried. The dry weight to wet weight ratio was 0.235 (n=45). All concentrations are expressed on a wet weight basis unless noted otherwise. Dried fish were combusted for one minute in a Packard Sample Oxidizer Model 306.

Carry-over during combustion was negligible. Recoveries of ^{14}C activity from injected dried fish were 46.9% for anthracene and 100% for B(a)P. The relatively low recovery for anthracene suggested some loss by volatilization during the freeze drying process. Therefore, all anthracene experiments were repeated using fish dried in a desiccator (recovery 100%) to minimize volatilization loss.

Water samples and solvent extracts were counted in 3a70B® cocktail (Research Products International Corp.). Samples were counted to a pre-set time of 10 min on a Beckman LS-8100 liquid scintillation counter. The samples were corrected for background, quench, and counting efficiency. The quench and counting efficiency correction was made using a quench curve based on the sample-channels ratio method. The counting error was SD $\leq$ 7%.

Anthracene, B(a)P, and metabolites were extracted from dried fish in a 40 ml TenBroeck homogenizer. Each fish was ground with successive 10 ml fractions of acidified benzene, diethylether (twice), and ethylacetate. The fractions were decanted, filtered, combined, dried over anhydrous sodium sulfate, and the volumes reduced. The remaining fish residue was combusted and counted to determine unextractable ^{14}C activity. Recoveries from the extraction of injected samples were 82 $\pm$ 9% for B(a)P and 93 $\pm$ 11% for anthracene.

Metabolites were determined by TLC using E. Merck silica gel plates without fluorescent indicator. Two solvent systems, hexane:benzene (9:1, V/V) and pentane:ether (9:1, V/V) were employed separately to resolve B(a)P from its biotransformation products. Anthracene samples were developed either in hexane:benzene (9:1, V/V) or in a two-directional system with pentane:ether (95:5, V/V) as the second solvent. Hydrocarbon spots were visualized under UV light, scraped, and the ^{14}C activity determined.

Extracts were also analyzed by high pressure liquid chromatography. Separations were made with a Micro-Pak MCH-10 reverse-phase column (35 cm long) equipped with a Whatman guard column of Co·Pel C_{18}ODS on 35 µm particles using gradient programmed elution conditions at 28°C. The gradient was from 45% acetonitrile in water to 90% acetonitrile in water. Acetonitrile (90%) was pumped through the column for five min before recreating the initial conditions.

Samples were detected by both fluorescence and 254 nm fixed wavelength detectors. The percentage of metabolite was calculated from the nonanthracene activity in the extract, plus the unextracted residue determined by combustion.

Rate Constants and Bioconcentration Factors

First-order rate constants for ^{14}C activity were calculated, assuming a single animal compartment, according to the first-order model described by Branson *et al.* (1975) and Neely (1979).

$$\frac{dC_a}{dt} = K_u \cdot C_w - K_d \cdot C_a \qquad (4.8.1)$$

$$C_a = \frac{K_u}{K_d} C_w (1 - e^{-(k_2 \cdot t)}) \qquad (4.8.2)$$

where C_a = concentration in fish ($ng \cdot g^{-1}$)

t = time (h)

C_w = concentration in water ($ng \cdot g^{-1}$)

K_u = uptake rate constant (ml $\cdot g^{-1} \cdot h^{-1}$) or ($h^{-1}$) assuming a tissue density of 1 g $\cdot$ ml^{-1}

K_d = depuration rate constant (h^{-1})

Underlying assumptions for the use of this model are discussed by Spacie and Hamelink (1980). The initial uptake rate was estimated by a tangent to the initial uptake curve (equation 4.8.3):

$$C_a = C_o + K_u \cdot C_w \cdot t \qquad (4.8.3)$$

where C_o is the initial concentration in fish. This was estimated from a linear regression and initial rates assumptions. For small values of t, the value of C_w is constant and C_a is negligible (Konemann and vanLecuwen, 1980). The apparent first-order elimination of ^{14}C activity during the depuration phase was calculated according to equation 4.8.4.

$$\log_e C_a = \log_e (C_t - K_d) \qquad (4.8.4)$$

where C_t is the concentration in fish at the beginning of depuration. The elimination half-life is described by equation 4.8.5.

$$t_{\frac{1}{2}} = \frac{\log_e 2}{K_d} \qquad (4.8.5)$$

Ideally, assuming the model described by equation 4.8.2, the bioconcentration factor (BCF) at steady state (as $t \to \infty$) is described by equation 4.8.6.

$$BCF = \frac{C_a}{C_w} = \frac{K_u}{K_d} \qquad (4.8.6)$$

Since the kinetic behavior of hydrocarbons may be more complex than this model would suggest, the ratio (K_u/K_d) will be termed the "estimated" BCF. The BCF values for anthracene and B(a)P were also calculated according to the regression of Veith et al. (1979b):

$$\log_{10} BCF = 0.85 \log_{10} P - 0.70 \qquad (4.8.7)$$

which relates bioconcentration to the n-octanol-water partition coefficient (P) of a chemical (Tulp and Hutzinger, 1978). This will be termed the "predicted BCF." The partition coefficients were calculated according to Leo et al. (1971).

The above BCF methods ordinarily relate to the bioconcentration of parent material, not to total ^{14}C activity which includes biotransformation products. To find a "corrected" BCF, the BCF calculated from the (K_u/K_d) ratio was corrected for the % parent material present in the fish at the end of the 4 h exposure. The equations describing the models were fit to the data by the Marquardt numerical methods (PROC NLIN, Barr et al., 1979).

RESULTS

Uptake Rates

Fish (mean weight 487 mg) were exposed to 20.5 $\mu g \cdot \ell^{-1}$ anthracene in aquaria for up to 16 h. The ^{14}C activity in the fish increased linearly ($r^2 = 0.93$) during the first 4 h with a flux of 1375 $\pm$ 105 ng $\cdot$ g^{-1} $\cdot$ h^{-1}, dry weight (Figure 4.8.1). This represents an uptake rate constant (K_u) of 67 $\pm$ 5 h^{-1}. The uptake rate declined after 4 h due to the depletion of a significant proportion of the dissolved anthracene: 8% after 1 h, 12% after 4 h, and 42% after 16 h (Figure 4.8.2). By comparison, a control tank without fish lost only 4.5% of initial activity in 16 h. Adsorption to walls represented 0.2% of the activity. Accountability for ^{14}C-anthracene from water, walls, and fish was 96 $\pm$ 2% and 98.3% for B(a)P after 4 h. Subsequent exposures were ended after 4 h to avoid problems of hydrocarbon depletion or water quality deterioration.

The effect of exposure concentration on K_u was investigated for anthracene concentrations of 0.7 to 16.6 $\mu g \cdot \ell^{-1}$ (Figure 4.8.3). The results (Table 4.8.1) show that K_u is essentially independent of the concentration of anthracene in the water. This is always assumed to be true but seldom tested. Another trial using larger fish (5140 mg), at 6.7 $\mu g \cdot \ell^{-1}$ produced a similar K_u of 31 h^{-1}. A slower uptake rate constant (K_u = 14 h^{-1}) was observed in a single group of 60 fish exposed to 11 $\mu g \cdot \ell^{-1}$ anthracene in a large 60-ℓ tank. In general, the fish in this group showed less swimming activity than those in the smaller 5-ℓ test tanks.

Accumulation of anthracene from well water (Figure 4.8.4) resulted in an uptake rate constant similar to that of stream water. The addition of humic acids does not affect the uptake rate significantly ($p = 0.1$). The uptake rate constants for equimolar solutions of B(a)P and anthracene in stream water were similar (Table 4.8.2). However, the accumulation of B(a)P from well water was greater than from the stream water containing refractory organics. The presence of humic acids in well water significantly reduced the rate of B(a)P accumulation by fish (Figure 4.8.4).

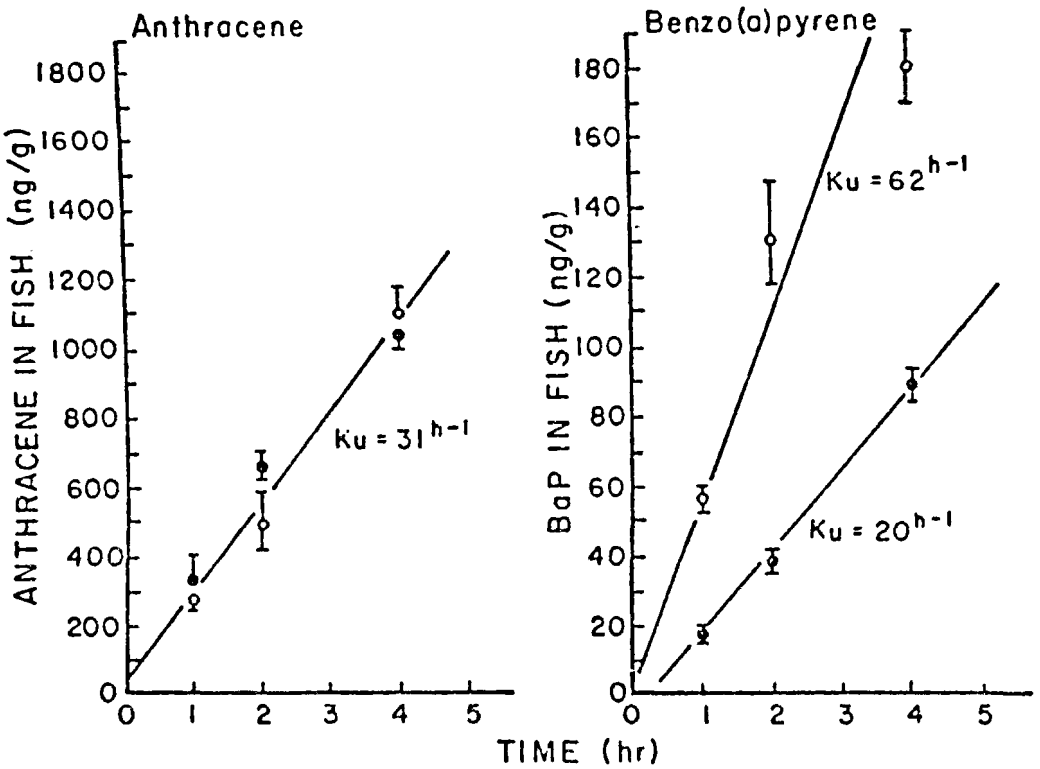

Figure 4.8.1. Accumulation of ^{14}C-anthracene and benzo(a)pyrene from well water with and without humic acids. Humics present (solid) circles), no humics (open circles).

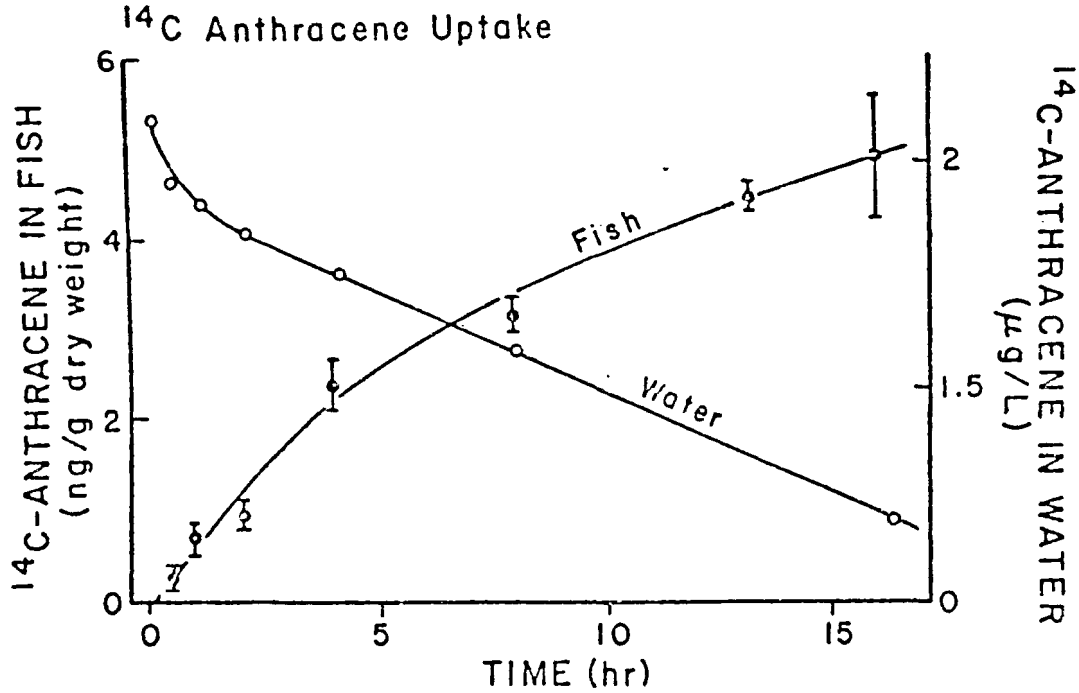

Figure 4.8.2. Accumulation of ^{14}C-anthracene by fish and depletion of ^{14}C-anthracene from water in a closed system.

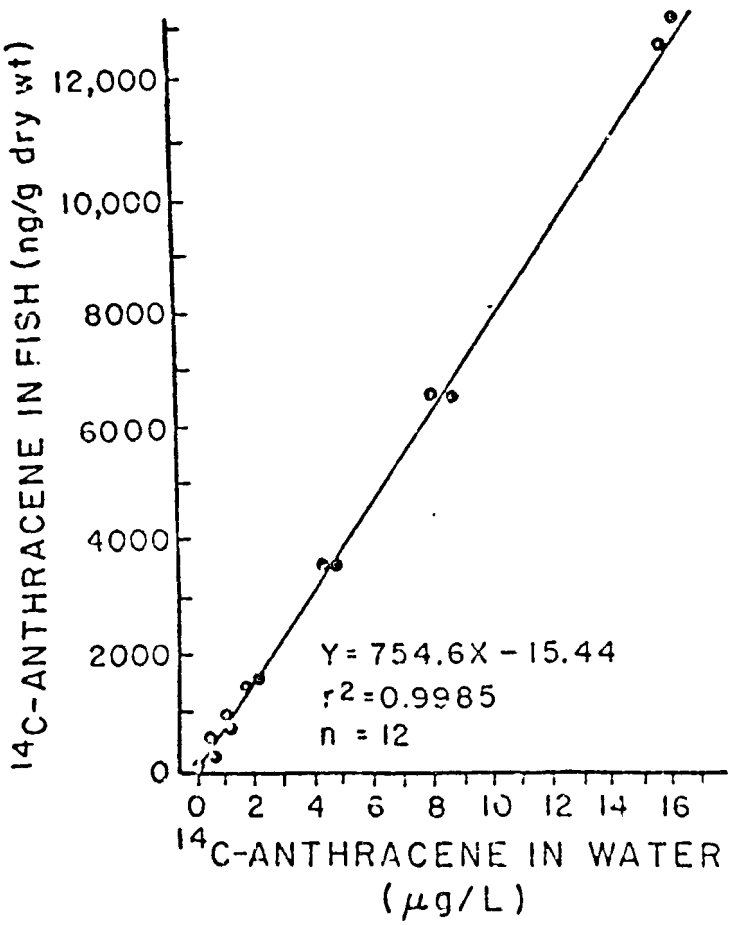

Figure 4.8.3. Concentration of ^{14}C-anthracene in bluegills after four hours exposure to ^{14}C-anthracene as a function of anthracene concentration in water.

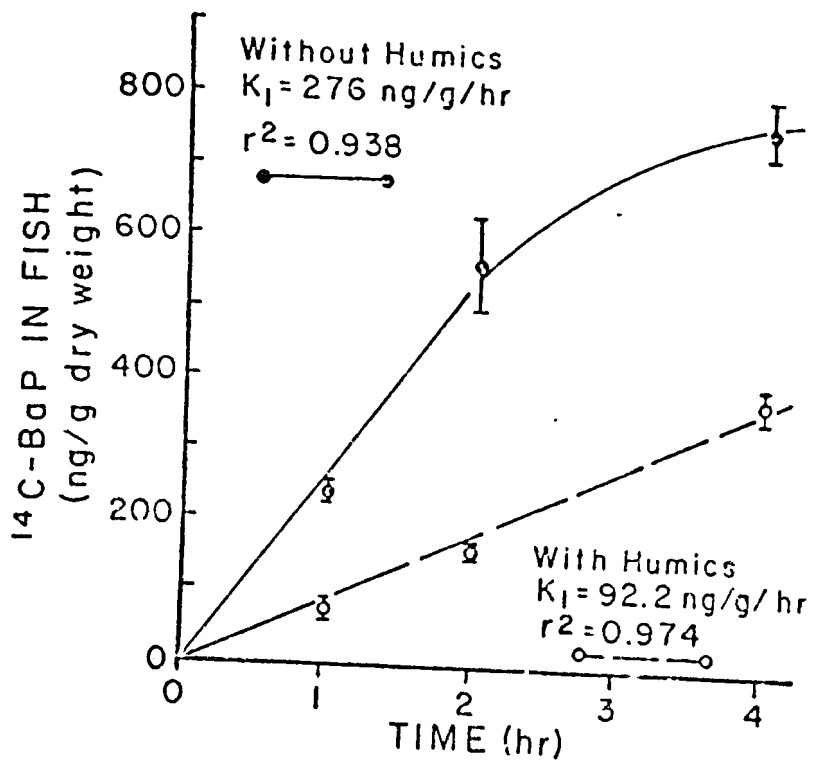

Figure 4.8.4. Accumulation of ^{14}C-B(a)P from water containing 1.0 ng·ml^{-1} in the presence or absence of humic acids.

TABLE 4.8.1. EFFECT OF VARYING EXPOSURE CONCENTRATION ON THE RATE OF UPTAKE OF ^{14}C ANTHRACENE BY BLUEGILLS.[a]

Conc. in water ($\mu g \cdot \ell^{-1}$)	Conc. in fish at 4 hr ($ng \cdot g^{-1}$)[b]	k_1 (h^{-1})
0.7	94 ± 4	36
1.1	170 ± 9	39
1.9	328 ± 18	43
4.6	786 ± 26	43
8.6	1439 ± 41	42
8.9	1591 ± 48	40
16.6	2777 ± 98	42

[a] Mean weight 620 mg.

[b] Mean ± SE.

Elimination Rates

Both anthracene and B(a)P ^{14}C activity in fish appeared to follow first-order kinetics during the depuration phase (Figure 4.8.5). However, the elimination of anthracene residues was approximately 4 times faster (Table 4.8.2). Elimination half-lives for total ^{14}C activity were 17 and 67 h for anthracene and B(a)P, respectively. The rate constants measured here predict that bluegills would reach 90% of their steady state concentrations in approximately 68 h for anthracene and 268 h for B(a)P.

Anthracene and metabolites excreted by the fish were trapped on resin columns placed below the depuration chamber. Approximately 47% of the total ^{14}C recovered from the columns was anthracene, according to TLC; the remainder was more polar material. A similar trapping technique for B(a)P was not completed because of the low concentration of excreted B(a)P in water and its' slow elimination from exposed fish.

Tissue Distribution and Biotransformation

Larger bluegills (4633 mg mean wt., n = 6) were exposed to either 5.8 $\mu g \cdot \ell^{-1}$ anthracene or 0.70 $\mu g \cdot \ell^{-1}$ B(a)P for 4 h to determine ^{14}C distri-

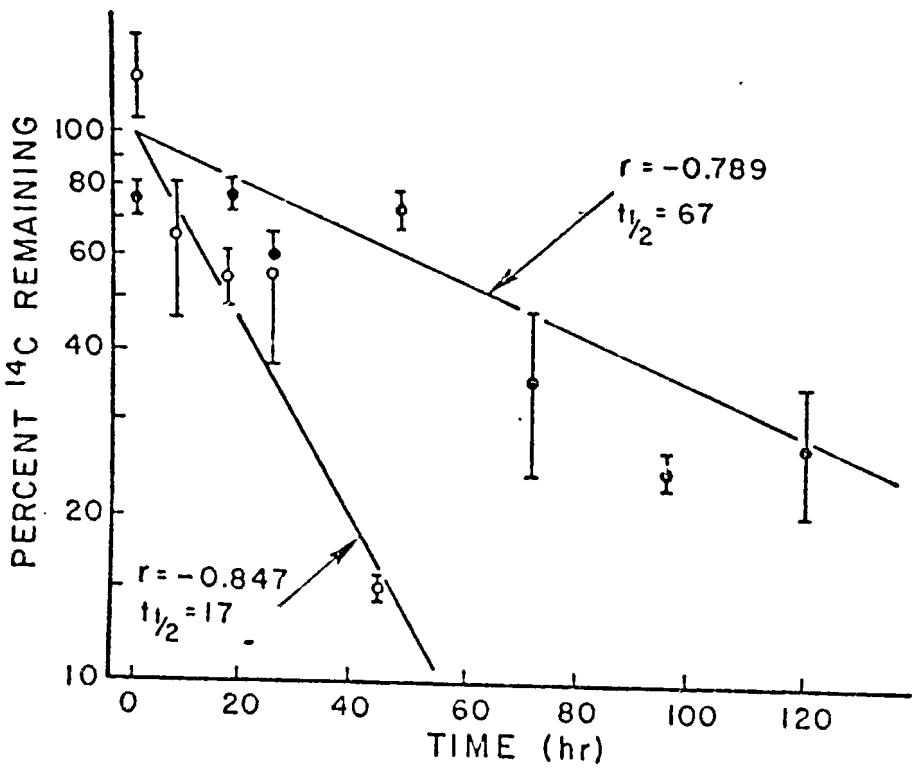

Figure 4.8.5. Depuration of ^{14}C-anthracene (open circles) and benzo(a)pyrene (solid circles) following an initial 4 h exposure x ± SE.

TABLE 4.8.2. RATES OF UPTAKE AND ELIMINATION OF ^{14}C ACTIVITY IN BLUEGILLS EXPOSED TO ANTHRACENE OR BENZO(A)PYRENE (B(A)P) IN STREAM WATER.

	Anthracene	B(a)P
Conc. in water[a] ($\mu g \cdot l$)	0.7	1.0
Conc. in fish at 4 h ($ng \cdot g^{-1}$)	94 ± 4[b]	207 ± 15
kU (h^{-1})	36 ± 3[c]	49 ± 4
kD (h^{-1})	0.040 ± .006[c]	0.010 ± .002
Elimination half-life (h)	17	67

[a] Approximately equimolar solutions.

[b] Mean ± SE.

[c] Slope ± standard deviation of regression coefficient.

butions in tissues (Table 4.8.3). Although the carcass had the largest quantity of both hydrocarbons, the gall bladder contained the greatest concentration on a weight basis. Liver, viscera, and brain all contained similar concentrations of anthracene. However, B(a)P residues were proportionately greatest in liver and least in brain. The very high rate of accumulation of ^{14}C-B(a)P in the gall bladder (14,000) suggests that B(a)P is rapidly metabolized and conjugated in the liver before transport to the bile.

The relative rate of biotransformation, expressed as the percentage of residue converted per hour, was greater for B(a)P than for anthracene (Table 4.8.4). The proportion of non-B(a)P biotransformation products increased from 36% after 1 h to 89% after 4 h. In contrast, only 7.9% of the anthracene activity had been biotransformed after 4 h. The rapid rate of biotransformation of B(a)P indicates that its' slower rate of elimination is due to excretion of metabolites rather than simple partitioning of the parent material.

Predicted Rates and Bioconcentration Factors

The measured rate constants (Table 4.8.2) yield estimated BCF values of 900 and 4900 for anthracene and B(a)P, respectively (Table 4.8.5). The

TABLE 4.8.3. DISTRIBUTION OF ^{14}C ACTIVITY IN BLUEGILLS EXPOSED TO 5.8 $\mu g \cdot \ell^{-1}$ ANTHRACENE (An) OR 0.70 $\mu g \cdot \ell^{-1}$ BENZO(A)PYRENE (BaP) FOR 4 HOURS.

Tissue	% Total Activity		Tissue conc. $ng \cdot g^{-1}$ dry		Uptake Coefficient[a]	
	An	B(a)P	An	B(a)P	An	B(a)P
Gall bladder	3.0 (0.7)[b]	16.7 (2.7)	43,800 (14,200)	39,000 (14,000)	1890	14,000
Liver	3.2 (0.8)	7.8 (1.7)	13,000 (1,100)	4,600 (640)	561	1,600
Viscera	20.3 (1.9)	17.2 (1.3)	14,900 (1,200)	2,200 (270)	641	770
Brain	1.5 (0.4)	0.3 (0.03)	12,900 (2,310)	250 (16)	555	90
Carcass	72.0 (2.0)	58.0 (3.4)	962 (194)	370 (26)	42	130

[a] (Tissue conc. at 4 h)/(conc. in water at 4 h).

[b] Mean (SE) for n = 6.

TABLE 4.8.4. RATES OF BIOTRANSFORMATION IN BLUEGILLS EXPOSED TO 8.9 $\mu g \cdot \ell^{-1}$ ANTHRACENE OR 0.98 $\mu g \cdot \ell^{-1}$ BENZO(A)PYRENE (B(a)P).

	Anthracene			B(a)P		
	1 h	2 h	3 h	1 h	2 h	3 h
Conc. of total residue ($nmol \cdot g^{-1}$)	6.2 (1.2)[a]	6.8 (0.3)	13.0 (0.4)	0.122 (-)	0.255 (-)	0.369 (-)
% metabolite	3.9 (1.0)	4.6 (0.4)	7.9 (0.2)	36 (5)	69 (2)	89 (4)
Biotransformation rate ($nmol \cdot g^{-1} \cdot hr^{-1}$)	0.24 (0.06)	0.16 (0.01)	0.26 (0.03)	0.044 (0.007)	0.088 (0.004)	0.082 (0.009)
% transformed per hr	3.9	2.3	2.0	36	35	22

[a] Mean (SE) for n = 3.

TABLE 4.8.5. COMPARISON OF BIOCONCENTRATION FACTORS DETERMINED BY THREE METHODS.[a]

Method	Anthracene	B(a)P
Predicted[b] (partition)	1209	28,250
Estimated (K_u/K_d)	900	4,900
Corrected (parent only)	675	490

[a] See Methods section for definitions.

[b] Using log P = 4.45 for anthracene and 6.06 for B(a)P (Leo, 1975).

estimated value for anthracene is reasonably close to its predicted value of 1209, based on partition coefficient. However, the estimated value for B(a)P is considerably lower than that predicted from the partition coefficient. Since the regression of BCF versus log P equation is derived primarily from inert or poorly metabolized chemicals (such as the polychlorinated biphenyls), it reflects an accumulation process dominated by a reversible exchange of the unaltered material. B(a)P is a clear exception to that pattern because of its rapid conversion to other products. In fact, a true steady state condition between fish and water may never occur.

The true corrected BCF values for both anthracene and B(a)P are well below the other estimates (Table 4.8.5). The % biotransformation product (Table 4.8.4) used to calculate the correct BCF may vary over time, depending on the length of exposure, enzyme activity, or other factors. If so, the corrected BCF values based on parent material would also change.

Although there are many BCF values in the literature for comparison, relatively few rate constants have been reported for fish. Spacie and Hamelink (1980) reported correlations for K_u and K_d versus log P for a series of chlorohydrocarbons and other organics. The correlations predict a slight increase in K_u and a relatively large decrease in K_d with higher log P. The predicted K_u values, 19 h^{-1} for anthracene and 33 h^{-1} for B(a)P, give reasonably good agreement with the measured values of 36 h^{-1} and 49 h^{-1}. The predicted K_d values based on partition coefficient are 0.02 h^{-1} for anthracene and 0.004 h^{-1} for B(a)P. They suggest slower rates of elimination and longer half-lives than were actually observed.

DISCUSSION

Anthracene and B(a)P were removed from water at similar rates from equimolar solutions. The rate constants are proportional to the octanol-water partition coefficient. This reflects the tendency of more nonpolar components to partition out of water (Chiou et al., 1977; Leo et al., 1971; Southworth et al., 1978; Veith et al., 1979b; Kenaga and Goring, 1980).

Similarly, the elimination rate constants were inversely proportional to the octanol-water partition coefficient. However, this cannot be totally attributed to the partition coefficients since significant biotransformation occurred, particularly for B(a)P. The formation of macromolecule-bound and polar biotransformation products will tend to reduce the depuration of the ^{14}C label. The bound material is not free to dissociate and the polar components may, in many cases, be more slowly eliminated (Landrum and Crosby, 1981a). Slow elimination of polar components by fish during these studies may have been enhanced if concentrated metabolites were not being emptied from the gall bladder due to the absence of feeding (Lech et al., 1973). The relative tissue distribution of anthracene and biotransformation products observed in the bluegill sunfish studied here were similar to that observed for anthracene in young Coho salmon (Roubal et al., 1977). In the study with salmon, gall bladder was the tissue containing the greatest concentration of ^{14}C-anthracene and biotransformation products.

The bioconcentration factor predicted from the log P relationship is much greater than that determined from K_u/K_d, and much greater than that corrected for biotransformation. This has also been observed by Southworth et al. (1980) for azaarenes in the fathead minnow and by Leversee et al. (1981b) for B(a)P in Chironomus riparius. Fish show this discrepancy due to the relatively slow uptake in proportion to the biotransformation rate. Thus, predictions of BCF from the log P can be expected to be higher than those actually found for compounds that undergo significant biotransformation.

Differences in the partition coefficients of the anthracene and B(a)P may account in part for the differences in observed biotransformation rates. Since B(a)P has a faster uptake rate from equimolar solutions, a greater concentration should be available for biotransformation. Additionally, B(a)P can be expected to be bound to serum proteins. This would result in lower whole-body concentrations and greater relative distribution to the liver. This could result in greater biotransformation, assuming the enzymes for biotransformation are not saturated. The biotransformation of B(a)P by fish on a dry weight basis was less than that found for either Daphnia or Chironomus riparius (Leversee et al., 1981 a and b). This reflects the compartmentalization of the biotransformation enzymes in the fish.

The rate of biotransformation appeared to increase in the case of B(a)P between 1 and 2 h. While B(a)P is a known cytochrome P-450 inducer (Ahokas, 1979), the short exposures (4 h) precluded the synthesis of more enzymes. However, adsorption of B(a)P or its metabolic products by endoplasmic reticular membranes may alter the specific activity of the enzymes. Such an apparent induction would affect K_d by altering the pool size of parent and biotransformation products. Induction would have its major effect on K_d if parent compound were the major excretion product and a minimal effect for the excretion of biotransformation products (Lech and Bend, 1980; Spacie and Hammelink, 1981). The length of exposure will tend to decrease the depuration rate constant, however, the uptake rate constant will not be affected by this induction. The decreased depuration rate results from the accumulation of a bound, unexchangeable, biotransformation product pool. This irreversible binding has been described for PAH as the mechanism for toxic response. Irreversible binding was observed in the kinetics of anthracene in Chironomus riparius (Gerould et al., 1981).

Thus, models used in describing the kinetics of uptake and depuration of PAH become biased when there is significant biotransformation, induction of PAH transforming enzymes, binding of biotransformation products, or translocation. In this study, we used short-term exposures and depuration periods to estimate rate constants. This avoided many of the problems mentioned above. Also, we chose to use simple one compartment, constant infusion models instead of two compartment mass balance models. The depletion of anthracene from water after 4 h in the static uptake study could be corrected for by a two compartment model. However, the other problems mentioned above would have resulted in a bias for both K_u and K_d. Thus, the creation of a multi-compartment model would be most appropriate, however, these models require large amounts of data for curve fitting. Since

the rate constants are highly correlated, many roots of the equation regression solutions may not result in real values or mechanistically realistic rate constants. Therefore, the use of simple models which fit one rate constant at a time provide good approximations to the overall processes for the fate of xenobiotics.

Veith et al. (1979a) suggested a technique for determining the log P or partitioning coefficient for organic compounds. This technique uses the retention time of the compound on reverse-phase, high-pressure liquid chromatography columns. This technique makes the measurement of this secondary property of compounds accurate and rapid. Since the partitioning coefficient is defined by several properties of compounds, such as molecular weight and polarity, it has been suggested as a possible integrator, which would be highly correlated with the bioconcentration factor (BCF) in fish (Leo et al., 1971; Chiou et al., 1977). However, the results of our studies indicate that the BCF predicted from the log P is greater than the observed BCF. This result is in agreement with those of Southworth et al. (1980) for azaarenes in fish and is most probably due to biotransformation. Therefore, if organisms are able to biotransform a compound of interest such as bluegills can biotransform B(a)P and anthracene, the use of the log P to predict steady state concentrations may result in error.

The biotransformation of PAH compounds, such as B(a)P and anthracene in fish, has been widely studied (Pedersen et al., 1974; Payne and Penrose, 1975; Gerhart and Carlson, 1978; Schnell et al., 1980; James and Bend, 1980). Because the microsomal mixed function oxidases can be induced, the rate of biotransformation can change with time of exposure. As discussed earlier, if the biotransformation products are bound tightly to macromolecules, the apparent BCF will change as a function of time due to: (1) induction of enzyme activity; (2) changes in the ratio of biotransformation products to parent compound; and (3) redistribution of both parent and biotransformed compound. Therefore, the short-term pharmacokinetic technique for determining steady-state concentrations of organic compounds by fish which was proposed by Branson et al. (1975) is appropriate only when biotransformation is minimal or the magnitude and rate of biotransformation is well known and constant.

The uptake rate constant for B(a)P was altered by the presence of dissolved humics. This reduced bioavailability was proportional to the log P, indicating that the more nonpolar materials interact strongly with the dissolved humics. Similar results have been observed for the uptake of hydrocarbons by sole (McCain et al., 1978) and for selected PAH by Daphnia (this report, Section 4.3).

SECTION 5

SIMULATION MODEL FOR PREDICTING PAH FATES

SECTION 5.1

INTRODUCTION

It is desirable to be able to predict the concentrations of PAH to which aquatic organisms will be directly exposed and humans will be exposed through food and drinking water. Thousands of different species of PAH's are chemically possible; therefore, application of elaborate screening protocols (Duthie, 1977) to individual PAH in order to quickly estimate major processes of transport, accumulation, and degradation are impractical for purposes of risk analysis. Assessment of health risks associated with introduction of PAH into the environment depends in part upon quantification of environmental transport and subsequent concentrations to which aquatic organisms are exposed (Crawford and Leggett, 1980). Estimates of transport and dose are independent of the specific nature of the threat to human health, either directly through contamination of potable water, for example, or indirectly through damage to ecological life support systems.

Several alternatives exist for the development of needed predictive capacity. Monitoring PAH content of stream components of interest following accidential pollution by PAH should provide sufficient data from which to generalize, given enough accidents. Statistical analysis of these data could facilitate prediction by providing regression models or correlation between measurable properties of specific PAH compounds and their observed fates in streams and rivers. Statistical models, however, depend solely upon available data. In addition, coefficients in statistical models often cannot be translated into mechanistic processes subject to control or manipulation by environmental decisionmakers.

Simulation models based upon mechanistic processes of PAH flux and accumulation represent a potentially more useful alternative to environmental monitoring or statistical models. These models are based upon "state of the art" understanding of processes, mathematical analogs of which translate directly into parameters or coefficients that can be estimated in the field or laboratory. Data collected in monitoring programs remain useful for model validation.

This section describes a model (Fates of Aromatics Models, FOAM) which simulates the transport of PAH compounds through lotic systems. Similar to models developed by Baughman and Lassiter (1978) this model has been designed to predict fates of PAH in a generalized stream environment. How-

ever, model structure permits parameterization for simulation of PAH dynamics in specific streams.

SECTION 5.2

MODEL STRUCTURE DESCRIPTION

Simulation of PAH transport in lotic systems requires an understanding of basic structure and function of streams and rivers, as well as, the physical, chemical and biological processes that govern PAH movement. Basic ecological information concerning species composition, standing crop and, in some instances, energy flow has accumulated for a variety of stream systems (Coffman et al., 1971; Fisher and Likens, 1972; McIntire, 1973; McIntire and Phinney, 1965; Minshall, 1978; Odum, 1957; Teal, 1957 and Tilly, 1968). Yet streams have not received the degree of attention from ecological modelers as have other aquatic systems (Patten, 1968). Models of lotic systems have classically been the purview of sanitation engineers. State variables in these models typically included dissolved oxygen, biological oxygen demand, and total solids. Model form typically divided a particular stream or river into a series of reaches, which individually may be quite different in hydraulic characteristics, but were assumed to be internally homogeneous. Reach models have become sophisticated in the realm of sanitation engineering, but little has been done to enhance their application to increase basic ecological understanding of stream structure and function. However, ecologists have recently begun to simulate energy and material flow through lotic systems, in some cases borrowing the reach model approach (Chen and Wells, 1976; Knowles and Wakeford, 1978; McIntire and Colby, 1978; Sandoval et al., 1976; Zalucki, 1978).

The major objective of this modeling effort was to predict the patterns of flow and accumulation in aquatic systems based on easily determined parameters for the compound of interest and the receiving environment. In this study we used laboratory studies to ascertain the most important vectors and mechanisms to be included in the simulation model. The effects of potentially mitigating factors on pathways and rate constants were also investigated. In some cases overall rate constants for uptake, depuration and biotransformation by biotic and abiotic matrices were determined in the laboratory for use in the model. Finally, the simulation model was parameterized for the conditions existing in the SREL channels microcosm facility (Giesy et al., 1979; Bowling et al. 1980). Simulation results were then compared to those of inputs of anthracene in the channels microcosms.

The general strategy was to adopt the reach approach (Figure 5.2.1) and to include fundamental biological production processes common to lotic systems. Specific processes known to influence PAH flux somewhat independent of ecological processes include photolytic degradation, volatiliza-

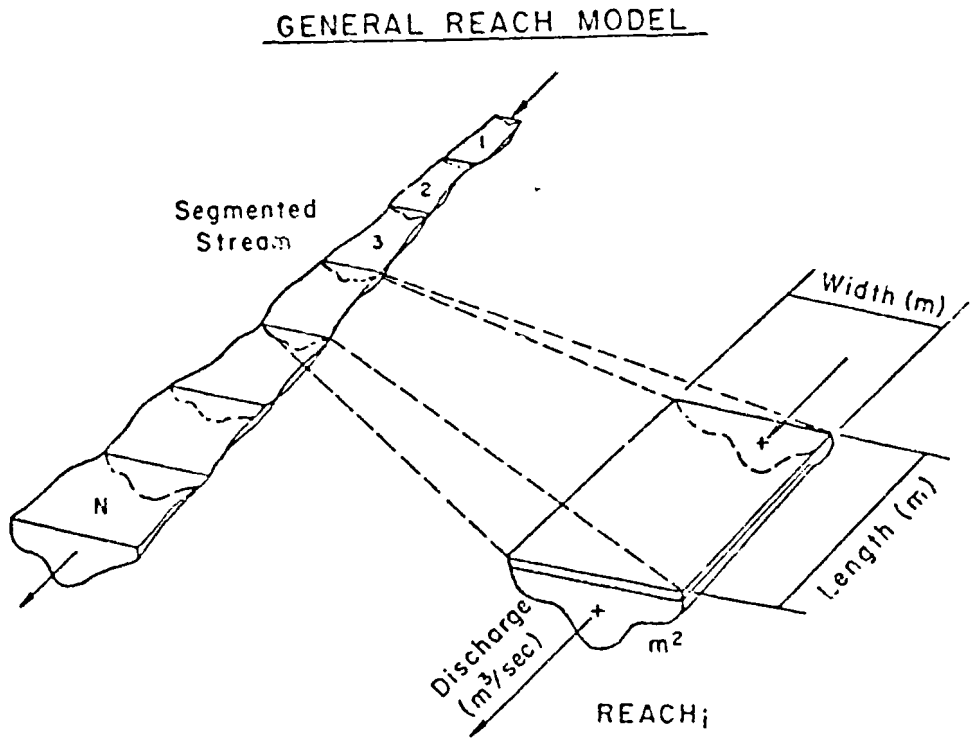

Figure 5.2.1. Conceptualization of generalized stream reach transport model.

tion losses and sorption to sediments and suspended particulates. These processes were, therefore, included in the model.

The fate of aromatics model (FOAM) predicted concentration of PAH in phytoplankton, periphyton, macrophytes, zooplankton, two benthic invertebrate compartments, bacteria, sediments, suspended particulate matter, and fish (Figure 5.2.2). The overall simulation model is organized as a main program (MAIN) which calls subroutines which calculate solar radiation (SOLAR) movement of water (HYDRO), solubility of PAH, and resuspension and calculates and graphs the relative and absolute mass of PAH in each compartment (Figure 5.2.3). Other submodels calculate the photolysis (PHOTO) volatilization (VOL) and sorption to sediments (SORP). The biotic components are coupled as in the representation given in Figure 5.2.4.

FOAM is programmed in FORTRAN. A modular structure was employed wherein individual processes were separated into subroutines (Figure 5.2.3). For example, subroutine HYDRO generates the hydraulic history used in subsequent calculations of state variable dynamics. Likewise, subroutine SOLAR simulates hourly values of incident solar radiation. The physical-chemical processes important in PAH dynamics: photolysis, volatilization and sorption, are modeled in routines PHOTO, VOL and SORP, respectively. Biological equations are contained in routine EQUA. Each routine calculates part of the overall derivative for change in biomass or PAH in each state variable (eg. equation 5.2.1). Modular structure facilitates modification of the submodels as directed by comparison of simulation results with observations to be made in the experimental streams.

Model Output

FOAM simulates the dynamics of biological production and PAH dynamics through time and space (reach) (Table 5.2.1). Each state variable value is printed in matrix form where row elements are values at a specific time for each reach. Column elements are temporal values in a particular reach. To assist in recognition of complex patterns in spatial-temporal dynamics, each state variable can be plotted simultaneously against reach number (distance downstream) and time (hour) to provide a three dimensional figure. A complete listing of the model code is beyond the scope of this report but can be obtained from the authors. It should be noted that model development is a dynamic process and FOAM is continually being updated. An overall mass balance approach was taken to model changes of biomass and PAH through time and space.

The first term on the right hand side of equation 5.2.1 represents time dependent changes in PAH concentration that result from processes such as volatilization, photolysis, biological transformation and translocation, and sorption to suspended particulate matter or sediments. The second term on the right hand side of equation represents downstream convective transport.

The general form of equation 5.2.1 implies independence between time dependent change and convective transport. However, as will be seen, cur-

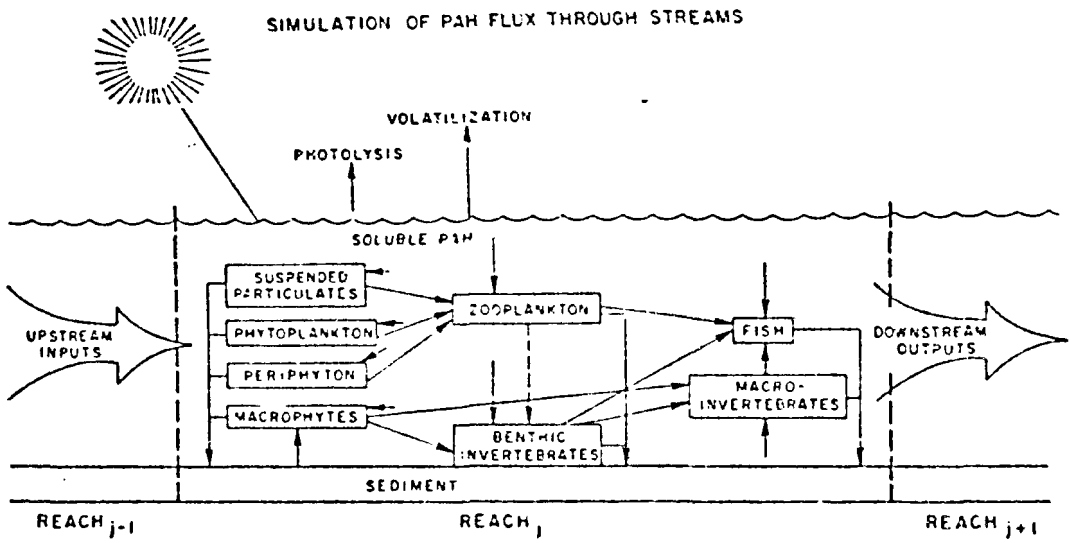

Figure 5.2.2. Schematic representation of Fates of Aromatic Molecules (FOAM) model.

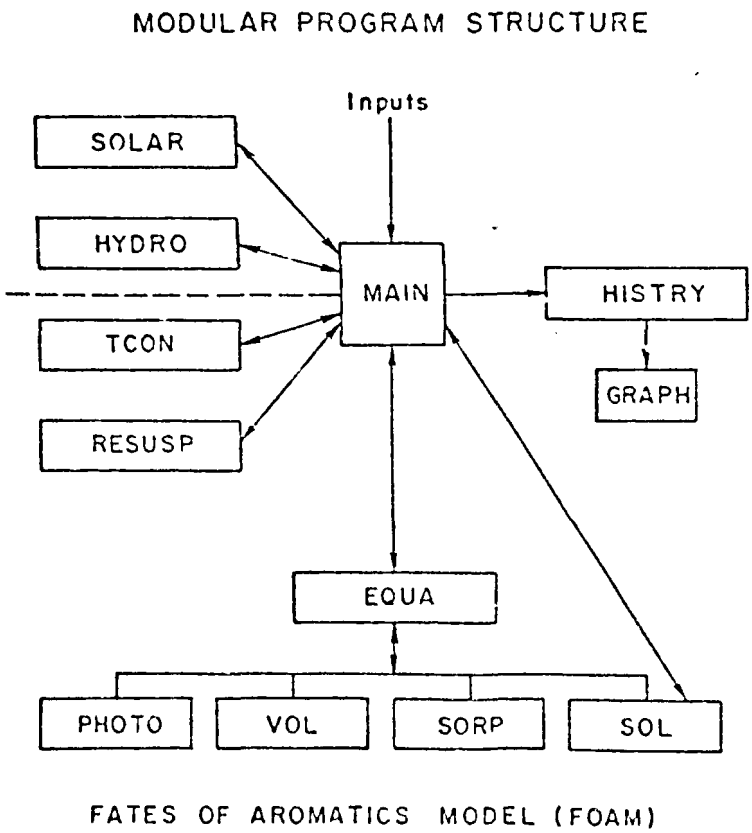

Figure 5.2.3. Schematic representation of modular subroutine structure of FOAM.

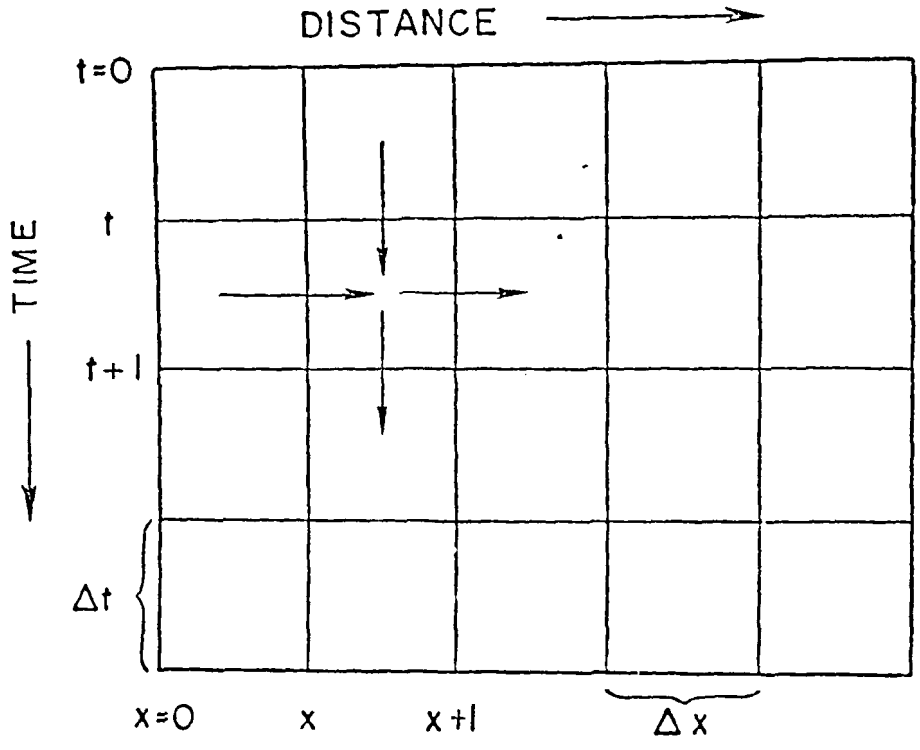

Figure 5.2.4. Movement of water mass through space and time.

Table 5.2.1. Output from FOAM. Each variable is simulated hourly.

Irradiance	langleys $\cdot h^{-1}$
Allochthanous organic matter	g $\cdot$ dry weight $\cdot m^{-2}$
External PAH loading	g $PAH \cdot m^{-2}$
Periphyton biomass	g $\cdot m^{-2}$
Macrophyte biomass	"
Benthic Invertebrate Biomass	"
Clam biomass	"
Bacteria biomass	"
Fish biomass	"
Suspended particulate organics	"
Dissolved organics	"
Bottom Sediments	"
Suspended inorganic particulates	"
Settled detritus	"
PAH in periphyton	μmol PAH $\cdot g^{-1}$, dry weight
PAH in macrophytes	"
PAH in Benthic Insects	"
PAH in Clams	"
PAH in Bacteria	"
PAH in Fish	
Predacious	"
Herbivorous	"
Suspended organic particulates	"
PAH in dissolved organic matter	"
PAH in bottom sediments	"
PAH in suspended inorganic particulates	"
PAH in settled detritus	"
PAH dissolved in water	μmol PAH $\cdot \ell^{-1}$
PAH which has been transferred	"

rent velocity directly affects some of the rates of time dependent processes, for example, rate of volatization of dissolved PAH or rates of settling and resuspension of particulate PAH. Time and space are to an extent the same thing coupled by current velocity.

Similar to Sandoval et al. (1976), a numerical approximation to the solution of equation 5.2.1 was used wherein the (x,t) plane was divided into an array and the derivatives approximated by differences (Figure 5.2.4).

$$\frac{\partial P}{\partial x} = \frac{P_{(x,t+1)} - P_{(x-1,t+1)}}{\Delta x} \qquad 5.2.1$$

$$\frac{\partial P}{\partial t} = \frac{P_{(x,t+1)} - P_{(x,t)}}{\Delta t} \qquad 5.2.2$$

An element in the array represents the PAH concentration in a given compartment, say periphyton, at a particular point in time and space. The actual value is the sum of the time dependent change (vertical arrow) and convective change (horizontal arrow). In another sense, the vertical arrow represents $\frac{\partial P}{\partial t}$ in equation 5.2.2 and the horizontal arrows, actually their sum, represents $U_{(x,t)}\frac{\partial P}{\partial xn}$ in equation 5.2.2. The time step was determined by a necessary relationship $\Delta t = U/\Delta x = 0.01\ M \cdot S^{-1}$ between reach length (M, 18.28 m) and current velocity (S^{-1}) (Bella and Dobbins, 1968).

SECTION 5.3

SUBMODELS

Hydrological Sub-model

Application of the model was constrained to conditions of constant reach morphometry under a constant discharge regime (Figure 5.3.1). Reach dimensions and flow rates are summarized in the facility description. A simple continuity equation was used to determine current velocity in relation to constant sectional area of each reach and discharge regime (equation 5.3.1).

$$Q = V_e \cdot A \qquad (5.3.1)$$

where,

Q = discharge into reach, $(M^3 \cdot t^{-1})$, 4.53 $m^3 \cdot h^{-1}$

V_e = current velocity $(m \cdot t^{-1})$, 18.3 $m \cdot h^{-1}$

A = cross sectional area of reach (m^2), 0.12 m^2

This hydrologic submodel appeared reasonable for the artificial streams, since the channels were of constant length, width, depth and flow rate.

Temperature Dependent Processes

In FOAM water temperature indirectly affected flow of PAH's through the food web by directly modifying rates of photosynthesis, consumption and respiration. An empirically derived equation (O'Neill et al., 1972; Shugart et al., 1974) was used to calculate the effect of water temperature in reach j at time t on rate estimates of photosynthesis and respiration for biological state variables (equation 5.3.2).

$$f(T) = V^x \cdot e^{x(1-V)} \qquad 5.3.2$$

where

$$V = (T_m - T)/(T_m - T_o)$$

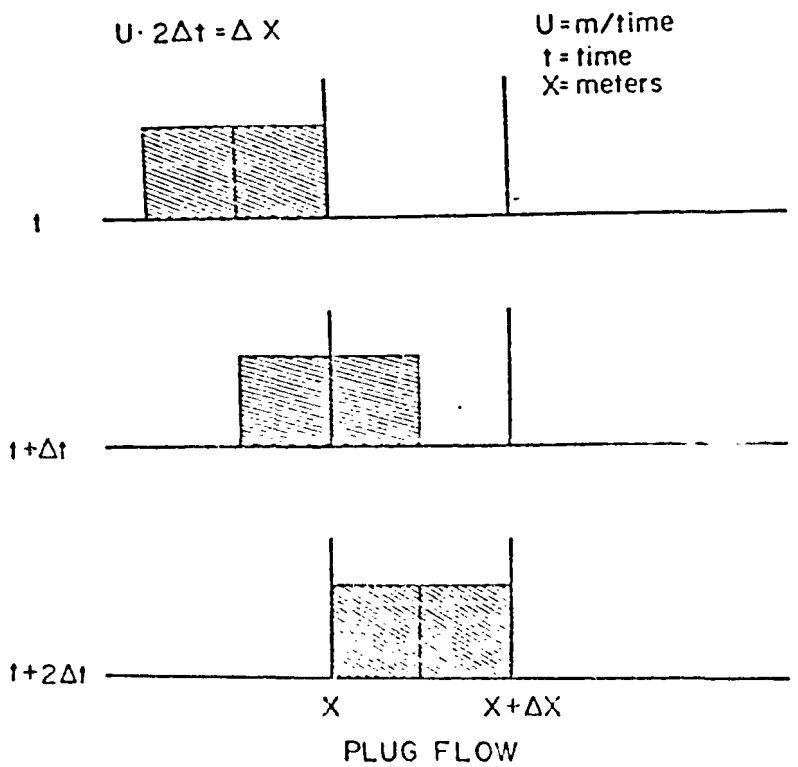

Figure 5.3.1. Schematic representation of plug flow used to represent water movement in reach model.

$$X = W^2 \, (1 + (1 + 40/Y)^{1/2})/400$$

$$W = (\ln Q_{10}) \, (T_m - T_o)$$

$$Y = (\ln Q_{10}) \, (T_m - T_o + 2)$$

T = water temperature°C; o = optimum, m = maximum

This function mimics a Q_{10} relationship at intermediate temperatures below T_o. At T_o, maximum rates are calculated. Beyond T_o, rates decrease rapidly to zero at T_m, which corresponds to an upper lethal temperature. Parameters were derived from published data for producer and consumer components (Table 5.3.1 - 5.3.3). Currently, FOAM requires a user specified input temperature regime for each reach j throughout the simulated time period.

Solar Radiation Sub-model

Incident solar radiation drives primary production and photolytic degradation of PAH in the biological submodel of FOAM. Therefore, realistic estimates of daily radiation inputs are required. FOAM incorporated, as a submodel, a modification of a solar radiation model (Satterlund and Means, 1978) to simulate surface radiation incident on reach j at time t (equation 5.3.3).

$$I_T = (I_{DS} + I_S F) \cdot (1 - C) + (I_{DO} + I_S) \, Ce^{-d_F} \qquad 5.3.3$$

where

I_T = radiation at surface of reach (ly/min)

I_{DS} = direct beam solar radiation, slope dependent

I_S = scattered clear sky solar radiation

I_{DO} = direct beam radiation on a horizontal surface

C = percent cloud over

F = slope correction factor for scattered clear sky radiation

d = parameter for seasonal cloud effects

Model inputs included latitude of stream (33 degrees N), slope direction, slope inclination (0) and daily estimates of mean cloud over. The model was calibrated with measurements recorded in the vicinity of the streams site. Figure 5.3.2 represents a simulation of the annual cycle of solar radiation.

FOAM includes the capacity to attenuate surface light with depth as a function of suspended sediments and phytoplankton biomass. Hyperbolic

Table 5.3.1. Parameter estimates for consumer components of fates of aromatic model (FOAM). See Table 5.3.3 for explanation of abbreviations.

Component	Parameter							
	DMAX (h^{-1})	Q10C	TOPTC (^{o}C)	TMAXC (^{o}C)	RMAX (h^{-1})	Q10R	TOPTR (^{o}C)	TMAXR (^{o}C)
Zooplankton	0.0375	2.0000	25.000	30.000	0.0042	1.8500	30.000	35.000
Benthic Invert	0.0150	2.0000	27.000	32.000	0.0042	2.8500	32.000	37.000
Macro Invert	0.0125	2.0000	25.000	30.000	0.0042	1.8500	30.000	35.000
Bacteria	0.0042	2.0000	27.000	32.000	0.0083	1.8500	32.000	37.000
Carnivore	0.0021	2.3000	27.000	31.000	0.0010	2.1000	30.000	34.000

Component	EXCR (h^{-1})	MORT (h^{-1})	EGEST (h^{-1})	LIPID (%)	DMAX (h^{-1})	QCi (h^{-1})	KP ($g \cdot m^{-2}$)
Zooplankton	0.0042	0.0001	0.0042	0.13	2.4×10^{-5}	4×10^{-6}	1.00
Benthic Invert	0.0042	0.0001	0.0042	0.13	0.00	0.0004	1.00
Macro Invert	0.0042	0.0001	0.0042	0.13	0.00	0.0004	1.00
Bacteria	0.0083	0.0001	0.0042	0.13	0.00	0.0004	1.00
Carnivore	0.0021	0.0001	0.0042	0.13	0.00	0.0004	1.00

Table 5.3.2. Parameter estimates for primary producer components of fates of aromatic model (FOAM). See Table 5.3.3 for explanation of abbreviations.

Component	Parameter								
	PSMAX (h^{-1})	Q10P	TOPTP (^{o}C)	TMAXP (^{o}C)	RMAX (h^{-1})	Q10R	TOPTR (^{o}C)	TMAXR (^{o}C)	EXCR (h^{-1})
Phytoplankton	0.0080	1.4900	20.000	35.000	0.0021	1.8000	30.000	37.000	0.0008
Periphyton	0.0060	1.4900	20.00	35.000	0.0021	1.8000	30.000	37.000	0.0008
Macrophytes	0.0050	1.4900	20.00	35.000	0.0021	1.8000	30.000	37.000	0.0008

Component	MORT (h^{-1})	SINK (h^{-1})	RK (FC)	LIPID (%)	DMAX (h^{-1})	QPi (h^{-1})	KP ($g \cdot m^{-2}$)
Phytoplankton	0.0001	0.0021	5.	0.15	0.00	0.0042	1.00
Periphyton	0.0001	0.0	5.	0.15	0.00	0.0042	1.00
Macrophytes	0.0001	0.0	5.	0.15	0.00	0.0042	1.00

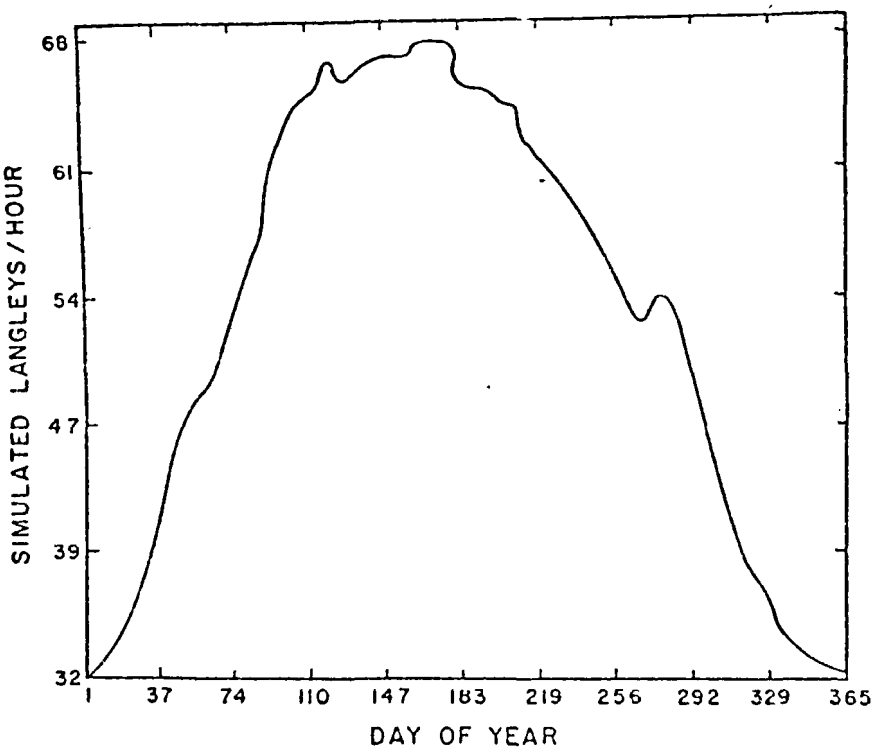

Figure 5.3.2. Simulation of solar radiation by sub-model solar.

Table 5.3.3. Key to parameter abbreviations used in FOAM for consumer and producer components.

DMAX	Maximum depuration rate
Q10C	Temperature dependence for consumption
TOPTC	Optimum temperature for consumption
TMAXP	Temperature of maximum photosynthesis
RMAX	Maximum respiration rate
Q10R	Temperature dependence for respiration
TOPTR	Temperature of maximum respiration
TMAXR	Temperature of which respiration goes to zero
EXCR	Rate of execution
MORT	Rate of mortality
EGEST	Rate of egestion
LIPID	Fraction lipid content
QC	Maximum PAH uptake rate by consumers
KP	Half saturation constant for uptake (half of max solubility)
PSMAX	Maximum photosynthesis rate
Q10P	Temperature dependence for producer
SINK	Sinking rate of phytoplankton
RK	Light saturation of photosynthesis
TMAXR	Temperature upper limit for respiration
QP	Maximum PAH uptake rate by producers
PUC	Uptake rate (flux) of PAH by consumers
PUP	Uptake rate (flux) of PAH by producers

functions provided partial extinction coefficients for each component which were summed to estimate an overall extinction rate used in a first order exponential decay function. Depth in past simulations was 0.21 m. Attenuated light drove the photosynthetic submodel for periphyton. Surface light intensity drove the phytoplankton photosynthesis submodel. Photolytic degradation of PAH was calculated with light intensities at several depths, integrated over the water column.

Photolytic degradation of PAH

Light dependent degradation of aromatic hydrocarbons represents a potentially important mechanism for physico-chemical transformation of these compounds in aquatic systems. Direct photochemical breakdown of dissolved PAH and degradation of photosensitized PAH sorbed to suspended particulates may both be important, however, Zepp and Cline (1977) indicate that indirect photolysis of sorbed PAH is minor in comparison with direct photolytic degradation of dissolved PAH. In the current version of FOAM, only direct photolytic degradation is simulated.

Incident light intensity, R_o, simulated by equation 5.3.3 is attenuated by suspended particulates via a diffuse attenuation coefficient calculated from a relationship (equation 5.3.4) based on published data (Zepp and Cline, 1977).

$$K = 0.20 + 0.00247 \cdot SS \quad (r^2 = 0.77) \qquad 5.3.4$$

where

K = diffuse attenuation coefficient, cm^{-1}

SS = suspended sediments, $mg \cdot \ell^{-1}$

In the subroutine that calculates photolytic degradation of PAH, dissolved PAH, assumed available for photolysis, is converted from units of grams per square meter to moles per liter for use in the equation for photolytic loss (equation 5.3.5) adapted from Zepp and Cline (1977).

$$\frac{d\ PAH_d}{dt} = \phi \Sigma_\lambda (k_\lambda \cdot PAH_d) \qquad 5.3.5$$

where

ϕ = yield coefficient

k_λ = light absorbed at wavelength λ and

PAH_d = dissolved PAH concentration

Reported yield coefficients range between 0.001 and 0.01 for polycyclic aromatic hydrocarbons (Zepp and Schlotzhauer, 1981). A linear regression based upon data presented by Zepp and Schlotzhauer (1981) was calculated to relate yield to molecular weight of PAH compounds with equation 5.3.6 (Figure 5.3.3) $\phi = 0.0235 - 8.38 \times 10^{-5} \cdot$ molecular weight ($r = -0.62$).

The value of k_λ represents light absorbance at wavelength λ by the PAH compound. Values of absorbance (photons $\cdot$ cm^2 $\cdot$ sec^{-1}) were summed at 10 nm increments between wavelengths of 300 and 500 nm, a region of peak absorbance and intense photochemical breakdown for PAH compounds. Each k_λ was calculated as the product of simulated light intensity and a measured molar extinction coefficient, ε_λ, at lambda. Values of ε_λ must be supplied as input to the model by the user.

Hourly light intensity simulated by subroutine solar is attenuated as a function of wavelength following some assumptions concerning the quality of light impinging upon the surface of each reach in the stream of interest. First, we assume that only 12% of the simulated light intensity, R_o is within the 300 to 500 nm range (Zepp and Cline, 1977). According to data presented in Miller and Zepp (1979), we determine the relative composition of light at each 10 nm increment between 300 and 500 nm (Table

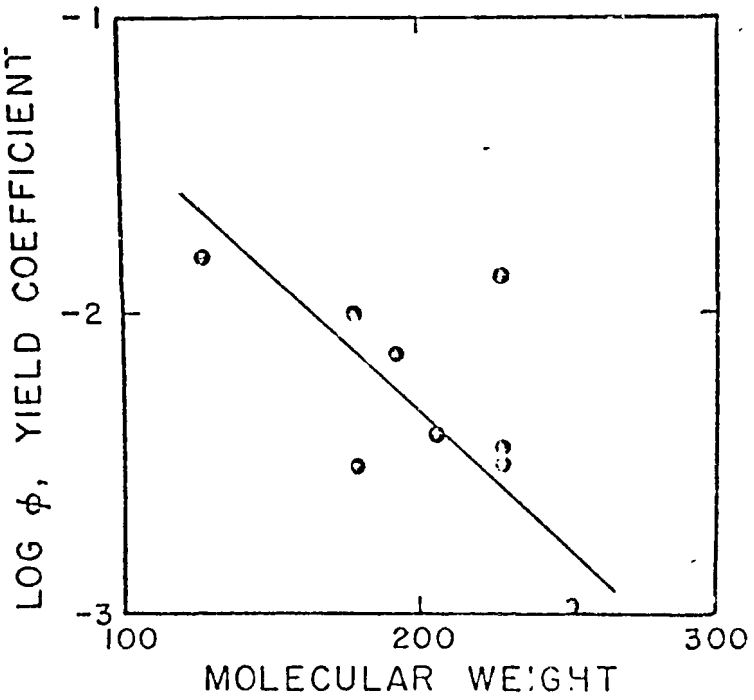

Figure 5.3.3. Log ϕ as a function of PAH molecular weight.

Table 5.3.4. Contribution of light of 10 nm increments to total spectrum between 300 and 500 nm.

Wavelength (nm)	Per Cent of Total
300	0.0050
310	0.1009
320	0.2749
330	1.7309
340	1.9876
350	2.1307
360	2.2715
370	2.5441
380	2.8167
390	3.3619
400	4.8157
410	6.3376
420	6.5193
430	6.2922
440	7.4279
450	8.3593
460	8.4501
470	8.7227
480	8.9499
490	8.4501
500	8.6319

5.3.4). Twelve per cent of R_o is multiplied by the appropriate value in Table 5.3.4 to estimate the incident light at each wavelength. Then, this quantity is attenuated according to an equation fit to the curve of light attenuation versus wavelength (equation 5.3.6) for 12 southeastern rivers (Zepp and Cline, 1979).

$$\alpha_\lambda = 0.42\ e^{(-4.4366\times10^{-3}\cdot\ \lambda)},\ (r^2 = 0.96) \qquad 5.3.6$$

where α_λ has units of cm^{-1}. A depth specific rate of photolysis is calculated at 1.0 cm intervals until either the depth of the reach has been equalled or the depth specific rate is less than 10% the rate calculated at the water surface. The depth specific rates are then integrated over the water column and converted to $g_2 PAH \cdot m_{-1}^{-2} \cdot h^{-1}$. Initial light intensity was converted to photons $\cdot\ cm^{-2} \cdot sec^{-1}$ from $ly \cdot h^{-1}$ by calculating the joules per Einstein for each wavelength λ between 300 and 500 nm at 10 nm increments. While ϕ, the yield coefficient, may reasonably be expected to be a function of wavelength, the model specifies ϕ as a constant for a

given compound over all wavelengths. Differences in photolytic degradation of specific compounds, as simulated by FOAM, occur as a result of a molecular weight dependent value of ϕ and different absorbance characteristics of each compound in the 300 to 500 nm region of the spectrum (Table 5.3.5). Photolytically degraded hydrocarbons were added to the pool of transformed PAH.

Table 5.3.5. Comparison of observed quantum yield coefficients for reaction of PAH in air saturated water to predicted quantum yields based upon regression with molecular weight.

Compound	Mol. Wt.	Predicted[a]	Observed
Napththalene	128	.0219	.0150
Phenanthrene	178	.0075	.0100
Anthracene[b]	178	.0075	.0030
9-Methylanthracene	192	.0055	.0075
9,10-Dimethylanthracene	206	.0041	.0040
Chrysene	228	.0026	.0028
Naphthacene	228	.0026	.0130
Benz(a)anthracene	228	.0026	.0033
Benz(a)pyrene	252	.0015	.009

[a] regression based upon data in Zepp and Schlotzhauer (1981)

[b] omitted from regression analysis, $\log \phi = -0.465 - 0.0093 \cdot$ mol. wt.

$r^2 = 0.87$

Volatilization of PAH

The submodel that quantifies losses of PAH through volatilization in reach j at time t was adapted from Southworth (1981). The rate of volatilization was modeled as a function of current velocity, wind velocity, reach depth and molecular weight of the PAH according to a hyperbolic equation involving Henry's Law (equation 5.3.7).

$$K_L = H \cdot K_g \cdot K_\ell / (H \cdot K_g + K_\ell) \qquad 5.3.7$$

where

H = molar concentration of PAH in air divided by molar concentration of PAH in water

K_g = gas phase exchange constant, $cm \cdot h^{-1}$

K_ℓ = liquid phase exchange constant, $cm \cdot h^{-1}$

The log of H can be estimated from molecular weight of the PAH compound (Zepp and Schlotzhauer, 1979, equation 5.3.8). Similarly, K_g was estimated from equation 5.3.9.

$$\log H = 0.7854 - 0.0191 \cdot \text{molecular weight} \qquad 5.3.8$$

$$K_g = 1137.5 \cdot (V+W) \cdot (18/\text{molecular weight})^{\frac{1}{2}} \qquad 5.3.9$$

where

V = current velocity $(m \cdot sec^{-1})$

W = wind velocity $(m \cdot sec^{-1})$

Values of K_ℓ result from application of two regressions for different wind velocity regimes (equations 5.3.10 and 5.3.11).

$$K_\ell = 23.51\ (V^{0.969}/R^{0.673}) \cdot (32/\text{molecular weight})^{\frac{1}{2}} \qquad 5.3.10$$

$$\text{if } W \leq 1.9\ m \cdot sec^{-1}$$

$$K_\ell = 23.51\ (V^{0.969}/R^{0.673}) \cdot (32/\text{molecular weight})^{\frac{1}{2}} \cdot (e^{0.526(W-1.9)}) \qquad 5.3.11$$

$$\text{if } W > 1.9\ m \cdot sec^{-1}$$

where

R = water depth (m)

FOAM uses calculated current velocities plus a user supplied wind regime in the volatilization model.

Microbial Biotransformation of PAH

Metabolic degradation of assimilated PAH is modeled as a function of respiration rate and was therefore indirectly affected by water temperature. Respiration was multiplied by $DMAX_i$ for compartment i. The units of $DMAX_i$ are grams PAH metabolized per gram dry weight respired per time. At present, all DMAX values are set at zero.

Sorption of PAH

Polycyclic aromatic hydrocarbons may be quickly lost from solution as a result of sorption to suspended particulate matter and settled sediments. Sorption to particulate matter provides a possible entry to the aquatic food web via filter feeding or sediment feeding animals.

The sorption sub-model in FOAM was based heavily upon data provided in Karickhoff et al. (1979) where the sorption of PAH was modeled as a first order relationship between dissolved PAH in the water and partitioning coefficient, Kp. The partition coefficient increased linearly as a function of the organic content of the sorbent material. The partition coefficient also correlated with the octanol/water partition coefficient (K_{ow}) of the PAH.

Depending upon available data, FOAM calculates rates of sorption in one of three ways. First, if K_{ow} and the organic fraction of the sorbent were known, a partition coefficient is calculated from equations 5.3.12 - 5.3.15.

$$K_p = K_{oc} \cdot oc \qquad 5.3.12$$

where

$$\text{Log } (k_{oc}) = \text{Log } (K_{ow}) - 0.21 \qquad 5.3.13$$

oc = fractional organic content of the sorbent.

Second, if K_{ow} is not known, k_{oc} is estimated from the solubility of the particular PAH:

$$\text{Log } (K_{oc}) = -0.54 \cdot \text{Log}(s) - 0.44 \qquad 5.3.14$$

where

s = solubility of the PAH mole fraction

Solubility can be estimated from molecular weight (Figure 5.3.4). Third, if neither k_{ow} nor the organic fraction of the sorbent were known, a partition coefficient was estimated directly from:

$$\text{Log}(K_p) = 4.16 - 0.51 \cdot \text{Log}(s) \qquad 5.3.15$$

where

s = solubility of the PAH, ppm

Equation 5.3.15 resulted from further analysis of data presented by Karickhoff et al. (1979).

Values of K_p were converted to units of inverse time by dividing by the duration of experiments (24h) of the experiments which generated data

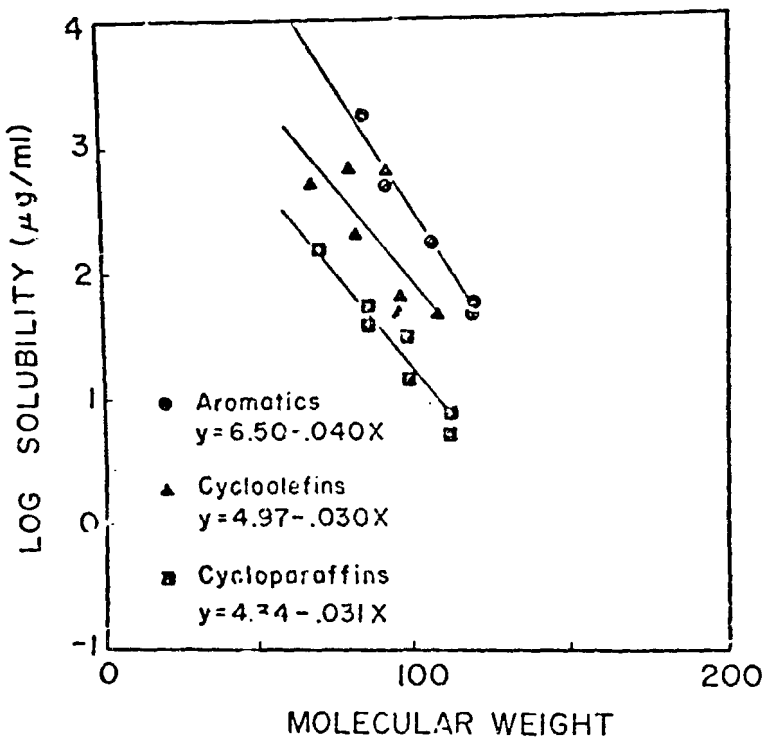

Figure 5.3.4. Log solubility of PAH in water as a function of PAH molecular weight.

for the regressions (equations 5.3.14 - 5.3.16). Because the experiments were performed with PAH concentrations that approached the maximum solubility of the compounds and because the sorbent was suspended by continuous stirring, we assumed that the K_p values provided estimates of a maximum rate of sorption, S_{max}. At each iteration of the model, the specific rate of sorption is calculated from equation 5.3.16.

$$S = S_{max} \cdot SBATE \cdot SBENT \cdot oc \; / \; [SBATE + (SBENT \cdot oc)] \qquad 5.3.16$$

where

S = rate of sorption, $gPAH \cdot m^{-2} \cdot h^{-1}$

S_{max} = maximum sorption rate, $\ell \cdot h^{-1}$

$SBATE$ = soluble PAH, $g \cdot m^{-2}$

$SBENT$ = sorbent, $g \cdot m^{-2}$

Biological Production Sub-model

Primary producers

Rates of biomass change were determined by first order mass balance differential equations. The overall biomass equation for producer i in reach j at time t (phytoplankton, periphyton, and macrophytes) is represented by equation 5.3.17.

$$\frac{dP_i}{dt} = (FI_i - FO_i) + P_i (PS_i - R_i - M_i - U_i - S_i) - G_i \qquad 5.3.17$$

where

P_i = biomass, g dry wt $\cdot m^{-2}$

FI_i = inflow of P_i from reach j-1

FO_i = outflow of P_i from reach j

PS_i = photosynthetic rate of P_i

R_i = respiration rate of P_i

M_i = non-predatory mortality rate

U_i = excretion rate

S_i = sinking rate

G_i = grazing loss of P_i

Photosynthesis

In FOAM, gross photosynthesis (of phytoplankton; periphyton and macrophytes) was modeled after Smith (1936) (equation 5.3.18).

$$P_{ijt} = f(T) \cdot P_{max} \cdot I(I_k^2 + I^2)^{-\frac{1}{2}} \qquad 5.3.18$$

where

P_{ijt} = photosynthesis per unit producer i in reach j at time t

P_{max} = light saturated photosynthetic rate for producer i

I = light intensity supplied by solar submodel

I_k = light saturation constant for producer i

$f(T)$ = temperature function, (equation 5.3.2)

Values of parameters for three primary producers in FOAM are listed in Table 5.3.2.

Consumption

Food consumption provided energy for biomass production and another potential PAH source to the non-photosynthetic biological components of FOAM. Consumption is modeled as a function of predator and prey biomass after DeAngelis et al. (1975) (equation 5.3.19).

$$C_{i,j} = f(T) \frac{C_{maxi} \cdot B_i \cdot W_{ij} \cdot B_j}{B_i + \sum_j (W_{ij} \cdot B_j)} \qquad 5.3.19$$

where

$C_{i,j}$ = input of prey j biomass to consumer i

C_{maxi} = maximum feeding rate of consumer i (day^{-1})

B_i = consumer biomass ($g \cdot m^{-2}$)

B_j = prey j biomass ($g \cdot m^{-2}$)

W_{ij} = Bayesian preference of predator i for prey j (unitless)

$f(T)$ = temperature dependent modifier of consumption rate (equation 5.3.2).

The behavior and stability properties of this function have been studied (De Angelis et al., 1975). This equation has been usefully applied to model feeding by zooplankton, benthic invertebrates and fish (Kitchell et

al., 1974; O'Neill, 1976; Smith et al., 1975). Figure 5.3.5 represents the prey items allowed for each consumer by FOAM. When prey are plentiful, consumption, C_{ij}, is proportional to predator biomass. Conversely, prey abundance regulates consumption in equation 5.3.19 when prey are scarce. The Bayesian parameter, W_{ij} (Table 5.3.6) can be estimated from data quantifying the relative abundance of prey j in predator i stomach samples and the relative abundance of prey j in the environment (O'Neill, 1971).

Foodweb transfer of PAH was modeled as C_{ij} multiplied by the PAH concentration in prey j summed over all j for consumer i. FOAM can therefore be used to examine the relative importance of direct uptake of PAH by consumers in association with respiration and trophic transfer of PAH through the foodweb. Appreciable amounts of polychlorinated biphenyls have been shown to accumulate from consumptive processes, especially at higher trophic levels (Weininger, 1978). Behavior of PAH's in this regard was essentially unknown. Calculation of the PAH derivative for P_i results from multiplying each term in equation 5.3.17 by the fractional PAH concentration of P_i and adding two terms that quantify PAH uptake and degradation as functions of photosynthesis and respiration, respectively (equation 5.3.20)

$$H_i = (Q_i \cdot PU_i \cdot PAH_d) \; / \; (K_i + PAH_d) \qquad 5.3.20$$

In equation 5.3.21 H_i ($g \cdot m^{-2} \cdot t^{-1}$) was the rate of PAH uptake mediated by photosynthesis, PAH_d was dissolved PAH ($g \cdot m^{-2}$) available for uptake and PU_i was a linear function of photosynthetic rate (equation 5.3.21)

$$PU_i = m \cdot PS_i \qquad 5.3.21$$

where

PU_i = g PAH assimilated per g producer i per time

PS_i = photosynthetic rate of producer i, $g \cdot g^{-1} \cdot t^{-1}$

m = slope, of PAH taken up per g photosynthetically fixed biomass

Respiratory mediated PAH biotransformation is represented by equation 5.3.22.

$$D_i = R_i \cdot d_i \cdot P_i \cdot h_i \qquad 5.3.22$$

where

D_i = rate of PAH degradation by producer i

d_i = fraction of respiration used to degrade PAH

h_i = fractional PAH content of P_i

R_i = temperature dependent respiration rate of P_i

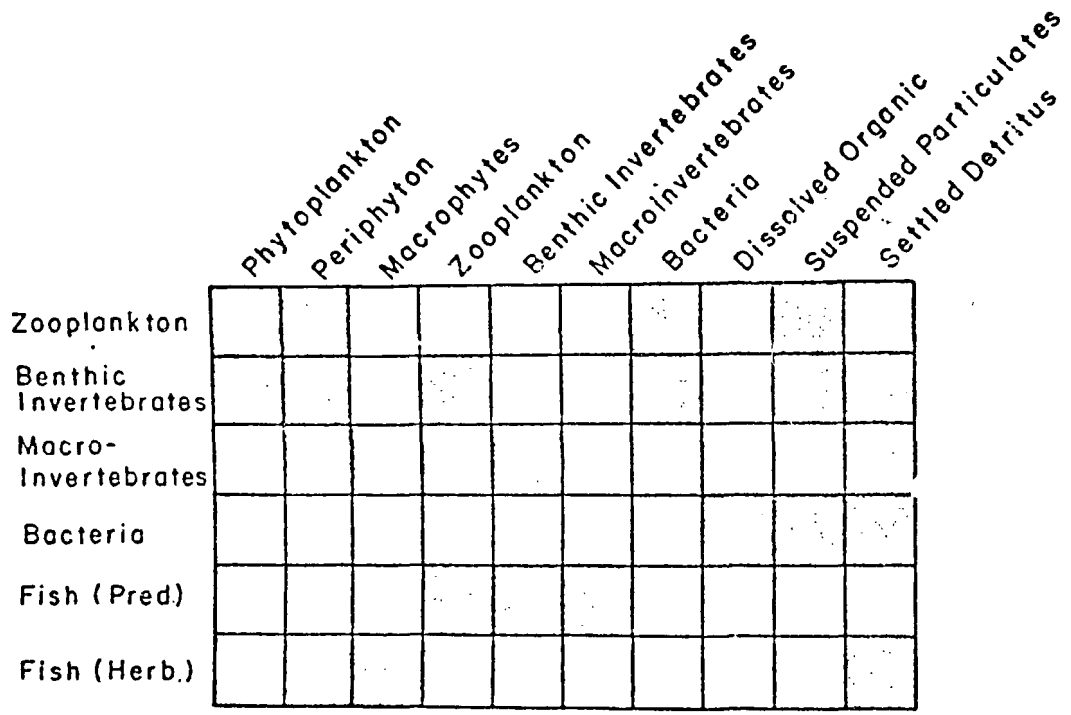

Figure 5.3.5. Matrix of consumers and food items which are considered by the production portion of FOAM.

Table 5.3.6. Continued

Predator	Food Item j						
	Predatory Fish	Herbivorous Fish	Suspended Organics	Dissolved Organics	Sediments	Suspended Inorganics	Settled Detritus
Zooplankton	0.0	0.0	0.1	0.0	0.0	0.1	0.0
	0.0	0.0	0.9	0.0	0.0	0.01	0.0
Benthic Invertebrates	0.0	0.0	0.9	0.0	0.0	0.01	0.0
	0.0	0.0	0.0	0.0	0.05	0.01	0.4
Clams	0.0	0.0	0.0	0.0	0.0	0.0	0.2
	0.0	0.0	0.0	0.0	0.0	0.0	0.2
Bacteria	0.0	0.0	0.25	0.25	0.0	0.0	0.5
	0.0	0.0	0.90	0.90	0.0	0.0	0.75
Fish (PRED)	0.0	0.0	0.0	0.0	0.0	0.0	0.0
	0.0	0.0	0.0	0.0	0.0	0.0	0.0
Fish (Herb)	0.0	0.0	0.0	0.0	0.5	0.0	0.15
	0.0	0.0	0.0	0.0	0.10	0.0	0.40

Consumer organisms

The overall mass balance equation for consumer compartment biomass is given by equation 5.3.23

$$\frac{dN_i}{dt} = (FI_i - FO_i) + \sum_j C_{ij} - N_i (R_i + F_i + U_i + M_i) - G_i \qquad 5.3.23$$

where

N_i = biomass of consumer i in reach at 5, (g dry wt $\cdot$ m^{-2})

C_{ij} = rate of consumption of prey j by consumer i

R_i = temperature dependent respiration rate of consumer i

F_i = fraction of ingested food that is egested

U_i = rate of biomass lost through excretion

M_i = natural mortality rate of i

G_i = predatory losses of i

FI-FO = net convective transport of consumer i

Respiration

For producers, a fraction of photosynthesis or for consumers, a fraction of standing crop is lost through respiration. Respiration was modeled as a temperature-dependent function by specifying an R_{max} value, which occurs at T_o, for each biological compartment.

For consumers, a respiration dependent direct uptake of PAH was included in FOAM. A limited amount of evidence suggests that Daphnia concentrate PAH in its lipid tissue (Southworth et al., 1978). These data further suggested an active uptake mechanism which resulted in steady-state concentrations after approximately 24 h. In FOAM, a hyperbolic function which relates respiratory rate and lipid concentration in the biomass is used to simulate direct PAH uptake by zooplankton, benthic invertebrates, macroinvertebrates and carnivores.

Biotransformation of PAH parent compound is modeled as a function of respiration rate. A variable fraction of the body load is removed from all biological compartments as a function of respiration rate. Biotransformation products are shunted to a dissolved pool of biotransformation products that acts as a final sink.

Excretion

It is assumed that part of the biomass of the plant and animal components is lost through excretion. Secretion might be a more appropriate interpretation of this process in plant metabolism. Excretion is modeled in a linear fashion. It is further assumed that PAH is lost through excretion in proportion to the concentration of PAH in the biomass component.

Rates of excretion (Tables 5.3.1 and 5.3.2) multiplied by the biomass in each component to calculate g, dry wt excreted$\cdot m^{-2} \cdot h^{-1}$ by each biological component. Multiplication of these rates by the concentration of PAH in each biological component, results in estimates of PAH excreted$\cdot m^{-2} \cdot h^{-1}$ by the biota. The model internally tracks the PAH concentration in each compartment during the simulation.

Mortality

As for excretion, it is assumed that a constant fraction (Tables 5.3.1 and 5.3.2) of biomass is lost from each compartment as the result of non-predatory mortality. Again, multiplication of mortality losses by the concentration of PAH in the biomass produces PAH losses to mortality.

Sinking losses

Phytoplankton sinking losses are modeled separately from settling of suspended particulate matter. Future versions of FOAM could incorporate more realistic coupling between hydraulic aspects of the model and net suspension of both phytoplankton and suspended particulate matter. Periphyton and macrophyte mortality are added to the sediment organic pool via the KSTL parameter. The sinking rate used is 0.0021 h^{-1}.

Egestion

A fraction of the consumed food is egested by the consumer components of the model (Tables 5.3.1 and 5.3.2). Egestion losses enter the suspended particulate pools for both biomass and PAH. Egested PAH is the product of egestion rate (0.0042 h^{-1}) and PAH concentration of the food item.

Direct uptake of dissolved PAH by producers and consumers.

Uptake of PAH by plants was modeled as a second order, non-linear Michaelis-Menten process (equation 5.3.24).

$$PU_i = P_i \cdot Q_i \cdot PAH/(KP_i + PAH) \qquad 5.3.24$$

where

PUC_i or PUP_i = uptake of PAH by producer (P) or consumer (C) i

P_i = biomass (g, dry wt·m^{-2}) of producer i

QP_i or QC_i = maximum uptake rate of PAH by producer (P) or consumer (C) i, (g PAH/g, dry wt·h^{-1})

PAH = dissolved PAH concentration (g PAH·m^{-2})

KP_i or KC_i = analagous to a half-saturation constant (g PAH·m^2)

Direct uptake by the producers was assumed, in the model, to be independent of photosynthetic or respiration rates. Q_i was 20 g PAH · g^{-1}, dry weight producers·h^{-1}. This constant was derived from laboratory accumulation studies and was specific for anthracene in this case. However, the Monod model was used so that structure/activity relationships could be used in future versions of the model. The Monod model is a relatively simple relationship to describe the saturation phenomenon observed in periphyton.

Direct uptake by consumers was coupled to the rate of respiration with the assumption that direct uptake takes place across respiratory membranes and is an active process. The equation is similar to (O'Neill et al., 1972), except respiration rate, $RSMAX_j$, appears in the numerator as a multiplier of Q_i and Q_i has units of g PAH accumulated·g^{-1}, dry wt·h^{-1}. Q_i was 42 · h^{-1} for all consumer components.

External loading

Polycyclic aromatic hydrocarbons enter the artificial streams by external loading of dissolved PAH from the head tanks. This is reproduced in the model structure, where dissolved PAH enters the uppermost reach as the product of the pre-defined discharge regime (m^3·day^{-1}) and the PAH concentrations of the influent (g PAH·m^{-3}). Future versions of FOAM could accomodate several point sources per reach.

A statistical relationship between solubility and molecular weight of PAH compounds was derived from published data (Braunstein et al. 1977) (equation 5.3.25 and Figure 5.3.4).

$$\log (PAH_d) = 6.50 - 0.04 \cdot \text{mol. wt.}, \quad r^2 = 0.77 \qquad 5.3.25$$

This regression was used to estimate solubility of a specific PAH and ensure that solubility constraints were obeyed throughout the simulation. PAH in excess of solubility limits was shunted to the sediments.

Initial conditions

Estimates of initial conditions (g dry wt $\cdot$ m^{-2}) of the biota for all 5 reaches were derived from previous experimental work at the channels microcosm facility, located on the Savannah River Plant site (Giesy et al., 1979) (Table 5.3.7). Each biological component of the system is discussed in greater detail in this section. Simulations of other aquatic systems would require parameterization for that system. Alternatively, for simulation to compare fates among compounds a generalized system could be parameterized.

Table 5.3.7. Initial biomass conditions for simulations reported here g dry weight $\cdot$ m^{-2}.

Compartment	Reach 1	2	3	4	5
Phytoplankton	0.0	0.0	0.0	0.0	0.0
Periphyton	0.18	0.18	0.18	0.18	0.18
Macrophytes	1.54	0.3	0.3	0.3	0.3
Zooplankton	0.0	0.0	0.0	0.0	0.0
Benthic Invertebrates	0.5	0.5	0.5	0.5	0.5
Clams	0.2	0.2	0.2	0.2	0.2
Bacteria	0.1	0.1	0.1	0.1	0.1
Predatory Fish	0.1	0.1	0.1	0.1	0.1
Herbivorous Fish	0.2	0.2	0.2	0.2	0.2
Suspended Organic Particulates	0.05	0.05	0.05	0.05	0.05
Dissolved Organic Matter	0.01	0.01	0.01	0.01	0.01
Sediments	1.0	1.0	1.0	1.0	1.0
Suspended Inorganic Matter	0.01	0.01	0.01	0.01	0.01
Settled Detritus	0.55	0.55	0.55	0.55	0.55

Primary procedures: phytoplankton, periphyton, macrophytes

Phytoplankton contribute to the production dynamics of large, slow moving rivers; however, previous experience with the SREL channels microcosms indicated that phytoplankton do not contribute substantially to overall system production. While parameters for phytoplankton growth and PAH metabolism have been generated for this model component, initial biomass was defined as zero for the current simulations (Table 5.3.7).

The algal component of the aufwuchs community was measured to be approximately 2 percent of the live volume (Giesy et al., 1979), of which members of the Chlorophyta and Cyanophyta comprised more than 95%. In 1977, algal volume collected from a reference channel ranged between 6 and 12 $cm^3 \cdot m^{-2}$. Assuming a density of 1.0, this volume translated to 0.12 - 0.24 $g \cdot m^{-2}$. Initial conditions for current simulations were defined as the midpoint of this observed range, 0.18 $g \cdot m^{-2}$.

Macrophyte flora that commonly colonized the artificial channels in past research included Juncus diffusissimusi, Gratiola virginiana, Callitriche heterophylla and Bacopa caroliniana. Colonization was assisted by transplants of J. diffusissimus which subsequently dominated the biomass of the macrophytic vegetation in the channels. Estimates of standing crop from the work of Giesy et al. (1979) suggested spatial heterogeneity in distribution of J. diffusissimus, with the greatest abundance upstream. Initial macrophyte biomass in the first reach was defined as 1.54 g dry wt $\cdot m^{-2}$. The remaining reaches were each set at 0.03 g $\cdot m^{-2}$.

Consumer components: zooplankton, benthic invertebrates, macroinvertebrates, bacteria, fish

As in the case of phytoplankton, pelagic zooplankton were assumed to be insignificant in the overall production dynamics of the SREL channels microcosms. While parameters have been defined for the growth and PAH metabolism by zooplankton, this component was initialized as zero for current simulations.

The benthic invertebrate component in the model is derived to simulate the growth and PAH dynamics of stream insects including the orders Ephemeroptera, Odonata, Coleoptera and families Notonectidae, Corixidae, Centropogonidae and Chironomidae. An estimate of their combined standing crop in previous research in the channels (Giesy et al., 1979) was 0.5 g dry wt per m^2. This value was used as an initial condition for all five reaches.

The macroinvertebrate compartment was defined to include larger invertebrate organisms such as crayfish and clams that have been incorporated in previous ecological studies involving the SREL channels microcosms. This compartment represents a complex fauna in natural systems; however, species used in the channels included Corbicula fluminea (Asian clam), Anodonta imbecilus (papershell clam), and Procamberus acutus acutus (crayfish). In experimental tests of the model, individual C. fluminea were

added and constrained in each reach by wire mesh. Clam biomass was 0.2 g dry wt·m^{-2} in each reach. Bacterial biomass was arbitrarily defined as 0.1 g dry wt · m^{-2}. In experimental tests of the model, 10 juvenile bluegill sunfish (Lepomis macrochirus) were caged in each reach. Fish biomass was estimated as 0.1 g dry wt · m^{-2}.

The biological state variable for simulations of the dynamics of anthrcene in the channels microcosms facility are given in Tables 5.3.8 and 5.3.9. The physical parameters for simulating volatilization and photolysis of anthracene in the channels microcosms are given in Tables 5.3.10 and 5.3.11.

Table 5.3.8. Biological state variables for simulation of anthracene dynamics. See Table 5.3.3 for explanation of abbreviations.

PRODUCERS	PSMAX (/HR)	Q10P	TOPTP (C)	TMAXP (C)	RMAX (/HR)	Q10R	TOPTR (C)	TMAXR (C)	EXCR (/HR)	MORT (/HR)	SINK (/HR)	RK (LY/H)
Photoplankton	0.3000	1.4900	20.000	35.000	0.1000	2.3000	27.000	31.000	0.0300	0.0001	0.0021	5.4
Periphyton	0.0300	1.4900	20.000	35.000	0.1000	1.8000	30.000	37.000	0.0300	0.0001	0.0	5.4
Macrophytes	0.0200	1.4900	20.000	35.000	0.1000	1.8000	30.000	37.000	0.0300	0.0001	0.0	5.4

CONSUMERS	CMAX (/HR)	Q10C	TOPTC (C)	TMAXC (C)	RMAX (/HR)	Q10R	TOPTR (C)	TMAXR (C)	EXCR (/HR)	MORT (/HR)	EGEST (/HR)
Zooplankton	0.0375	2.0000	25.000	30.000	0.0080	1.8500	30.000	35.000	0.0042	0.0001	0.0042
Benth Invert	0.0150	2.0000	27.000	32.000	0.0042	1.8500	32.000	37.000	0.0042	0.0001	0.0042
Macro Invert	0.0125	2.0000	25.000	30.000	0.0042	1.8500	30.000	35.000	0.0042	0.0001	0.0042
Bacteria	0.0042	2.0000	27.000	32.000	0.0083	1.8500	32.000	37.000	0.0083	0.0001	0.0042
Fish (Pred)	0.0021	2.3000	27.000	31.000	0.0005	2.1000	30.000	34.000	0.0022	0.0001	0.0042
Fish (Herb)	0.0021	2.3000	27.000	31.000	0.0005	2.1000	30.000	34.000	0.0021	0.0001	0.0042

Table 5.3.9. Biological state variables for anthracene dynamics simulation.

	Lipid Content (%)	Maximum[a] Uptake (QMAX)	Uptake half[b] Saturation Constant	Minimum[c] Depuration DMAX
Producers				
Phytoplankton	15	$2x10^{-6}$	1.0	$2.4x10^{-5}$
Periphyton	"	"	"	"
Macrophytes	"	"	"	"
Consumers				
Zooplankton	13	$4.2x10^{-6}$	"	"
Benthic Invertebrates	"	"	"	"
Clams	"	"	"	"
Bacteria	"	"	"	"
Predatory Fish	"	"	"	"
Herbivorous Fish	"	"	"	"

[a] a_h^{-1}

[b] b_g PAH$\cdot m^{-2}$

[c] c_h^{-1}

Table 5.3.10. Parameters for the simulation of volatilization of anthracene.

Gas phase constant, $K_g = 3.6 \times 10^{2}$
liquid phase constant, $K_\ell = 1.8 \times 10^{-1}$
overall rate constant, $KL = 7.3 \times 10^{-3}$

Table 5.3.11. Parameters for photolytic degradation of anthracene. Quantum yield coefficient = 7.5×10^{-3}.

Wave length (nm)	Molar extinction coefficient
300	4.84×10^{2}
310	1.17×10^{3}
320	1.90×10^{3}
330	2.1×10^{3}
340	4.9×10^{3}
350	3.4×10^{3}
360	4.8×10^{3}
370	3.2×10^{3}
380	2.7×10^{3}
390	5.4×10^{2}
400	2.2×10^{1}

SECTION 5.4

SIMULATION OF ANTHRACENE IN CHANNELS MICROCOSMS

RESULTS AND DISCUSSION

Water

FOAM was used to simulate a constant infusion of 0.056 $\mu mol \cdot \ell^{-1}$ of anthracene into the uppermost reach of the experimental channels. Parameter estimates were based solely upon laboratory measurements or published data; only the initial conditions were measured in the channels.

During daylight hours the model predicts a decrease from 0.056 to 0.036 µmoles in a distance of 81 meters, between reach one and reach five. At night, this concentration gradient is absent and all reaches exhibited a concentration similar to the input concentration. Regardless of light conditions, reach one exhibited a constant anthracene concentration of 0.056 µmol anthracene$\cdot\ell^{-1}$. The model predictions compared favorably with the average day and nighttime measurements made in the channels (Table 5.4.1). Simulated values were somewhat lower, and the rate of loss downstream was slower in the model. Nevertheless, the general behavior of the dissolved "pool" was predicted by the model. When the constant infusion was stopped, the concentration of dissolved anthracene quickly decreased to 0.006 $nmol \cdot \ell^{-1}$ within 24 h.

Table 5.4.1. Predicted and observed concentrations of dissolved anthracene in channels microcosms.

Time	µmol anthracene$\cdot\ell^{-1}$ Reach 1	Reach 3	Reach 5
Dawn			
observed	.066	.065	.063
predicted	.056	.056	.055
Noon			
observed	.067	.045	.028
predicted	.056	.045	.036

Sediments

Simulations of anthracene dynamics in the channels microcosms predicted that the bottom sediments would accumulate anthracene linearly. Steady-state concentrations of 0.09, 0.004 and 0.0035 $\mu mol \cdot g^{-1}$, dry weight were predicted for reaches 1, 3 and 5, respectively (Figure 5.4.1). The simulation predicted a rapid desorption of anthracene from the sediments, which was not consistent with the p tern observed in the channels microcosms (Table 5.4.2). FOAM also underestimated the rate of flux into the sediments. The simulation model did, however, predict a downstream gradient of anthracene concentrations in the sediments similar to the observed gradient.

The routines to simulate sorption will need to be improved to give better predictability in future simulation models. Sorption to sediments is complicated by resuspension, transport and convective processes, which are difficult to represent by either deterministic or statistical models. Long term simulations will be affected by large rainfall events, which may cause great deviations from the patterns of sediment transport throughout most of an annual cycle. The scaling of such events will probably be such that good predictability will only be available on geologic time scales and will cause large uncertainties in short-term simulations. Even beyond this, differences in diffusion rates and micro-dynamics have not yet been adequately described by FOAM to predict anthracene dynamics in bottom sediments. Descriptions of thoroughly mixed suspended sediments are much more adequately described by FOAM and other existing relationships. We suggest that more research on sediment sorptive and desorptive processes as well as interfacing to sediment transport models is required before PAH concentrations in this important PAH accumulating matrix can be made.

Periphyton

The simulated anthracene dynamics in periphyton showed a rapid uptake to a quasi-equilibrium concentration of about 0.17 $\mu mol \cdot g^{-1}$ dry weight, by day 3 (Figure 5.4.2). Anthracene concentrations in the periphyton decreased downstream and are greater at night in all reaches. These patterns probably reflect both the greater concentration of dissolved anthracene at night and the initial assumption that depuration rate is physiologically coupled to photosynthesis. This assumption is probably violated because some depuration is due to passive diffusion from the surface and interior of the cells. The day-night pattern results in the broad envelope of anthracene observed in periphyton in the simulations represented in Figure 5.4.2.

The steady state concentration of anthracene in periphyton predicted by the simulation was similar to the results observed in the channels. However, the great variability in measured anthracene concentrations made comparisons difficult (see Section 6.4). The 2 SE confidence intervals for the steady state anthracene concentrations measured in periphyton from the channels microcosm ranged from 0.07 to 0.15 $\mu mol\ anthracene \cdot g^{-1}$ dry weight, which was in the same range as the simulated concentrations (Figure 5.4.2).

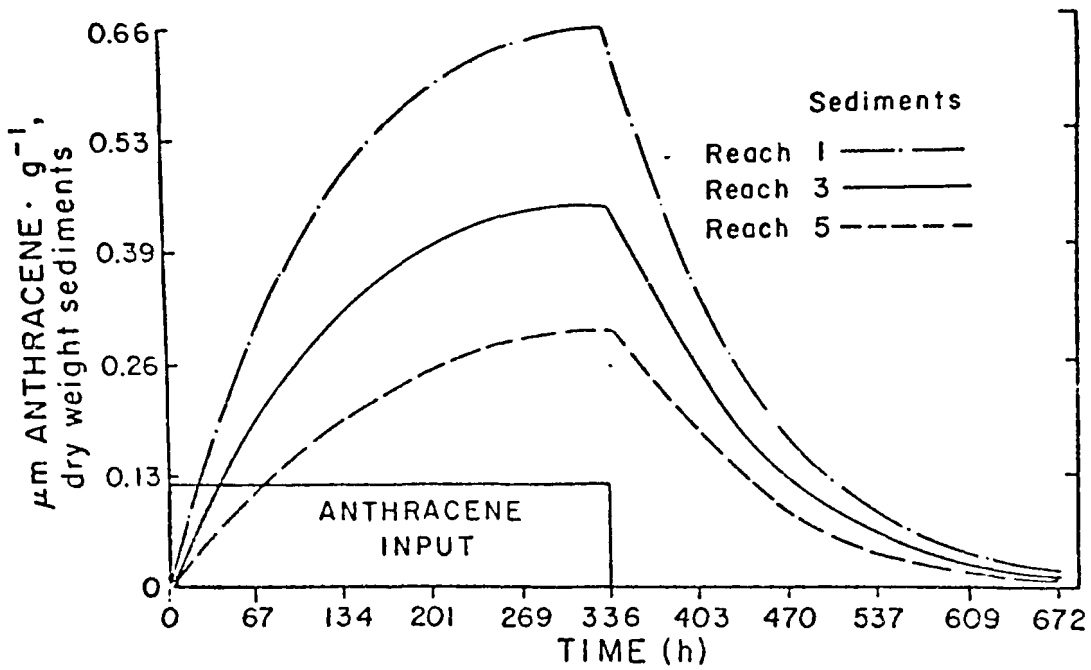

Figure 5.4.1. Simulation of anthracene dynamics in bottom sediments of the channels microcosms.

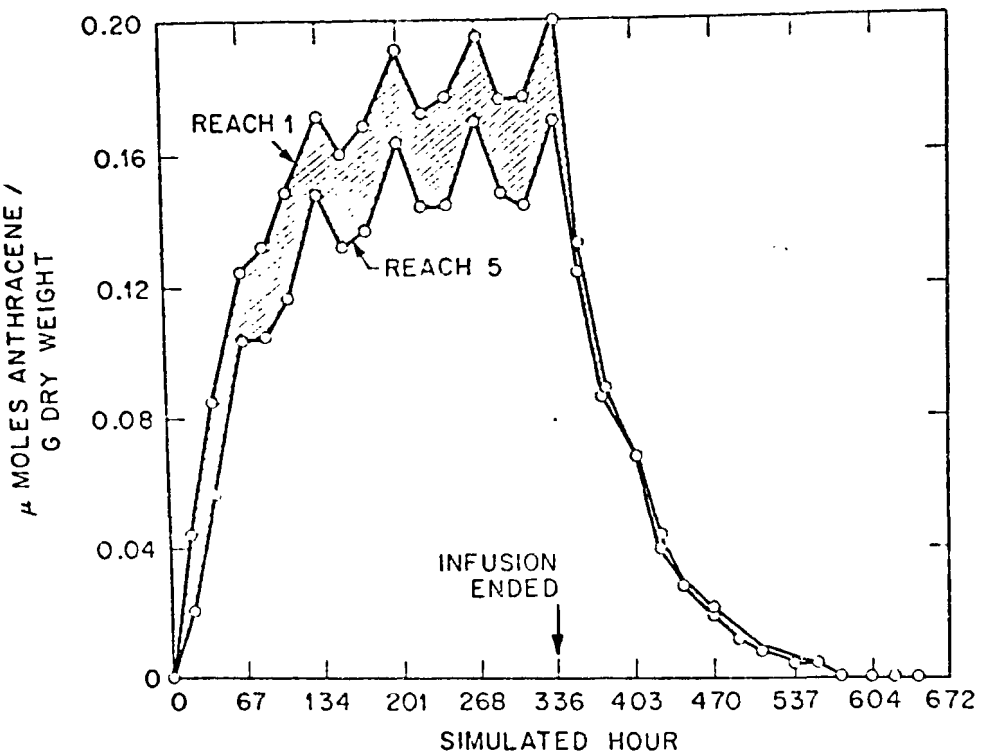

Figure 5.4.2. Simulated concentration of anthracene in periphyton through time in reaches 1 and 5. Hatched area contains transient concentrations for reaches 2 - 4.

Table 5.4.2. Comparison of predicted and observed concentrations of anthracene in stream sediments.

Time (h)	Anthracene Concentration ($\mu mol \cdot g^{-1}$, dry weight) Reach 1 Obs	Reach 1 Pre	Reach 3 Obs	Reach 3 Pre	Reach 5 Obs	Reach 5 Pre
24	.0024	.00026	.0023	.00020	.0021	.00017
67	.0044	.00059	.0040	.00045	.0034	.00037
134	.0070	.0014	.0060	.00096	.0053	.00080
201	.0096	.0027	.0086	.0018	.0073	.0015
269	.0149	.0073	.0134	.0040	.0123	.0033
336	.0137	.0079	.0118	.0041	.0106	.0034
403	.0108	.0084	.0104	.0043	.0104	.0035
470	.0113	.0092	.0116	.0044	.0107	.0035
537	.0092	.0096	.0076	.0044	.0065	.0035
672	.0072	.0092	.0065	.0042	.0053	.0034

Parameter values for anthracene uptake were derived from experimental work with cultures of periphyton grown on glass slides in natural streams located on the SRP. The uptake kinetics were determined for these actively growing cultures (see Section 4.4). Periphyton in the artificial channels was comprised of less luxuriant growth. Extrapolation of laboratory determined uptake kinetics, via the model, to the field situation seems to be justified in this case. However, the comparison between half-lives of anthracene in simulated periphyton and that measured for periphyton shows the model results to be in close agreement. The depuration rate constant determined in the laboratory studies with natural cultures appears to be a reasonable estimate of the rate of depuration by periphyton in the channels. During daylight hours, photolysis reduced the dissolved anthracene concentration, making less compound available for uptake. In addition, the depuration process of the periphyton should be operating to reduce the concentration of anthracene in periphyton. In absolute terms, the equilibrium concentration does not agree within two orders of magnitude with the anthracene concentrations measured in the periphyton in the channels. The half-time for elimination of anthracene in periphyton following termination

of the constant input, however, agrees within 2-3 h with the measured half-time for elimination of anthracene from periphyton in the channels. Uptake might have been overestimated in the model, as parameters for uptake rate were derived from actively growing cultures of periphyton that colonized glass slides placed in streams located on the Savannah River Plant site. Whereas, the periphyton in the channels microcosms did not appear to be growing at the rate of the cultured plants and consisted of a different flora.

Clams

The simulation of anthracene predicted that the maximum anthracene concentration in clams would not be attained until after the anthracene input was terminated (Figure 5.4.3). This is because the simulation model assumes that the clams are accumulating anthracene both directly from the water and from suspended particulates, which still had anthracene associated with them after the anthracene input was terminated. The maximum was reached earlier in reach 1 than 3 or 5 because the amount of anthracene associated with suspended particulates was greatest downstream. The maximum anthracene concentration was attained in clams in reach 3 because this reach had the greatest exposure concentration between water and particulates.

The concentration of anthracene predicted to be in the soft tissues of clams at the time of termination of anthracene input was 4.16 μmol anthracene· g^{-1} dry weight of soft tissue (Figure 5.4.3). This is equivalent to 740 $\mu g \cdot g^{-1}$, dry weight, which is greater than the 16.6 $\mu g \cdot g^{-1}$, dry weight, actually observed in clams exposed to approximately 10 $\mu g \cdot \ell^{-1}$ anthracene in the channels. This value is probably an overestimate of actual accumulation because the simulation allows uptake from particulates, which have been shown to be less important for accumulation of PAH by clams than accumulation directly from water (Dobroski and Epifanio, 1980). Also the model assumes that filtering is a continuous process, which was not observed in the channels microcosms. The clams living in the channels were also under environmental stress (Giesy et al., 1979) because of factors other than anthracene, which may have reduced the frequency and rate of filtering as well as metabolism.

FOAM considers a component which we have called benthic invertebrates. This term is somewhat misleading and needs to be defined here. We have considered only macroinvertebrates such as insects and oligochetes and not protozoans in this class of organisms. FOAM also includes another macroinvertebrate component which for the anthracene simulation is the clam component. This component can also be used to include other macroinvertebrates such as crayfish. If better precision of accumulation by clams is desired, this component needs to be separated and better mechanistic predictions made.

The results of the simulation of anthracene dynamics in benthic macroinvertebrates cannot be compared to analogous results from the channels microcosm because the benthic macroinvertebrate community had not developed

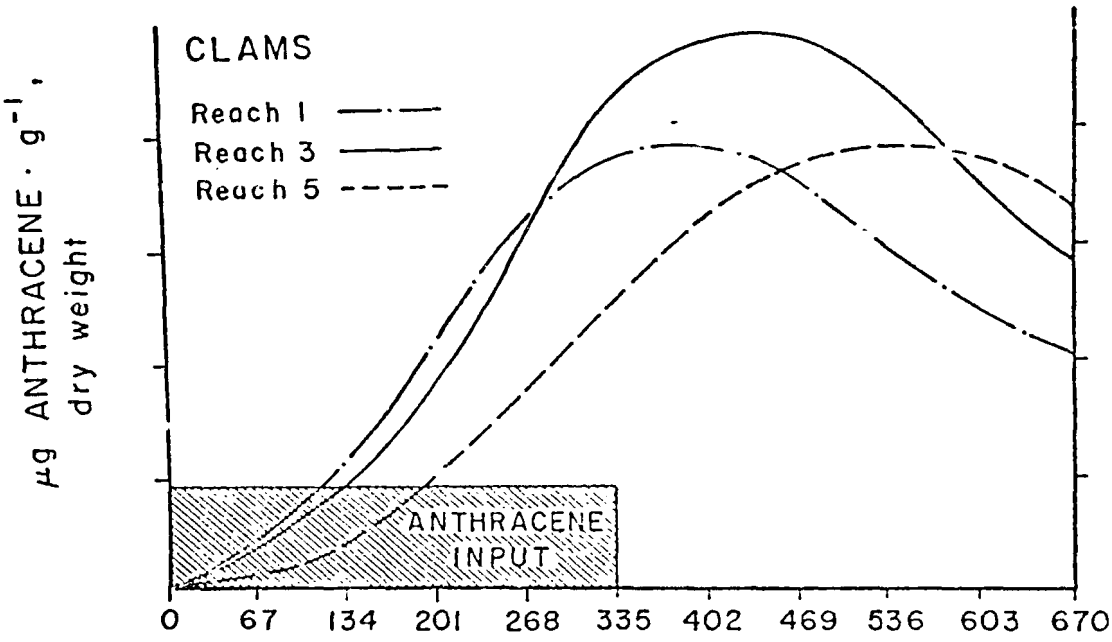

Figure 5.4.3. Simulation of anthracene dynamics in clams in channels microcosm.

to a great enough extent to allow sampling of enough biomass for representative, destructive sampling.

The results of the simulation of anthracene dynamics in the macroinvertebrate community (Figure 5.4.4) show that anthracene concentration is greater in the upstream reaches because the anthracene concentration in the water and periphyton is greater. Also, it should be noted that the anthracene concentration in the benthic macroinvertebrate component continues to increase after the anthracene input was terminated. This is a function of the ingestion of anthracene-containing food (periphyton and detritus) after the anthracene input period. Even though we cannot compare this simulation to the macroinvertebrates in the channels microcosm study we feel that the prolonged increase predicted by the simulation is unrealistic. The main reason is that the relative importance of accumulation c PAH, anthracene in this case, from food and directly from the water is not known. We suggest further research be conducted to determine the relative importance of flow materials along these pathways and determine better estimates of KP_i, KC_i, QP_i and QC_i (equation 5.3.24).

Fish

As with the macroinvertebrate organisms, we were unable to compare results from the simulation to results from the channels microcosms because of anthracene induced mortality (see section 6.6). The simulation model includes components for both herbivorous and carnivorous fish. The herbivorous fish and carnivorous fish attain approximately the same concentrations of anthracene during the input period (Figures 5.4.5 and 5.4.6). However, after the input of anthracene was stopped the concentrations of anthracene in the herbivorous fish stopped increasing while that of the carnivorous fish continued to increase. This is a result of rapid depuration from the periphyton, which was the major source to the herbivorous fish. Alternatively, loss from the macroinvertebrates, which were the source of ingestion for the carnivorous fish was much slower, which caused the simulation to predict a continued accumulation of anthracene. Some preliminary laboratory studies indicate that bluegill sunfish (see section 4.8) accumulate most of their body concentrations of PAH directly from the water. Thus, to improve the prediction capabilities of FOAM we will need to have better estimates of the maximum uptake rates and relative importance of various pathways under different conditions.

Relative Importance Along Biotic and Abiotic Pathways

We have calculated the relative importance of non-advective physical-chemical processes and biological processes in determining the overall flux of anthracene through the simulated lotic system. The periodic behavior of anthracene corresponded to the light-dark cycle and emphasized the importance of photolytic degradation of anthracene in the overall dynamics. During the anthracene simulations, the continued processes of photolysis, sorption and volatilization accounted for more than 50% of the total anthracene flux along pathway which allowed for either uptake and depuration

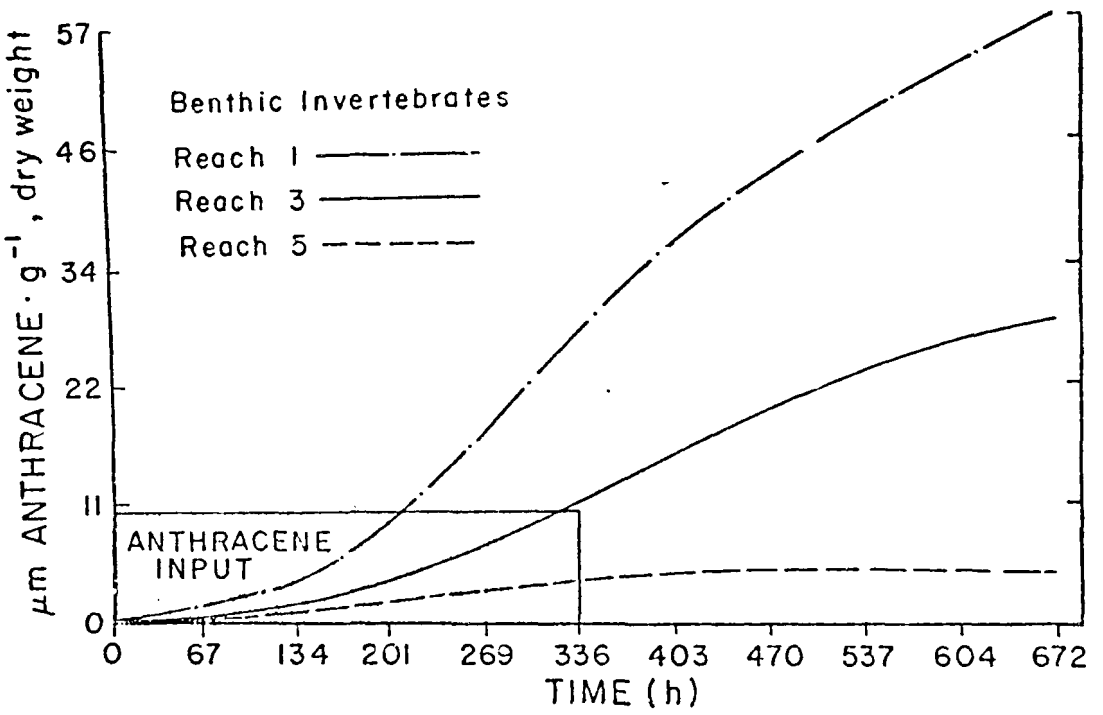

Figure 5.4.4. Simulation of dynamics of anthracene in benthic macroinvertebrates other than clams.

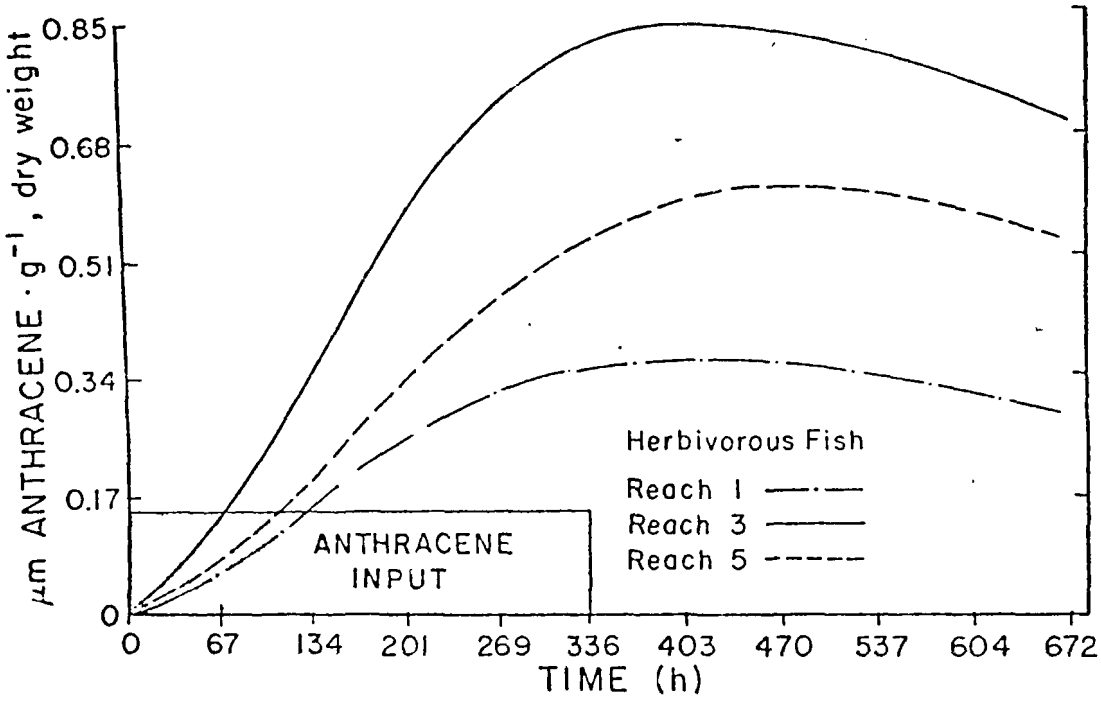

Figure 5.4.5. Simulation of dynamics of anthracene in herbivorous fish

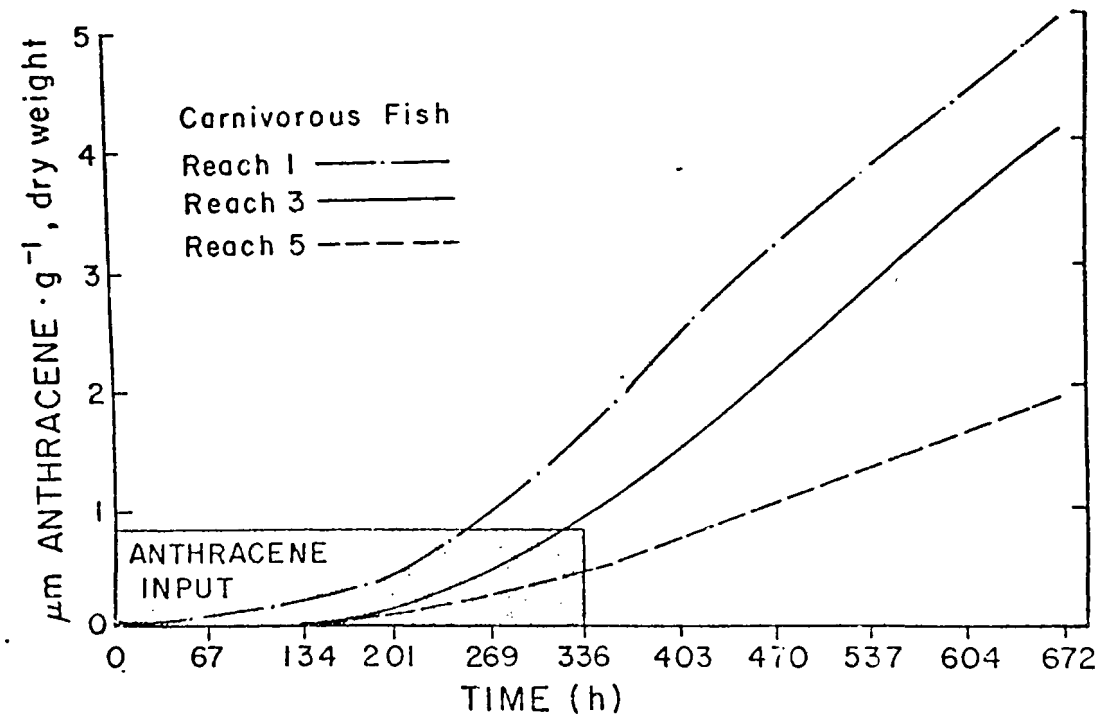

Figure 5.4.6. Simulation of anthracene dynamics in carnivorous fish.

or transformation. As more anthracene entered biological components the relative importance of the biological processes increased. This was especially true at night when the photosynthesis rate was zero. When the anthracene input was terminated, the physical chemical processes became unimportant and biological degradation processes assumed control over the fate of anthracene. Of all biological processes, consumer egestion and defecation of anthracene laden prey items accounted for more than 40 percent of anthracene flux. Plant uptake represented about 6 percent of the total flux. The remaining anthracene moved fairly equally among the other biological pathways: depuration and excretion by plants, mortality losses to plants and consumers, flux along the food web and uptake and depuration of anthracene by consumers.

Comparison of Naphthalene Benzo(a)Pyrene and Anthracene Simulations.

One of our initial premises for constructing a model from first principles of compounds to be released to the environment stated that the dynamics of PAH compounds could be predicted from a few readily available pieces of information about a compound. These include molecular weight, functional groups and molecular stereochemistry. There was given some agreement between trends of the simulations and channels microcosms experiments for anthracene, (mol. wt. = 178). The experiment was simulated again with equal infusion rates of napthalene (mol. wt. = 128) and B(a)P (mol. wt. = 252). The initial conditions and parameter estimates were identical to the anthracene simulation. Only the molecular weight and absorbance spectra were changed to correspond to naphthalene or B(a)P.

Without data for comparison with the FOAM simulation, discussion of the dynamics of individual state variables becomes rather meaningless. However, it is reasonable to examine the relative importance of various pathways simulated in light of available information concerning observed behavior of these compounds in natural or experimental systems. The simulated fate of naphthalene was similar to anthracene with respect to the relative importance of physical/chemical versus biological processes. Physico-chemical processes accounted for more than 90% of the napthalene flux through the channels in simulations (Figure 5.4.7). However, the absence of periodic behavior corresponding to the light-dark cycle indicated that, unlike anthracene, photolysis was not the dominant process but that volatilization was the dominant physico-chemical pathway of napthalene loss from the channels, according to the simulations. These results are similar to the conclusions of Lee et al. (1978), that volatilization was an important process in the overall loss of naphthalene from large pelagic enclosures. Similar to the anthracene simulation, the process of consumer egestion and defecation assumed importance in the overall flux of naphthalene following the termination of naphthalene infusion in simulations of naphthalene dynamics in the channels.

The transport of benzo(a)pyrene (B(a)P) in the simulation was dominated by biological processes in contrast to the lighter weight anthracene and naphthalene (Figure 5.4.7). Following an initial 8 h period of infusion, where photolytic degradation was important, uptake by primary pro-

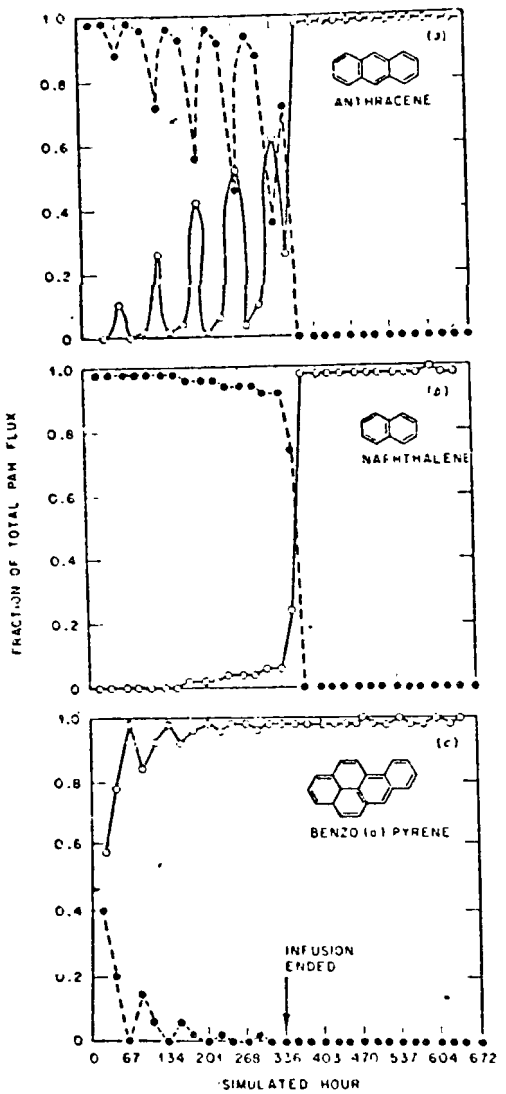

Figure 5.4.7. Relative importance of non-advective physical/chemical processes (solid dots, dashed line) and biological processes (open circles, solid line) in total transport of (a) anthracene, (b) naphthalene, and (c) benzo(a)pyrene through artificial streams.

ducers, movement through the foodweb, and consumer processes of egestion and defecation played the determining role in the non-advective transport and fate of B(a)P in the modeled stream. Lu et al. (1977) measured biomagnification of B(a)P by biota in a simple aquatic microcosm that contained algae, mosquito larvae, daphnia, snails, and fish. Lee et al. (1978) found 40 percent of B(a)P added to marine pelagic enclosures in samples of sediments. Of the physical/chemical processes simulated, sorption to suspended particulates and settled sediments was the most important vector simulated for B(a)P by FOAM.

Discussion

To be useful, a model of the transport of PAH should be capable of several functions. The model should trace the entry of PAH into ecosystem components potentially affected by, or involved in the transfer of, PAH throughout the system. Second, the model should quantitatively characterize the movement of PAH among system components and across system boundaries. Third, the disposition of PAH within components should result from model application. Finally, transport through the system to ultimate sinks following removal of the PAH input should be simulated.

Examination of initial results of FOAM simulations suggests that this model could become a useful tool for synthesizing current understanding of PAH dynamics and developing capacity to reasonably predict the transport of PAH in lotic systems.

Initial results of simulations showed that FOAM predicted the spatial-temporal dynamics of dissolved anthracene with reasonable accuracy (Table 5.4.1). This success might reflect the observation that photolytic degradation is the major pathway of degradation for this PAH. The photolysis submodel has a firm foundation in theory and photolysis information for PAH in general exists in greater amount and sophistication than for other processes. Given that the photolytic submodel is perhaps the most realistic process submodel within FOAM and photolysis appears as a key pathway for degradation of anthracene, it is not surprising that FOAM predicts the diurnal and downstream fluctuations measured for soluble anthracene in the artificial stream channels.

The absence of rate coefficients for biological transport processes in relation to molecular weight or other fundamental chemical properties of PAH reflected the limited amount of data available for estimation of correlations. Therefore, the model depended on extrapolation of rate constants measured in the laboratory or published in the literature. As the number of necessary rate parameters that must be directly measured in the system of interest increases, specific application of the model becomes more difficult. Lack of close agreement between simulated and measured concentrations of anthracene in periphyton, clams, and sediments likely reflected the difficulties in extrapolating laboratory determined rate constants to the streams. For example, rate of uptake by periphyton was overestimated.

The cultures of algae used in the laboratory experiments to determine uptake did not resemble the flora that was growing in the experimental channels.

While no data from the artificial streams are available to evaluate the simulated transport of naphthalene and B(a)P, the agreement between predicted and measured anthracene transport and several general aspects of the simulated behavior of naphthalene and B(a)P generated some confidence in the model's general applicability over a wide range of possible PAH compounds. In the naphthalene simulation, volatilization proved to be the single most important process that determined transport of naphthalene. This agrees favorably with general experience with this low molecular weight PAH.

Photolysis initially accounted for 40 percent of the degradation of B(a)P inputs to the simulated streams. The modeled importance of photolysis agrees with the observations of Zepp and Schlotzhauer (1981) and are consistent with expectations based upon the relatively high molecular weight of this compound. However, the low solubility of B(a)P in water ($\sim 1 \mu g \cdot ml^{-1}$) resulted in most of the external input being shunted to the sediments where it entered the food web via the feeding activity of benthic invertebrates. Given the observation that B(a)P was input in excess of its solubility limits during this simulation, strict comparison with the anthracene and napthalene simulations may be unjustified. In future model application, equimolar concentrations might provide results that are more valid for purposes of comparison.

Initial results of application of the model indicated that molecular weight carries considerable information concerning transport of PAH compounds through lotic systems. Nevertheless, much work is still required to evaluate the overall utility of FOAM. Rigorous sensitivity analysis will identify a set of parameters, of which the values must be measured with as much accuracy as possible, as well as point out those parameters that need only be estimated, say, within an order of magnitude. Systematic variation of individual parameters in repeated simulations will accomplish this aspect of the sensitivity analysis. From past experience with functional forms used in FOAM (Bartell et al., 1981), likely candidates for sensitive parameters in the production submodel are the Bayesian food preference values, W_{ij}, and assimilation values, a_{ij}.

The dynamics of PAH transport implicit in molecular weight are mechanically translated by several regressions into variable parameters associated with the processes of photolysis, sorption, volatilization, and solubilization. As a function of available data, each regression has its' own band of confidence limits about the regression equation. For a particular molecular weight, regression derived parameters can be selected randomly about the regression within the 95 percent confidence limits. Use of these stochastic parameters in repeated simulations constitutes another aspect of the necessary sensitivity analysis of FOAM. This analysis will evaluate the robustness of the regressions and indicate which relationships should receive additional attention or which ones require larger data bases.

Even without the results of rigorous sensitivity testing, there are several aspects of the model that require modification. The version of FOAM used in present simulations fails to link hydraulic power to net suspension. Resuspension and settling rates of particulates are now independent of current velocity, clearly an unrealistic assumption. Given the importance of PAH sorption to particulates, dynamics of particulate suspension are potentially important in terms of removing dissolved PAH from the water column and introduction of PAH into organisms that either filter feed or work the sediments. The submodel for net suspension should incorporate hydraulic power, reach dimensions, and size distributions of suspended and settled particulates to more realistically simulate particle processing in lotic environments.

The hydrologic routine is only capable of simulating constant flow conditions. All reaches are identical in morphometry, and discharge into the uppermost reach equals discharge between all reaches; the simulated stream is hydrologically in a dynamic steady-state. While this limitation does not constrain application of the model to the artificial channels, model application to natural lotic systems depends upon the degree of similarity between the stream segment of interest and the constant geometry of the model reaches. Clearly, to make the model useful to the majority of streams and rivers of interest, many of which are impounded, the hydrologic submodel needs to be modified or replaced by an algorithm that can handle variable reach dimensions and discharge regimes.

Simulation of B(a)P transport suggested, counter-intuitively, that sorption was not an important process in determining the fate of this PAH. Previous research (Karickhoff et al., 1979) indicated that this high molecular weight, relatively insoluble PAH should readily sorb to particulate matter. The regression was derived from analysis of data that described sorption kinetics for a variety of PAH compounds and river sediments (Karickhoff et al., 1979). The derived regression has an opposite slope from a regression based upon sorption data from another source (SRI Report in EPA file). Clearly, the analyses that lead to the present submodel must be re-examined. It may be worthwhile to test the implication of the regression based upon the SRI data base in the sorption submodel and overall transport of compounds that appear readily sorbed to particulates, such as B(a)P.

Another potential mechanical modification of FOAM resides in the current integration scheme. The mass balance equations, while conceptualized as a set of coupled partial differential equations (e.g., equation 5.3.1), are mathematically handled as a set of different equations with a simple Euler integration routine. Results of simulations repeated at different time steps should be compared in order to determine a time step that optimizes precision and computing time. It might be necessary to include a more sophisticated numerical integration algorithm (e.g., variable step size Runge-Kutta method) to maximize precision at the expense of increased computer costs per simulation.

A major conceptual weakness of the model lies in the production of metabolic or degradation products of the particular PAH simulated. The

current revision of FOAM directs a constant fraction of metabolized parent compound into the metabolite pool. We assume for the moment that the metabolite pool does not undergo further degradation. No molecular weight was assigned to the metabolite. In future versions of the model it may be possible to simulate some characteristics of the degradation products based upon the structure of the parent compound. For example, the number of rings and the kind, location, and number of functional groups that comprise the parent compound might be used to predict the chemical structure of degradation compounds that result from photolytic and metabolic processes.

The physiological process structure of the equations for PAH transport through the food web encourages linkage of lethal and sublethal toxicity to the overall transport model. In the past, fate and effects have been largely examined independently. As information accumulates concerning the processes affected by toxic components of PAH, the component of the growth derivative can be modified appropriately. For example, low molecular weight fractions of certain oils have been shown to decrease the rate of photosynthesis of marine algal species. This effect could be translated into a concentration dependent term that multiplies the simulated photosynthetic rate by the appropriate factor to model the toxic effect. Similarly, rates of other processes (feeding, respiration, excretion, etc.) might be adjusted to simulate toxic effects. Incorporation of these toxic effect multipliers would directly link effects to transport through the food web.

Feedback between the modeling effort, analysis of published data, and evaluation of laboratory and field microcosm experiments will result in modification of FOAM to increase the model's usefulness as a management tool for predicting PAH dynamics in lotic systems.

SECTION 6

CHANNELS MICROCOSM STUDIES

SECTION 6.1

FACILITY DESCRIPTION

The channels microcosm facility used in this study is located on the Department of Energy's (DOE) Savannah River Plant (SRP), a 507 km^2 reserve, including portions of Aiken, Barnwell and Allendale Counties in South Carolina, U.S.A.

The channels microcosms facility (Figure 6.1.1) is a pass-through system consisting of six separate cinder-block channels, each 91.5 m long, 0.61 m wide, and 0.31 m deep. Located at the upper end of each channel is a pool 3.1 m long, 1.5 m wide, and 0.9 m deep. At the lower end of the six channel facility is a single large pool 10.2 m long, 3.1 m wide, and 1.0 m deep. For these studies, the channels and headpools were lined with a 0.05 cm thick black polyvinyl chloride (PVC) film and covered with 0.05 meters of washed quartz sand substratum.

Water for the channels was pumped from the Tuscaloosa aquifer via a deep well located near the facility, treated to remove CO_2, and hydrated lime added to produce inorganic water quality similar to that of surface waters in the local upper coastal plain (Table 6.1.1). Water flows were monitored by v-notch weirs on each head pool where water enters the channel. Flow rates of 75.7 $\ell \cdot min^{-1}$ were maintained manually by input valves located above each headpool; this resulted in a current velocity of 1.0×10^{-2} $m \cdot sec^{-1}$ and a retention time of 2.5 h. The water depth in each channel was maintained at 20 cm by use of control gates located at the lower end of each channel.

Effluent water from the channels was pumped from the tail pool at a rate of 108 gpm, into a large steel treatment tank where it was gravity fed through a filter of activated charcoal and gravel prior to final release to the local environment. At the point of release anthracene and anthracene degradation compound concentrations in the process water were at or below background levels for water supplying the facility.

At the time water flow was commenced four channels were seeded with a 50-ℓ slurry of water, sediment and biological material (i.e., algae, zooplankton, macroinvertebrates) from seven locations around the SRP site: Brinkley Well, Skinface Pond, Ellenton Bay, Dicks Pond, Asphalt Pond and Upper Three Runs Creek. Seeding was conducted weekly from March 11, 1979

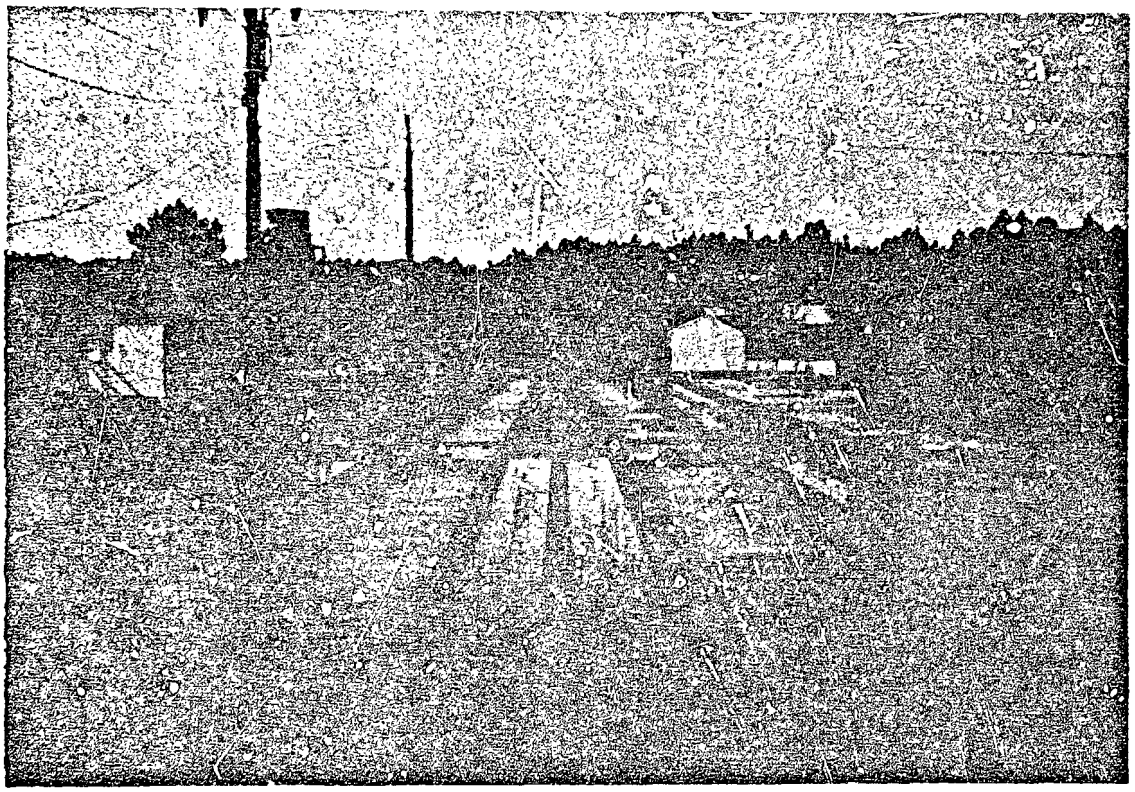

Figure 6.1.1. View of channels microcosms facility.

Table 6.1.1. Mean water quality of treated well water

Total alkalinity	17.5 mg/ℓ as $CaCO_3$
Hardness	21.5 mg/ℓ as $CaCO_3$
pH	6.6
Specific conductance	31 μ mho/cm
Ionic strength (I)	2.5×10^{-4}
DO	8.5 mg/ℓ
CO_2	3.25 mg/ℓ
SO_4^{-2}	1.9 mg/ℓ
Total P	10.1 μg/ℓ
Nitrogen (NO_2 + NO_3)	19.2 μg/ℓ
Ca	3.17 mg/ℓ
Cu	3.4 μg/ℓ
Co	2.5 μg/ℓ
Cd	0.023 μg/ℓ
Cr	0.3 μg/ℓ
Fe	1.7 μg/ℓ
K	1.1 μg/ℓ
Mg	246 μg/ℓ
Mn	7.0 μg/ℓ
Na	1.8 mg/ℓ

through June 13, 1979 and daily from June 13, 1979 to July 16, 1979 after which these channels were allowed 10 weeks of additional colonization prior to the introduction of anthracene. Also, during the early stages of the seeding processes the macrophytic angiosperm Juncus canadensis was transplanted to the system. Juncaceae represent the dominant macrophytic group which has naturally colonized the channels during past studies (Kania et al., 1976, Giesy et al., 1979).

METHODS AND MATERIALS

Anthracene (Aldrich Chemical Co.) was made up to 649±86 $mg \cdot \ell^{-1}$ in pharmaceutical grade ethanol. Stock was introduced via a peristaltic pump at 2.12±0.2 $ml \cdot min^{-1}$ for a nominal anthracene concentration of 18.2 $\mu g \cdot \ell^{-1}$ and a nominal ethanol concentration of 28 $mg \cdot \ell^{-1}$. Fresh stock solution was prepared daily and was introduced through stainless steel tubing (excepting 15 cm of silicon rubber tubing within the pump) directly into the turbulent mixing zone of the channel. Nominal anthracene concentrations were not obtained. The average observed input of anthracene was 16.2 and 13.8 $\mu g \cdot \ell^{-1}$ for the abiotic and biotic experiments, respectively.

Anthracene was introduced into a newly lined uncolonized channel microcosm (abiotic study) for five days (August 18-22, 1980) and samples of water, sediment (sand) and plastic liner material were taken from reaches one, two and five. Samples of water, sand and plastic liner were taken on days two and four at dawn and 1530. Samples of water, sand and plastic liner were taken at noon on day one and three and at 1030 on day five. No samples were taken after the five day input period.

Anthracene was subsequently introduced into a biologically colonized channel (biotic study) for 14 d of exposure (September 22 - October 6, 1980). Samples of water, organic sediment, periphyton, fish, clams and plastic liner were taken from reaches one, three and five on days 1, 2, 3, 5, 8 and is during the period of anthracene input. Samples were also taken 1, 2, 4, 8, and 14 days after anthracene input was terminated (October 6-20). For sampling and modeling purposes, the channels were divided conceptually into five 8.3 m long reaches. Samples were taken at 4.58, 9.15, and 13.7 m from the beginning of each sampled reach. For the abiotic study, water samples only were taken on days two and four at dawn and 1530 to evaluate photolysis losses. Water, sand, and plastic were also sampled at noon on days one and three, and at 1030 on day five.

In the biotic study, water samples were taken at noon on days 1, 2, 3, 5 and at dawn on days 2, 5, 8, 15, 16, 17, 19, 23 and 29 from reaches one, three and five. Sediments and periphyton were sampled from reaches one, three and five on days 2, 3, 5, 8, 15, 16, 17, 19, 23 and 29 at 0830. Clams, fish and plastic were sampled from reaches one and five at 0830 on the same days as the sediment and periphyton.

Water

One-liter water samples were acidified with 1 ml of concentrated HCl. Control and blank water samples were taken at the weir prior to the addition of compound. The control was spiked with 3135 ng (abiotic study) or 5371 ng (biotic study) anthracene and 4578 ng (abiotic study) or 5076 ng (biotic study) anthraquinone in 30 µl acetonitrile. The water samples were passed through Amberlite® XAD-4 resin (Rhom and Haas, Philadelphia, PA) macroreticular adsorbant for anthracene and anthraquinone. The resin columns were 1.5 cm diameter x 25 cm long equipped with a 250 ml reservoir and a stopcock. A plug of glass wool was placed in the column and 30 ml of wet precleaned XAD-4 resin was added to the column. The resin was precleaned with and stored under nanograde methanol. Prior to use the columns were drained and rinsed with 10 bed volumes of deionized water. Water samples were percolated through the resin at a flow rate of 0.8-1.2 $\ell \cdot hr^{-1}$. The columns were eluted sequentially with two bed volumes each of anhydrous diethylether and nanograde acetone. The solvents were combined and dried over anhydrous sodium sulfate. The solvent volume was reduced to ~ 200 µl by a combination of rotary flash evaporation and evaporation under a stream of nitrogen. Acetonitrile (2.0 ml), containing the chrysene internal standard, was added to each sample. This was mixed and 25 µl analyzed by high pressure liquid chromatography (HPLC). The recovery from fortified control samples was 62.3±9.8% ($\bar{x}$ ± SE) for anthracene (n = 7) and 84±13% for anthraquinone (n = 7) in the abiotic study. For the biotic study the recoveries were 89.2±2% for anthracene (n = 24) and 105±3.4% for anthraquinone (n = 24).

Sediment

Sand sediment to be sampled during the abiotic study was placed in the channel in 3.3 cm deep crucibles. One crucible was removed from each station at each sampling time. The interstitial water was removed by vacuum filtration. Samples were extracted in a soxhlet apparatus for 18 h with benzene:acetonitrile (65:35, v/v). The samples were dried over sodium sulfate and prepared for HPLC analysis as previously described. Blanks and control samples were removed from the stream prior to the addition of compound, filtered and stored frozen under acetonitrile. Prior to analysis, controls were spiked with 1045 ng anthracene and 1526 ng anthraquinone.

Organic sediments for the biotic study were collected from a silt bank at Box Landing on Upper Three Runs Creek. The sediment was sieved through a 5 mm stainless steel screen, mixed and placed in 144, 15 x 60 mm glass petri dishs. Twelve of the sediment filled petri dishes were placed at each sampling station in reaches 1, 3 and 5. One randomly chosen petri dish from each sampling station was removed at each sampling time. Three control sediments from an adjacent channel, which did not receive anthracene, were removed per sampling time. Figure 4.2.1 (Section 4.2 this report) shows a flow diagram of the extraction and analytical procedure utilized for sediment samples during the biotic study. Each sample was filtered through Whatman number 41 filter paper using ~20 ml of distilled water to rinse the petri dish. The sediment was weighed and ~10 g sub-

sampled for extraction and analysis. The remainder was dried at ~50°C for 1 to 2 weeks and dry weight determined. Each subsample for extraction was mixed with ~10 g of granular anhydrous Na_2SO_4, transferred to a Whatman 22 x 80 mm cellulose extraction thimble and stored under 35 ml of acetonitrile, at -20°C. The three control sediments were treated identically except that one sediment was spiked prior to addition of sodium sulfate with 1045 or 1790 ng of anthracene and 1526 ng or 1685 ng anthraquinone in acetonitile.

One sample set corresponding to one sampling date consisted of 9 experimentals, 2 background controls and 1 spiked control. The sediments and acetonitrile for each sample set were placed in soxhlet extractors with 65 ml of benzene and extracted for 18 h. The crude extracts were rotary flash evaporated to ~2 ml; passed through a 7 cm column of Florisil®, eluted with three benzene rinses (~2 ml each) of the round bottom flask and 10 ml of 90% Benzene:methylene Cl_2(9:1, V/V). The sample volume was reduced by rotary flash evaporation and evaporation under a stream of nitrogen to 200 µl. Two or four milliliters of acetonitrile containing a chrysene, internal standard was added to each sample. The samples were mixed and placed in a freezer overnight. Precipitates that formed overnight were removed by centrifugation and the superantant was transferred and stored at -20°C until HPLC analysis. Recovery of anthracene from spiked sediment was 73.3 ± 7%, n = 5. Anthraquinone could not be quantified in extracts from sediments because of an interfering compound, which could not be resolved from anthraquinone by HPLC (see Section 4.2).

Periphyton

A constant area of 75 cm^2 of periphyton was scraped from the walls of the channel. This was removed as an aqueous suspension. After all the samples were taken, the water was removed by filtration and a wet weight determined.

Subsamples from each reach were removed for subsequent species identification. Samples for identification were stored in a mixture of 60% deionized water, 30% ethanol (95%) and 10% formalin, prior to microscopic analysis. A second subsample was stored under ethylacetate:acetone (4:1, V/V) at -20°C. Three controls and one blank were taken from a non-exposed channel. The controls were spiked with 1790 ng anthracene and 1685 ng anthraquinone in 10 µl acetonitrile.

The samples were extracted by homogenization in a TenBroeck tissue grinder with 2 x 12 ml ethylacetate:acetone (4:1, V/V) and 2 x 12 ml cyclohexane. The extracts were combined, dried over Na_2SO_4 and the volume reduced to ~ 300 µl. The internal standard was added initially in 2 ml acetonitrile. However, problems of a two phase separation occurred; subsequently, 1 ml ethanol was used to add the internal standard. The samples were analyzed by HPLC. The recovery of anthracene from fortified samples was 70.1±2%. Samples were corrected for background, which averaged 107 ng anthracene per sample.

Fish

The conditions for the subsequent experiments on fish in the channels were slightly different. Juvenile bluegills, Lepomis macrochirus, of mean length 5.0 ± 0.1 cm (± 2SE, N = 58), mean wet weight 1.2 ± 0.1 grams (N = 58), and with a dry to wet weight ratio of 0.222 (N = 45), were obtained from the National Fish Hatcheries at Millen, Georgia and Orangeburg, South Carolina. Only fish appearing in excellent condition were used. The fish were acclimated for 48 h in a control channel and then transferred to glass and stainless steel mesh cages in the experimental channel 12 h before the initiation of anthracene dosing. During both the acclimation and experimental periods fish were fed with Tetra Min® staple food flakes once a day.

Fish for anthracene assays were collected by dip net, wet weights were determined and whole fish were placed into vials containing ethylacetate: acetone (4:1 v/v) and stored at -20°C until analyzed. Prior to analysis fish were homogenized in 2 x 12 ml ethylacetate acetone (4:1, V/V) and 2 x 23 ml cyclohexane in a TenBroeck glass tissue grinder. Extracts were combined, dried over anhydrous Na_2SO_4 and volume reduced to ~ 300 µl. Control fish were spiked with 895 ng anthracene and 843 ng anthraquinone in 5 µl of acetonitrile. A chrysene internal standard was added to each sample in 2 ml of acetonitrile. Analysis was by HPLC and anthracene recovery from fortified controls was 94.5 ± 2.5%. Reported fish whole body anthracene concentrations after 24 - 144 h of depuration are freshly dead animals collected when observed or taken at the end of the experiment. Analysis of dead fish became necessary due to unexpected acute phototoxicity (see Section 6.6).

Clams

Individual clams were sampled from each sampling station and a wet weight determined. The tissue and all fluid from the closed animal were blended and a homogeneous subsample taken for analysis. The weight of the subsample and shell were determined. The sample was added to 40-60 ml of anhydrous Na_2SO_4 for desiccation and stored under either cyclohexane or cycohexane:ethylacetate (1:1, V/V) at -20°C. Three controls and two blanks were prepared in the same manner from an unexposed population. The controls were spiked with 895 ng anthracene and 843 ng anthraquinone respectively.

The sodium sulfate coated with desiccated clam was extracted by shaking with 2 x 50 ml cyclohexane:ethylacetate (1:1, V/V) and 2 x 50 ml cyclohexane. The volume was reduced to ~ 200 µl and internal standard added in acetonitrile. The recovery of anthracene from fortified samples was 87±7% (n = 6).

Plastic Liner

Plastic strips were placed at mid-reach in reaches one, two and five (abiotic study) and one, three and five (biotic study). These were sampled

using a cork borer which yielded plugs of 1.45 cm^2. Six plugs were taken at each sampling time. The plastic was stored in the freezer prior to analysis. The plastic was extracted by shaking 5 min in (2 x 20 ml) ethylacetate:acetone (4:1, V/V). Recovery for fortified samples was 91±7% for anthracene. The samples were prepared for HPLC analysis as previously described for water extracts.

Weather and Sunlight

Air temperature, water temperature and general weather conditions were recorded at each sampling time. Solar radiation was determined using a Belfort Instrument Company Pyranograph Cat. No. 5-3850A located approximately 10 miles southwest of the channels microcosms.

Quantification

The samples were analyzed for anthracene and anthraquinone using a Varian Model 5000 HPLC system with a 254 nm fixed wavelength detector. Separations were made with a 35 cm Micro-Pak MCH-10 reverse-phase column, which was equipped with a Whatman guard column of Co·Pel C_{18} ODS on 35 µm particles. Compounds were eluted from the column at 28°C by programming the moble phase from a 75% acetonitrile: 25% water mixture to 90% acetonitrile: 10% water (Johnson et al., 1977). Acetonitrile (90%) was pumped through the column for five min before recreating the initial conditions. The sediments required a gradient to 100% acetonitrile to remove late eluting compounds.

Quality Control/Quality Assurance

The recovery and precision for each of the matrices was determined by applying the proposed method to fortified samples (Table 6.1.2). Many of these studies were performed with ^{14}C-anthracene. The storage stability was checked by storing fortified samples the same length of time as the samples.

The background determinations were made from samples analyzed at the same time as the environmental samples. The limit of detection was taken to be 3 σ + background (Table 6.1.3). The linearity of the analysis was determined with each sample set by creating a standard curve.

The accuracy of the analysis was determined by analyzing a standard PAH mixture Alltech (PAH-I) which contained anthracene. The relative amount of anthracene determined over several months was 96.5 ± 8% (n = 10).

Double peaks at or near the retention time for anthraquinone for some sediment samples were confirmed by GC-mass spectrometry (see Section 4.2).

Table 6.1.2. Recovery and precision of anthracene and anthraquinone from various matrices.

MATRIX	% RECOVERIES	
	Anthracene[a]	Anthraquinone[a]
Sediments		
A) Sand	15.5 ± 2	b
B) Organic	71.2 ± 12	b
Fish	87.7 ± 6	92.3 ± 8
Periphyton	78.5 ± 2	82.2 ± 3
Clams	78.9 ± 2	93.2 ± 3
Water	81 ± 2	97.6 ± 4
Plastic Liner	91.1 ± 7	b

[a] $\bar{x}$ ± 1SD

[b] not determined because of interferences

Table 6.1.3. Background and limits of detection for analysis of Anthracene and Anthraquinone from various matrices.

Matrix	Background		Limit of Detection	
	Anthracene	Anthraquinone	Anthracene	Anthraquinone
Water				
Input Phase	56 ± 44 $ng \cdot \ell^{-1}$	322 ± 336	188 $ng \cdot \ell^{-1}$	1330 $ng \cdot \ell^{-1}$
Depuration Phase	3.8 ± 8.5 $ng \cdot \ell^{-1}$	ND	29.3 $ng \cdot \ell^{-1}$	-
Periphyton	0.68 ± .64 $ng \cdot cm^{-2}$	ND	2.6 $ng \cdot cm^{-2}$	-
Fish	47.6 ng/fish	ND	116.9 ng/fish	
Clams	103 ± 70 $ng \cdot g$ dry wt^{-1}	ND	315.75 $ng \cdot g$ dry wt^{-1}	
Sediments	53.3 ± 26 $ng \cdot g$ dry wt^{-1}	ND	131.6 $ng \cdot g$ dry wt^{-1}	
Plastic	ND	ND		

ND Not detected. Instrument Detection limit 0.25 ng = S x 2N

Statistical Methods

Rate constants for accumulation and elimination from each geological and biological matrix as well as steady state concentrations were estimated by least-square fits of the data to first-order, donor-dependent models. Each data set was fit independently by the methods of Giesy et al. (1980) with the Marquardt iterative least square procedures (NLIN of the Statistical Analysis System, Barr et al., 1979).

Dynamics of anthracene in each component were calculated by fitting data to equations with the general form given in equation 6.1.1

$$\frac{dC_a}{dt} = K_u \cdot C_w - K_d \cdot C_a \qquad 6.1.1$$

where

K_u = uptake rate constant

K_d = depuration rate constant

C_w = concentration of anthracene in the water

C_a = concentration of anthracene in the component

t = time

To avoid biases introduced by making inappropriate assumptions, most parameters were estimated by several different equations, which made different assumptions.

Plastic Liner

Accumulation of anthracene by the PVC liner was linear during the period which anthracene was input into the channels (Fig. 6.2.3). After anthracene inputs were terminated, anthracene desorbed slowly from the PVC.

Because organic compounds such as anthracene tend to partition into organic matrices an estimate of the possible loss to the PVC liner was made by exposing PVC strips, which were not colonized by periphyton. Sorptive losses to PVC estimated in this manner are a conservative estimate. That is, because the PVC extracted was not covered by periphyton, this number represents a maximum loss to the liner that would be expected.

The uptake flux into any component can be described by equation 6.1.2

$$J = C_w \cdot K_u \qquad 6.1.2$$

By making the initial rates assumptions, that the amount of anthracene in the component of interest is small during the initial uptake period, one can estimate the uptake rate constant by taking a tangent to the uptake curve (J) and dividing by the water concentration.

Because the water concentration C_w is relatively constant for a given period of exposure the equation which describes the dynamics of anthracene in a given component can be simplified to

$$C_a = \frac{K_u}{K_d} \cdot (C_w)\ (1 - e^{-(K_d \cdot t)}) \qquad 6.1.3$$

the concentration of anthracene in the component of interest approaches steady state as $t \to \alpha$. Thus, at $t \to \alpha$

$$BCF = \frac{C_a}{C_w} = \frac{K_u}{K_d} \qquad 6.1.4$$

Equation 6.1.4 gives the relationship between the bioconcentration factor (BCF) or steady state distribution between the water and component of interest. Also, from equation 6.1.4 it can be seen that the steady state concentration can be predicted from equation 6.1.5, when the water concentration is constant

$$C_a = C_{ss}\ (1 - e^{-(K_d \cdot t)}) \qquad 6.1.5$$

where

C_{ss} = steady state concentration in component.

We have given equations for estimating KU, KD and CSS during the period of exposure. To test for biases in fitting equations to estimate KD during only the uptake period, the concentration of anthracene in each component was followed during the depuration period, when no anthracene was being added to the channels. Estimations of multiple depuration rate constants were made by fitting the observed data to equation 6.4.1

$$C_{at} = \sum_{i=1}^{n} Ca_i \cdot e^{-(K_{di} \cdot t)} \qquad 6.1.6$$

where

C_{at} = concentration in component at time t

C_{ai} = initial concentration in ith component

i = individual depuration component

K_{di} = depuration rate constant for ith component

n = number of independent depuration components

RESULTS AND DISCUSSION

CHANNELS MICROCOSM STUDIES

SECTION 6.2

WATER

In the abiotic study the control samples for the water had recoveries of 62.3 ± 9.8% ($\bar{x}$ ± SE) for anthracene and 84 ± 13.1% for anthraquinone (Table 6.2.1). These values were considerably lower than those determined

Table 6.2.1. Percent recovery of anthracene and anthraquinone from control water samples in abiotic channels experiment.[a]

Sample Set	Anthracene $ng \cdot \ell^{-1}$	% Recovery[b]	Anthraquinone $ng \cdot \ell^{-1}$	% Recovery[b]
1	1745	56	5442	119
2	2960	94	5178	113
3	1917	61	3192	70
4	2172	69	3493	76
5.	674	22	1451	32
6	2265	72	4298	94
7	3096	99	5705	125

[a]One liter control water samples were taken upstream of anthracene input (weir) at each sampling period and spiked as follows: 3135 ng anthracene and 4578 ng anthraquinone in 30 µl acetone. Blank water (no additions) recorded anthracene (91.8 ± 78 $ng \cdot \ell^{-1}$) and anthraquinone (298 ± 213 $ng \cdot \ell^{-1}$).

[b]Calculated as: $ng \cdot \ell^{-1}$ detected/$ng \cdot \ell^{-1}$ spiked.

for samples of the same water fortified in the laboratory -- 81.1 ± 1.5% for anthracene and 97.6 ± 3.9 for anthraquinone. This may have occurred due to the additional handling and transport time (30 minutes) in the heat from the channels microcosms to the laboratory.

After correcting for recovery, some loss occurred between the input and the first sampling station which was not accounted for by the sum of the anthracene and anthraquinone (Table 6.2.2). The average accountability was

Table 6.2.2. Calculated input of anthracene to channel and measured values in reach one.

Day	Calculated Anthracene Input ($\mu g \cdot \ell^{-1}$)	Measured Anthracene Concentration ($\mu g \cdot \ell^{-1}$)
1	17.7	11.4 ± 0.4[a,b]
2	12.6	11.4 ± 0.7[c]
3	21.1	7.3 ± 1.3[b]
4	21.8	18.4 ± 1.7[c]

[a] $\bar{x}$ ± 1SD, all values corrected for average control recovery

[b] Values recorded at noon

[c] Values recorded at dawn (7:30 am)

76 ± 5.3% and ranged from 48-95%. The average actual anthracene concentra- just below the input in both the biotic and abiotic studies were approximately 12 $\mu g \cdot \ell^{-1}$. Anthracene concentrations in the water showed significant diurnal variation. Maximum water concentrations (steady state) were achieved and maintained during periods of darkness. However concentrations decreased significantly with distance downstream during daylight periods. Photolysis accounts for 100% of the loss down the channel, with the other matrices falling in the experimental error of our ability to measure water concentration. In the absence of photolysis (dawn samples) the anthracene concentration in the water was at steady state within 24 h in both the abiotic and biotic studies (Table 6.2.3 and 6.2.4) (Figs. 6.2.1 and 6.2.2). Samples taken at noon or 1530 h had lower concentrations of anthracene than dawn samples in reaches 3 and 5 (Table 6.2.3 and 6.2.4, Figs. 6.2.1 and 6.2.2). The loss rate constant for all noon and afternoon samples was 0.016 ± 0.006 min^{-1} which is a half life of 4[illegible]3 ± 12 min. Since the loss of anthracene was observed in both the abiotic and biotic study the most probable cause is photolysis rather than photo-respiration by microbial populations in the water and benthos.

Table 6.2.3. Concentration ($\mu g \cdot \ell^{-1}$) of anthracene and anthraquinone in water.

Day	Time	Reach 1		Reach 2		Reach 3	
		Anthracene $\mu g \cdot \ell^{-1}$	Anthraquinone $\mu g \cdot \ell^{-1}$	Anthracene $\mu g \cdot \ell^{-1}$	Anthraquinone $\mu g \cdot \ell^{-1}$	Anthracene $\mu g \cdot \ell^{-1}$	Anthraquinone $\mu g \cdot l^{-1}$
1	12:00 pm	7.7 ± 0.3	2.4 ± 0.3	3.1 ± 0.1	3.9 ± 2	1.8 ± 0.1	2.4 ± 0.7
2	8:00 am	7.7 ± 0.4	0.09 ± 0.05	8.2 ± 0.3	0.08 ± 0.03	7.9 ± 0.2	0.08 ± 0.05
2	3:00 pm	5.3 ± 0.8	0.8 ± 0.4	3.4 ± 0.3	2.1 ± 0.5	1.7 ± 0.3	1.7 ± 0.3
3	12:00 pm	4.9 ± 1.0	3.0 ± 0.4	3.4 ± 1.0	3.1 ± 0.4	1.3 ± 0.1	2.7 ± 0.3
4	8:00 am	15.8 ± 13.3	0.8 ± 0.5	13.1 ± 0.3	0.6 ± 0.3	11.7 ± 1.3	0.3 ± 0.08
4	3:00 pm	14.1 ± 12.2	3.6 ± 1.2	4.7 ± 0.6	4.6 ± 1.4	0.9 ± 0.2	3.0 ± 0.9
5	10:30 am	5.2 ± 3.4	1.5 ± 0.6	9.9 ± 1.5	4.9 ± 1.5	9.0 ± 0.2	4.8 ± 1.2

All values mean ± SD of three sampling stations in each reach.

Table 6.2.4. Percent accountability nM anthracene + nM anthraquinone/actual anthracene input (nM).

	Reach 1	Reach 3	Reach 5
Dawn	102	106	103
Noon	96	77	48
Dry & Heavy Cloud cover Noon	110	95	80

Concentrations of anthraquinone were more variable than those of anthracene. Anthraquinone concentrations were near zero in samples taken at dawn (Table 6.2.5). Concentrations of anthraquinone in water samples taken during the day ranged from 1-5 $\mu g \cdot \ell^{-1}$. This suggests that the anthraquinone was due to photolysis of anthracene.

Plastic Liner

Accumulation of anthracene by the PVC liner was linear during the period during which anthracene was input into the channels (Fig. 6.2.3). After anthracene inputs were terminated, anthracene desorbed slowly from the PVC.

Because organic compounds such as anthracene tend to partition into organic matrices an estimate of the possible loss to the PVC linear was made by exposing PVC strips, which were not colonized by periphyton. The estimate of sorptive losses to PVC estimated in this manner are a conservative estimate. That is, because the PVC extracted was not covered by periphyton, this number represents a maximum loss t the liner that would be expected.

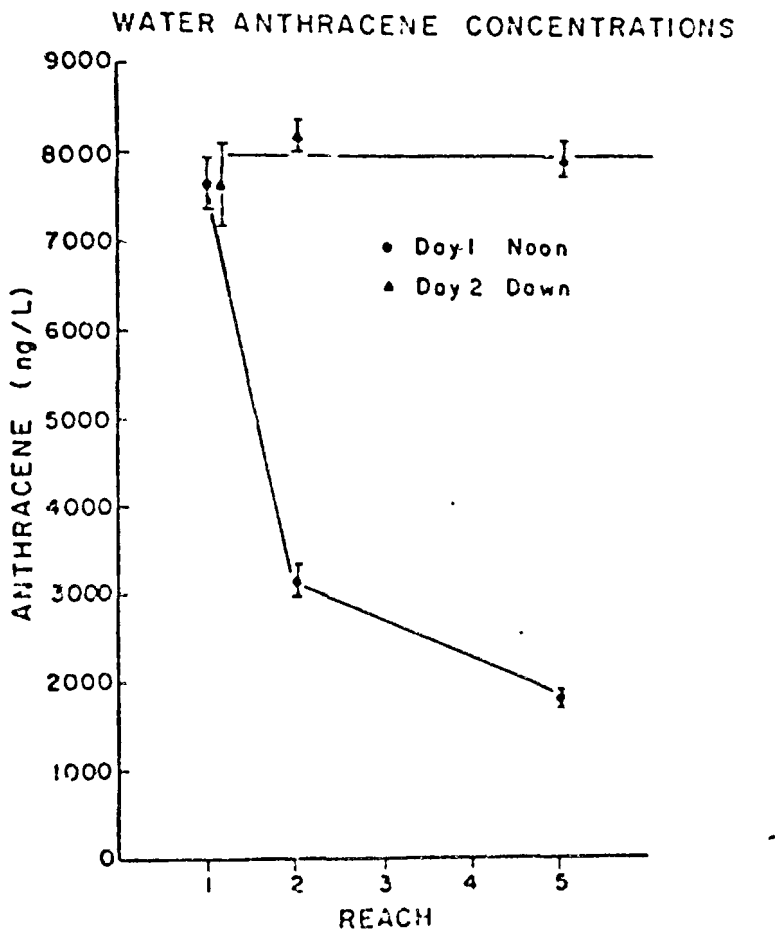

Figure 6.2.1. Anthracene concentrations in reach 1 during the input period of the abiotic study. The closed triangles represent samples taken at dawn, while closed circles represent samples taken at noon. Each point represents the mean of replicate samples. The confidence interval is 1SD.

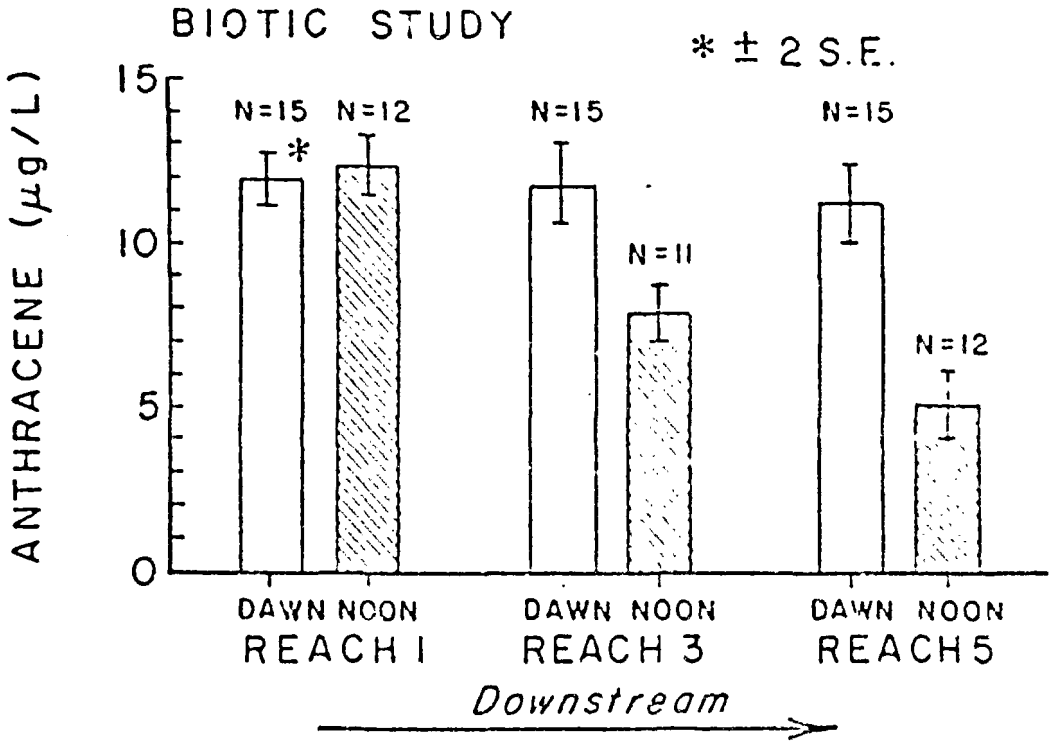

Figure 6.2.2. Histogram representing anthracene concentrations in water from reaches 1, 3 and 5, during the biotic study.

Table 6.2.5. Input and mass balance of anthracene/anthraquinone in reach one.

Day	Sample Time	Calculated Input Anthracene (nM)	Measured Concentration Anthracene (nM)	Measured Concentration Anthraquinone (nM)	Percent Accountability
1	12:00 pm	99	63.9	13.1	77.8
2	7:00 am	99	63.6	0.4	64.7
2	3:30 pm	71	44.7	4.3	68.7
3	12:00 pm	118	40.4	15.8	47.7
4	7:00 pm	118	108.7	3.3	94.7
4	3:30 pm	122	58.4	19.2	63.6
5	10:30 am[b]	0	43.5	8.1	-

[a]Accountability = nM anthracene + nM anthraquinone/calculated anthracene input (nM).

[b]Input stopped 1 h prior to sampling.

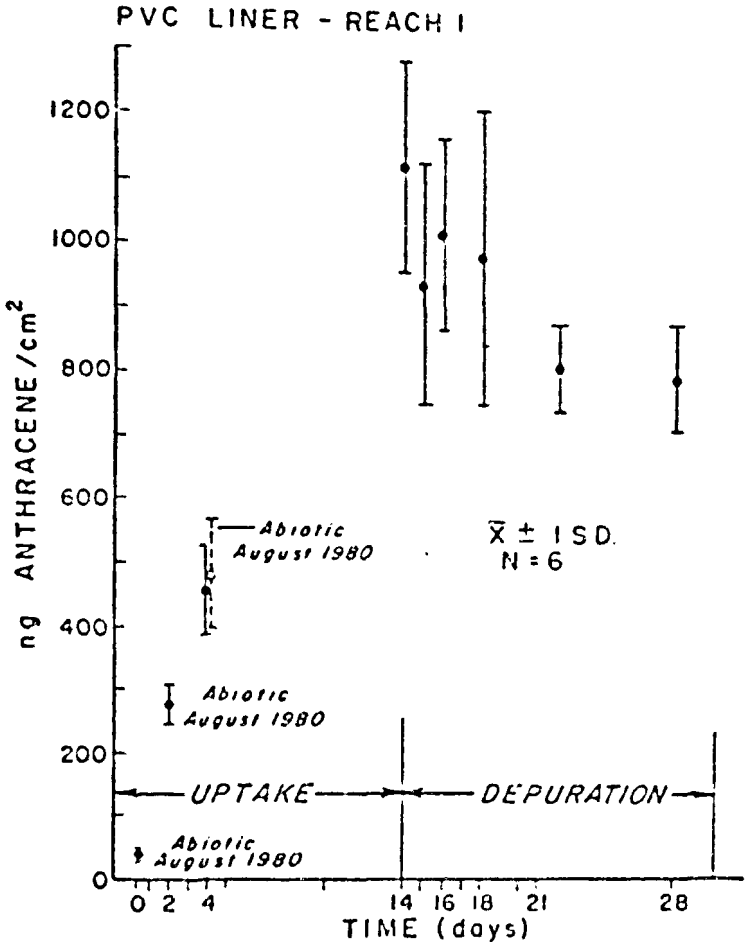

Figure 6.2.3. Concentrations of anthracene associated with plastic liner during the two channel microcosm studies. The points which represent samples taken during the abiotic study are labeled as such. The other points are from the biotic study. Each point represents the mean of 6 samples. The confidence interval is 1SD.

SECTION 6.3

SEDIMENTS

The rate constants for uptake and depuration from sediments were not significantly different among the three reaches (Table 6.3.1 and Fig. 6.3.1). This indicates that the rates of accumulation were indeed first-order with respect to water concentrations of anthracene because the mean concentrations of anthracene in the water varied and fluxes into the sediments varied in proportion to the water concentrations. Depuration from the sediments was also first order with respect to the concentration in the sediment (Table 6.3.1 and Fig. 6.3.1). Because the rate of accumulation could be related to the rate of diffusion into the sediment, we normalized the concentration of anthracene in the sediments on both a weight (Table 6.3.1) and area basis (Table 6.3.2). The relative variabilities of the K_u, K_d and C_{ss} values from the three reaches were less when normalized to area but not greatly so (Tables 6.3.1 and 6.3.2).

The sorption and desorption of PAH are some of the most difficult mechanisms to model and predict. Most previous models have used steady state partitioning coefficients in completely mixed systems to predict the proportion of PAH associated with the sediment. It is difficult to develop a probabilistic model to predict the PAH sorbed to settled sediment or to quiescent sediment. Also, the rate of sorption and desorption of PAH from quiescent sediment may be determined by the rates of diffusion into and out of the sediment as well as settling and resuspension processes.

The results of the experiments presented in Section 4.2 indicate that PAH diffuse into organics and clay lattice spaces as a function of time and become less available. One of the most difficult hydraulic processes to model is bed movement of sediment. This process may be potentially important in determining the dynamics of PAH associated with sediments. Furthermore, catastrophic (i.e., storm) events may be the most important process in determining the overall movement of PAH associated with sediment. Bioturbation has been found to be an important process in determining the transport of PAH into and out of sediments. Even though many of these transport and resuspension mechanisms are known and quantifiable, developing a mathematical simulation model will be difficult. One of the main reasons is the temporal scaling of catastrophic effects, relative to the time steps required to attain adequate resolution of other processes. For this reason we feel that simulation of the dynamics of PAH associated with sediments will always be one of the least accurate components of simulation models. This will be a severe limitation of simulation models because of the great affinity of sediments for PAH in aquatic systems (Giddings et al., 1978). We suggest that for short-term simulations the top

2 cm be considered as a homogeneous completely mixed storage pool for which the sorption and desorption fluxes are not diffusion limited.

TABLE 6.3.1. First order rate constants for uptake and release of anthracene from organic sediments during the channels microcosm experiment based on dry weight of sediment. Data was fit by the Marquardt iterative least squares procedure. $\bar{X} \pm SE$, $n = 3$, $PF < 0.001$ for all regressions.

	Reach 1	Reach 3	Reach 5
K_u [a]	1.3 ± 0.093	1.4 ± 0.13	1.4 ± 0.11
K_d [b]	0.0048 ± 0.0007	0.0049 ± 0.0009	0.0040 ± 0.0007
K_d [c]	0.0022 ± 0.0003	0.0022 ± 0.0004	0.0025 ± 0.0003
C_{ss} [d]	3265 ± 266	2980 ± 298	2917 ± 306

[a] $ml \cdot g^{-1} \cdot h^{-1}$

[b] h^{-1}, assuming density of sediment is near 1, estimated from data collected during anthracene input.

[c] h^{-1}, estimated from data collected during period of no anthracene input.

[d] ng anthracene$\cdot g^{-1}$ sediment, dry weight

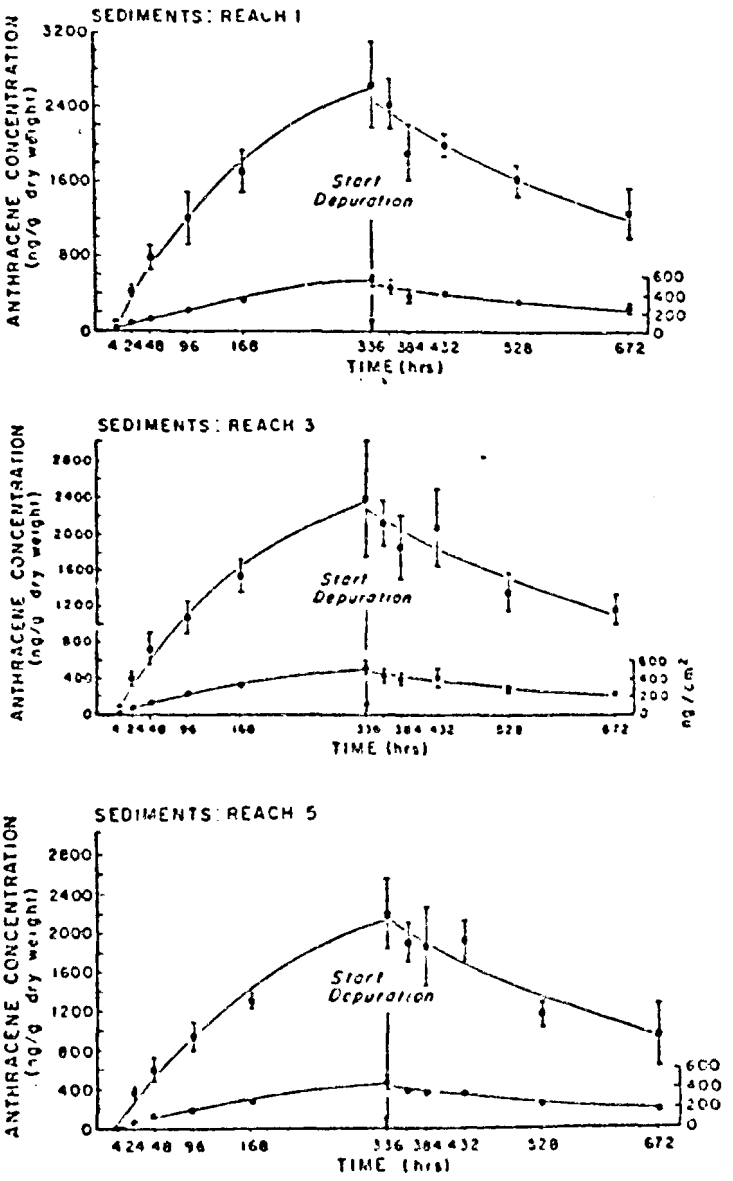

Figure 6.3.1. Uptake and depuration of anthracene by organic sediments in petri dishes in the channel microcosm. Closed squares represent the concentration of anthracene on a dry weight basis while closed circles represent the same data normalized to an areal basis.

TABLE 6.3.2. First order rate constants for uptake and release of anthracene from organic sediments, based on area of sediment. Data was fit by the Marquardt iterative least squares procedure. $\bar{X} \pm SE$, n = 3, PF < 0.0001 for all regressions.

	Reach 1	Reach 3	Reach 5
K_u [a]	0.22 ± 0.014	0.27 ± 0.016	0.26 ± 0.019
K_d [b]	0.0034 ± 0.00056	0.0039 ± 0.0005	0.0032 ± 0.0006
K_d [c]	0.002 ± 0.0003	0.0023 ± 0.00033	0.0027 ± 0.00028
C_{ss} [d]	800 ± 80	685 ± 57	680 ± 87

[a] $ml \cdot cm^{-2} \cdot h^{-1}$

[b] h^{-1}, estimated from data collected during period of anthracene exposure

[c] h^{-1}, estimated during period of no anthracene input

[d] ng anthracene $\cdot cm^{-2}$ sediment

SECTION 6.4

PERIPHYTON

The anthracene concentrations reported are not corrected for extraction efficiency which was 71% ± 0.1 ($\bar{X}$ ± SD). Thus, the numbers reported are approximately 30% less than the total amount of anthracene contained in the periphyton. Since the reported values would be corrected by a constant this does not affect the trends reported. Since there is an error associated with determining the extraction efficiency at each point we decided not to confound this error with that of the extractions and quantifications of anthracene in periphyton. The dry to wet ratio for periphyton was 0.034 ± 0.016 (SD, n = 11).

Concentrations of anthracene in the periphyton community were normalized to both an area and a wet weight basis. Similar trends were observed for data reported in both ways (Figs. 6.4.1, 6.4.2, and 6.4.3). The coefficient of variation was generally less when concentrations were reported on an area basis but this was not always true. There was a general increase during the first 48 h of exposure, however, there was some decrease between 24 and 48 h in reach 1. Concentrations in periphyton from reach 1 were much greater than those in reach 3 which were in turn approximately four times greater than those in reach 5. The trend of greater concentrations at the upstream sites was consistent at all sampling times during anthracene exposure.

Because of the variability of anthracene concentrations in periphyton, no rate constants were calculated. Uptake of anthracene was rapid, and reached steady state within 168 h. Furthermore, desorption of anthracene was very rapid (Figs. 6.4.1, 6.4.2, and 6.4.3). The anthracene concentration was not significantly different from background after 48 h. The half-time for elimination was less than 1 day.

The concentration of anthraquinone in periphyton was variable and not very different from background. An interferring peak could not be resolved by HPLC so anthraquinone concentrations are not reported here.

Removal of anthracene from the water column by periphyton was not a significant vector. After day 4 and 14, 0.09 and 0.04% of the anthracene added to the channels had been removed by periphyton. While this is not a significant reduction of the mass of anthracene added to the water, consideration of the periphyton component could be much more important as a potential for food web accumulation. While it is our opinion that the vector of food is not as important as that of direct exposure from water,

for aquatic organisms, more data are needed to determine the relative importance of this vector.

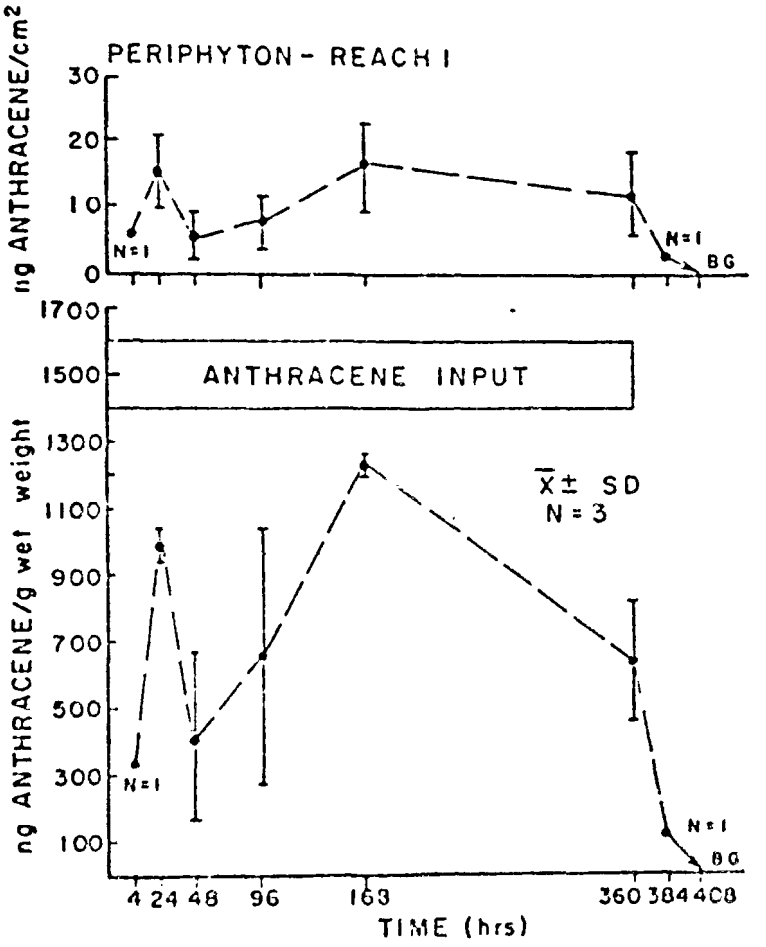

Figure 6.4.1. Anthracene concentrations in periphyton in reach 1 as a function of time. Upper figure represents anthracene·cm^{-2}, while the lower figure represents anthracene·g^{-1}, dry weight, periphyton.

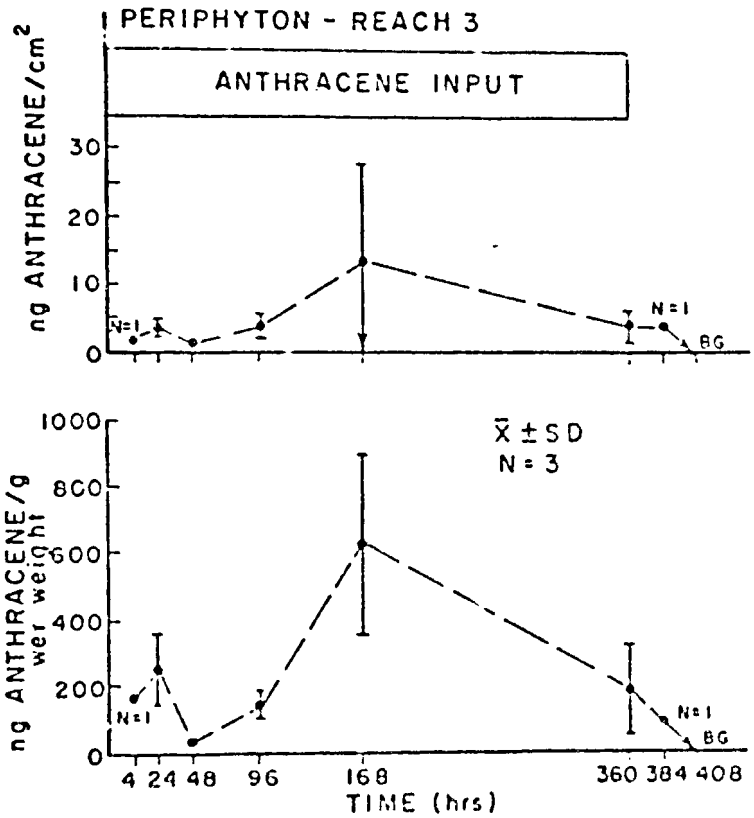

Figure 6.4.2. Anthracene concentrations in periphyton in reach 3 as a function of time. Upper figure represents anthracene·cm^{-2}, while the lower figure represents anthracene·g^{-1}, dry weight, periphyton.

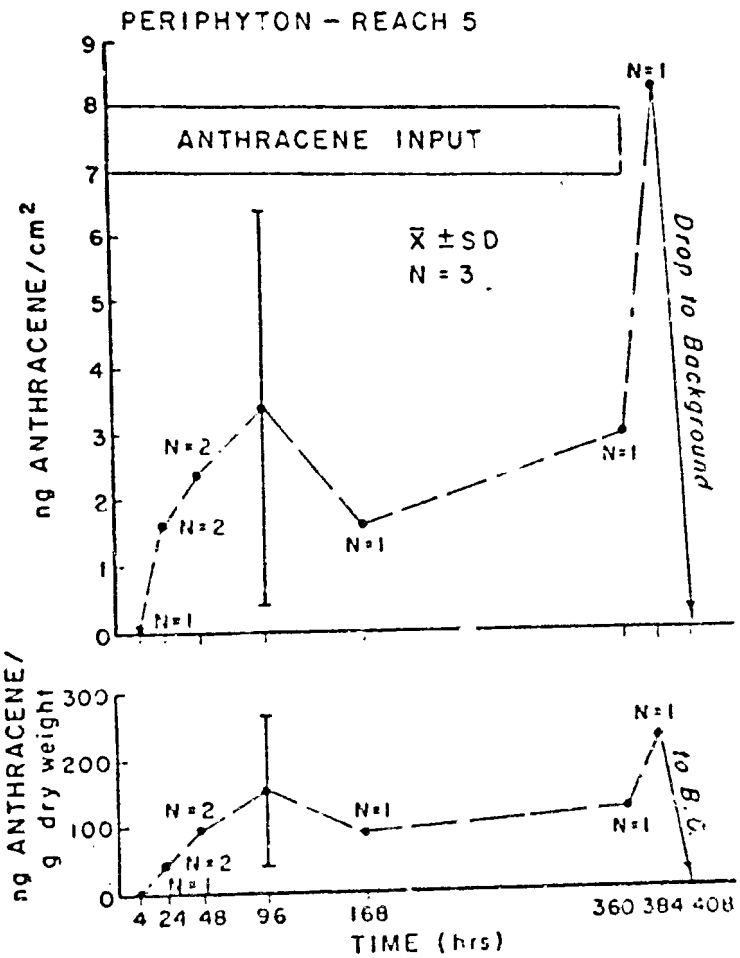

Figure 6.4.3. Anthracene concentrations in periphyton in reach 5 as $ng \cdot cm^{-2}$ function of time. Upper figure represents $anthracene \cdot cm^{-2}$, while the lower figure represents $anthracene \cdot g^{-1}$, dry weight, periphyton.

SECTION 6.5

CLAMS

After 336 h of exposure to anthracene, papershell clams, Anodonta imbecillis, had attained 96% of the projected steady state concentration of 17,580 ng anthracene·g^{-1}, dry weight of soft tissue which could be attained at approximately 500 h of exposure (Fig. 6.5.1). The first order uptake and depuration rate constants estimated simultaneously during the 336 h exposure period were 13.99 ± 1.7 (asymptotic standard error, $ml \cdot g^{-1} \cdot h^{-1}$) and 0.0080 ± 0.0015 h^{-1} respectively. This depuration rate constant corresponds to a half time for elimination of approximately 88 h. See Section 4.7 for a discussion of PAH accumulation and depuration by molluscs and the lack of oxidative biotransformation observed in most molluscs.

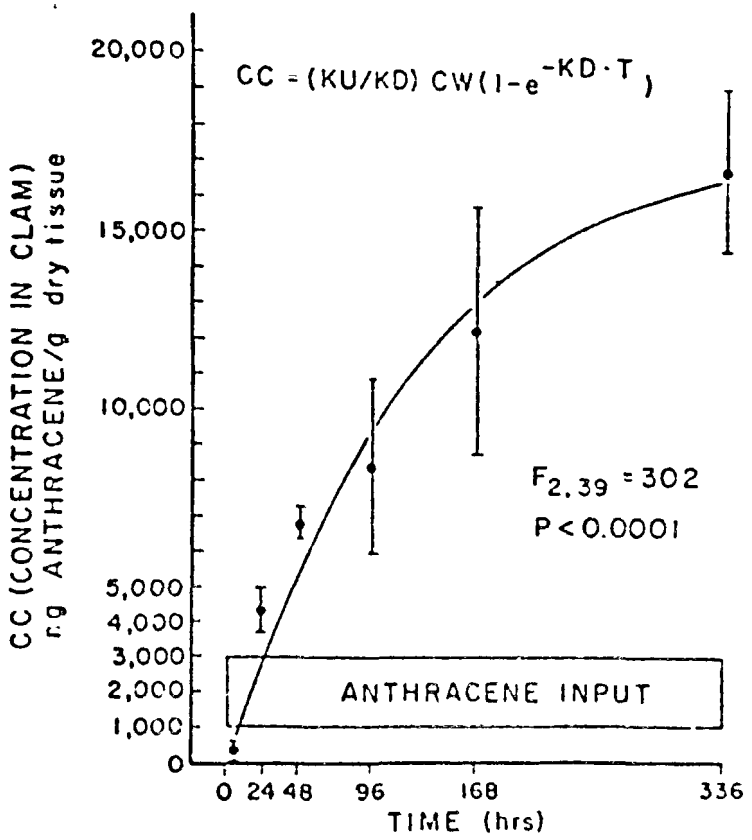

Figure 6.5.1. Uptake of anthracene by soft tissues of clams during the period of anthracene input to the channels. Each point represents the mean of 6 clams. Confidence intervals of 2SE are presented. The least squares predicted regression curve for the indicated model is given.

SECTION 6.6

FISH

During the channels microcosm study, we observed mortality of bluegill sunfish. The first fish mortality was observed as early as 1530 hrs, 7 h after the anthracene infusion was started. By 1700 hrs, 9 h of exposure, all of the fish in reach 1 of the experimental channels were dead. In reach 5, the reach farthest from the input, no fish died during the first day of the experiment. All of the fish in this reach were alive at 0800 hrs of day 2 of the experiment. Fish in reach 5 started dying at 1000 hrs and were all dead within an hour.

Bluegills were collected just after death in reach 1 and alive from reach 5 after 4 h exposure. Fish were also collected from reach 5 at 0800 hrs on day 2 (24 h after anthracene infusion was initiated), which was prior to any observed mortality. The total anthracene concentrations in fish in reach 1 after 4 h was 2389, $ng \cdot g^{-1}$, wet weight (SD = 275, n = 3). Anthracene concentrations in reach five were 457 (SD = 182, n = 3) and 7763 (SD = 1325, n = 3) after 4 and 24 h exposure, respectively. Subsequent studies showed that the mortality was not due to the ethanol carrier.

From the anthracene concentrations measured at the times when fish died, we suspected a photo-induced mortality of anthracene contaminated fish. To try and elucidate this possibility we considered several experiments. A brief description of the design as well as the results and discussion of each experiment are given in this section.

Initially, we repeated the anthracene exposure to determine if the mortality observed during the channels microcosms study could be repeated (Figure 6.6.1). Again all of the fish in both reaches were killed. The onset of mortality was more rapid in reach 1 than in reach 5, as in the first biotic channels microcosm experiment. However, in this second study of fish mortality, which was conducted on 8-10 January, the mortality was less rapid than in the first experiment. Also, the solar radiation was less during the second experiment, due to partly cloudy skies.

A second study was conducted to determine if the mortality observed was due directly to light on the fish or indirectly from a photo-product. In this study fish in reaches 1 and 5 were shaded so there was no sunlight and one reach (reach 3) which was between then was unshaded. In reaches 1 and 5, which were shaded, only 1 mortality was observed (Figure 6.6.2). However, in reach 3, which was not shaded, all of the fish died between 0800 and 1800 hrs of the second day of the experiment. These results

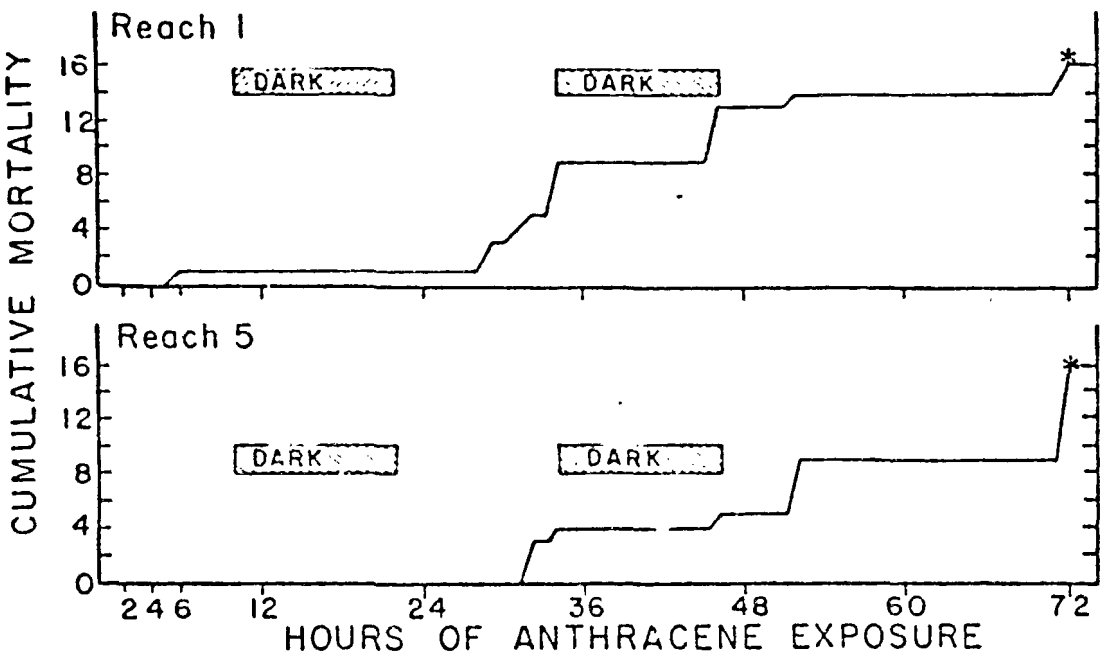

Figure 6.6.1. Cumulative mortality of bluegill sunfish in the channels microcosm. Mean dawn anthracene concentrations were 12 $\mu g \cdot \ell^{-1}$. Two cages at each reach with 8 fish per cage. Time is given as cumulative exposure to anthracene. Periods of light and dark are given. * denotes time at which all fish were dead.

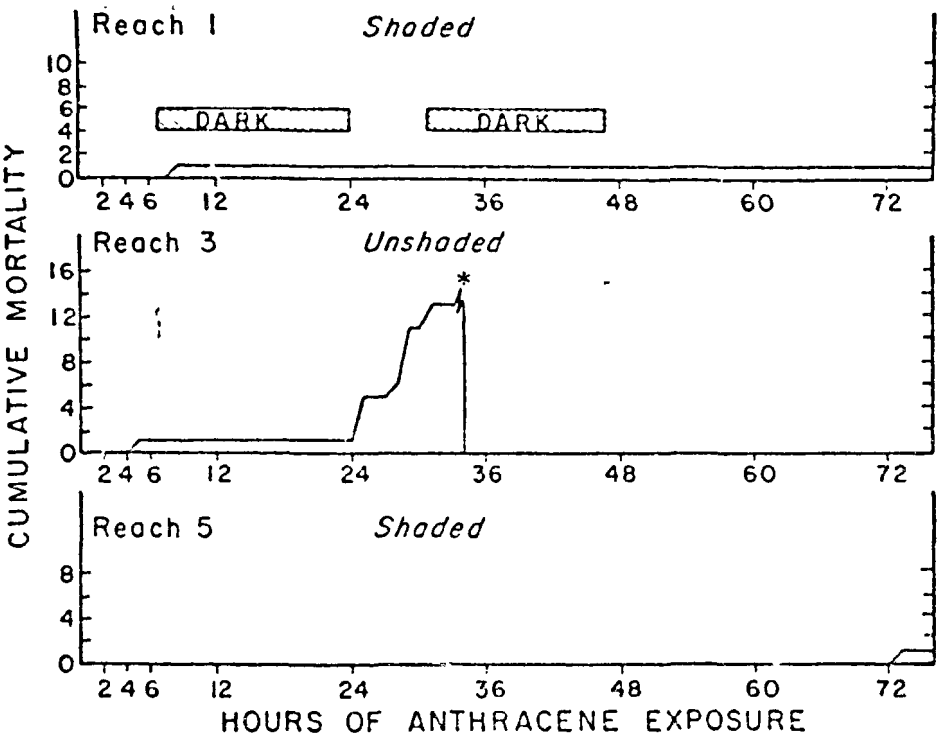

Figure 6.6.2. Cumulative mortality of bluegill sunfish in shaded and unshaded reaches of the channels microcosms. The weighted averages (day - night) of anthracene were 13 $\mu g \cdot \ell^{-1}$ (dawn = 13); 9.38 $\mu g \cdot \ell^{-1}$ (dawn = 12.54, n = 13; noon = 7.4, n = 21) and 9.5 dawn = 12.5, n = 42; noon = 5.6, n = 53) for reaches 1, 3 and 5 respectively. Two cages with 8 fish per cage were placed in each reach. * denotes time at which all fish were dead.

support the hypothesis that the mortality observed was an anthracene-light mortality.

In another experiment fish were dosed for 72 h in the dark (reaches 1 and 5) and in the light reach 3 (Figure 6.6.2). After 72 h of dosing at 0800 hrs the anthracene input was terminated and the fish which had been shaded (reaches 1 and 5) were unshaded at 1000 hrs.

All of the fish which had been dosed in the unshaded reach 3 were dead at the end of the 72 h dosing period. One fish had died in both reach 1 and 5 after the 72 h dosing period. Upon being exposed to light after accumulating anthracene, all of the fish in reaches 1 and 5 died within 24 h (Figure 6.6.3). These results suggest that the mode of action is by anthracene or an anthracene transformation product in the organisms since we allowed a washout period to remove anthracene from the water column prior to removing the shading.

An additional experiment was conducted to determine the time necessary for fish held in clean water to depurate photoactive contaminants. Caged fish were dosed continuously for 48 h with anthracene (14.6 $\mu g \cdot \ell^{-1}$) at the shaded 9 meter station. The anthracene infusion was stopped and fish were transferred from the shaded 4m station, after 24, 48, 72, 96 and 144 h of depuration in shaded, uncontaminated water (eight fish) to an unshaded, uncontaminated section.

After 48 h of exposure whole fish had attained an average anthracene concentration of 318 $\mu g \cdot g^{-1}$, dry weight (n = 8, SD = 79). No fish had died during dosing in the dark.

The first group was removed from the dark at 0800 (following 24 h depuration in the dark). The mean anthracene concentration in whole fish was 47.3 $\mu g \cdot g^{-1}$, dry weight (n = 6, SD = 18.9). All of these fish were dead by 1500 h (7 h exposure to light) (Figure 6.6.4).

Fish which were allowed 48 h of depuration in the dark had a mean anthracene concentration 36.0 $\mu g \cdot g^{-1}$ (n = 5, SD = 28.3) dry weight. The mortality of fish in this group was less than those which had been allowed only 24 h of depuration in the dark before exposure to light (Figure 6.6.4). After 48 h four of the eight fish were still alive. The fish which were allowed 72 and 96 h of depuration in the dark exhibited rates of mortality, which were similar to that observed for fish which were allowed to depurate for 48 h. After 72 h of depuration the anthracene concentration had decreased to 73 $\mu g \cdot g^{-1}$, dry weight (SD = 37). After 144 h the concentrations were not different from those in control fish. Some of these fish were able to survive in sunlight and reduce the concentration of anthracene in their bodies until they were undetectable. We observed no mortality in fish which had been allowed to depurate until their whole body concentrations had decreased to background (Figure 6.6.4).

The rapid depuration of anthracene from fish, which we observed, is consistent with those reported for many different fish species and PAH (Lee *et al.*, 1972; Roubal *et al.*, 1978). Elimination mechanisms reported for

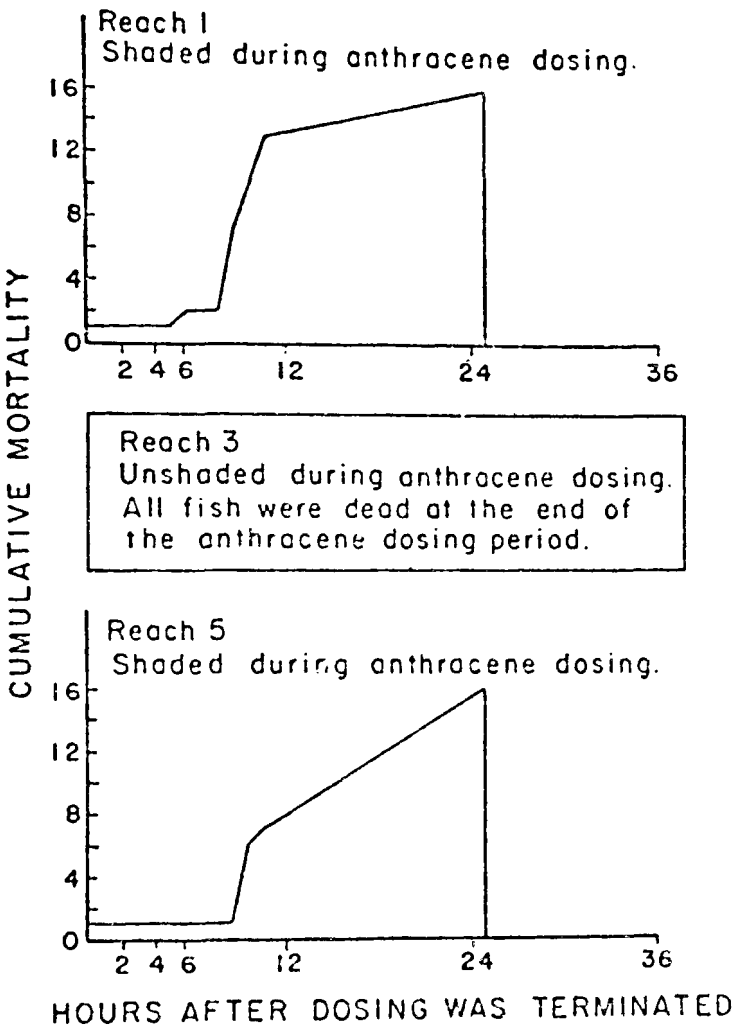

Figure 6.6.3. Cumulative mortality of bluegill sunfish after 72 hr of exposure to anthracene in shaded or unshaded reaches. After 72 hr of anthracene dosing, anthracene inputs were stopped and fish exposed to light.

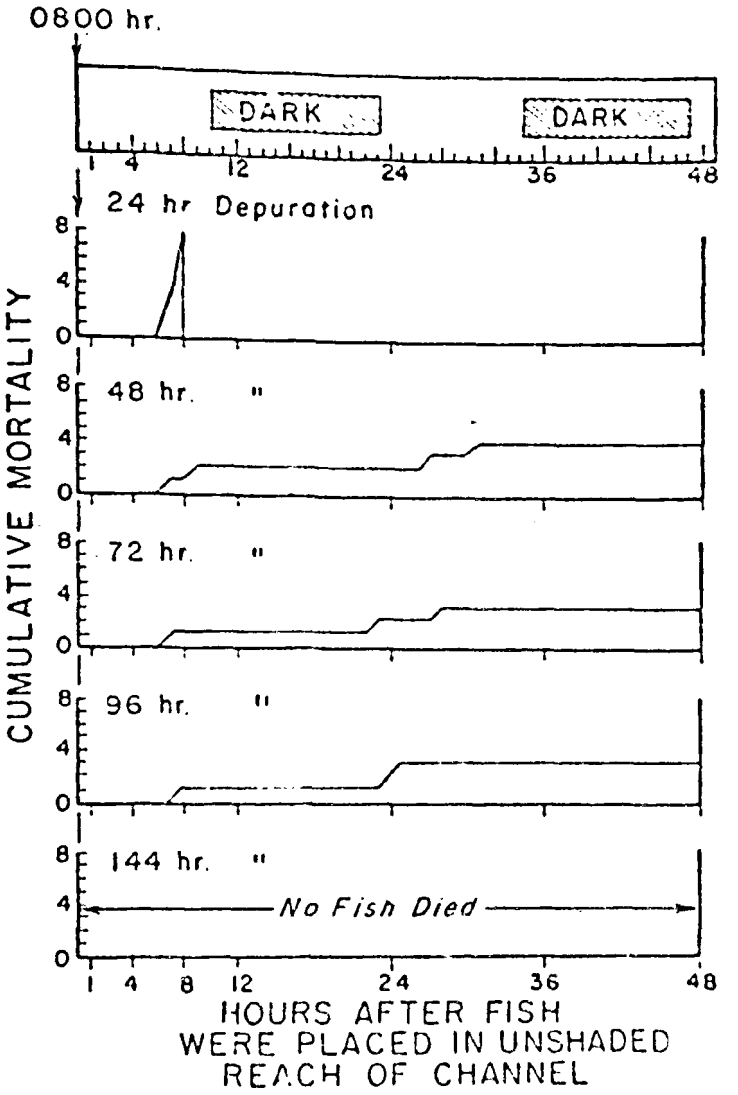

Figure 6.6.4. Cumulative mortality of bluegill sunfish as a function of time. Fish were exposed to 14.6 µg anthracene·ℓ^{-1} for 48 h in the dark. Sets of 8 fish were allowed to depurate into clean water for 24, 48, 72, 96 and 144 h then placed in clean water in the light. Each set of fish were placed in the light at 0800 hrs and observed for 48 h.

fish include partitioning of PAH into clean water as well as active biotransformation and excretion (Neeley et al., 1974; Melancon and Lech, 1979).

The mechanism of anthracene phototoxicity is unknown, but can be postulated to involve photooxidation of anthracene to form toxic products within fish or, more likely, to involve sensitized photooxidation of macromolecules binding anthracene. The oxidative photo-chemistry of anthracene has been well studied. Solution phase formation of endoperoxides by singlet oxygen as well as further oxidation to anthraquinone has been reported (Foote, 1968). Anthracene derived fluorescent dyes, used as environmental probes of protein structure, cause photooxidation of histidine and other amino acid residues (Harrington et al., 1956).

Photooxidation in the presence of sensitizing dyes has been reported to cause cell death, in vitro and in vivo damage to nucleic acids, enzyme inactivation and degradation of proteins and carbohydrates (Means and Feeney, 1971; Spikes, 1977). Light is also known to increase fish activity levels and trigger many complex physiological processes which could contribute indirectly to mortality under stress conditions of anthracene contamination.

Phototoxicity effects may be widespread among PAH. Death of E. Coli due to photodynamic action of benzo(a)pyrene in the presence of oxygen has been reported (Harrison and Raabe, 1967). Mutagenic and potentially toxic photoproducts have been formed from fuel oil exposed to sunlight (Larson et al., 1977) and on PAH contaminated atmospheric particulate matter (Fox and Oliver, 1981). While many PAH are known to be photolabile, to our knowledge phototoxic effects in aquatic biota have not been reported previously. Tests of phototoxicity should be included in protocols for risk assessment of compounds known to be photolabile. The common practice of studying PAH fate and effects under laboratory conditions which minimize photo-degradation should be re-examined until additional studies determine the potential ecological significance of PAH phototoxicity in aquatic biota.

APPENDIX I

Open literature publications containing information collected during this study are given below.

1. Bartell, S. M., P. F. Landrum, J. P. Giesy, and G. J. Leversee. 1981. Simulated transport of polycyclic aromatic hydrocarbons in artificial streams. in: Energy and Ecological Modeling Mitsch, W. J., R. W. Bosserman and J. M. Klopatek (eds.), Elsevier, N. Y. 839 p.

2. Leversee, G. J., J. P. Giesy, P. F. Landrum, S. Gerould, J. W. Bowling, T. E. Fannin, J. D. Haddock, and S. M. Bartell. 1981. Kinetics and Biotransformation of Benzo(a)Pyrene in Chironomous riparius. Arch. Environ. Contam. Toxicol. 11:25-31.

3. Leversee, G. J., J. P. Giesy, P. F. Landrum, S. Gerould, M. Bruno, A. Spacie, S. Bartell, J. Bowling, J. Haddock, and T. Fannin. 1981b. Disposition of benzo(a)pyrene in aquatic systems components: periphyton, chironomids, fish. pp. 357-366. In: Chemical Analysis and Biological Fate: Polynuclear Aromatic Hydrocarbons. M. Cooke and A. J. Dennis (eds.), Battelle Press, Columbus, Ohio.

4. Landrum, P. F. and J. P. Giesy. 1981. Anomolous Breakthrough of Benzo(a)pyrene During Concentration with Amberlite XAD-4 from Aqueous Solutions. Chapter 22 in: Advances in the Identification and Analysis of Organic Pollutants in Water, L. H. Keith (ed.), pp. 345-355, Ann Arbor Science, Ann Arbor, Michigan.

5. Gerould, S., P. F. Landrum and J. P. Giesy. 1982. Anthracene bioconcentration and biotransformation in chironomids: Effects of temperature and concentration. Environ. Poll. (in press).

6. Bruno, M. G., T. E. Fannin and G. J. Leversee. 1982. The disposition of benzo(a)pyrene in the periphyton communities of two South Carolina streams. Can. J. Bot. (in press).

7. J. W. Bowling, G. J. Leversee, P. F. Landrum and J. P. Giesy. 1982. Photo-induced Toxicity in Anthracene Contaminated Fish Exposed to Sunlight. Aquatic Toxicol. (in press).

8. Leversee, G. J., P. F. Landrum, J. P. Giesy, and T. Fannin. 1982. Effect of Humics on Polycyclic Aromatic Hydrocarbons: Accumulation by Daphnia magna and Coprecipitation at Estuarine Salinities. Can. J. Fish. Aquat. Sci. (submitted).

9. Spacie, A., P. F. Landrum and G. J. Leversee. 1982. Uptake, Depuration and Biotransformation of Anthracene and Benzo(a)pyrene in Bluegill Sunfish. Ecotox. Environ. Safety. (In Press).

REFERENCES

Abedi, Z. H. and A. W. A. Brown. 1961. Peritrophic membrane as vehicle for DDT and DDE excretion in Aedes aegypti larvae. Ann. Ent. Soc. Amer. 54:539-542.

Ahokas, J. T , H. Saarni, D. W. Nebert and O. Pelkonen. 1979. The in vitro metabolism and covalent binding of benzo(a)pyrene to DNA catalysed by trout liver microsomes. Chem. Biol. Interactions 25: 103-111.

Ahokas, J. T. 1979. Cytochrome P-450 in fish liver microsomes and carcinogen activation. In: Pesticide and Xenobiotic Metabolism in Aquatic Organisms. M. A. Q. Kahn, J. J. Lech, and J. J. Menn (Eds.), American Chemical Society, ACS Symposium Series 99, Washington, D. C., pp. 279-296.

American Petroleum Institute. 1978. Fate and Effects of Polynuclear Aromatic Hydrocarbons in the Aquatic Environment. Publication No. 4297, 23 p.

Anderson, J. W., J. M. Neff, B. A. Cox, H. E. Tatum and G. M. Hightower. 1974. The effects of oil on estuarine animals: Toxicity, uptake, depuration, respiration. pp. 285-310. In: Pollution and Physiology of Marine Organisms. F. J. Vernberg and W. B. Vernberg (Eds.), Academic Press, New York.

Andelman, J. B. and J. E. Snodgrass. 1974. Incidence and significance of polynuclear aromatic hydrobarbons in the water environment. CRC Critical Reviews in Environmental Control 4:69-83.

Ausmus, B. S., G. K. Eddlemon, S. J. Draggan, J. M. Giddings, D. R. Jackson, R. J. Luxmoore, E. G. O'Neill, R. V. O'Neill, Monte Ross-Todd and P. Van Voris. 1980. Microcosms as Potential Screening Tools for Evaluating Transport and Effects of Toxic Substances. Edited by W. F. Harris. ORNL/EPA 4, EPA-600/3-80-042 U. S. Environmental Protection Agency, Athens, Ga. p 379.

Archer, S. R., T. R. Blackwood and G. E. Wilkins. 1979. Status Assessment of Toxic Chemicals: Polynuclear Aromatic Hydrocarbons I. EPA-600/2-79-210L, U. S. Environmental Protection Agency, Cincinnati, OH.

Barnsley, E. A. 1975. The bacterial degradation of fluoranthrene and benzo(a)pyrene. Can. J. Microbiol. 21:1004-1008.

Barr, A. S., J. H. Goodnight, J. P. Sall and J. T. Helwig. 1979. SAS User's Guide. SAS Institute, Inc., Raleigh, N. C. pp. 317-329.

Bartell, S. M., P. F. Landrum, J. P. Giesy and G. J. Leversee. 1981. Simulated transport of polycyclic aromatic hydrocarbons in artificial streams. pp. 1-31. In: Proceedings of the International Symposium on Energy and Ecolgoical Modeling. Louisville, Kentucky, April 20-28, 1981.

Baughman, G. L. and R. R. Lassiter. 1978. Prediction of environmental pollutant concentration. pp. 35-54. In: Estimating the Hazard of Chemical Substances to Aquatic Life. J. Cairns, Jr., K. L. Dickson and A. W. Maki, (eds.). American Society for Testing Materials, ASTM STP 657.

Bella, D. A. and W. E. Dobbins. 1968. Difference modeling of stream pollution. J. Sanitary Engineering ASCE. 94:995-1016.

Bend, J R., L. M. Ball, T. H. Elmamlouk, M. O. James and R. M. Philpot. 1979. Microsomal mixed-function oxidation in untreated and polycyclic aromatic hydrocarbon-treated marine fish. pp. 297-318. In: Pesticide and Xenobiotic Metabolism in Aquatic Organisms M. A. Q. Kahn, J. J. Lech and J. J. Menn (Eds.). American Chemical Society, ACS Symposium Series 99, Washington, D. C.

Bend, J. R., M. O. James and P. M. Dansetts. 1977. In vitro metabolism of xenobiotics in some marine animals. Ann. N. Y. Acad. Sci. 298: 505-521.

Bjorseth, A. and A. J. Dennis. 1979. Polynuclear Aromatic Hydrocarbons: Chemistry and Biological Effects. Battelle Press, Columbus, Ohio. 1097 p.

Blanchard, F. A., I. T. Takahashi, H. C. Alexander and E. A. Bartlett. 1977. Uptake, clearance and bioconcentration of ^{14}C-sec-buty-14-chlorodiphenyl oxide in rainbow trout. pp. 162-177. In: Aquatic Toxicology and Hazard Evaluation, F. L. Mayer and J. L. Hamelink (eds.), American Society for Testing and Materials. ASTM STP 634.

Blumer, M., G. Souza and J. Sass. 1970. Hydrocarbon pollution of edible shellfish by an oil spill. Mar. Biol. 5:195-202.

Boehm, P. D. and J. G. Quinn. 1974. The solubility behavior of No. 2 fuel oil in sea water. Marine Pollut. Bull. 5:101-105.

Boehm, P. D. and J. G. Quinn. 1976. The effect of dissolved organic matter in sea water on the uptake of mixed individual hydrocarbons and number 2 fuel oil by a marine filter-feeding bivalve (Mercenaria mercenaria). Estu. Coastal Mari. Sci. 4:93-105.

Bowling, J. W., J. P. Giesy, H. J. Kania and R. L. Knight. 1980. Large-scale microcosms for assessing fates and effects of trace contaminants. pp. 224-247. In: Microcosms in Ecological Research J. P. Giesy (ed.). U. S. Department of Energy Technical Information Center, Oak Ridge, TN.

Branson, D. R., G. E. Blau, H. C. Alexander and W. B. Neely. 1975. Bioconcentration of 2,2',4,4'-tetrachlorobiphenyl in rainbow trout as measured by an accelerated test. Trans. Am. Fish. Soc. 104-785-792.

Braunstein, H. M., E. D. Copenhaver and H. A. Pfuderer (ed.). 1977. Environmental, Health and Control Aspects of Coal Conversion: An Information Overview Vols. 1 and 2. ORNL/EIS-94.

Bravo, H. S., S. L. Salazar, A. V. Botello and E. F. Mandelli. 1978. Polyaromatic hydrocarbons in oysters from coastal lagoons along the eastern coast of the Gulf of Mexico, Mexico. Bull. Environ. Contamn. Toxicol. 20:171-176.

Brown, R. A. and P. K. Starnes. 1978. Hydrocarbons in the water and sediment of Wilderness Lake II. Marine Poll. Bull. 9:162-165.

Bruno, M. G. and R. L. Lowe. 1980. The distribution of some bog diatoms: a cluster analysis. Am. Midl. Nat. 104:70-79.

Canton, J. H., R. C. C. Wegman, T. J. A. Vulto, C. H. Verhoef and G. J. van Esch. 1978. Toxicity-, accumulation-, and elimination studies of α-Hexachlorocyclohexane (αHCH) with saltwater organisms of different trophic levels. Water Res. 2:687-690.

Carlson, G. P. 1972. Detoxification of foreign organic compounds by the quahaug, Mercenaria mercenaria. Comp. Biochem. Physiol. 43B:295-302.

Chen, C. W. and J. T. Wells, Jr. 1976. Boise river ecological modeling. pp. 171-203. In: Modeling Biochemical Processes in Aquatic Ecosystems. R. P. Canale, (ed.), Ann Arbor Science, Ann Arbor, Mich. 389 p.

Chiou, C. T., V. H. Freed, D. W. Schmedding and R. K. Kohnert. 1977. Partition coefficient and bioaccumulation of selected organic chemicals. Envir. Sci. Technol. 11:475-478.

Christensen, H. E., T. T. Lugin Byhl and B. S. Carroll. 1975. Registry of toxic effects of chemical substances. U. S. Dept. of Health Education and Welfare. Rockville, MD.

Coffman, W. P., K. W. Cummings and J. C. Wuycheck. 1971. Energy flow in a woodland stream ecosystem: Tissue support trophic structure of the autumnal community. Arch. Hydrobiol. 68:232-276.

Crawford, D. J. and R. W. Leggett. 1980. Assessing the risk of exposure to radioactivity. Amer. Sci. 58:524-636.

Collier, T. K., L. C. Thomas and D. C. Malins. 1978. Influence of environmental temperature on disposition of dietary naphthalene in coho salmon (Oncorhynchus kisutch): isolation and identification of individual metabolites. Comp. Biochem. Physiol. 61C:23-28.

Crosby, D. G., P. F. Landrum and C. C. Fischer. 1979. Investigations of xenobiotic metabolism in intact aquatic animals. pp. 217-231. In: Pesticide and Xenobiotic Metabolism in Aquatic Organisms. M. A. Q. Kahn, J. J. Lech and J. J. Menn (Eds.), American Chemical Society, ACS Symposium Series 99, Washington, D. C.

DeAngelis, D. L., Goldstein, R. A. and R. V. O'Neill. 1975. A model for trophic interaction. Ecology 56:881-892.

Deickman, W. B. and H. W. Gerarde. 1969. Toxicology of Drugs and Chemicals. Academic Press, New York. 805 p.

Derr, S. K. and J. J. Zabik. 1972. Biolobically active compounds in the aquatic environment: the uptake and distribution of (1, 1-dichloro 2,2-bis (p-chlorophenyl) ethylene), DDE by Chironomus tentans Fabricius (Diptera: Chironomidae). Trans. Amer. Fish. Soc. 101:323-328.

DeSalvo, L. H., H. E. Guard and L. Hunter. 1975. Tissue hydrocarbon burden of mussels as potential monitor of environmental hydrocarbon insult. Environ. Sci. Technol. 9:247-251.

Dobroski, C. J. and C. E. Epifanio. 1980. Accumulation of benzo(a)pyrene in a larval bivalve via trophic transfer. Can. J. Fish. Aquat. Sci. 37:2318-2322.

Douglas, B. 1958. The ecology of attached diatoms and other algae in a small stony stream. J. Ecol. 46:295-322.

Dunn, B. P. 1976. Techniques for determination of benzo(a)pyrene in marine organisms and sediments. Environ. Sci. Technol. 10:1018-1021.

Dunn, B. P. and H. F. Stitch. 1975. The use of mussels in estimating benzo (a)pyrene contamination of the marine environment. Proc. Soc. Exp. Biol. Medicine 150:49-51.

Dunn, B. P. and H. F. Stitch. 1976. Release of the carcinogen benzo(a) pyrene from environmentally contaminated mussels. Bull. Environm. Contam. Toxicol. 15:398-401.

Duthie, H. C. 1965. A study of the distribution and periodicity of some algae in a bog pool. J. Ecol. 53:343-349.

Duthie, J. R. 1977. The importance of sequential assessment in test programs for estimating hazard to aquatic life. pp. 17-35. In: Aquatic Toxicology and Hazard Evaluation, F. L. Mayer and J. L. Hamelink (eds.). American Society for Testing and Materials, ASTM STP 634.

Estenik, J. F. and W. J. Collins. 1979. In vivo and in vitro studies of mixed function oxidase in an aquatic insect Chironomus riparius. pp. 349-370. In: Pesticides and Xenobiotic Metabolism in Aquatic Organisms, M. A. Q. Khan, J. J. Lech and J. J. Menn (Eds.). American Chemical Society, Washington, D. C.

Evans, W. C., H. N. Fernley and E. Griffiths. 1965. Oxidation metabolism of phenanthrene and anthracene by soil pseudomonads. Biochem. J. 95: 819-831.

Fisher, S. G. and G. E. Likens. 1972. Stream ecosystem: Organic energy budget. Biosci. 22:33-35.

Foote, C. S. 1968. Mechanisms of photosensitized oxidation. Science 162:963-970.

Fox, M. A. and S. Olive. 1981. Photooxidation of anthracene on atmospheric particulate matter. Science 205:582-583.

Fossato, V. U. and W. J. Canzonier. 1976. Hydrocarbon uptake and loss by the mussel Mytilus edulis. Marine Biol. 36:243-250.

Fucik, K. W. and J. M. Neff. 1977. Effects of temperature and salinity of napthalenes uptake in the temperature clam Rangia cuneata and the boreal clam Protothaca staminea. pp. 305-312. In: Fate and Effects of Petroleum Hydrocarbons in Marine Organisms and Ecosystems, D. A. Wolfe (ed.), New York, Pergamon Press.

Gardner, W. S. and D. W. Menzel. 1974. Phenolic aldehydes as indicators of terrestrially derived organic matter in the sea. Geochim. Cosmochim. Acta. 38:813-822.

Garnas, R. L. 1975. Comparative metabolism of pesticides by marine invertebrates. Doctoral dissertation, University of California, Davis.

Gearing, J. N., P. J. Gearing, T. F. Lytle and J. S. Lytle. 1978. Comparison of thin-layer and column chromatography for separation of sedimentary hydrocarbons. Anal. Chem. 50:1833-1835.

Gearing, P. J., J. N. Gearing, R. J. Pruell, T. C. Wade and J. G. Quinn. 1980. Partitioning of No. 2 fuel oil in controlled estuarine ecosystems. Sediments and suspended particulate matter. Environ. Sci. Technol. 14: 1129-1136.

Gehrs, C. W. (coordinator). 1976. Coal Conversion: description of technologies and necessary biomedical and environmental research. ORNL5192. Oak Ridge National Laboratory, Oak Ridge, TN. 288 p.

Gerhart, E. H. and R. M. Carlson. 1978. Hepatic mixed-function oxidase activity in rainbow trout exposed to several polycyclic aromatic compounds. Environ. Res. 17:284-295.

Gerould, S., P. Landrum and J. P. Giesy. 1981. Anthracene bioconcentration and biotransformation in chironomids: Effects of temperature and concentration. Environ. Pollut. (In Press).

Giddings, J. M., B. T. Walton, G. K. Eddlemon and K. G. Olson. 1979. Transport and fate of anthracene in aquatic microcosms. pp. 312-320. In: Microbial Degradation of Pollutants in Marine Environments, EPA-60019-79-012. U. S. Environmental Protection Agency, Gulf Breeze, FL. 551 p.

Giddings, J. M. 1979. Acute toxicity to Selenastrum capricornutum of aromatic compounds from coal conversion. Bull. Environ. Contam. Toxicol. 23:360-364.

Giesy, J. P. (ed.). 1980. Microcosms in Ecological Research. CONF-781101. U. S. Department of Energy Technical Information Center, Oak Ridge, TN. 1110 p.

Giesy, J. P. and L. A. Briese. 1978. Trace metal transport by particulates and organic carbon in two South Carolina streams. Vech. Internal. Vereln. Limnol. 20:1401-1417.

Giesy, J. P., K. J. Kania, J. W. Bowling, R. L. Knight, S. Mashburn and S. Clarkin. 1979. Fate and Biological Effects of Cadmium Introduced into Channel Microcosms. EPA-6002/3-79-039. U. S. Environmental Protection Agency, Athens, Ga. 157 p.

Giesy, J. P., J. W. Bowling and H. J. Kania. 1980. Cadmium and zinc accumulation and elimination by freshwater crayfish. Arch. Environ. Contam. Toxicol. 9:683-697.

Goldberg, E. D. 1975. The mussel watch--A first step in global marine monitoring. Mar. Poll. Bull. 6:111.

Gower, A. M. and P. J. Buckland. 1978. Water quality and the occurrence of Chironomus riparius Meigan (Diptera:Chironomidae) in a stream receiving sewage effluent. Freshwater Biol. 8:153-164.

Graham, J. E. S. and T. C. Hutchinson. 1975. The role of temperature and heterotrophism in determining crude oil toxicity. Proc. 10th Canadien Symp. Water Poll. Res. Canada. p. 73-83.

Gude, W. D. 1968. Autoradiographic Techniques: Localization of Radioisotopes in Biological Material. Prentice-Hall, Inc., Englewood Cliffs, NJ. 113 p.

Hamelink, J. L. 1977. Current bioconcentration test methods and theory. pp. 149-161. In: Aquatic Toxicology and Hazard Evaluation. F. L. Mayer and J. L. Hamelink (eds.), American Society for Testing and Materials, ASTM STP 634.

Harrington, W. F., P. Johnson and R. H. Ottewill. 1956. Bovine serum albumin and its behavior in acid solution. Biochem. J. 62:569-582.

Harris, R. P., V. Berdugo, E. D. S. Corner, C. C. Kilvington and S. C. M. O'Hara. 1977. Factors affecting the retention of a petroleum hydrocarbon by marine planktonic copepods. pp. 286-304. In: Fate and Effects of Petroleum Hydrocarbons in Marine Systems and Organisms, D. A. Wolfe (ed.). Pergamon Press, New York.

Harrison, A. P. and V. E. Raabe. 1967. Factors influencing the photodynamic action of benzo(a)pyrene on Excherichia coli. J. Bacteriol. 93:618-626.

Harrison, R. M., R. Perry and R. A. Wellings. 1975. Polynuclear aromatic hydrocarbons in raw, potable and waste waters (Review paper). Water Res. 9:331-346.

Hassett, J. P. and M. A. Anderson. 1979. Association of hydrophobic organic compounds with dissolved organic matter in aquatic systems. Environ. Sci. Technol. 13:1526-1529.

Hedges, J. I. and P. L. Parker. 1976. Land-derived organic matter in surface sediments from the Gulf of Mexico. Geochim. Cosmochim. Acta. 40:1019-1029.

Herbes, S. E. and G. F. Risi. 1978. Metabolic alteration and excretion of anthracene by Daphnia pulex. Bull. Environ. Contam. Toxicol. 19: 147-155.

Herbes, S. E. and L. R. Schwall. 1978. Microbial transformation of polycyclic aromatic hydrocarbons in prsitine and petroleum-contaminated sediments. Appl. Environ. Microbiol. 35:306-316.

Herbes, S. E., L. R. Schwall and G. A. Williams. 1977. Rate of microbial transformation of polycyclic aromatic hydrocarbons: a chromatographic quantification procedure. Appl. Environ. Microbiol. 34:244-246.

Herbes, S. E., G. R. Southworth and C. W. Gehrs. 1976. Organic contaminants in aqueous coal conversion effluents: Environmental consequences and research priorities. pp. 295-303. In: Trace Substances in Environmental Health, D. D. Hemphill (ed.). University of Missouri, Columbia.

Hinga, K. R., Pilson, M. E. Q., R. F. Lee, J. W. Farrington, K. Tjessem and A. C. Davis. 1980. Biogeochemistry of benzoanthracene in an enclosed marine ecosystem. Environ. Sci. Technol. 14:1136-1143.

Hites, R. A., R. E. Laflamme and J. W. Farrington. 1977. Sedimentary polycyclic aromatic hydrocarbons: The historical record. Science 198:829-831.

James, M. O. and J. R. Bend. 1980. Polycyclic aromatic hydrocarbon induction of cytochrome P-450-dependent mixed-function oxidases in marine fish. Toxicol. Appl. Pharm. 54:117-133.

Jackim, E. and L. Wilson. 1977. Benzo(a)pyrene accumulation and depuration in the soft-shell clam (Mya arenia). pp. 92-94. In: Proceedings Tenth National Shellfish Sanitation Workshop. Hunt Valley, Maryland.

Jonasson, P. M. 1978. Edgardo Baldi Memorial Lecture, Zoobenthos of lakes. Verh. Internat. Verein. Limnol. 20:13-37.

Johnson, E., A. Abu-Shumaya and S. R. Abbott. 1977. Use of fluorescence detection in high performance liquid chromatography. J. Chromatogr. 134:107-119.

Jones, P. W. and P. Leber (eds.). 1979. Polynuclear Aromatic Hydrocarbons. Third International Symposium on Chemistry and Biology - Carcinogenesis and Mutagenesis. Ann Arbor Science, Ann Arbor, Mich. 892 p.

Kania, H. J., R. L. Knight and R. J. Beyers. 1979. Fate and biological effects of mercury introduced into artificial streams. EPA-60013-76-060. U. S. Environmental Protection Agency, Athens, Ga. 129 p.

Karickhoff, S. W., D. S. Brown and T. A. Scott. 1979. Sorption of hydrophobic pollutants on natural sediments. Water Res. 13:241-248.

Kawatski, J. A. and M. A. Bittner. 1975. Uptake, elimination and biotransformation of the lampricide 3-trifluormethyl 4nitrophenol (TFM) by larvae of the aquatic midge Chironomus tentans. Toxicol. 4:183-194.

Kenaga, E. E. and C. A. I. Goring. 1980. Relationship between water solubility, soil sorption, octanol-water partitioning, and concentration of chemicals in biota. pp. 62-77. In: Aquatic Toxicology. J. G. Eaton, P. R. Porrish and A. C. Hendricks (eds.), American Society for Testing and Materials, ASTM STP 707.

Kitchell, J. F., J. F. Koonce, R. V. O'Neill, H. H. Shugart, Jr., J. J. Magnuson and R. S. Booth. 1974. Model of fish biomass dynamics. Trans. Amer. Fish. Soc. 103:786-798.

Knowles, G. and A. C. Wakeford. 1978. A mathematical deterministic river-quality model. Part I: Formulation and description. Water Res. 12:1149-1153.

Konemann, H. and K. vanLeeuwen. 1980. Toxicokinetics in fish: Accumulation and elimination of six chlorobenzenes by guppies. Chemosphere 9:3-19.

Kooke, R. M. M., J. W. A. Lustenhouwer, K. Olie and O. Hutzinger. 1981. Extraction efficiencies of polychlorinated dibenzo-p-dioxins and polychlorinated dibenzofurans from fly ash. Anal. Chem. 53:461-463.

LaFlamme, R. E. and R. A. Hites. 1978. The global distribution of polycyclic aromatic hydrocarbons in recent sediments. Geochimica et Cosmochimica Acta. 42:289-303.

LaFlamme, R. E. and R. A. Hites. 1979. TETRA- and pentacyclic, naturally-occurring, aromatic hydrocarbons in recent sediments. Geochemica et Cosmochimica Acta. 43:1687-1691.

LaVoie, E., L. Tulley, V. Bedenko and D. Hoffman. 1979. Mutagenicity, tumor initiating activity, and metabolism of tricyclic polynuclear aromatic hydrocarbons. pp. 1041-1058. In: Polynuclear Aromatic Hydrocarbons: Chemistry and Biological Effects. A, Bjorseth and A. J. Dennis (eds.). Battelle Press, Columbus, Ohio. 1097 p.

Lake, J. L., C. W. Dimock and C. B. Norwood. 1980. A comparison of Methods for the Analysis of hydrocarbons in Marine Sediments. Advances in Chemistry: Petroleum in the Marine Environment. (in press.)

Lake, J. L. and C. Kershner. 1977. Petroleum sulfur-containing compounds and aromatic hydrocarbons in the marine mollusks Modiolus clemissus and crassastrea virginica. Oil Spill Conf., pp. 627-632.

Landrum, P. F. and D. G. Crosby. 1981a. Comparison of the disposition of several nitrogen containing compounds in the sea urchin and other marine invertebrates. Xenobiotica 11:351-361.

Landrum, P. F. and G. D. Crosby. 1981b. The Disposition of p-Nitroanisole by the sea urchin, Strongylocentrolus purpuratus, biotransformation and bioconcentration. Ecotoxicol. Environ. Safety 5:240-254.

Landrum, P. F. and J. P. Giesy. 1981. Anomolous breakthrough of benzo(a) pyrene during concentration with Amberlite® XAD-4 resin from aqueous solutions. pp. 345-355. In: Advances in the Identification and Analysis of Organic Pollutants in Water. L. H. Keith (ed.). Ann Arbor Science, Ann Arbor, Mich..

Larson, R. A., L. L. Hunt and D. W. Blankenship. 1977. Formation of toxic products from #2 fuel oil by photooxidation. Environ. Sci. Technol. 11:492-496.

Lech, J. J. and J. R. Bend. 1980. Relationships between biotransformation and the toxicity and fate of xenobiotic chemicals in fish. Envir. Health Perspect. 34:115-131.

Lee, R. F., C. Ryan and M. L. Neuhauer. 1976. Fate of petroleum hydrocarbons taken up from food and water by the blue crab Callinectes sapidus. Marine Biol. 37:363-370.

Lee, R. F., R. Sauerheber and A. A. Benson. 1972. Petroleum hydrocarbons: Uptake and Discharge by the marine mussel Mytilus endulis. Sci. 177: 344-346.

Lee, R. F., R. Sauerheber and G. H. Dobbs. 1972b. Uptake, metabolism and discharge of polycyclic aromatic hydrocarbons by marine fish. Mar. Biol. 17:201-208.

Lee, R. F., S. C. Singer, K. R. Tenore, W. S. Gardner and R. M. Philpot. 1979. Detoxification system in polychaete worms: importance in the degradation of sediment hydrocarbons. pp. 23-37. In: Marine Pollution: Functional Responses, W. B. Vernberg, F. P. Thurberg, A. Calabrese and F. J. Vernberg (eds.). Academic Press, New York.

Lee, R. F. and M. Takahashi. 1977. The fate and effect of petroleum in controlled ecosystem enclosures. Rapp. P.V-Reun. Cons. int. Explor. Mer. 171:150-156.

Lee, R. F., W. S. Gardner, J. W. Anderson, J. W. Blaylock and J. Barwell-Clark. 1978. Fate of polycyclic aromatic hydrocarbons in controlled ecosystem enclosures. Environ. Sci. Technol. 12:832-838.

Lehr, R. E., H. Yagi, D. R. Thakker, W. Levin, A. W. Wood, A. H. Couney and D. M. Jerina. 1978. The bay region theory of polycyclic aromatic hydrocarbon induced carcinogenicity. In: Carcinogenesis, Vol. 3. P. W. Jones and R. I. Freudenthof (eds.). A, Raven Press, New York.

Leo, A., C. Hansch and D. Elkins. 1971. Partition coefficients and their uses. Chemical Reviews 71(G):525-616.

Leo, A. J. 1975. Calculation of partition coefficients useful in the evaluation of the relative hazards of various chemicals in the environment. In: Symposium on Structure-Activity Correlations in Studies of Toxicity and Bioconcentration with Aquatic Organisms. G. D. Veith and D. E. Konasewich (eds.), Internat. Joint Commission. Winsor, Ontario, Canada.

Leversee, G. J., J. P. Giesy, P. F. Landrum, S. Gerould, J. W. Bowling, T. Fannin, J. Haddock and S. Bartell. 1981a. Kinetics and biotransformation of Benzo(a)pyrene by Chironomus riparius. Arch. Environ. Contamn. Toxicol. 11:25-31.

Leversee, G. J. J. P. Giesy, P. F. Landrum, S. Gerould, M. Bruno, A. Spacie, S. Bartell, J. Bowling, J. Haddock and T. Fannin. 1981b. Disposition of benzo(a)pyrene in aquatic systems components: periphyton, chironomids, fish. pp. 357-366. In: Chemical Analysis and Biological Fate: Polynuclear Aromatic Hydrocarbons. M. Cooke and A. J. Dennis (eds.), Battelle Press, Columbus, Ohio.

Lu, P., R. L. Metcalf, N. Plummer and D. Mandel. 1977. The environmental fate of three carcinogens: Benzo(a)Pyrene, Benzidine and Vinyl Chloride evaulated in laboratory model ecosystems. Arch. Environ. Contam. Toxicol. 6:129-142.

Lu, P. Y., R. L. Metcalf and E. M. Carlson. 1978. Environmental fate of five radio-labeled coal conversion by-products evaluated in a laboratory model ecosystem. Environ. Health Perspect. 24:201-208.

McCain, B. B., H. O. Hodgins, W. D. Gronlund, J. W. Hawkes, D. W. Brown, M. S. Myers and Vandermeulen. 1978. Bioavailability of crude oil from experimentally oiled sediments to English sole (Parophrys vetulus), and pathological consequences. J. Fish. Res. Board Can. 35:657-664.

McIntire, C. D. 1973. Periphyton dynamics in laboratory streams: A simulation model and its implications. Ecol. Monogr. 43:399-420.

McIntire, C. D. 1975. Periphyton assemblages in laboratory streams. pp. 403-430. In: River Ecology. B. A. Whitton (ed.). University of California Press, Berkeley.

McIntire, C. W. and J. A. Colby. 1978. A hierarchical model of lotic ecosystems. Ecol. Monogr. 48:167-190.

McIntire, C. D. and H. K. Phinney. 1965. Laboratory studies of periphyton production and community metabolism in lotic environments. Ecol. Monogr. 35:237-258.

McLeese, D. W., V. Zitko and D. B. Sergeant. 1979. Uptake and excretion of fenitrothione by clams and mussels. Bull. Environ. Contam. Toxicol. 22:800-806.

Maher, W. A., J. Bagg and D. Smith. 1978. Determination of polycyclic aromatic hydrocarbons in marine sediments, using solvent extraction, thin layer chromatography and spectrofluorimetry. Intern. J. Environ. Anal. Chem. 4:1-11.

Means, G. E. and R. E. Feeney. 1971. Chemical Modifications of Proteins. Holden-Day, San Francisco, 149 p.

Melancon, M. J., Jr. and J. J. Lech. 1978. Distribution and elimination of naphthalene and 2-methylnaphthalene in rainbow trout during short and long-term exposures. Arch. Environ. Contam. Toxicol. 7:207-220.

Melancon, M. J., Jr. and J. J. Lech. 1979. Uptake, a biotransformation, disposition, and elimination of 2-methylnaphthalene and naphthalene in several fish species. pp. 5-22. In: Aquatic Toxicology, L. L. Marking and R. A. Kimerle (Eds.), pp. 5-22. American Society for Testing and Materials, ASTM STP 667.

Metcalf, R., G. K. Sangha and I. P. Kapoor. 1971. Model ecosystem for the evaluation of pesticide biodegradability and ecological magnification. Environ. Sci. Technol. 5:709-713.

Miller, G. C. and R. G. Zepp. 1979. Effects of suspended sediments on photolysis rates of dissolved pollutants. Water Res. 13:453-459.

Minshall, G. W. 1978. Autotrophy in Stream Ecosystems. Bio-science 28: 707-771.

Moore, M. N. 1979. Cellular responses to polycyclic aromatic hydrocarbons and phenobarbital in Mytilus edulis. Marine Environ. 2:255-263.

Muller, G., G. Grimmer and H. Böhnke. 1977. Sedimentary record of heavy metals and polycyclic aromatic hydrocarbons in Lake Constance. Naturwissenschaften 64: 427-431.

National Academy of Science (USA). 1972. Particulate Polycyclic Organic Matter. Washington, D. C.

Neal, E., B. Patten and C. DePoe. 1967. Periphyton growth on artificial substrates in a radioactively contaminated lake. Ecology 48:918-924.

Nebert, D., and H. Gelboin. 1968. Substrate inducible microsomal aryl hydrocarbon hydroxylases in mammalian cell cultures. J. Biol. Chem. 243:6242-6249.

Neely, W. B. 1979. Estimating rate constants for the uptake and clearance of chemicals by fish. Environ. Sci. Technol. 13:1506-1510.

Neely, W. B., D. R. Branson and G. E. Blau. 1974. Partition coefficient to measure bioconcentration potential of organic chemicals in fish. Env. Sci. Technol. 8:1113-1115.

Neff, J. M., B. A. Cox, D. Dixit, and J. W. Anderson. 1976. Accumulation and release of petroleum-derived aromatic hydrocarbons by four species of marine animals. Mar. Biol. 38:279-289.

Neff, J. M. 1982. Polycyclic aromatic hydrocarbons in the aquatic environment and cancer risk to aquatic organisms and man. In: Symposium: Carcinogenic Polynuclear Aromatic Hydrocarbons in the Marine Environment. N. L. Richards and B. L. Jackson (eds.), EPA-600/9-82-013, U. S. Environmental Protection Agency, Pensacola, Florida.

Neff, J. M. 1979. Polycyclic Aromatic Hydrocarbons in the Aquatic Environment. Applied Science Publishers Ltd., London. 262 p.

Norden, B., U. Edlund and S. Wold. 1979. Carcinogenicity of polycyclic aromatic hydrocarbons studied by SIMCA pattern recognition. pp. 345-366. In: Polynuclear Aromatic Hydrocarbons: Chemistry and Biological Effects. A, Bjorseth and A. J. Dennis (eds.). Battelle Press, Columbus, Ohio. 1097 p.

Nunes, P. and P. E. Benville. 1979. Uptake and depuration of petroleum hydrocarbons in the Manila clam, Tapes semidecussata Reeve. Bull. Environm. Contam. Toxicol. 21:719-726.

O'Neill, R. V. 1971. Systems approaches to the study of forest floor arthropods. pp. 441-477. In: Systems Analysis and Simulation in Ecology. Vol. I. Pattern, B. C. (ed.). Academic Press, New York. 607 p.

O'Neill, R. V. 1976. Ecosystem persistence and heterotrophic regulation. Ecology 57:1244-1253.

O'Neill, R. V., R. A. Goldstein and H. H. Shugart. 1972. Terrestrial Ecosystem Energy Model. USIBP-EDFB Memo Rep. 72-19.

Odum, H. T. 1957. Trophic structure and productivity of silver springs, Florida. Ecol. Monogr. 27:55-112.

Oliver, D. R. 1971. Life history of the Chironomidae. Ann. Rev. Entomol. 16:211-230.

Overton, E. B., J. Bracken and J. L. Caseter. 1977. Application of glass capillary columns to monitor petroleum-type hydrocarbons in marine sediments. J. Chromatog. Sci. 15:169-173.

Payer, H. D. and C. J. Soeder. 1975. Accumulation of polycyclic aromatic hydrocarbons in cultivated microalgae. Naturwissenschafte 62:536-537.

Payne, J. F. and W. R. Penrose. 1975. Induction of aryl hydrocarbon (benzo(a)pyrene) hydroxylase in fish by petrolem. Bull. Environ. Contamn. Toxicol. 14:112-116.

Patten, B. C. 1968. Mathematical models of plankton production. Int. Rev. Ges. Hydrobiol. 53:357-408.

Pedersen, M. G., W. K. Hershberger, and M. R. Juchau. 1974. Metabolism of 3,4-benzpyrene in rainbow trout (Salmo gairdneri). Bull. Environ. Contam. Toxicol. 12:481-486.

Pitts, J. N., K. A. Van Cauwenbetghe, D. Grosjean, J. P. Schmid, D. R. Fitz, W. L. Belser, G. B. Knudson, and P. M. Hynds. 1978. Atmospheric reactions of polycyclic aromatic hydrocarbons: Facile formation of mutagenic nitro derivatives. Science 202:515-519.

Prahl, F. G. and R. Carpenter. 1979. The role of zooplankton fecal pellets in the sedimentation of polycyclic aromatic hydrocarbons in Dabob Bay, Washington. Geochim. Cosmochim. Acta. 43:1959-1972.

Rose, F. L. and C. E. Cushing. 1970. Periphyton: autoradiography of zinc-65 adsorption. Science 168:576-577.

Roubal, W. T., T. K. Collier, and D. C. Malins. 1977. Accumulation and metabolism of carbon-14 labeled benzene, naphthalene, and anthracene by young coho salmon (Oncorhynchus kisutch). Arch. Environ. Contam. Toxicol. 5:513-529.

Roubal, W. T., S. I. Stranahan, and D. C. Malins. 1978. The accumulation of low molecular weight aromatic hydrocarbons of crude oil by coho salmon (Oncorhynchus kisutch) and starry flounder (Platichthys stellatus). Arch. Environ. Contam. Toxicol. 7:237-244.

Sandoval, M., F. H. Verhoff and T. H. Cahill. 1976. Mathematical modeling of nutrient cycling in rivers. pp. 205-232. In: Modeling Biochemical Processes in Aquatic Ecosystems. R. P. Canale (ed.), Ann Arbor Science, Ann Arbor, Mich. 389 p.

Satterlund, D. R. and J. E. Means. 1978. Estimating solar radiation under variable cloud conditions. Forest Sci. 24:363-373.

Schnell, J. V., E. H. Gruger, Jr. and D. C. Malins. 1980. Mono-oxygenase activities of coho salmon (Oncorhynchus kisutch) liver microsomes using three polycyclic aromatic hydrocarbon substrates. Xenobiotica 10: 229-234.

Sheldon, L. S., Hites, R. A. 1978. Organic Compounds in the Delaware River. Env. Sci. Technol. 12:1188-1194.

Shindler, D. B., B. F. Scott and D. B. Carlisle. 1975. Effect of crude oil on populations of bacteria and algae in artificial ponds subject to winter weather and ice formation. Verh. Internal. Verein. Limnol. 19:2138-2144.

Shugart, H. H., R. A. Goldstein and R. V. O'Neill. 1974. TEEM: A terrestrial ecosystem energy model for forests. Oecol. Plant. 25: 251-284.

Smith, E. L. 1936. Photosynthesis in relation to light and carbon dioxide. Proc. Nat. Acad. Sci. 22:504-511.

Smith, O. L., H. H. Shugart, R. V. O'Neill, R. S. Booth and D. C. McNaught. 1975. Resource competition and an analytical model of zooplankton feeding on phytoplankton. Amer. Nat. 109:571-591.

Soto, C., J. A. Hellebust and T. C. Hutchinson. 1975. Effect of naphthalene and aqueous crude oil extracts on the green flagellate Chlamydomonas angulosa. II. Photosynthesis and the uptake and release of naphthalene. Can. J. Bot. 53:118-126.

Soto, C., J. A. Hellebust, T. C. Hutchinson and R. G. Sheath. 1979. The effect of crude oil on the morphology of the green flagellate Chlamydomonas angulosa. Can. J. Bot. 57:2717-2728.

Soto, C., J. A. Hellebust, T. C. Hutchinson and R. G. Sheath. 1979b. The effect of the hydrocarbon naphthalene on the morphology of the green flagellate Chlamydomonas angulosa. Can. J. Bot. 57:2729-2739.

Southworth, G. R. 1979. The role of volatilization in removing polycyclic aromatic hydrocarbons from aquatic environments. Bull. Environ. Contamn. Toxicol. 21:507-514.

Southworth, G. R., J. J. Beauchamp and P. K. Schmieder. 1978. Bioaccumulation potential of polycyclic aromatic hydrocarbons in Dephnia pulex. Water Res. 12:973-977.

Southworth, G. R., C. C. Keffer, and J. J. Beauchamp. 1980. Potential and realized bioconcentration. A comparison of observed and predicted bioconcentration of azaarenes in the fathead (Pimephales promelas). Environ. Sci. Technol. 14:1529-1531.

Spacie, A. and J. Hamelink. 1981. Recent advances in the prediction of bioconcentration in fish. J. Environm. Toxicol. Chem. (in press).

Spikes, J. D. 1977. Photosensitization. pp. 87-112. In: The Science of Photobiology, K. C. Smith (ed.), Plenum Press, New York, 87 p.

Statham, C. N., C. R. Elcombe, S. P. Szyjka, and J. J. Lech. 1978. Effect of polycyclic aromatic hydrocarbons on hepatic microsomal enzymes and disposition of methylnaphthalene in rainbow trout in vivo. Xenobiotica 8:65-71.

Stegeman, J. J. and S. M. Teal. 1973. Accumulation, release and retention of petroleum hydrocarbons by the oyster Crassostrea virginica. Marine Biol. 22:37-44.

Suess, M. J. 1976. The environmental load and cycle of polycyclic aromatic hydrocarbons. Sci. Total Environ. 6:239-250.

Teal, J. M. 1957. Community metabolism in a temperate cold spring. Ecol. Monogr. 27:283-302.

Teal, J. M., K. Burns and J. Farrington. 1978. Analyses of aromatic hydrocarbons in intertidal sediments resulting from two spills of No. 2 fuel oil in Buzzards Bay, Massachusetts. J. Fish. Res Board Can. 35:510-520.

Tilly, L. J. 1968. The structure and dynamics of Cone Spring. Ecol. Monogr. 38:169-197.

Tulp, M. T. M. and O. Hutzinger. 1978. Some thoughts on aqueous solubilities and partition coefficients of PCB, and the mathematical correlation between bioaccumulation and physico-chemical properties. Chemosphere 10:849-860.

Varanasi, U., D. J. Gmur, and W. L. Weichert. 1981. Effect of environmental temperature on naphthalene metabolism by juvenile starry flounder (Platichthys stellatus). Arch. Environm. Contam. Toxicol. 10: 203-214.

Veith, G. D., D. L. DeFoe, and B. V. Bergstedt. 1979a. Measuring and estimating the bioconcentration factor of chemicals in fish. J. Fish. Res. Bd. Canada. 36:1040-1048.

Veith, G. D., K. J. Macek, S. R. Petrocelli, and J. Carroll. 1979b. An evaluation of using partition coefficients and water solubility to estimate bioconcentration factors for organic chemicals in fish. Fed. Regist. 15926 (March 15, 1979).

Wagner, J. G. 1975. Fundamentals of Clinical Pharmacokinetics. Drug Intelligence Publications Inc., Hamilton Press, Hamilton, IL.

Walsh, G. E., K. E. Ainsworth and L. Faas. 1977. Effects and uptake of chlorinated naphthalenes in marine unicellular algae. Bull. Environ. Contamn. Toxicol. 18:297-301.

Walshe, B. M. 1949. The function of haemoglobin in Chironomus plumosus under natural conditions. J. Exp. Biol. 27:73-95.

Weininger, D. L. 1978. Accumulation of PCB's by lake front in Lake Michigan. Ph.D. Thesis, University of Wisconsin, Madison, 232 p.

Wershaw, R. L., P. J. Burcar, and M. C. Goldberg. 1969. Interaction of pesticides and natural organic material. Environ. Sci. Technol. 3(3):271-273.

Wilkes, F. G., and C. M. Weiss. 1971. The accumulation of DDT by the dragonfly nymph Tetragoneuria. Trans. Amer. Fish. Soc. 100:222-236.

Windsor, J. G. and R. A. Hites. 1979. Polycyclic aromatic hydrocarbons in Gulf of Maine sediments and Nova Scotia soils. Geochim. Cosmochim. Acta. 43:27-33.

Zalucki, M. P. 1978. Modeling and simulation of the energy-flow through Root Spring, Massachusetts. Ecology 59:654-659.

Zepp, R. G. and D. M. Cline. 1977. Rates of direct photolysis in aquatic environment. Environ. Sci. Technol. 11:359-366.

Zepp, R. G. and P. F. Schlotzhauer. 1979. Photoreactivity of selected aromatic hydrocarbons in water. pp. 141-158. In: Polynuclear Aromatic Hydrocarbons. Third International Symposium on Chemistry and Biology - Carcinogensis and Mutagenesis. P. W. Jones and P. Leber (eds.). Ann Arbor Science, Ann Arbor, Mich.